DIFFERENTIAL PATHOPHYSIOLOGY IN MELAS SYNDROME

Tesis doctoral

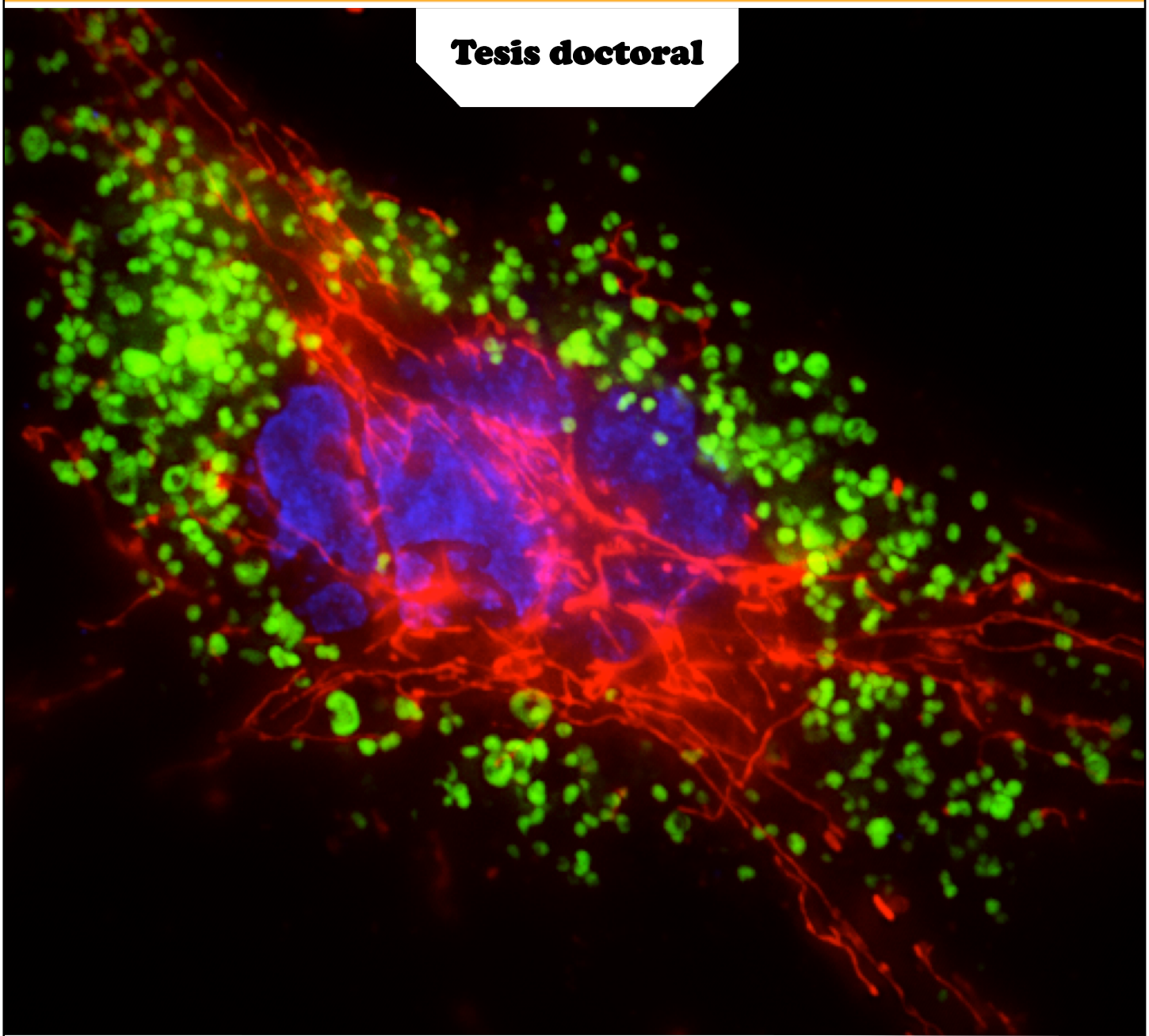

Juan Garrido Maraver
Sevilla, 2015

DIFFERENTIAL PATHOPHYSIOLOGY IN MELAS SYNDROME

Tesis doctoral

Juan Garrido Maraver

Sevilla, Octubre de 2015

Centro
Andaluz
de Biología
del Desarrollo

DIFFERENTIAL PATHOPHYSIOLOGY IN MELAS SYNDROME

Tesis doctoral

Memoria de tesis doctoral presentada por **JUAN GARRIDO MARAVER**, licenciado en Biotecnología, para optar al título de Doctor enmarcado en el programa de Doctorado en Biotecnología y Tecnología Química. Esta tesis doctoral ha sido realizada en el Centro Andaluz de Biología del Desarrollo (CSIC-UPO-JA), financiada por el Centro de Investigación Biomédica en Red de Enfermedades Raras (CIBERer) durante 2009 y por el Consejo Superior de Investigaciones Científicas (CSIC) desde 2011 hasta 2015. Esta tesis está inscrita al Departamento de Fisiología, Anatomía y Biología Celular de la Universidad Pablo de Olavide.

Juan Garrido Maraver

Sevilla, Octubre de 2015

Centro
Andaluz
de Biología
del Desarrollo

EL DIRECTOR
José Antonio Sánchez Alcázar
Profesor Titular de la Universidad Pablo de Olavide

D. JOSÉ ANTONIO SÁNCHEZ ALCÁZAR, Doctor en medicina por la Universidad Complutense de Madrid y profesor titular del área de Biología celular en el departamento de Fisiología, anatomía y biología celular de la Universidad Pablo de Olavide de Sevilla

INFORMA

Que **D. JUAN GARRIDO MARAVER,** licenciado en Biotecnología por la Universidad Pablo de Olavide de Sevilla, ha realizado bajo su dirección la tesis doctoral titulada **DIFFERENTIAL PATHOPHYSIOLOGY IN MELAS SYNDROME**, y que a su juicio reúne los méritos suficientes para superar el programa de Doctorado en Biotecnología y Tecnología Química.

Y para que conste, firmo el presente en Sevilla, a 7 de Octubre de 2015.

Fdo.: José Antonio Sánchez Alcázar

“Desocupado lector, sin juramento me podrás creer que quisiera que este libro [...] fuera el más hermoso, el más gallardo y más discreto que pudiera imaginarse.”

Miguel de Cervantes, Don Quijote de la Mancha

A mis padres

ABSTRACT

MELAS (mitochondrial encephalomyopathy, lactic acidosis and stroke-like episodes) is a mitochondrial disorder caused mainly by the m.3243A>G mutation in mitochondrial DNA. In this thesis, we report on how the severity of pathophysiological alterations is differently expressed in fibroblasts derived from patients with MELAS disease. We evaluated mitophagy activation and mitochondrial biogenesis, which are the main mechanisms regulating the degradation and genesis of mitochondrial mass, in transmitochondrial cybrids and fibroblasts derived form MELAS patients. Our results suggest a critical balance between mitophagy and mitochondrial biogenesis which leads to the expression of different degrees of pathological severity among MELAS fibroblast cell lines according to their heteroplasmy load and the activation of AMP-activated protein kinase (AMPK). AMPK-activators such as 5-aminoimidazole-4-carboxamide 1-β-D-ribofuranoside (AICAR) or coenzyme Q_{10} (CoQ) increased peroxisome proliferator-activated receptor alpha (PGC-1α) nuclear translocation, mitochondrial biogenesis, antioxidant enzyme system response, autophagic flux, and ultimately improved pathophysiological alterations in MELAS fibroblasts with the most severe phenotypes. Our findings support the hypothesis that mitochondrial biogenesis, increased antioxidant response and autophagy clearance serve as compensatory mechanisms in response to mitophagic degradation of dysfunctional mitochondria and point out that AMPK is an important player in this balance.

These results are particularly important since currently no efficient treatments are available for this chronic progressive disorder. In this thesis we propose the evaluation of the effectiveness of putative beneficial pharmacological agents in the treatment of MELAS by using cellular models such as transmitochondrial cybrids and fibroblasts with high mutational load. According to our results, supplementation with riboflavin or coenzyme Q_{10} effectively reversed the pathologic alterations in MELAS cybrid and fibroblast cell models. Our results indicate that cell models manifesting severe pathophysiological alterations and high heteroplasmy load have great potential as a screening and validation assays of novel drug candidates for MELAS treatment and presumably also for other diseases with mitochondrial impairment.

RESUMEN

MELAS (del inglés, *mitochondrial encephalomyopathy, lactic acidosis and stroke-like episodes*) es una enfermedad mitocondrial principalmente causada por la mutación m.3243>G en el ADN mitocondrial. En esta tesis, se estudia cómo la severidad de las alteraciones fisiopatológicas pueden expresarse diferencialmente en fibroblastos derivados de pacientes con este síndrome. Además, se evalúa dos mecanismos claves en la degradación y génesis de la masa mitocondrial celular, como son, la mitofagia y la biogénesis mitocondrial. Para ello se ha utilizado dos modelos celulares: cíbridos transmitocondriales y fibroblastos derivados de pacientes diagnosticados con el síndrome MELAS. Los resultados obtenidos sugieren la existencia de un equilibrio crítico entre ambos procesos, que conduce finalmente a la expresión de diferentes niveles de severidad patológica entre los fibroblastos según su carga mutacional y la activación de la proteína AMPK (del inglés, *AMP-activated protein kinase*). Los resultados obtenidos en esta tesis indican que activadores de AMPK como el 5-aminoimidazole-4-carboxamide 1-β-D-ribofuranoside (AICAR) o la coenzima Q_{10} (CoQ) fueron capaces de incrementar la translocación al núcleo de PGC-1α (del inglés, *Peroxisome proliferator-activated receptor gamma coactivator 1-alpha*), la biogénesis mitocondrial, el sistema enzimático antioxidante, el flujo autofágico y la mitofagia, mejorando en última instancia las alteraciones fisiopatológicas mostradas por los fibroblastos MELAS que manifiestan un fenotipo más severo. Nuestros resultados respaldan la hipótesis de que la biogénesis mitocondrial, el incremento de la respuesta antioxidante y la autofagia actúan como mecanismos de compensación en respuesta a la degradación de mitocondrias disfuncionales mediante mitofagia, señalando que la proteína AMPK juega un papel clave en este equilibrio.

Estos resultados revisten gran importancia ya que actualmente no existen tratamientos efectivos para tratar este desorden progresivo y crónico. Por ello, en esta tesis se propone la evaluación de la efectividad de agentes farmacológicos potencialmente beneficiosos en el tratamiento del síndrome MELAS, utilizando para ello modelos celulares de elevada carga mutacional y alta severidad patológica. Nuestros resultados indican que el tratamiento con riboflavina o la CoQ revierten de forma efectiva las alteraciones patológicas mostradas por cíbridos y fibroblastos de esta enfermedad. Así, los modelos celulares con alta heteroplasmia y alta severidad fisiopatológica se postulan como candidatos válidos para el cribado de nuevos fármacos en el tratamiento de enfermedades mitocondriales en general, y del síndrome MELAS en particular.

DIFFERENTIAL PATHOPHYSIOLOGY IN MELAS SYNDROME

CONTENTS

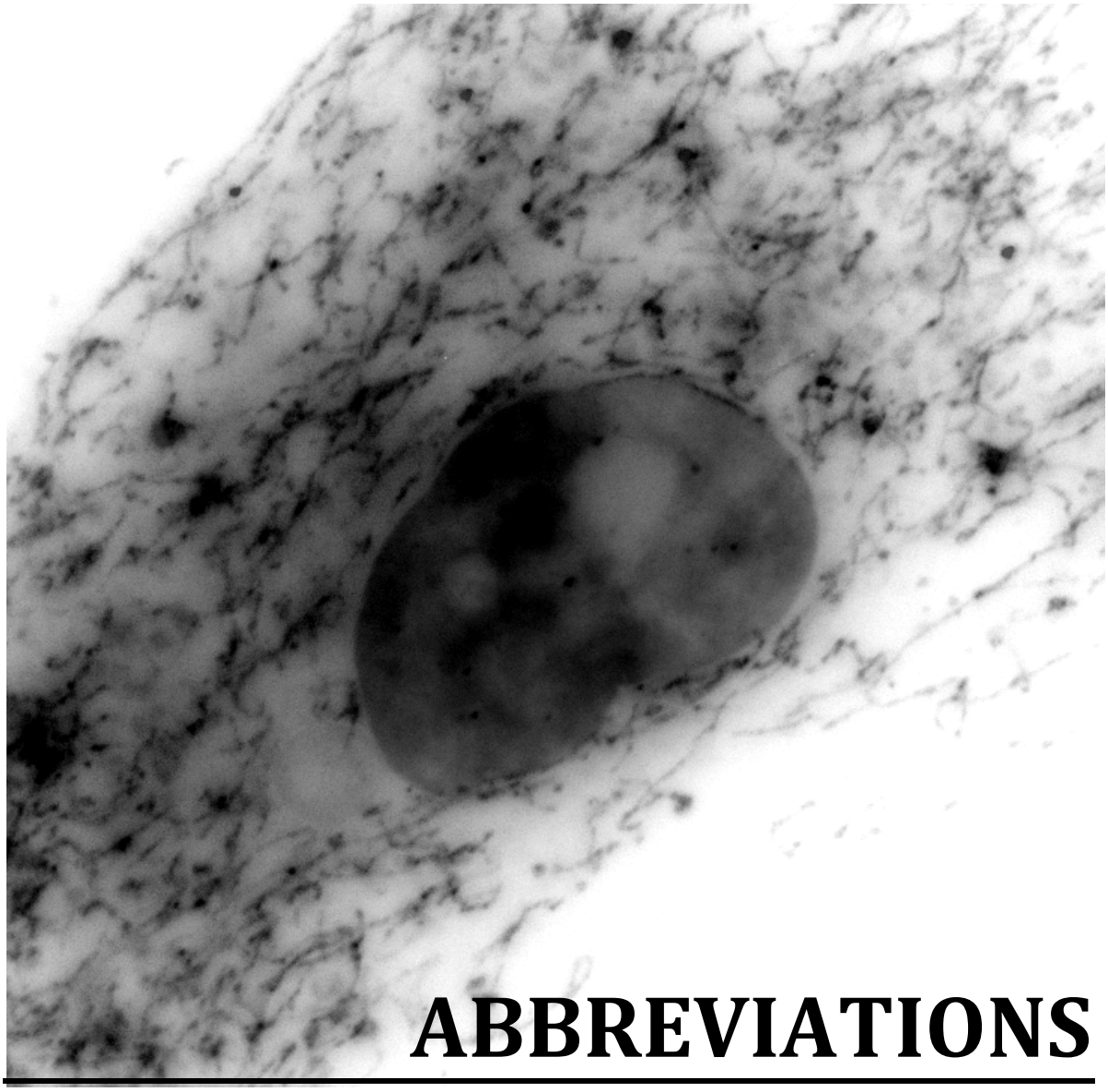

ABBREVIATIONS

ABBREVIATIONS

aaRSs: Aminoacyl-tRNA synthetases

AD: Alzheimer disease

ADN: Ácido desoxirribonucleico

AICAR: 5-aminoimidazole-4-carboxamide 1-β-D-ribofuranoside

ADP: Adenosine diphosphate

AMP: Adenosine monophosphate

AMPK: AMP-activated protein kinase

ANT1: Adenine nucleotide translocator

AOX: CoQ/O_2 alternative oxidase

ATF-2: Activating transcription factor 2

ATG: Autophagy-related

ATP: Adenosine triphosphate

AAVs: Adeno-associated viral vectors

BNIP3: BCL2/adenovirus E1B 19 kDa protein-interacting protein 3

BNIP3L: BNIP3-like

BN-PAGE: Blue-native PAGE

BTHS: Barth syndrome

BSA: Bovine serum albumin

cAMP: cyclic adenosine monophosphate

CaMK: Calcium/calmodulin-dependent protein kinase

CBS: Cystathionine binding domain

CnA: Calcineurin A

CoA: Coenzyme A

CoQ: Coenzyme Q_{10}

CoQ_1: Coenzyme Q_1

CoQ_9: Coenzyme Q_9

COXs: Complex IV subunits

CPT: Carnitine palmitoyltransferase

CREB: Cyclic AMP-response binding protein

CS: Citrate synthase

CSF: Cerebrospinal fluid

DAMP: Damage-associated molecular patterns

DBH2: Reduced decylubiquinone

DCPIP: Dichlorophenolindophenol

dGK: Deoxyguanosine kinase

DM1: Myotonic dystrophy type 1

DMEM: Dulbecco's modified Eagle's medium

DNA: Deoxyribonucleic acid

dNTP: Deoxyribonucleotides

DRP1: Dynamin-like protein 1 (Mitochondrial fission)

DTNB: 5,5'-dithiobis-(2-nitrobenzoic acid)

DTT: Dithiothreitol

EDTA: Ethylenediaminetetraacetic acid

EE: Ethylmalonic encephalopathy

ER: Endoplasmic reticulum

ERR: Oestrogen-related receptors

ETF: Electron-transferring-flavoprotein

FAD^+: Oxidised Flavin adenine dinucleotide

$FADH_2$: Reduced Flavin adenine dinucleotide

FBS: Fetal bovine serum

FCCP: Carbonyl cyanide-4-(trifluoromethoxy)phenylhydrazone

FDA: Food Drug Administration

Fis1: Fission related protein

GAPDH: Glyceraldehyde 3-phosphate dehydrogenase

GRACILE: Growth retardation, aminoaciduria, cholestasis, iron overload, lactic acidosis, and early death

GTP: Guanosine-5'triphosphate

HDAC: Histones deacetylase

HEPES: 4-(2-hydroxyethyl)-1-piperazineethanesulfonic acid

HPLC: High-performance liquid chromatography

HRP: Horseradish peroxidase

HSPs: Heavy-strand transcription promoters

IMM: Inner mitochondrial membrane

IS: Intermembrane space

JC-1: 5,5', 6,6'-tetrachloro-1,1'3,3'-tetraethylbenzimidazolecarbocyanine iodide

KSS: Kearns-Sayre syndrome

LC3: Microtubule-associated protein light chain 3

LC3-I: LC3 cleaved at the C terminus by Atg4

LC3-II: LC3-I lipided by conjugation to PE

LC3B: LC3 isoform (antibody against LC3B was used during this thesis)

LHON: Leber's hereditary optic neuropathy

LIR: LC3-interacting region

LSP: Light-strand transcription promoter

MAM: Mitochondria-associated ER membrane

MAPK: Mitogen-activated protein kinase

MELAS: Mitochondrial encephalomyopathy, lactic acidosis and stroke-like episodes

MERRF: Myoclonus epilepsy with ragged red fibers

MFNs: Mitofusin proteins

MIRO: Mitochondrial rho 1

MNGIE: Mitochondrial neurogastrointestinal encephalomyopathy

MOPS: 3-(N-morpholino)propanesulfonic acid

MPT: Mitochondrial permeability transition

MPTP: MPT pore

MR: Magnetic resonance

MRC: Mitochondrial respiratory chain

mtDNA: Mitochondrial DNA

mtEFs: Mitochondrial translation elongation factors (Tu, Ts and G1)

mtIF: Mitochondrial translation initiation factor

mt-LeuRS: mt-leucyl-tRNA synthetase

mTOR: Mammalian target of rapamycin

mTORC1: mTOR complex 1

MTS: Mitochondrial targeting sequence

mtSSB: Mitochondrial single-strand binding protein

mtTERM: Mitochondrial transcription terminator factor

mtTFA: Mitochondrial transcription factor A

mtTFBs: Mitochondrial transcription factors B

mt-ValRS: mt-valyl-tRNA synthetase

N or N_0: Number of cells

n: Proliferation rate

NAC: N-acetylcysteine

NAD^+: Oxided nicotinamide adenine dinucleotide

NADH: Reduced nicotinamide adenine dinucleotide

NAO: Nonyl acridine orange

NARP: Neuropathy, ataxia, retinitis pigmentosa

NBR1: Neighbor of BRCA1

Ndi1: NADH dehydrogenase/CoQ reductase

nDNA: Nuclear DNA

NO: Nitric oxide

NR: Nicotinamide riboside

NRFs: Nuclear respiratory factors

O_L: Replication origin of light strand of mtDNA

O_H: Replication origin of heavy strand of mtDNA

OMM: Outer mitochondrial membrane

OPA1: Optic atrophy-1 protein

OXPHOS: Oxidative phosphorylation system

P: P-value (statistics)

PAGE: Polyacrylamide gel electrophoresis

PARL: Presenilin-associated rhomboid-like

Parp1: Poly(ADP) ribosyl-polymerase 1

PBS: Phosphate-buffered saline

PCR: Polymerase chain reaction

PCR-RFLP: PCR - Restriction fragment length polymorphism

PDH: Pyruvate dehydrogenase

PE: Phosphatidylethanoalmine

PEO: Progressive external ophthalmoplegia

PGC – 1: Peroxisome proliferator-activated receptor gamma coactivator 1

PGC – 1 α: PGC-1 alpha

PGD: Pre-implantation genetic diagnosis

Pi: Phosphate

PI3K: Phosphatidylinositol 3-kinase

PKA: Protein kinase A

PKC: Protein kinase C

POLRMT: Mitochondrial RNA polymerase

Polγ: Polymerase γ

PINK1: Serine/threonine kinase phosphatase and tensin homolog (PTEN)-induced kinase 1

PMSF: Phenylmethylsulfonyl fluoride

PNAs: Protein nucleic acids

PS: Pearson syndrome

PTP: Permeability transition pore

p160MBP: p160 myb binding protein

RIPA: Radioimmunoprecipitation assay (buffer)

RLU: Relative light units

RNA: Ribonucleic acid

RNS: Reactive nitrogen species

ROS: Reactive oxygen species

RRF: Ragged-red fibers

SD: Standard deviation

SDH: Succinate dehydrogenase

SDS: Sodium dodecyl sulphate

SOD: Superoxide dismutase

TALENs: Transcription activator-like effector nucleases

TAZ: Tafazzin

TBS: Tris-buffered saline

TCA: Tricarboxylic acid

TEMED: Tetramethylethylenediamine

TFEB: Transcription factor EB

TG: Transfer buffer (25 mM Tris, 190 mM glycine, 20% methanol, pH 8.3)

TGS: Running buffer (25 mM Tris, 190 mM glycine, 0.1% SDS, pH 8.3)

Thr: Threonine

TIM: Translocase of inner membrane

TMRE: Tetramethylrhodamine ethyl ester

tm^5U: 5-taurinomethyluridine

TOM: Translocase of outer membrane

TP: Thymidine phosphorylase

T-PBS: PBS 0.05% Tween

tRNA: Transfer RNA

T-TBS: TBS with 0.05% Tween

U: Activity units

UBA: Ubiquitin binding domain

ULK1: Unc-51 like autophagy activating kinase 1

UV: Ultraviolet

VDAC: Voltage-dependent anion channel

VLCAD: Very long-chain acyl-CoA dehydrogenase

Vps15: Vacuolar protein sorting 15

Wt: Wild type

ZFNs: Zinc finger-endonucleases

ZMP: 5-aminoimidazole-4-carboxamide 1-b-D-ribofuranosyl monophosphate

$\Delta\Psi_m$: Mitochondrial membrane potential

ε: Extinction molar coefficient

λ: Wavelength

3D: Three-dimensional

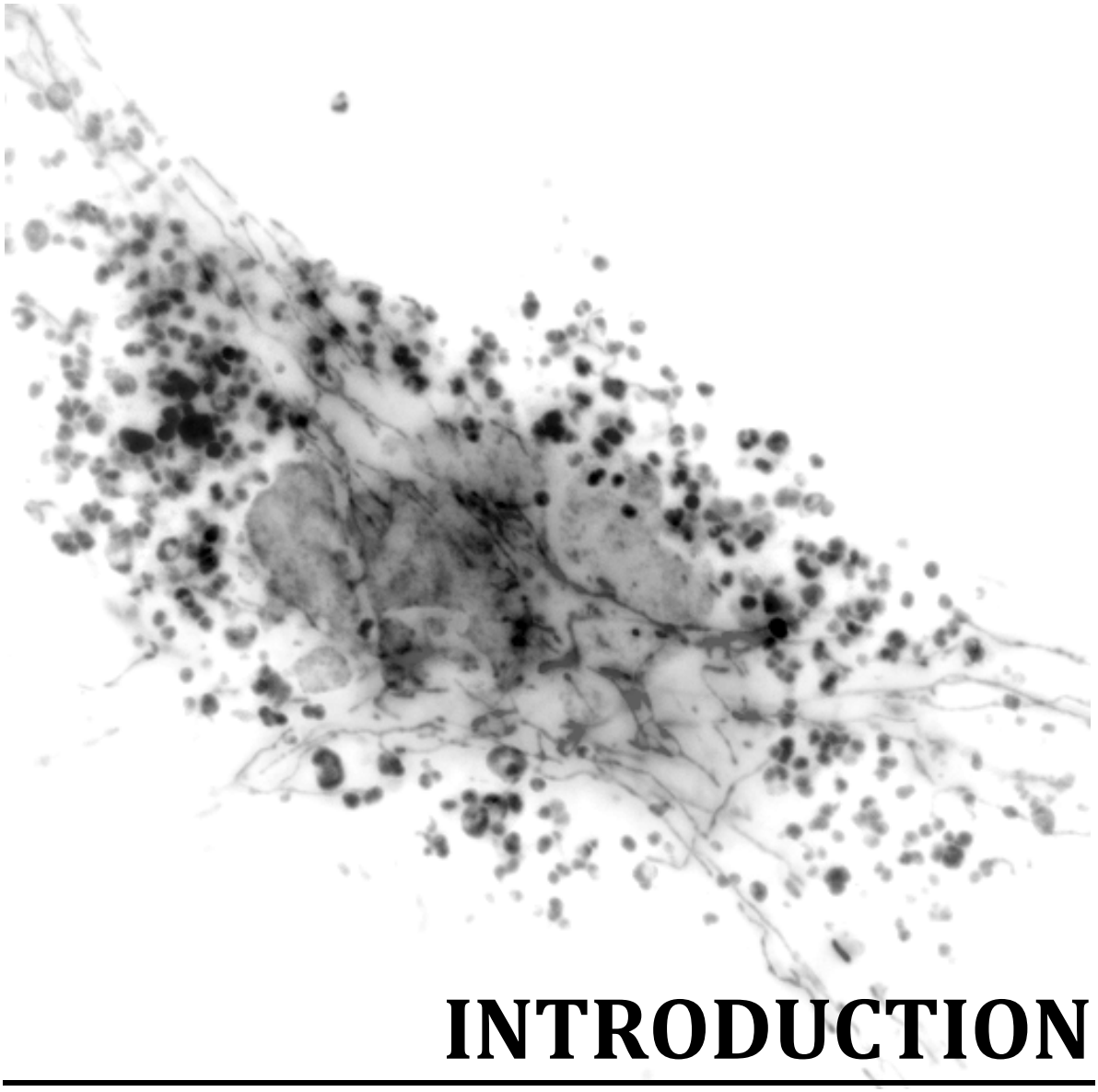

INTRODUCTION

INTRODUCTION

I-I. Mitochondrion

Mitochondrial bioenergetics

Mitochondria are fundamental organelles that ensure the proper energetic functioning of the cells. The discovery of mitochondria came during the mid-1800s, when different researchers such as Albert von Kölliker and Richard Altman described what they called "granules" or "bioblasts" in the cells of muscles. Later, in 1898, Carl Benda coined the term *mitochondria*, which derives from the Greek *mitos,* "thread", and *khondrion*, "little granule". These cytoplasmic organelles, ubiquitously found in most of eukaryotic cells, are surrounded by two membranes, and harbour a circular genome without intron structures similarly to bacterial genomes. These atypical characteristics are thought to be due to the origin of this organelle, which is explained by different theories. The most accepted theory, the endosymbiont theory, proposes that mitochondria were originally prokaryotic cells, capable of implementing oxidative mechanisms that were not possible for eukaryotic cells; they became endosymbionts living inside the eukaryote and maintained during evolution[1,2]. Alternatively, the less accredited autogenous hypothesis proposes that mitochondria are a portion of nuclear DNA enclosed by cytoplasmic membranes[3].

Structurally, mitochondria are difficult to define due to its high plasticity and active dynamism. Even though classically represented as small bean-shaped organelles (0.5-1 μm in diameter and variable in length), mitochondria are frequently found as complex 3D tubular branching networks due to their ability to move, fuse and split[4,5]. The abundance of mitochondria varies from tissue to tissue according to energy requirements. Thus, neurones and cardiac and skeletal muscle have a high density of mitochondria, which, to some extent, explains their vulnerability to energy-dependent defects resulting from mitochondrial abnormalities[4].

Mitochondria contain two membranes composed of phospholipid bilayers and proteins[6]: an outer membrane (OMM) and an inner membrane (IMM). OMM encloses the whole mitochondria and has a similar composition that plasma membrane in relation to protein: phospholipid ratio (1:1). OMM contains a large number of integral membrane proteins forming channels that allow the free diffusion of molecules smaller than 5 kDa[6]. Larger mitochondria-targeted proteins can cross this membrane through large multisubunit protein called translocase[7] such as the translocase of outer membrane (TOM). OMM can be associated with the endoplasmic reticulum (ER), forming mitochondria-associated ER membrane (MAM) that has a key role in lipid transference and calcium signalling[8], or with the cytoskeleton which has an essential role in determining mitochondrial distribution, shape and function[9].

IMM, with a higher protein: phospholipids ratio than OMM (4:1), is characterised by presenting an unusual phospholipid typical of bacteria, cardiolipin. This lipid

constitutes about 20% of the total lipid composition in mitochondria[10]. Unlike OMM, IMM is highly impermeable since ions and proteins require special membrane transporter to enter or exit the matrix, such as translocase of inner membrane (TIM)[11]. IMM is tremendously compartmentalized into numerous cristae, which expand the surface area of the inner membrane, enhancing its ability to anchor crucial proteins in mitochondrial functioning. In fact, in liver mitochondria and other tissues with high demand of energy, the area of the inner membrane increases around five times the OMM area[12] (**Figure I1**).

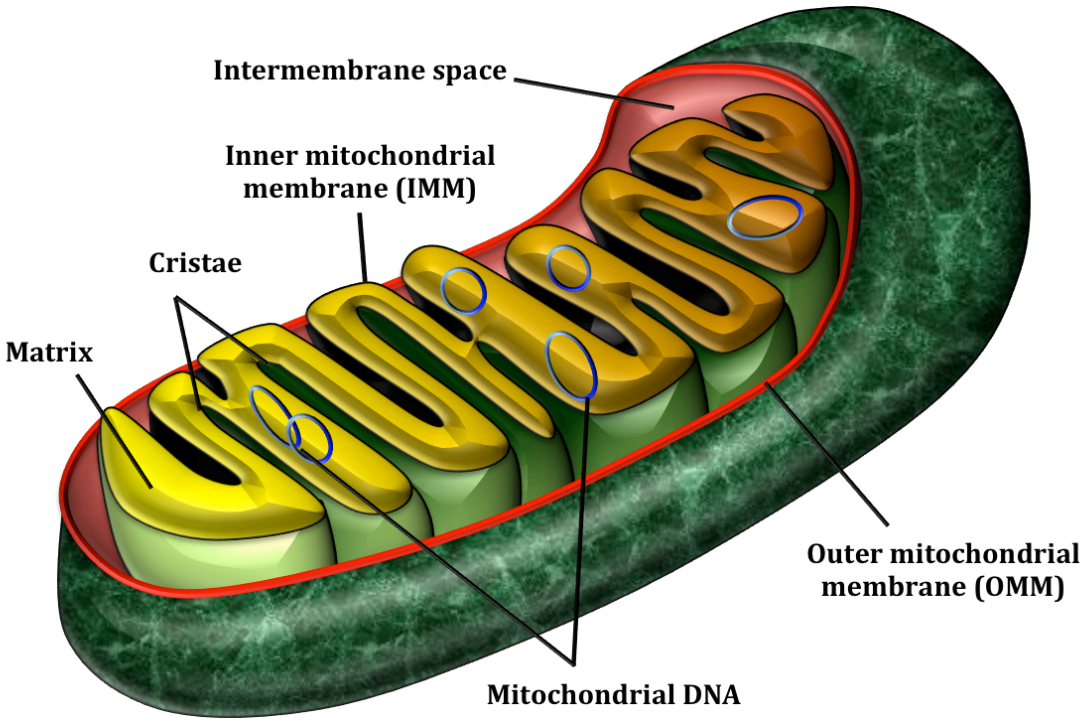

Figure I1. Mitochondrion ultrastructure. Mitochondria contain two membranes composed of phospholipid bilayers and proteins: an outer membrane (OMM) and an inner membrane (IMM). IMM, which is compartmentalized into cristae, delimits different spaces with specialised functions such as intermembrane space and mitochondrial matrix.

IMM delimits different spaces with specialised functions such as the intermembrane space (IS) and the mitochondrial matrix. IS is the space located between OMM and IMM. It is freely permeable to small molecules like ions and sugars, therefore, the composition of cytoplasm and IS is quite similar[6]. However, protein composition of IS is slightly different from cytosol because of selective transportation of proteins across the OMM. Cytochrome c is an example of protein specific for intermembrane space[13]. On the other hand, the mitochondrial matrix is the space enclosed by IMM that contains a highly concentrated mixture of enzymes, mitochondrial ribosomes, tRNA and several copies of mtDNA. Oxidation of pyruvate and fatty acid and citric acid cycle are the most relevant biochemical pathways that take place in mitochondrial matrix[6].

At functional level, apart from intracellular regulation of Ca^{+2}, thermogenesis and control of apoptosis[14,15], mitochondria play a critical role in providing most of energy supply of the cells. The generation of adenosine triphosphate (ATP) is the function *par excellence* of mitochondria and is achieved through the mitochondrial respiratory chain (MRC) (**Figure I2**).

Proteins integrated in IMM are the ultimate responsible for ATP synthesis by a metabolic pathway termed oxidative phosphorylation (OXPHOS) that is achieved by the transfer of electrons form NADH or $FADH_2$ to O_2 through MRC. MRC is comprised by 4 associated complexes (Complex I-IV) into the inner mitochondrial membrane and 1 ATP synthase (often named Complex V)[6,16]:

- Complex I or NADH:coenzyme Q oxidoreductase
- Complex II or Succinate-coenzyme Q oxidoreductase
- Complex III or Coenzyme Q-cytochrome c oxidoreductase
- Complex IV or Cytochrome c oxidase
- Complex V or ATP synthase

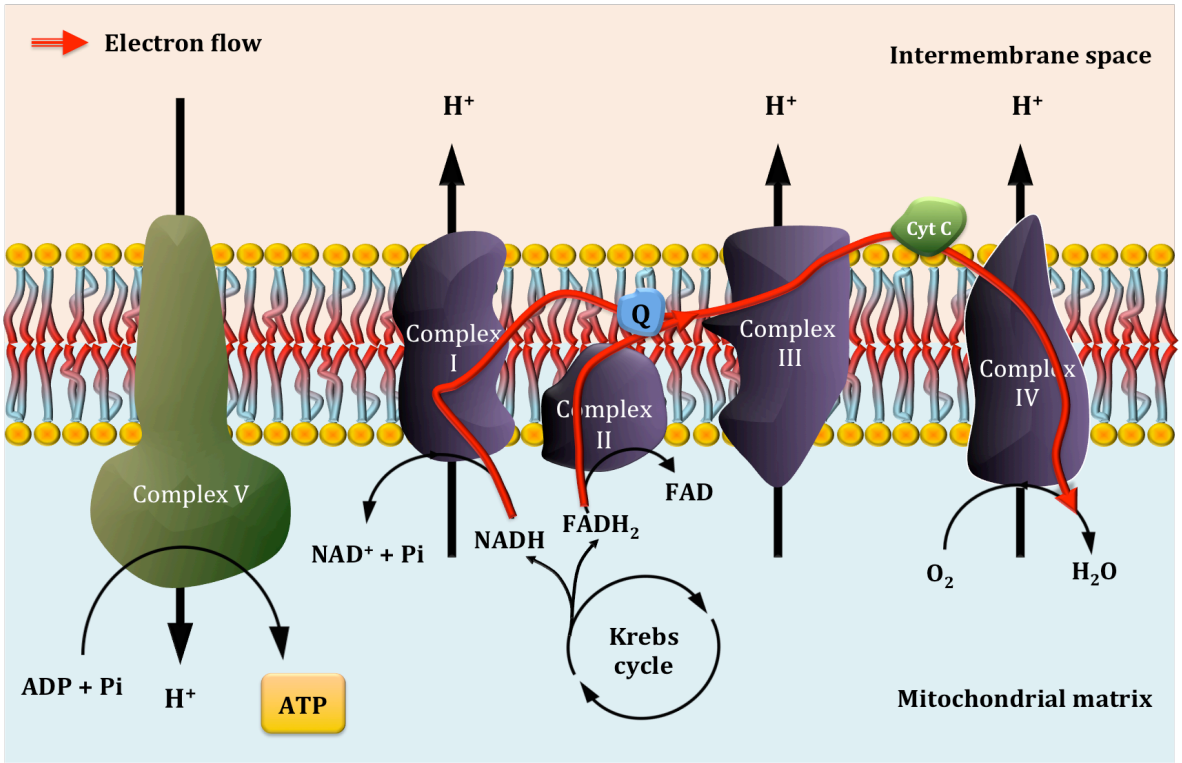

Figure I2. Mitochondrial respiratory chain (MRC). In mammals, MRC is comprised by 4 associated complexes (Complex I-IV) into the inner mitochondrial membrane and 1 ATP synthase (Complex V) in charge of oxidative phosphorylation system (OXPHOS).

Mitochondrial respiratory complexes (complexes I to IV) are responsible for the oxidation of the reducing equivalents coming through NADH or $FADH_2$ originated by different metabolic pathways (glycolysis, fatty acid oxidation or the Krebs cycle). Oxidation of NADH and $FADH_2$ is coupled to a pumping of protons into the IS resulting

in a proton gradient, which provides mitochondrial membrane potential ($\Delta\Psi_m$) that determines the polarisation degree of mitochondria. This proton gradient in mitochondria is dissipated by the ATPase (complex V) generating utilizable energy in the form of ATP.

NADH reducing equivalents enter the MRC through complex I, whereas $FADH_2$ reducing equivalents enter through complex II or other dehydrogenases such as electron-transferring-flavoprotein (ETF) dehydrogenase. The electrons are then passed to coenzyme Q_{10}, and subsequently to complex III, which passes them to cytochrome c, and this to complex IV, where are definitively transferred to oxygen as the final acceptor to generate water[17–21]. In an tightly coupled electron transport chain, approximately 1–3% of mitochondrial oxygen consumed is incompletely reduced; those "leaky" electrons can quickly interact with molecular oxygen to form superoxide anion, the predominant reactive oxygen species (ROS) in mitochondria[22–25]. Increases in cellular superoxide production have been implicated in cardiovascular diseases, including hypertension, atherosclerosis, and diabetes-associated vascular injuries[25–27], as well as in neurodegenerative diseases such as Parkinson's, Alzheimer's, and amyotrophic lateral sclerosis[22,28–31].

Mitochondrial DNA: a very particular genome

OXPHOS complexes consists of a total of 90 protein subunits, 13 of which are encoded by the mitochondrial genome, making this organelle the only location of extrachromosomal DNA within mammalian cells. Mitochondrial DNA (mtDNA) was firstly discovered in 1960s by Margit MK Nass and Sylvan Nass by electron microscopy as DNAase-sensitive threads inside mitochondria[32] and Ellen Haslbrunner, Hans Tuppy and Gottfried Schatz by biochemical assays on highly purified mitochondrial fractions[33].

Each mitochondrion is estimated to contain from 2 to 10 copies[34] of mtDNA, and its structure, genetic content and organisation are highly conserved in a large number of species. Unlike nuclear genome, mtDNA contains no introns in protein coding sequences and some codons code differently. For example, TGA codes for tryptophan instead of stop, AGA and AGG code for stop instead of arginine and ATA codes for methionine instead of isoleucin[35,36].

The mtDNA is composed by a circular double-stranded DNA molecule of 16,569 base pairs encoding 2 ribosomal RNAs (12S and 16S), 22 transfer RNAs and 13 proteins that form part of the multi subunits complexes of the OXPHOS system [7 subunits of complex I (ND1, ND2, ND3, ND4, ND4L, ND5 and ND6), 1 subunit of complex III (Cyt b), 3 subunits of complex IV (COX I, COX II and COX III) and 2 subunits of complex V (ATP6 and ATP8)]. The two strands of mtDNA are differentiated by their nucleotide content, with a guanine-rich strand referred to as the heavy strand (H-strand) and a cytosine-rich strand referred to as the light strand (L-strand). The H-strand encodes for 28 genes (for the 2 rRNAs, 12 of the polypeptides and 14 of the tRNAs), whereas the L-strand encodes for 9 genes (only one of the polypeptides (ND6) and 8 transfer RNAs). All the remaining MRC subunits, including the whole Complex II, are encoded

by nuclear genes. Therefore, mitochondrial function depends on the coordination of both nuclear and mitochondrial genomes[16,35,36] (**Figure I3**).

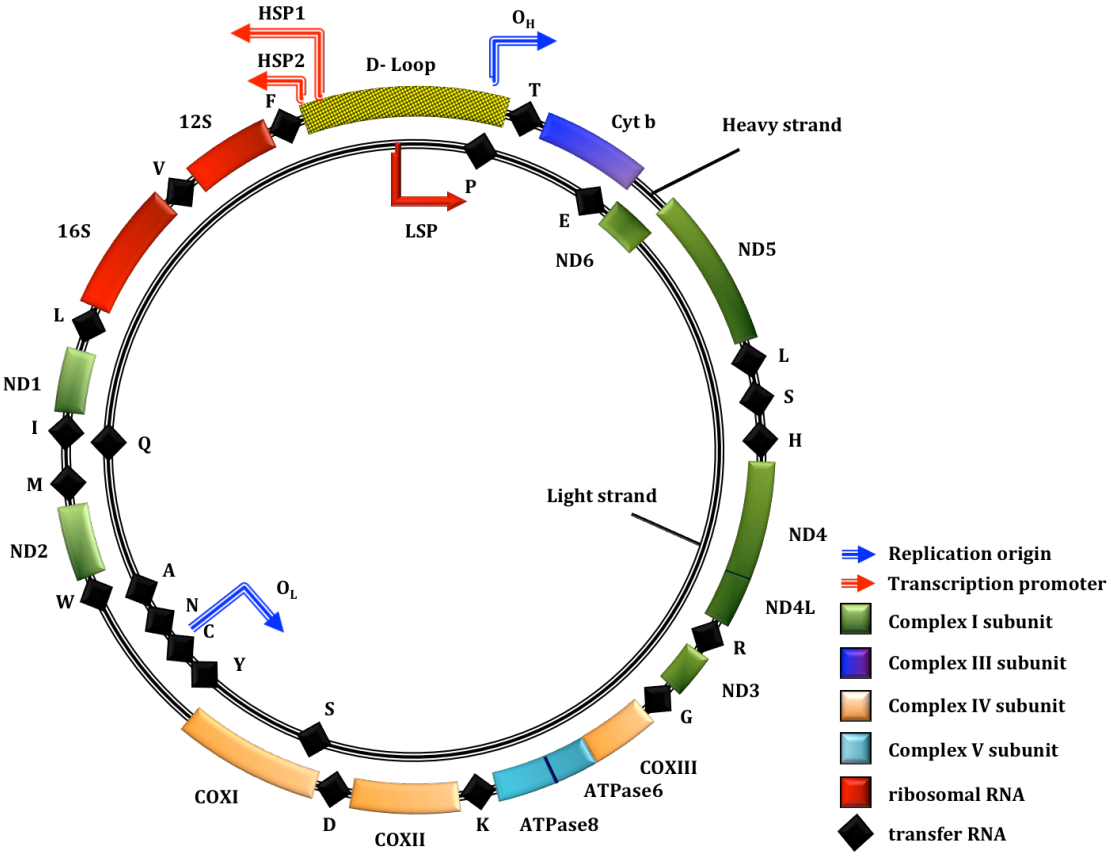

Figure I3. Mitochondrial DNA structure. The mtDNA is composed by a circular double-stranded DNA molecule of 16,569 base pairs encoding 2 ribosomal RNAs, 22 transfer RNAs and 13 proteins of the multi subunits complexes of the OXPHOS system. Replication of mtDNA starts from replication origins (O_H and O_L). Heavy strand has 2 transcription promoters (HSP1 and HSP2) and light strand only one (LSP).

Recent studies have demonstrated how mtDNA is associated with several proteins by forming packed structures denominated nucleoids. The mitochondrial transcription factor A (mtTFA), polymerase γ (Polγ), helicase TWINKLE, the mitochondrial single-strand binding protein (mtSSB), the E2 subunit of pyruvate dehydrogenase and a-ketoglutarate dehydrogenase, aconitase and some cytoskeletal proteins seem to bind mtDNA and anchor it to the inner mitochondrial membrane[37].

The mtDNA replication is closely linked to the transcription because of the first RNA sequence synthesised by the mitochondrial RNA polymerase (POLRMT) in the light-strand promoter (LSP) serves as an RNA primer to initiate DNA replication at the origin of replication of the heavy-strand (O_H) located in the displacement loop (D-loop)[38]. The mtDNA replication is carried out by POLγ assisted by TWINKLE that unwinds the DNA duplex, and by mtSSB proteins that keep the DNA in a single stranded form. Currently, there are two proposed models for DNA replication: i) a

unidirectional and asynchronous replication that starts at O_H and proceeds displacing the parental heavy strand until it reach the origin of replication of the other strand (O_L) to start again now in the opposite direcction[39,40]; and ii) a coupled replication of both leading and lagging strands[41].

The mechanism of mtDNA transcription is similar to bacteria. It starts from the promoters present in each strand (HSP and LSP) producing polycistronic RNAs. In the HSP there are two sites of initiation, the H_1 site, that produces a short transcript containing the 12S RNA, 16S RNA and the $tRNA^{leu}$, and the H_2 site, that produces a polycistronic transcript of the length of the full genome. However, in the LSP there is only one initiation site, L_1[42–44]. The transcription is carried out by the before commented POLRMT assisted by mtTFA that recruits POLRMT to the promoter site and by mitochondrial transcription factor B1 or B2 (mtTFB1 and mtTFB2). The termination of transcripts seems to be dependent on the mitochondrial transcription terminator factors (mtTERM)[45].

In spite of components responsible for the proper mitochondrial translation are different from their cytosolic counterparts and they are more related to those of bacteria, the mechanisms of the translation follows the same major steps: initiation, elongation, termination and recycling of the ribosome[44,46]. Translation of the polycistronic transcript involves the participation of mitochondrial ribosomes, or mitoribosomes[47], initiation factors (mtIF)[48], elongation factor (mtEF-Tu, mtEF-Ts and mtEF-G1)[49] and protein related with ribosome recycling (mtRRF and EF-G2mt)[50].

Mitochondrial turnover

Mitochondria forms a complex, interconnected, and highly dynamic network that is maintained by the continuous opposing and counterbalanced events of mitochondrial fusion and fission[51,52], which have as main role to share genome and matrix contents to maintain mitochondrial homeostasis. Defective energy functioning, low yield or aged proteins in mitochondria induce the dissipation of $\Delta\Psi_m$, a signal that triggers selective elimination of mitochondria or mitophagy. Mitochondrial fission and fusion serve as a quality control mechanism or turnover to preserve healthy mitochondria via fusion, and eliminate dysfunctional mitochondria via fission and subsequent mitophagy. The dynamic nature of mitochondria protects these organelles by ensuring that regional losses of membrane potential are always transient. In particular, when mitochondrial damage is still considered mild, defective mitochondria can be rescued by fusion with the healthy network[53,54] and therefore, restored local depletions to maintain the whole mitochondrial function[55]. This continuous turnover occurs during mitochondria life cycle (about 9-25 days)[56] (**Figure I4**).

Fission-related proteins are dynamin-like protein 1 (Drp1) and Fis1. Drp1 is a member of the conserved dynamin large GTPase superfamily that controls membrane fission, existing constitutively in a cytosolic pool and being recruited to specific points of the OMM supposed to be future fission sites. The putative mechanistic action of Drp1 on mitochondrial membrane relies on the formation of a ring-like complex

structure within the mitochondrial surface that constricts the organelle upon the hydrolysis of GTP, initiating fission[57]. Fis1 is a mitochondrial outer membrane protein suggested to act as a receptor for Drp1[58], which lacks a mitochondrial target sequence. As result of mitochondrial fission, two spherical mitochondria arise[59,60]. The process of mitochondrial fission usually occurs in all cells in normal conditions. However, mitochondrial fission has mainly been associated with conditions of metabolic stress[61] as well as autophagy[53] and apoptosis[62].

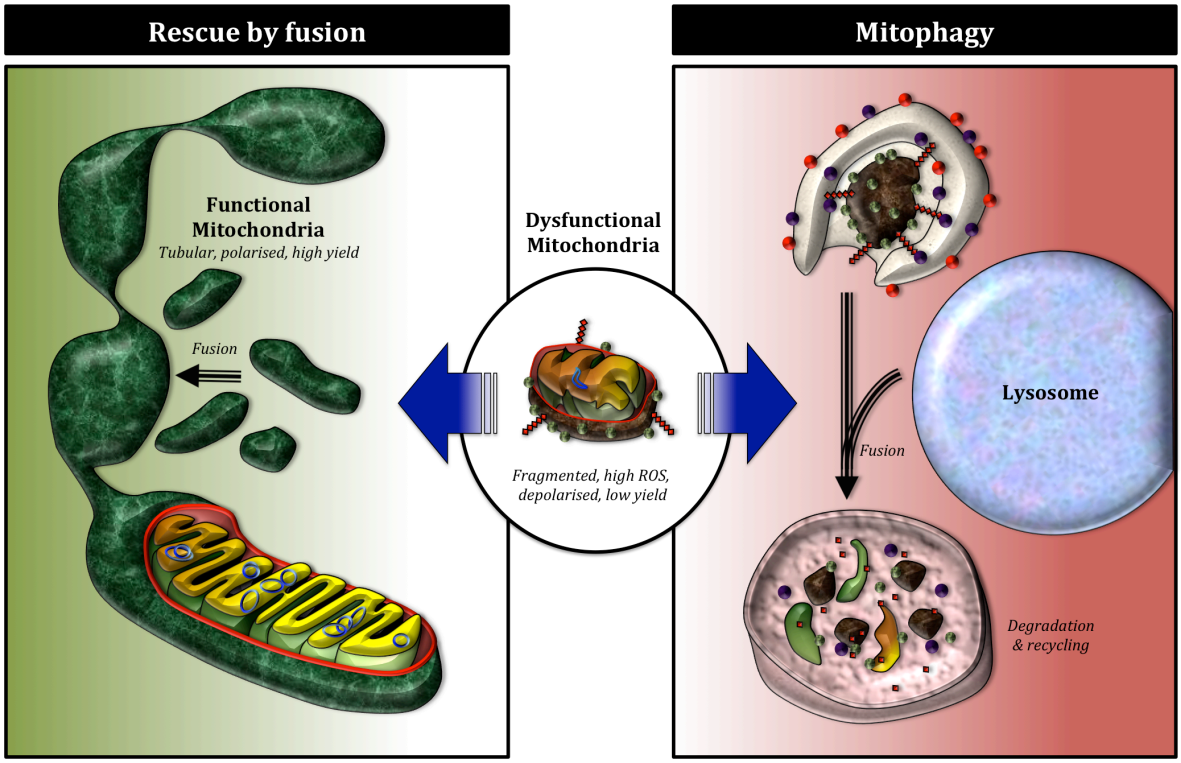

Figure I4. The fate of dysfunctional mitochondria. Defective mitochondria can be functionally restored by mitochondrial fusion or removed by selective degradation. When mitochondrial damage is still considered mild, defective mitochondria can be rescued by fusion with the healthy network. However, severe damage in mitochondria triggers mitophagic pathway.

The main regulators of mitochondrial fusion in humans are the mitofusin proteins (Mfn1 and Mfn2) and the optic atrophy-1 protein (OPA1), three large GTPase proteins that assume different functions and ultrastructural locations. For the fusion of the outer membrane to occur, Mfn1 and Mfn2 interact by their coiled-coil domains, forming homo- and heterooligomeric complexes, connecting the mitochondrial outer membranes of close mitochondria[63,64]. Whereas Mfn1 and Mfn2 interact with each other to coordinate fusion of the OMM, OPA1 participates in the remodelling of the mitochondrial crests and the approach and fusion of the IMM[65,66], requiring Mfn1, but not Mfn2, to mediate this process[67]. Several studies have associated low mitochondrial ATP levels, dissipation of the membrane potential across the inner membrane, or apoptotic stimuli with OPA1 cleavage[68] resulting in the loss of long isoforms and impairing mitochondrial fusion[69–72] (**Figure I5**).

Both mitochondrial fusion and fission have a crucial role by removing defective mitochondria in order to maintain cellular homeostasis. Apart from fusion/fission processes, mitophagy and mitochondrial biogenesis also play crucial roles in mitochondrial turnover of the cell in order to maintain a proper mitochondrial mass for energy production[36].

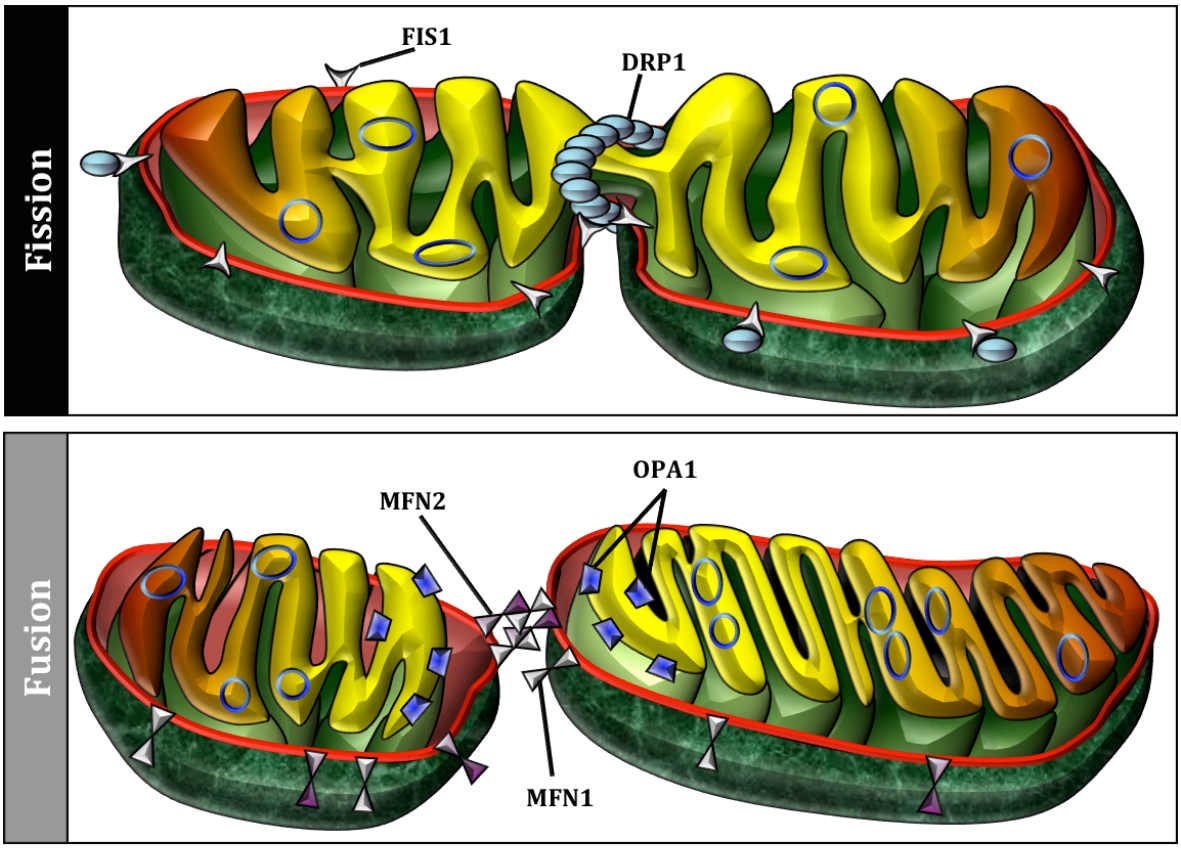

Figure I5. Mitochondrial fission and fusion. Mitochondria forms a dynamic network that is maintained by the continuous opposing and counterbalanced events of mitochondrial fission and fusion. In the process of fission, Drp1 subunits, which are targeted to the mitochondrial surface by Fis1 receptor, form a ring-like complex structure that constricts and splits the organelle. During fusion, Mfn1 and Mfn2 interact with each other to coordinate fusion of the OMM and OPA1 participates in the remodelling of the mitochondrial crests and the approach and fusion of the IMM.

Mitophagy: selective degradation of mitochondria

As commented above, mitochondria are involved in pivotal roles such as energy supply and cellular homeostasis. Therefore, impaired mitochondrial quality control and accumulation of damaged mitochondria can generate high levels of ROS[73] into the cell, produce ATP inefficiently[74], release cytochrome *c* resulting in apoptosis[75], undergo mitochondrial permeability transition pore (MPTP) opening resulting in necrosis[76], or release mitochondrial components (mtHSP60, oxidized

mitochondrial DNA) into cytosol where its recognition by receptors for damage-associated molecular patterns (DAMP) activates inflammation[77]. Therefore, proper maintenance of a healthy population of mitochondria is vital to ensure an efficient energy supply into the cells. This is particularly interesting since OXPHOS leads to oxidative damage to mitochondrial proteins over time[78] and unbalances between nuclear and mitochondrial biosynthesis of respiratory chain subunits can generate futile protein overprovision. Mitochondria contain proteases responsible for protein quality control[79] and for degradation of proteins via the proteasome[80]. However, this system is not sufficient for rapid removal of whole dysfunctional mitochondria. To address this matter, cells rely on a selective autophagy-based system in order to eliminate damaged mitochondria, mitophagy.

Selective degradation of mitochondria or mitophagy is a complex process that shares elements and mechanisms of general autophagy, which was first observed in mammalian cells by early electron microscopy studies in 1962[81]. The term "mitophagy" was coined later to describe the engulfment of mitochondria into vesicles that are coated with the marker microtubule associated light chain 3 (LC3)[82]. In mammals, the double membrane in charge of engulf mitochondria is thought to develop from a pre-existent structure known as phagophore which can derive from the plasma membrane[83], the endoplasmic reticulum (ER)[84], the trans Golgi network[85], or even mitochondria[84].

The different steps of autophagy are regulated by over 30 autophagy-related (Atg) proteins[86,87]. The formation of autophagosomes undergoes a multistep process of nucleation to form the phagophore. During the vesicle nucleation process, two kinases are involved: i) the Ser/Thr protein kinase mammalian target of rapamycin (mTOR), with an inhibitory action on autophagy and being negatively modulated by rapamycin; and ii) the Class III phosphatidylinositol 3-kinase (Class III PI3K) complex, composed of three proteins, the protein kinase vacuolar protein sorting 15 (Vps15), the phosphatidylinositol 3-kinase Vps34, and a modulatory component named Beclin 1/Atg6, with a positive modulatory action on autophagy and being negatively modulated by 3-methyladenine[88,89].

The assembly of autophagosomes requires two evolutionarily conserved ubiquitin-like conjugation systems of Atg proteins[90]: i) Atg12-ATG5 and Atg16 are one of the conjugation systems and the other ii) is composed by lipidated LC3 (LC3-II), the mammalian homologue of yeast Atg8[91]. The autophagy process starts by the recruitment and transient association of the conjugated protein At12-Atg5 conjugated into a precursor vesicle (LC3-II) that elongates along the perimeter of the mitochondrion until both ends fuse forming the double membrane of the autophagosome. Despite the relevance of these proteins in the autophagic process, a recent work demonstrated the existence of an alternative process, independent of Atg5, in which the lipidation of LC3 to form LC3-II does not occur and is regulated by several autophagic proteins including ULK1 and Beclin1[92]. Once the autophagosome is completely formed, it matures through the dissolution of the inner membrane and fusion with lysosomes to form the autolysosome, where cargo is degraded through the action of hydrolases, and macromolecules release[93]. This fusion process of the

autophagosome to the lysosomes can be inhibited by bafilomycin A1[94] . On the other hand, in order to facilitate and initiate mitophagy, mitochondrial dynamics (fusion and fission) play a critical role in mitochondrial turnover, favouring fission and suppressing fusion, enabling engulfment by autophagosomes. As before commented, fission of reticulate mitochondria into smaller fragments is a crucial requirement for mitophagy to occur[53]. Otherwise, fusion-related proteins like mitofusin and OPA-1 are degraded by the UPS and mitochondrial proteases during mitophagy, respectively[95,96] (**Figure I6**).

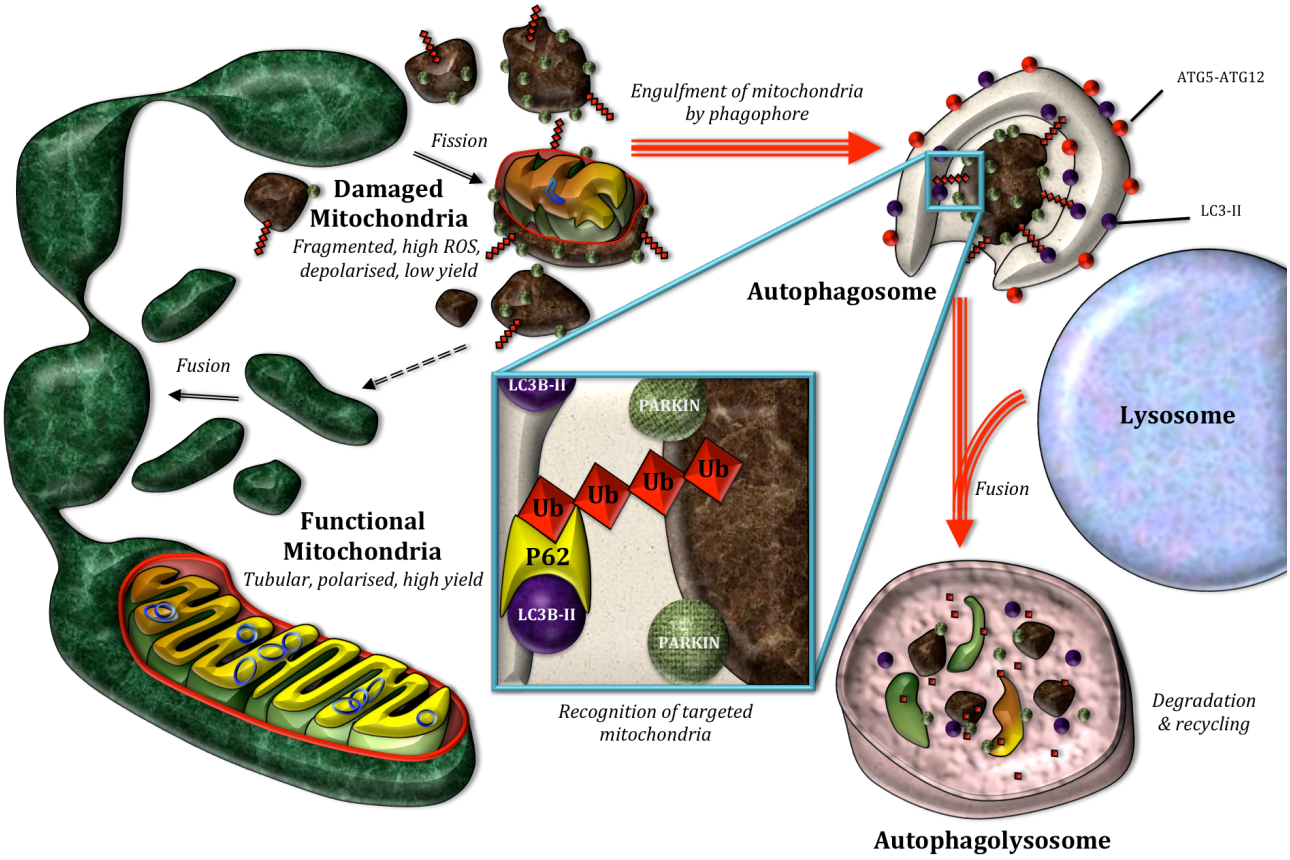

Figure I6. Selective degradation of mitochondria. Inefficient mitochondria are targeted to degradation by mitophagy. The phosphorylation of outer membrane proteins such as VDAC or Mfn1/2 leads to their ubiquitination by Parkin. The fission machinery separates the dysfunctional mitochondrion from the network, and the ubiquitinated proteins serve as binding sites for autophagy adaptor proteins such as p62. These proteins contain LC3 binding sites, leading to encapsulation of the organelle in an autophagic vesicle, which is delivered to the lysosome for degradation.

Different theories have reported evidences for unravelling the triggers involved in mitophagy activation[53,97,98]. Overall, all of them seem to suggest that the induction of mitophagy is triggered by energy deficiency following by the depolarization of mitochondria and PTP opening[76]. Importantly, coenzyme Q_{10} deficiency in human fibroblasts was shown to be associated with decreased efficiency in the electron transport chain, decreased $\Delta\Psi_m$, increased ROS production, and susceptibility to PTP

opening, and these features strongly correlate with increased expression of autophagy-related genes, lysosomal markers, and mitophagy[99–101].

One of the best-characterized pathways of mitochondrial labelling depends on mitochondrial membrane potential. Mitochondrial depolarisation results in stabilization of the serine/threonine kinase phosphatase and tensin homolog (PTEN)-induced kinase 1 (PINK1) on the outer mitochondrial membrane. PINK1 is constitutively made and continuously degraded by the mitochondria-specific proteases presenilin-associated rhomboid-like protein (PARL) and mitochondrial processing peptidase (MPP). These proteases are inactivated by the loss of membrane potential resulting in the accumulation of PINK1 on the OMM where it can phosphorylate the OMM proteins and facilitates the recruitment of several proteins[102,103]. One of these proteins is the E3 ubiquitin ligase Parkin, whose recruitment allows the attachment of ubiquitin tags to OMM proteins[104–107]. The targets of PINK1 include Parkin itself[107], mitofusin 2 (Mfn2)[108], mitochondrial rho 1 (MIRO)[109] and voltage-dependent anion channel 1 (VDAC1)[110]. In addition, the presence of ubiquitin tags on those proteins facilitates recruitment of autophagy adapter proteins such as neighbor of BRCA1 (NBR1) or sequestosome-1 (p62/SQSTM1). These adaptor proteins have an ubiquitin binding domain (UBA) and a LC3-interacting region (LIR) which serves as an anchor for the developing autophagosomal membrane in proximity to the tagged mitochondrion in a zipper-like process[111,112]. Recently, other two possible actors in Parkin-dependent mitophagy seems to come to light: SMAD-specific E3 ubiquitin ligase 1 (SMURF1)[113] and Beclin 1-regulated autophagy (Ambra1)[114]. Ambra1 seems to dissociate from mitochondrial Bcl-2 to bind Beclin1 to initiate autophagy[115]. Furthermore, recent studies seem to indicate a novel mode of Parkin activation by PINK1, through the phosphorylation of ubiquitin at its Serine 65 residue ($ubiquitin^{Phospho-Ser65}$)[116,117].

On the other hand, Parkin-independent mitophagy can be triggered through proteins such as BCL2/adenovirus E1B 19 kDa protein-interacting protein 3 (BNIP3) and BNIP3-like protein (BNIP3L aka NIX). These proteins insert into the OMM and facilitate engulfment by the double membrane through LIR domains that interact with LC3 isoforms (GABARAP)[118,119]. Mitophagy can also be initiated by Bnip3, which seems to recruit Drp1 to mitochondria to promote fission[120], and FUN14 domain containing 1 (FUNDC1), which contains a LIR domain that can interact with LC3[121].

Moreover, mTOR is also an essential autophagy regulator. Amino acid starvation, growth factor deprivation, the drop of ATP or oxygen levels, and accumulation of ROS trigger autophagy pathway through the participation of mTOR[122–125]. ATP depletion either due to glucose starvation or mitochondrial dysfunction can activate AMP-activated protein kinase (AMPK) which can inhibit the mTOR complex, and phosphorylate ULK1 to activate autophagy[126–128]. Apart from ULK1 activation, downstream of mTOR inhibition, autophagy is activated by VPS34 activation[129], as well as transcription factor EB (TFEB) activation[130].

Finally, in order to monitor autophagic activation one of the most direct methods is the detection of LC3 processing by Western blot analysis and the detection of

autophagosome formation by fluorescence and electron microscopy[131]. LC3 proteins are specifically cleaved at the C terminus by Atg4 to become LC3-I. Once cleaved, LC3-I is lipided by conjugation to phosphatidylethanolamine (PE) to form LC3-II[131], which is degraded in autolysosomes. Thus, the level of LC3-II is widely used as a marker for monitoring the autophagic process[132]. However, it is necessary to consider that autophagy is a highly dynamic process and an accumulation of LC3-II signal is not always indicative of increased autophagy. In fact, the accumulation of autophagosomes could indicate autophagic activation, but also an inefficient fusion with lysosomes or blockage in autophagosome maturation[132,133]. Therefore, the analysis of the number of autophagosomes or the presence of LC3 processing is insufficient for evaluating the whole autophagic process. To address this matter, the term "autophagic flux" is particularly used to include the whole process of autophagy: autophagosome formation, maturation, fusion with lysosomes, subsequent breakdown and the release of macromolecules back into the cytosol. Interestingly, impaired autophagic progress has been involved in a growing list of pathologies, including neurodegeneration, cancer, myopathy, cardiovascular diseases and immune-mediated disorders[134]. To measure autophagic flux, LC3-II signal must be detected in the presence and absence of lysosomal degradation inhibitors (pepstatin A, E64d, bafilomycin A1, chloroquine or NH_4Cl[135,136]), which are able to block the degradation of autophagosome and, hence, of LC3-II[137]. Whereas an extra accumulation of LC3-II in presence of autophagic flux inhibitors suggests autophagic induction and proper autophagic flux, the absence of any increase could indicate autophagic flux blockage.

Mitochondrial biogenesis

The cellular control on adaptive changes in the mitochondrial content requires a capacity to sense the need for additional mitochondrial energy production, followed by triggering of signalling pathways that culminate in an increased and coordinated expression of respiratory genes. The activation of mitochondrial biogenesis (defined as the growth and division of pre-existing mitochondria) needs to be orchestrated by the subtle regulation of both nuclear and mitochondrial biosynthetic pathways. The most important regulatory steps of mitochondrial biogenesis appear to take place at the level of transcriptional regulation of nuclear genes[138,139], but coordinated transcription of mitochondrial genome is also required to produce new mitochondria[140].

Despite the complexity of the various signalling pathways that converge to regulate mitochondrial biogenesis, they all seem to share the common key component of the PGC-1 family of co-transcription factors, PGC-1α (**Figure I7**). PGC-1α seems to act as a master regulator of energy metabolism and mitochondrial biogenesis[141] by coordinating the activity of multiple transcription factors such as the NFRs or mtTFA. NRF-1 and NRF-2 are important contributors to the sequence of events leading to the increase in transcription of key mitochondrial enzymes, and they have been shown to interact with mtTFA, which drives transcription and replication of mtDNA[142]. Significant evidences indicate that PGC-1α co-actives the transcriptional function of

NRF-1 on the promoter for mtTFA[143]. In addition to NRFs, PGC-1α also interacts with and co-activates other transcription factors such as PPARs, thyroid hormone, glucocorticoid, oestrogen and ERRs (oestrogen-related receptors) α and γ[144]. Otherwise, PGC-1β, in spite of sharing a similar molecular structure and function with PGC-1α (transcriptional activation of mitochondrial biogenesis), is not up-regulated in the same way[145]. This suggests that PGC-1α and PGC-1β are stimulated independently, although both clearly regulate mitochondrial biogenesis through NRF-1 to enable mitochondria to meet the energetic requirements of the cell.

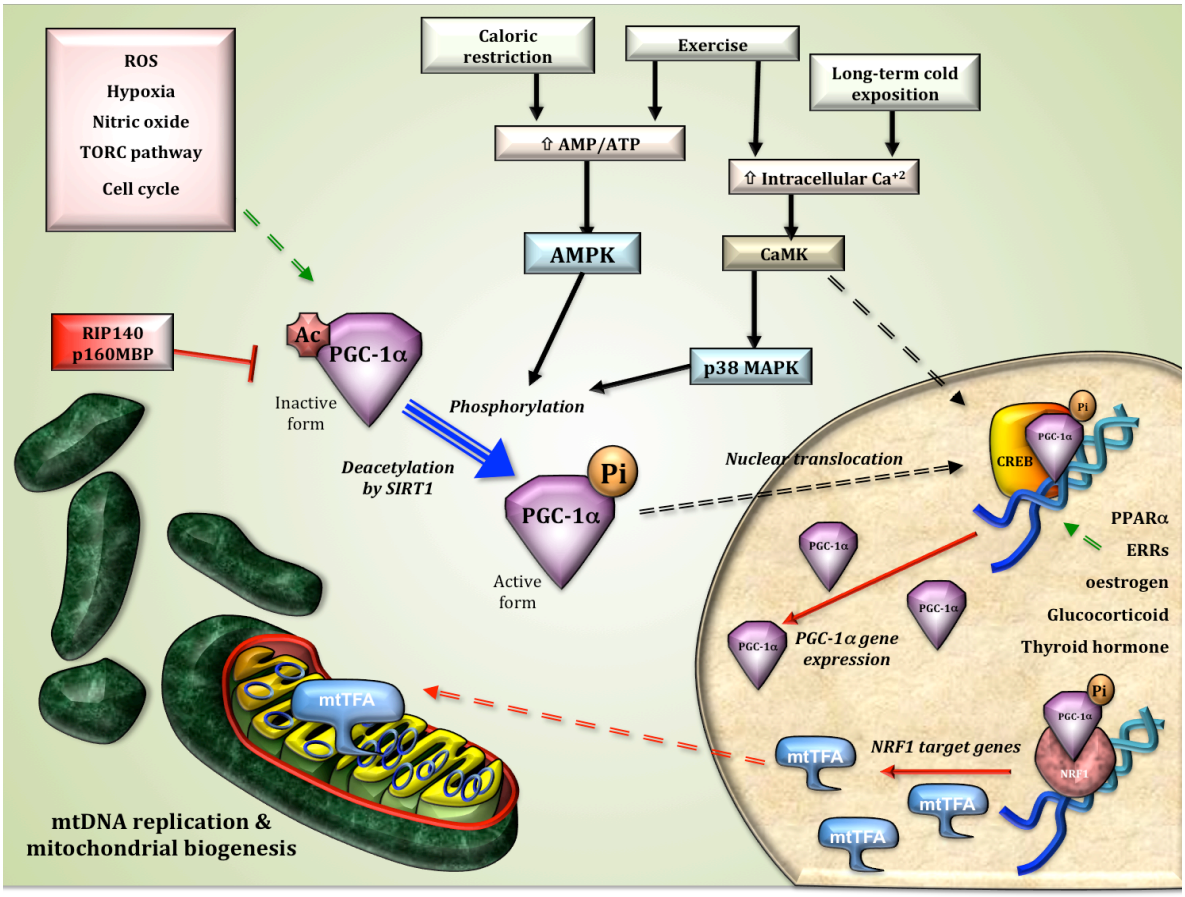

Figure I7. Mitochondrial biogenesis pathway. The activation of mitochondrial biogenesis needs to be orchestrated by the subtle regulation of both nuclear and mitochondrial biosynthetic pathways. Both nuclear and mitochondrial pathways share a common key component PGC-1 alpha that acts as a master regulator of energy metabolism and mitochondrial biogenesis by coordinating the activity of multiple transcription factors such as the NFRs or mtTFA.

As a multi-responsive factor, many agents and events can regulate the activation of PGC-1α by different intracellular mediators. Mitochondrial biogenesis is increased, among other factors, by endurance exercise and caloric restriction[146]. Several observations in different animals unravelled the role of exercise in mitochondrial biogenesis activation[147,148] and further studies in humans confirmed these results later[149–151]. In skeletal muscle, endurance exercise induces an increase in mitochondrial mass that is mediated by the increase in intracellular calcium levels

during fiber contraction[152]. Furthermore, increased levels of intracellular calcium activates cytoplasmic protein kinases such as protein kinase C (PKC) or calcium/calmodulin-dependent protein kinase (CaMK) that in turn stimulate the expression of several nuclear and mitochondrial genes[153]. The activation of CaMK occurs upstream of the activation of p38 mitogen-activated protein kinase (p38 MAPK), which is responsible for phosphorylating, activating and inducing PGC-1α expression[154,155]. In addition to p38 MAPK, other kinases like AMP-activated protein kinase (AMPK) can directly bind and phosphorylates PGC-1α[156]. The induction of PGC-1α expression is also mediated through ATF-2 (activating transcription factor 2) that binds to the PGC-1α promoter in the CREB (cyclic AMP-response binding protein) element binding site[157,158]. TORCs proteins seem to be related with the induction of PGC-1α and its downstream target genes in the mitochondrial respiratory chain and TCA (tricarboxylic acid) cycle (Krebs cycle)[159]. In addition to phosphorylation, another post-translational modification that regulates PGC-1α activity has been identified. Specifically, deacetylation mediated by SIRT1 during fasting promotes the expression of mitochondrial genes involved in lipid oxidation[160].

Apart from endurance exercise and intracellular calcium signalling, recent evidences relate mitochondrial biogenesis with changes in cell cycle. Indeed, the mitochondrial mass and membrane potential increased during the progression of G1 to mitosis and after cell division these parameters were reduced again. The levels of mtDNA also increased in G1/S to G2 transition concomitant with increase of NRF-1 levels[161]. Moreover, mitochondrial biogenesis, can also be stimulated by other pathways like ROS[162], nitric oxide (NO)[163] and hypoxia[164], which can be caused by ischemic insults or mitochondrial disorders. In fact, mitochondrial biogenesis is stimulated in mitochondrial disorders[165,166] and commonly observed as abnormal mitochondrial proliferation in muscle[165].

On the other hand, exposure of mammals to low-temperature environment for prolonged periods of time induces a marked increase in mitochondrial mass in brown adipocytes, originating an important control mechanism to maintain body energy balance and core temperature[167]. More recently, the control of PGC-1α expression by CaMK IV and the protein phosphatase calcineurin A (CnA) in muscle cells has been investigated, and it has been reported that the PGC-1α promoter is subject to positive regulation[168,169].

In contrast to the growing list of PGC-1α-activating factors identified to date, little is known about cellular factors that act as negative regulators. One of these negative regulators could be RIP140, which has been proposed as suppressor of mitochondrial biogenesis and oxidative metabolism in mammalian cells[170–172]. Moreover, PGC-1α also contains a negative regulatory domain that attenuates its transcriptional activity, and the p160 myb binding protein (p160MBP) acts as a repressor of PGC-1α by binding to this regulatory region. This interaction is further regulated by p38 MAPK, which phosphorylates the inhibitory domain of PGC-1α, efficiently disrupting p160MBP-binding and releasing PGC-1α from its inhibition[173]. In summary, the confluence of several activating and repressing pathways on PGC-1α affects the

complex system that coordinates the demand of energy in the cell with mitochondrial biogenesis.

Finally, there are evidences of nuclear PGC-1α translocation when it is phosphorylated and hence activated by other proteins as Protein kinase A (PKA). It seems that PGC-1α is a protein whose subcellular localization is in the nucleus but is permanently interacting with nuclear transporters like CRM1 in order to be exported to the cytoplasm. Phosphorylation of PGC-1α by PKA prevents nuclear export and increases PGC-1α in the nucleus[174]. Therefore, the subcellular localization seems to have great importance for the functional activation of pathways like mitochondrial biogenesis.

AMPK pathway

As commented in previous sections, another important pathway involved in both mitochondrial biogenesis and mitophagy, is AMP-activated protein kinase (AMPK) pathway. AMPK plays a key role as a master regulator of cellular energy homeostasis. The kinase is activated in response to stresses that deplete cellular ATP supplies such as low glucose, hypoxia, ischemia, and heat shock. This kinase is essentially expressed in all eukaryotic cells as a heterotrimeric complex containing a catalytic α subunit and two regulatory subunits (β and γ subunits). AMPK activity is regulated by phosphorylation of Threonine 172 in α subunit. This phosphorylation is allosterically regulated by AMP binding to CBS/Bateman domains in γ subunit, which are able of binding adenine nucleotides[175,176]. Binding of AMP to the γ subunit enables the phosphorylation on Thr[172] in the activation loop of the α subunit by its major upstream AMPK kinase, LKB1[177]. Importantly, AMPK can also be phosphorylated on Thr[172] in response to calcium flux, independently of LKB1, via CAMKK2 kinase[178]. The activation of AMPK depends on intracellular adenosine nucleotide levels (AMP/ATP ratio). High AMP or ADP levels, or even modest decreases in ATP production, result in activation of AMPK[179,180]. Once activated, AMPK positively regulates signalling pathways that replenish cellular ATP supplies, including fatty acid oxidation and autophagy. Likewise, AMPK negatively regulates ATP-consuming biosynthetic processes including gluconeogenesis, lipid and protein synthesis. AMPK accomplishes this through direct phosphorylation of a number of enzymes directly involved in these processes as well as through transcriptional control of metabolism by phosphorylating transcription factors, co-activators, and co-repressors[181].

In conditions where nutrients are scarce, AMPK acts as a metabolic checkpoint inhibiting cellular growth. One of the mechanism by which AMPK regulates cell growth is via suppression of the mammalian target of rapamycin complex 1 (mTORC1) pathway. AMPK directly phosphorylates Raptor (regulatory associated protein of mTOR) which blocks the ability of the mTORC1 kinase complex to phosphorylate its substrates[182,183]. Consistent with this negative function of AMPK in mTORC1 signaling, AMPK positively regulates autophagy in mammalian cells[184,185]. In addition, AMPK also phosphorylates and inhibits some family members of the class IIa family of histones deacetylases (HDACs)[186,187]. Normally, class IIa HDACs regulates the activity of FOXO family transcription factors, stimulating their de-acetylation and

activation, increasing expression of gluconeogenesis genes[188]. Therefore, a proper activation of AMPK can suppress glucose production by reducing the expression of FOXO target genes via class IIa HDAC inactivation[181]. Moreover, AMPK has also been shown to regulate the activity of other deacetylases like SIRT1[189,190]. As SIRT1 targets a number of transcriptional regulators for deacetylation, this adds yet another layer of temporal and tissue specific control of metabolic transcription by AMPK. Altogether, there seem to be that AMPK is able to induce a metabolic reprogramming, which requires PPARβ/δ[191] and likely involves PGC-1α as well[156] (**Figure I8**).

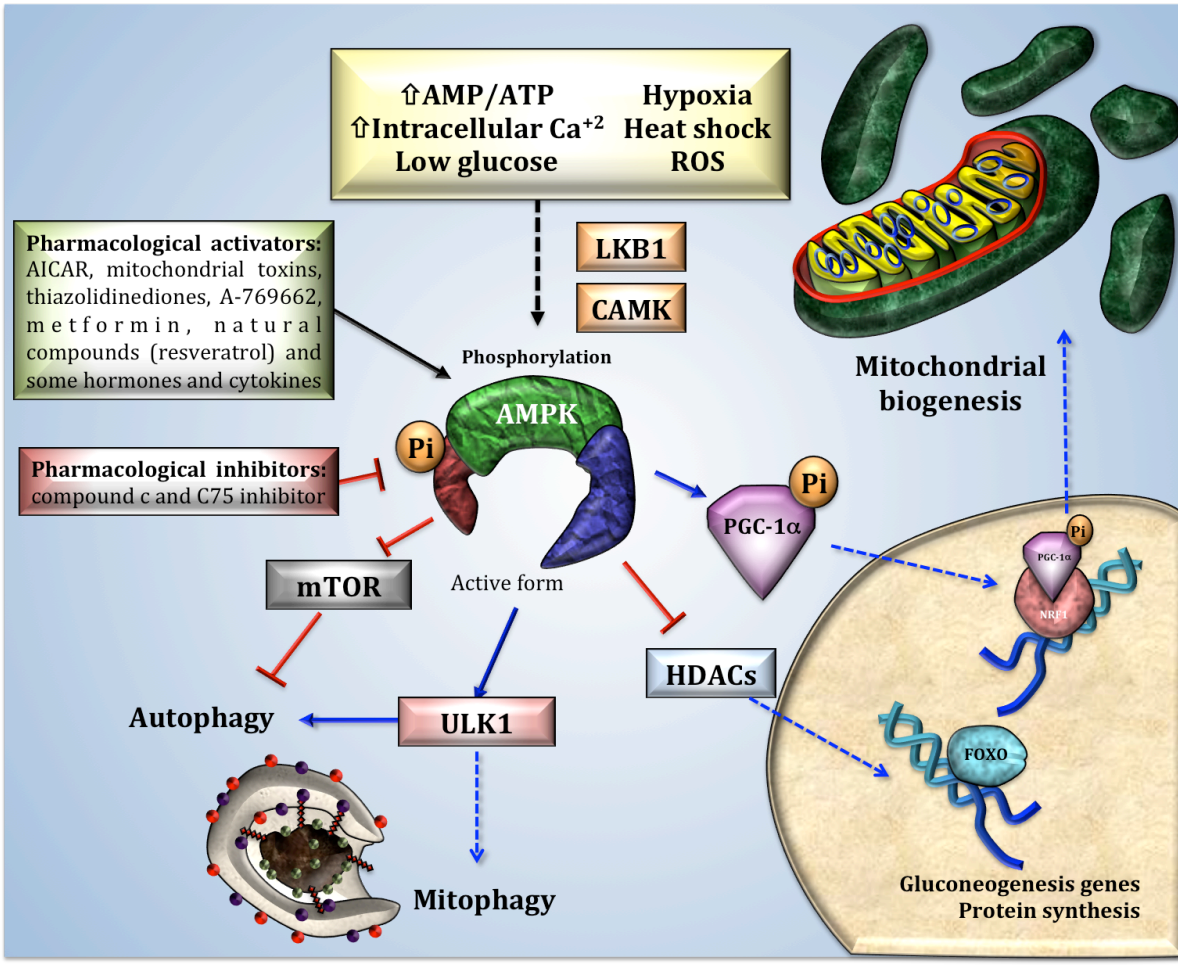

Figure I8. AMPK pathway. AMPK is a mater regulator that controls mitochondrial homeostasis by regulating mitochondrial biogenesis and selective degradation of defective mitochondria.

On the other hand, it has been reported that AMPK can be activated by reactive oxygen/nitrogen species (ROS/RNS), which in turn lead to the increase of glycolysis and mitochondrial biogenesis. While ROS are normally produced in the normal cellular respiration, high levels are cytotoxic. ROS are mainly produced as a result of mitochondrial dysfunction[192–198]. Ultraviolet (UV) irradiation, hydrogen peroxide (H_2O_2), nitric oxide (NO) and peroxynitrite ($^{\cdot}ONOO^-$) have been demonstrated to active AMPK in several human cell lines[199–202]. Therefore, high ROS production and the

activation of ROS sensor proteins as AMPK are required for the activation of the defensive anti-ROS system[203].

In addition to regulating cell growth and reprograming the metabolism, AMPK seems to play a key role to control autophagy. In contrast to inhibitory phosphorylation from mTORC by AMPK commented before, the ULK1 complex is activated via direct phosphorylation by AMPK[204,205], which is critical for its function in autophagy and mitochondrial homeostasis[206]. In fact, the lack of either AMPK or ULK1 result in defective mitophagy and elevated levels of p62[204] suggesting that ULK1 is definitively required for cell survival and autophagy. In addition, mTOR also seems to phosphorylate ULK1 which appears to manage AMPK binding to ULK1[207]. Collectively, these studies show that AMPK can trigger autophagy in a double mechanism of directly activating ULK1 and inhibiting the suppressive effect of mTORC1 on ULK1[181]. Moreover, recently it has been reported that AMPK-dependent phosphorylation of ULK1 is critical for translocation of ULK1 to mitochondria and for mitophagy in response to hypoxic stress[208]. Therefore, AMPK seems to enhance a subtle degradation of defective mitochondria through an ULK1-dependent stimulation of mitophagy, as well as stimulating de novo mitochondrial biogenesis through PGC-1α dependent transcription. Thus, AMPK controls mitochondrial homeostasis concomitant with selective degradation of defective mitochondria[181] (**Figure I8**).

Given the functional knowledge of AMPK, a growing list of different drugs have been identified to date to activate AMPK pathway and, consequently, reprogram antioxidant system response and mitochondrial biogenesis. Among these compounds, the most frequently mentioned in the literature are the followings: AICAR[209], mitochondrial toxins (dinitrophenol, rotenone, KCN)[175,210], thiazolidinediones (rosiglitazone and pioglitazone)[175,210], A-769662[211,212], metformin[213], natural compounds (salidroside[214], D-xylose[215], quercitin[216], capsaicin[217], curcumin[218] berberin[219], EGCG[220], genistein[217], resveratrol[221] and several others) and some hormones and cytokines (leptin, interleukin-6, resistin, ghrelin, and adiponectin)[222]. Otherwise, compound C[223] and C75 inhibitor[224] have been described as AMPK inhibitors.

The link between AMPK signalling and multiple metabolic pathways reinforces the concept that there is a small number of regulators that control distinct aspects of biology to act as master coordinators of cell growth, metabolism, and ultimately cell fate.

I-II. Mitochondrial diseases

The concept of mitochondrial disease was first introduced in 1962, when Luft *et al* reported a case of a young Swedish woman with severe hypermetabolism not due to thyroid dysfunction (Luft syndrome)[225]. In this investigation, three sets of clinical characteristics were established to describe this kind of disorders not reported to date: (i) abnormal morphology of mitochondria in muscle; (ii) biochemical uncoupling of OXPHOS system in isolated muscle mitochondria; and (iii) correlation between biochemical defects and clinical features. The excessive proliferation of mitochondria in muscle, which is known as "ragged-red fibers" (RRF) and detected by Gomori trichrome stain[226], was considered the main pathological hallmark of mitochondrial diseases, although its lack does not exclude a mitochondrial aetiology. Along with abnormal proliferation of mitochondria, these disorders are often accompanied by energy deficiencies mainly caused by OXPHOS dysfunction. Mitochondrial diseases are renowned for their variability in clinical and biochemical features, mainly affecting organs with high-energy requirements. Indeed, the tissues most affected are often those that demand more energy such as nervous system and muscle[165,166], hence the term "mitochondrial encephalomyopathy". The onset and severity of the symptoms varies from one patient to another. Interestingly, mitochondrial diseases may range from life-threatening to asymptomatic or oligosymptomatic mutation carriers. This differential manifestation severely complicates the diagnosis of mitochondrial diseases[227]. Currently, the clinical diagnosis in mitochondrial diseases remains uncertain until muscle biopsies or genetic tests confirm the abnormality. There have been published several diagnostic criteria to guide the practitioners for diagnosis, which are based on a combination of clinical, laboratory, pathologic, biochemical, and genetic findings. The best-known are the Walker criteria[228,229] and other attempts such as the Nijmegen Center for Mitochondrial Disorders scoring system[230] and the Mitochondrial Disease Criteria[231].

The symptomatology in these disorders may present anytime from birth to late adulthood. Indeed, children often present different clinical features when compared to adults. Common clinical presentations of children include failure to thrive, motor regression, metabolic encephalopathy, seizures, ptosis, external ophthalmoplegia and cardiomyopathy. In adults, manifestations include exercise intolerance, sensorineural hearing loss, ophthalmological abnormalities (retinal pigmentary changes, ptosis, progressive external ophthalmoplegia, optic atrophy), muscle weakness (proximal limb weakness, dysphagia, dysarthria), central nervous system involvement (focal neurological deficits, migraine, seizures), cardiac manifestations (cardiac arrhythmia, hypertrophic cardiomyopathy, conduction block), gastrointestinal system abnormalities (pseudo-obstruction, constipation) and endocrine abnormalities (diabetes, short stature and rarely hypoparathyroidism and hypogonadism)[227] (**Figure I9**).

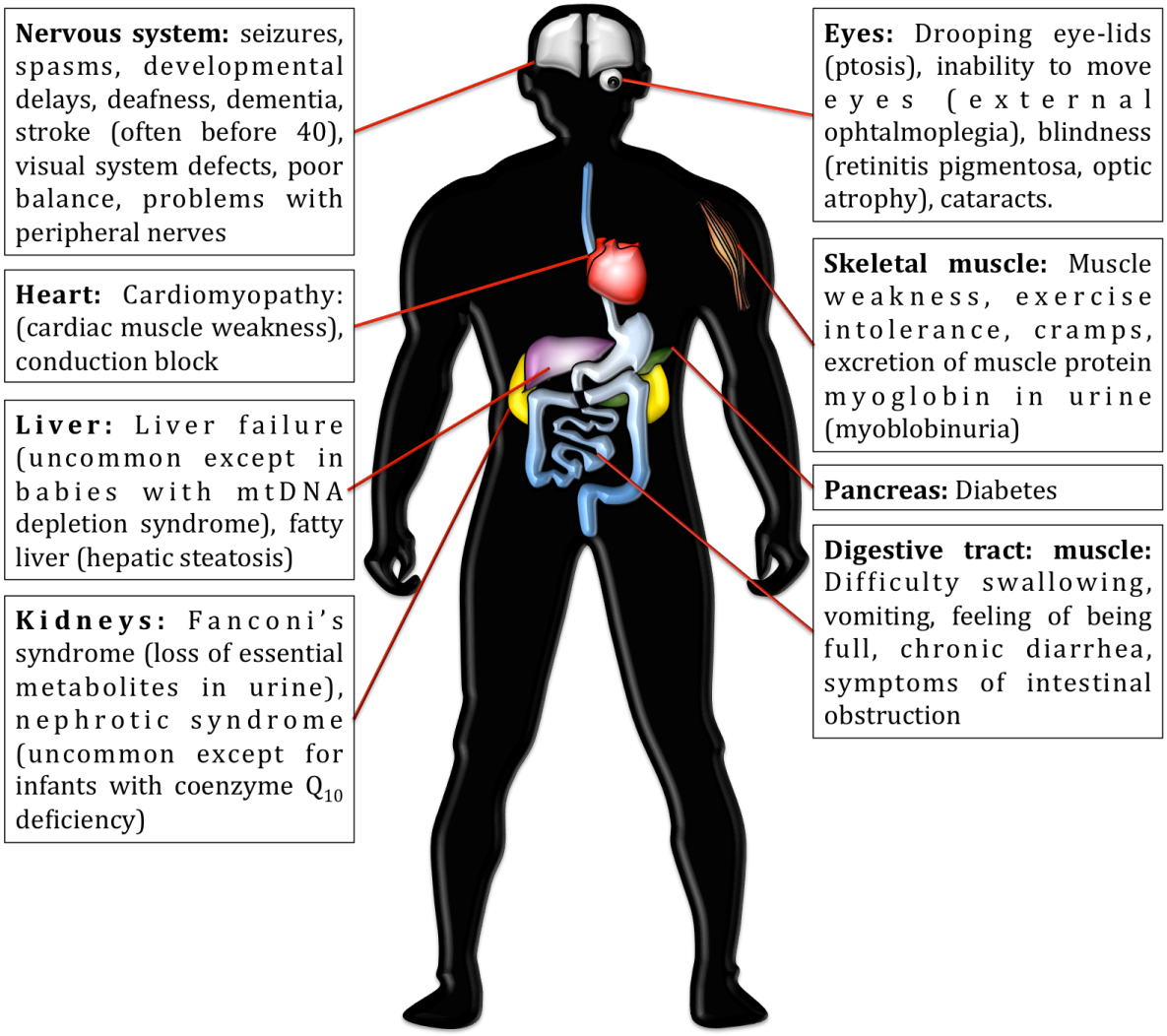

Figure I9. Symptomatology in mitochondrial diseases. Common clinical presentations of patients with mitochondrial diseases.

Classification

The broad variety of symptoms led to try to classify mitochondrial diseases. First, the emergence of the biochemical assays in the 1970s was concomitant with the description of several defects of mitochondrial metabolism, including pyruvate dehydrogenase (PDH) deficiency[232], carnitine deficiency[233], carnitine palmitoyltransferase (CPT) deficiency[234], as well as, the first example of cytochrome *c* oxidase (COX) deficiency in Leigh syndrome[235]. Not long after, DiMauro *et al* proposed a biochemical classification of the mitochondrial diseases based on defects in the five major steps of mitochondrial metabolism: substrate transport, substrate utilization, Krebs cycle, electron transport chain, and oxidation/phosphorylation coupling[236]. However, because of the extremely variable clinical presentations of mitochondrial diseases and the difficulty to define them, these disorders ended up being grouped as

defects of the MRC, the bioenergetic pathway *par excellence*[165] and the common link between them. Mitochondrial respiratory chain is the only metabolic pathway in the cell that is under the dual control of the mitochondrial genome (mtDNA) and the nuclear genome (nDNA), therefore, a genetic classification seems to better distinguish disorders due to mutations in mtDNA, ruled by mitochondrial genetics, and disorders due to mutations in nDNA, which are governed by mendelian genetics[237].

- **Mitochondrial diseases due to mutations in mtDNA**
  - **Defects in mitochondrial protein synthesis**
    - **mtDNA rearrangements**. Single deletions of mtDNA have been associated with three usually sporadic conditions[238]: Pearson syndrome (PS), Kearns–Sayre syndrome (KSS) and Progressive external ophthalmoplegia (PEO).
    - **mtDNA point mutations**: Multiples point mutations in mtDNA have been identified, but the most common are: Mitochondrial encephalomyopathy, lactic acidosis, and stroke-like episodes (MELAS)[239,240] and Myoclonus epilepsy with ragged red fibers (MERRF)[241,242].
  - **Defects of protein-coding genes.** The most representative cases are: first, Neuropathy, ataxia, retinitis pigmentosa (NARP) and Maternally inherited Leigh syndrome (MILS) with the same gene affected, the ATPase6 gene[243–245] and, secondly, Leber's hereditary optic neuropathy (LHON)[246] with mutations affecting genes of complex I (ND genes).

- **Diseases due to mutations in nDNA.** Mitochondrial diseases due to mutations in nDNA not only include mutations in nuclear-encoded subunits of the MRC, but also those related with their correct assembly, transport to mitochondria, maintenance and functioning.
  - **Mutations in genes encoding subunits or auxiliary proteins of the MRC.** In addition to completely synthesise complex II, nDNA encodes most subunits of the other four complexes as well as both electron transporters (coenzyme Q_{10} and cytochrome c). Therefore, mutations in any of them might presumably involve MRC deficiency directly or indirectly. Some examples of direct affectations are mutations in subunits of complex I[247] and of complex II[248] which have been associated with autosomal recessive forms of Leigh syndrome, or mutations in the biosynthetic pathway of coenzyme Q_{10}[249]. On the other hand, mutations in genes non-coding for MRC proteins may also generate deficiency like those related with the proper assembly of the MRC complexes. This is the case of mutations in auxiliary proteins associated with complex IV deficiency such as SURF1, SCO2, SCO1, COX10 and COX15[250,251]; mutations in a complex III assembly protein, BSC1L, associated with GRACILE syndrome[252]; and mutations in a complex V assembly protein, ATP12[253].
  - **Defects of intergenomic signaling.** mtDNA replication requires numerous factors encoded by nuclear genes, which in case of mutation cause mendelian disorders characterized by qualitative or quantitative alterations of mtDNA[254–256]. For instance, qualitative alterations include multiple deletions of mtDNA in

the gene of the adenine nucleotide translocator (ANT1), Twinkle or POLG that may be responsible for PEO, or deletions in the gene of thymidine phosphorylase (TP) which may be responsible for Mitochondrial neurogastrointestinal encephalomyopathy (MNGIE)[257–261]. Quantitative alterations of mtDNA include mutations in two genes, thymidine kinase 2 (TK2) and deoxyguanosine kinase (dGK), both involved in mitochondrial nucleotide homeostasis, which have been associated with mtDNA depletion syndromes [262,263].

- **Defects of mitochondrial protein importation.** Transport across outer and inner membranes of proteins synthesised in the cytoplasm requires a set of factors which includes docking proteins, chaperonins, and proteases, and it involves unfolding and refolding of the protein to be translocated[264]. Several mutations in targeting sequences have been documented, but few genetic defects in the general transport machinery[265]. In particular, two gene are reported to cause defects in the transport machinery: the TIMM8A gene, which is associated with Mohr-Tranebjaerg syndrome[266], and the chaperonin HSP60[267].
- **Alterations of the lipid composition of the inner mitochondrial membrane.** Mutations in the tafazzin (TAZ) gene are associated with Barth syndrome (BTHS) and decreased cardiolipin levels[268,269].
- **Alterations of mitochondrial motility or fission.** Mutations in a gene encoding a dynamin-related guanosine triphosphatase (OPA1) have been associated with the mendelian counterpart of LHON[270] showing clumped mitochondria in the cytoplasm of monocytes.
- **Late-onset neurodegenerative diseases and aging.** In this group, several neurodegenerative disorders associated with mitochondrial dysfunction and oxidative stress are grouped. Some examples are Parkinson disease, Huntington disease, Alzheimer disease, amyotrophic lateral sclerosis and aging[271–273].

Particular considerations

The study of mitochondrial diseases caused by mtDNA mutations involves a series of difficulties associated with the nature of mtDNA, which is ruled by different mechanisms than nuclear genome. Mitochondria are semi-autonomous organelles governed by their own rules. Cells may contain from one mitochondrion to hundreds depending on their energy requirements. Likewise, each mitochondrion is estimated to contain from 2 to 10 mtDNA copies[34], which are continuously mixing in the mitochondrial network by fusion and fission events. The biggest difficulty in the study of mitochondrial diseases lies in the fact that several particularities need to be considered[237]:

- ***Heteroplasmy load***. Each cell may contain hundreds or even thousands of mtDNA copies, which are randomly distributed among daughter cells. Homoplasmy is considered when all these copies are identical between them. By contrast, heteroplasmy is considered when mutations in mtDNA affect some

but not all copies. Overall, these mitochondrial patients usually harbour a mixture of normal and mutant copies of mtDNA, whose relative proportion is considered heteroplasmy load in a tissue.

- ***Threshold effect***. The clinical expression of a pathogenic mtDNA mutation is largely determined by heteroplasmy load in different tissues. According to energy requirements into the cells, the critical number of mutant mtDNAs to cause mitochondrial dysfunction in a particular organ or tissue may vary. This threshold is typically reached when 60-90% of the mtDNA molecules carry an identical mutation[274]. Thus, neurones and cardiac and skeletal muscle are more vulnerable to energy-dependent defects[4].
- ***Random segregation***. During mitosis, mitochondria and hence mutant mtDNA are distributed randomly in daughter cells. However, according to that distribution the heteroplasmy load may shift and, therefore, the phenotype may change accordingly. This phenomenon explains how patients with mtDNA-related disorders may have variable heteroplasmy load in different tissues and manifest their disease differentially.
- ***Maternal inheritance***. Apart from one exception[275], all mitochondria derives from the oocyte at fertilisation. The mode of transmission of mtDNA definitively differs from Mendelian inheritance. Therefore, only mothers carrying mtDNA point mutations will pass them on to all their children (males as well as females). A disease expressed in both sexes but with no evidence of paternal transmission is strongly suggestive of a mtDNA point mutation.

Overall, the analysis of mitochondrial mutations must take into account these particularities in order to better understand the complexity of diseases under study.

Therapeutic approaches

Mitochondrial diseases are known by huge clinical, biochemical and genetic heterogeneity, which hampers the collection of homogeneous cohorts of patients to establish the efficacy of a treatment. Based on this, cellular and animal models are recently been used to try different therapeutic strategies[276]:

- **Pharmacological and metabolic interventions**
  - ***Increasing mitochondrial biogenesis***. Mitochondrial biogenesis up-regulation could partly explain cases of incomplete penetrance in LHON disorder[277]. As commented in previous sections, the induction of mitochondrial biogenesis involves three axis of activation: PGC-1α, AMPK and SIRT1. In order to induce PGC-1α, bezafibrate treatment was successfully used in different models of mitochondrial diseases such as fibroblasts form patients[278], muscle-specific PGC-1α transgenic mouse[279], cybrids harbouring pathological tRNA mutations[280] and the nervous tissue of a brain-specific*Cox10* knockout mouse[281]. On the other hand, AMPK activation can also result in mitochondrial biogenesis[156]. The AMPK agonist, AICAR, reported interesting results in three models of COX deficiency, a *Surf1* constitutive knockout mouse (*Surf1*$^{-/-}$), a

Sco2 knockout/knockin (*Sco2*^{KOKI}) mouse and a muscle-specific *Cox15*(*ACTA-Cox15*$^{-/-}$) mouse[282]. Interestingly, AICAR was found the most effective compound in inducing mitochondrial biogenesis in complex I deficient cells[283]. Finally, other strategy to activate PGC-1α is to promote its deacetylation via Sirt1 activation. Both diet supplementation with nicotinamide riboside (NR), natural precursor of NAD^+ that activates Sirt1, or by genetic or pharmacological inhibition of poly(ADP) ribosyl-polymerase 1 (Parp1), a NAD^+ consumer and Sirt1 competitor, seem to increase mitochondrial respiration by inducing OXPHOS genes via the PGC-1α axis in *Sco2*^{KOKI} mice[284] and in *deletor* mouse, another model of mitochondrial myopathy due to expression of a mutant variant of the mitochondrial helicase Twinkle[285]. In addition to bezafibrate, AICAR and NR, other compound like resveratrol, metformin and retinoic acid seem to increase mitochondrial biogenesis in some studies[286–288].

- ***Endurance training.*** Endurance training has also been exploited to trigger mitochondrial biogenesis in patients affected by mitochondrial myopathy[289], in muscle-specific *Cox10* knockout mice[290], and in the mtDNA *mutator* mice, where it seems to rescue progeroid aging[291]. Importantly, these beneficial effects were not limited to skeletal muscle but also involved other organs, including the brain.
- ***Scavenging toxic compounds***. Mitochondrial diseases are often characterized by metabolic blockages in mitochondria that lead to accumulation of toxic substances. An example is found in ethylmalonic encephalopathy (EE), which accumulates high levels of hydrogen sulphide (H_2S). Administration of N-acetylcysteine (NAC) and metronidazole, which facilities the H_2S clearance, were successfully tested in *Ethe1*$^{-/-}$mouse model and in a cohort of EE patients[292]. Other harmful metabolites are generated as by-products of mitochondrial respiration. Increased ROS may occur as a consequence of respiratory chain dysfunction due to aging[293] or OXPHOS defects[294]. Cocktails of antioxidant compounds, including lipoic acid, vitamins C and E, and CoQ, have been used in the therapy of mitochondrial diseases[294–296].
- ***Supplementation of nucleotides***. Some disorders like Mitochondrial neurogastrointestinal encephalomyopathy (MNGIE) show an unbalance in the pool of mitochondrial dNTPs due to mutations in enzymes involved in their metabolism[297]. Supplementation with deoxyribonucleotides can ameliorate mtDNA depletions derived from the disease in fibroblasts derived from patients[298,299].
- ***Targeting autophagy*.** As before commented, different pathways can regulate autophagy: (i) mTORC1, which inhibits autophagy in presence of nutrients; (ii) cAMP, which provokes the release of Ca^{+2} from ER and inhibits autophagy; and (iii) AMPK, which activates ULK1 and triggers autophagy under nutrients deprivation. Some mutations of NDUFS4, subunit of complex I, are associated with Leigh disease in humans and with neurodegenerative failure in the *Ndufs4*$^{-/-}$ mouse model[300]. Chronic treatment with the mTOR inhibitor rapamycin, which activates autophagy, significantly delayed the disease progression and corrected the accumulation of abnormal metabolic biomarkers.

- ***Dietary manipulations*.** High-fat or low-carbohydrate diets are proposed to stimulate mitochondrial beta-oxidation and generate ketones, which constitute an alternative energy source for the brain, heart and skeletal muscle. Ketone bodies are metabolized to acetyl-CoA and ultimately generate ATP via OXPHOS. Ketogenic diets have been associated to increased synthesis of succinate, expression of OXPHOS genes and activation of mitochondrial biogenesis through SIRT1, AMPK and PGC-1α[301]. In addition, ketogenic treatments seem to reduce heteroplasmy load in cybrids derived from a Kearns–Sayre syndrome patient[302] and delay the progression of mitochondrial myopathy in the *deletor* mouse[303] and neurological symptoms in Harlequin mice[304]. Other compounds that release succinate in mitochondria is triheptaoin, which ameliorates symptoms in patients with VLCAD deficiency[305] and CPT2 deficiency[306].
- ***Targeting the PTP*.** The opening of the permeability transition pore (PTP) in mitochondria can trigger dissipation of the mitochondrial membrane potential, osmotic swelling and ultimately mitochondrial disruption. Finally, as a consequence of the release of cytochrome c, cells can undergo apoptosis[307]. Cyclosporine A, which inhibits the PTP, was successfully used in patients with Bethlem/Ullrich congenital muscular dystrophy[308].

➢ **Molecular approaches to treat mitochondrial diseases**

- ***Targeted re-expression of the mutated gene***. Some attempts to correct mutations for gene replacement are being recently performed in mice by expressing the wild-type gene in critical organs such as skeletal muscle, brain, heart, liver and retina. In the context of mitochondrial disease models, several serotypes of adeno-associated viral (AAVs) vectors have been tested[309,310] such as AAV2, administered by local injections to correct the myopathy associated with *Ant1*$^{-/-}$ mice[311] or AAV2/8 expressing a recombinant construct from human *Ethe1*^{wt} in *Ethe1*$^{-/-}$mice[312]. In addition, AAV2/8 was also tested in other disorders like MNGIE, both on *Tymp*$^{-/-}$ mice[313] and on patients[314]. Other serotypes like AAV5 and AAV2 were tested in in liver[315] and retina[316], respectively. On the other hand, other strategy proposes to correct mtDNA mutation by using allotropic expression, which consists of expressing a recombinant wild-type protein in the nuclear genome with a mitochondrial targeting sequence (MTS). This method was tested in fibroblasts carrying mutations in ND1, ND4 and ATP6 genes[317–319] and in a rat model of LHON[320]. Due to the fact that the mitochondrial transport of recombinant protein not always successes, other alternative strategies have been proposed with promising results. Protein nucleic acids (PNAs) are hybrid synthetic DNA-like molecules that links to DNA sequences with greater affinity than natural DNA sequences. PNAs complementary to the mtDNA containing the 8344A>G MERRF mutation in mt-tRNA^{Lys} was imported into mitochondria, where they inhibited the replication of mutant but not wild type mtDNA[321]. Finally, the allotopical expression in nuclei of tRNAs and mRNAs and transported to the mitochondria through a specialized system of translocation of the RNase P was used to correct mt-tRNA and COII gene mutations in cell lines[322,323].

- ***Manipulating mtDNA heteroplasmy.*** Therapeutic approaches to reduce heteroplasmic mutations of mtDNA were successfully tested in cellular models by targeting to mitochondria recombinant restriction endonucleases[324–326], zinc finger-endonucleases (ZFNs)[327] or transcription activator-like effectors nucleases (TALENs)[328]. Some examples of mitochondrially targeted restriction enzymes are a recombinant form of *Sma*I to reduce the 8399T>G mutation in NARP disorder[329] and *ApaL*1 in NZB/BalbC heteroplasmic mice[330,331]. Whereas restriction endonucleases need to recognise restriction site generated by mutations, ZFNs[332,333] and TALENs[328] can recognise multiple sequences. In the three cases, a reduction of mtDNA content takes place as a consequence of the elimination of mutant copies, however, the mtDNA content is restored by wild-type mtDNA replication[327].
- ***Stabilizing mutant mt-tRNA*.** MELAS or MERRF syndromes are caused by mtDNA mutations localised in tRNA genes. In order to attenuate these point mutations, some therapeutic approaches try to overexpress aminoacyl-tRNA synthetases (aaRSs), which are in charge of the attach between the specific tRNA and their amino acids[334]. For instance, overexpression of mt-leucyl-tRNA synthetase (mt-LeuRS) restored the MRC deficiency of transmitochondrial cybrids harbouring the MELAS mutation in the mt-tRNA$^{Leu(UUR)}$ gene (*MTTL1*)[335] and mt-valyl-tRNA synthetase (mt-ValRS) ameliorated defects in the cybrids with mutated mt-tRNA^{Val}[336]. On the other hand, in yeast some mt-tRNA can also be synthesised by nuclear genome and then imported into mitochondria. Some experiments with human cells expressing the yeast version of nuclear-encoded tRNA achieved to restore mitochondrial dysfunction derived from MERRF[337] and Kearns-Sayre syndromes[338].
- ***Targeting fission and fusion***. Alterations in the genes encoding fusion and fission-related proteins lead to disease in humans such the autosomal dominant optic atrophy (OPA1 mutations)[339] and Charcot–Marie–Tooth disease type 2A (MFN2 mutations)[340]. Some approaches propose to overexpress OPA1, which improved fusion of IMM and stabilisation of supercomplexes[341]. On the other hand, pharmacological treatments are been tested like MDIVI-1[342] and M1-hydrazone[343], which seem to regulate fusion and fission.
- ***Bypassing the block of the respiratory chain*.** OXPHOS system is often blocked in mitochondrial diseases by particular deficiencies in MRC complexes. NADH dehydrogenase/CoQ reductase (Ndi1), which substitutes complex I in yeast, and CoQ/O_2 alternative oxidase (AOX), which bypasses complexes III and IV in plants, can be alternatively used in human for bypassing the blockage, but without pumping protons across the membrane and without increasing ATP production directly[344–346].
- **Somatic nuclear transfer.** Given the difficulty of using gene therapies in adult patients harbouring mtDNA mutations, prenatal or pre-implantation genetic diagnosis (PGD) seem to be the available way to avoid inheriting pathogenic mtDNA mutations. Recent studies in non-human primates[347] and non-viable human embryos[348,349] have demonstrated the viability of replacing the mutated

maternal mtDNA with that obtained from a healthy woman, by transferring either the spindle-chromosomal complex of mature oocytes, or the pronuclei during the pre-zygotic stage of fertilized egg. A child born by these procedures will carry the nuclear genes of the affected mother (and healthy father) but the healthy mitochondrial genes of the donor.

I-III. MELAS syndrome

Pathogenesis

Since 1984, the syndrome of mitochondrial encephalopathy, lactic acidosis, and stroke-like episodes (MELAS) has been one of the most useful model to study the complex interplay of factors that define mitochondrial disease[350]. Ever since Holt described the first pathogenic mtDNA mutations[351], more than 200 disease-causing point mtDNA mutations have been reported[352], 29 of which associated with MELAS syndrome[240,353]. The pathogenesis of MELAS syndrome is closely related to the mutations, which often disrupt mitochondrial protein synthesis and lead to a decreased activity of the MRC components and a subsequent ATP deficiency. These energy imbalances generate a shifting into the cells to alternative metabolic pathways, resulting in the accumulation of metabolic by-products like lactate (lactic acidosis)[240], that cause cellular injury and tissue damage[354]. Normally, in order to rebalance the energy supply, MRC deficiencies are accompanied by a compensatory increase of mitochondrial mass observed as RRFs. Moreover, in the absence of a proper electron transport in MRC system, toxic ROS are accumulated exacerbating cellular damage[24]. Abnormal calcium levels due to the incapacity to control proper calcium influx may cause neuronal injury and contribute to the central nervous system impairment in the disease[355]. Indeed, failure of energy-dependent ion transport in the context of defective OXPHOS system may result in increased extracellular potassium or glutamate within the synaptic cleft, driving neuronal hyperexcitability and the development of the clinical phenotype with prolonged seizures, migraines and stroke-like episodes[356]. Other theories point to nitric oxide that can displace heme-bound oxygen and decrease oxygen availability to the tissues. High cytochrome c oxidase levels may lead to stroke-like symptoms because they produce a relative shortage of nitric oxide with consequent inhibition of cerebral vasodilation. A possible dysfunction in nitric oxide production and catabolism might result in angiopathy and stroke-like episodes observed in MELAS syndrome[357]. Likewise, the inability of dysfunctional mitochondria to generate sufficient ATP along with the nitric oxide deficiency may be behind the myopathic manifestations of this syndrome. In fact, decreased nitric oxide availability can lead to impaired basal muscular perfusion resulting in a limited availability of nutrients like amino acids in tissues that decreases muscle protein synthesis contributing to the myopathy and muscle wasting observed in MELAS syndrome[358,359]. On the other hand, diabetes developed in MELAS syndrome can be due to several defects in insulin and glucose metabolism including insulin deficiency, increased gluconeogenesis, and insulin resistance[360].

In addition, MELAS syndrome is renowned by its variable phenotype, from patients with the whole spectrum of symptoms to asymptomatic individuals. Between these two extremes, intermediate phenotypes exist including single organ involvement (cardiomyopathy) and multi-organ involvement (myopathy, diabetes, and deafness). This wide variety of phenotypes seems to be associated with heteroplasmy load and the tissue affected. Indeed, heteroplasmy load seems to correlate with oxygen uptake and workload, resting plasma lactate, and muscle morphology abnormalities in

individuals with MELAS syndrome. Interestingly, the threshold of muscle mutation load seems to be about 50%[361].

Genetics

The complexity of mitochondrial genetics is made manifest through the study of MELAS syndrome. The molecular basis of MELAS syndrome was initially discovered in 1990 when an adenine to guanine transition at position 3243 (m.3243A>G) of mtDNA was associated with this syndrome[362,363]. Specifically, this mutation affects the MT-TL1 gene encoding a transference RNA for leucine ($tRNA^{leu(UUR)}$). The m.3243A>G mutation impairs termination[364], pre-processing[365], aminoacylation[366] and conformation[367] of the normal $tRNA^{leu(UUR)}$, which ultimately reduces the synthesis of mitochondrial proteins. In particular, m.3243A>G disrupts the taurinomethylation at the C5 position of wobble uridine (tm^5U; 5-taurinomethyluridine), which enables the double recognition and decoding of UUA and UUG codons. The altered $tRNA^{leu(UUR)}$ affects severely the UUG translation but do not repress the UUA translation[368,369] (**Figure I10**).

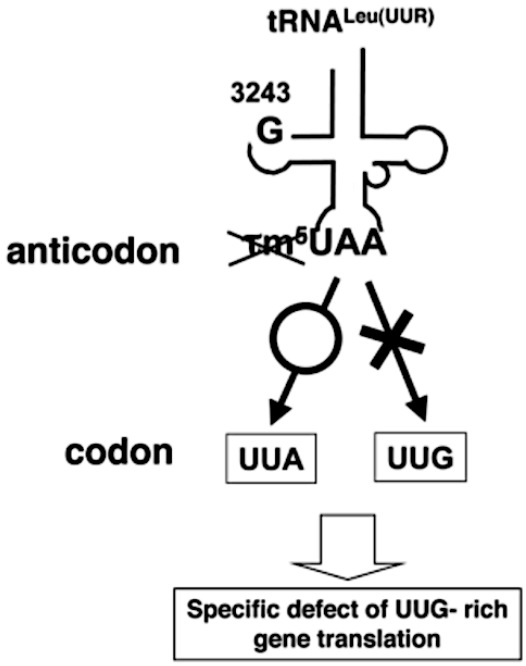

Figure I10. Proposed molecular pathogenesis caused by the wobble modification deficiency of mutant tRNAs associated with MELAS syndrome. The pathogenic point mutation m.3243A>G impairs the wobble modification of the mutant tRNA and the pattern of codon recognition. ***Adapted from Kirino, Y. & Suzuki, T (2005)[369].***

The lack of the modification subsequently causes a UUG-codon–specific translational defect, possibly leading to a translational depression of protein rich in UUG codons in

mtDNA base substitution diseases: coding and control region point mutations						mtDNA base substitution diseases: rRNA/tRNA mutations			
Locus	Disease	Allele	Nucleotide position	Nucleotide change	Amino acid change	Locus	Disease	Allele	RNA
MT-ND1	MELAS; DEAF modulator	T3308C	3308	T→C	M→T	MT-TF	MELAS/MM & EXIT	G583A	tRNA Phe
MT-ND1	LHON/MELAS overlap	G3376A	3376	G→A	E→K	MT-TV	MELAS	G1642A	tRNA Val
MT-ND1	MELAS	G3481A	3481	G→A	E59→K	MT-RNR2	MELAS	C3093G	16S rRNA
MT-ND1	MELAS	G3697A	3697	G→A	G→S	MT-TL1	MELAS	A3243G	tRNA Leu (UUR)
MT-ND1	MELAS	G3946A	3946	G→A	E→K	MT-TL1	MELAS	G3244A	tRNA Leu (UUR)
MT-ND1	MELAS	T3949C	3946	T→C	Y→H	MT-TL1	MELAS	A3252G	tRNA Leu (UUR)
MT-CO3	PEM[a]; MELAS; NAION[b]	T9957C	9957	T→C	F→L	MT-TL1	MELAS	C3256T	tRNA Leu (UUR)
MT-ND4	MELAS	A11084G	11084	A→G	T→A	MT-TL1	MELAS/myopathy	T3258C	tRNA Leu (UUR)
MT-ND5	MELAS	A12770G	12770	A→G	E→G	MT-TL1	MELAS	T3271C	tRNA Leu (UUR)
MT-ND5	MELAS/LHON/ Leigh overlap syndrome	A13045C	13045	A→C	M→L	MT-TL1	MELAS	T3291C	tRNA Leu (UUR)
MT-ND5	MELAS/Leigh disease	A13084T	13084	A→T	S→C	MT-TQ	Encephalopathy/ MELAS	G4332A	tRNA Gln.
MT-ND5	MELAS/Leigh disease	G13513A	13513	G→A	D→N	MT-TK	MELAS	T8316C	tRNA Lys
MT-ND5	MELAS	A13514G	13514	A→G	D→G	MT-TH	MERRF-MELAS/ cerebral edema	G12147A	tRNA His
MT-ND6	MELAS	G14453A	14453	G→A	A→V	MT-TL2	MELAS	A12299C	tRNA Leu (CUN)
MT-CYB	PD/MELAS	14787del4	14787	TTAA→;	I-frameshift				

Table I1. MELAS-associated mutations in mtDNA. [a]PEM, Progressive encephalomyopathy; [b]NAION, Non-arteritic anterior ischemic optic neuropathy. ***From Sproule, D. M. & Kaufmann, P (2008)[240]*****.**

mitochondria, like ND6 subunit of respiratory chain complex I (NADH-coenzyme Q reductase)[369,370], which contains eight UUG codons that constitute 42.1% of the total leucine codons[368]. Thus, MELAS disease is often associated with a general defect in mitochondrial protein synthesis and severe mitochondrial respiratory chain defects[274,371].

Apart from m.3243A>G mutation, which is found in 80% of patients, MELAS is indeed a polygenetic disorder associated with up to 29 specific point mutations (Table I1). In addition to at least seven identified point mutations in the mitochondrial $tRNA^{(Leu)}$ gene, mutations affecting other mitochondrial tRNA genes (His, Lys, Gln, and Glu) and protein-coding genes (MT-ND1, MT-CO3, MT-ND4, MT-ND5, MT-ND6, and MT-CYB) have been associated with the MELAS syndrome[372]. Moreover, mutations in the nuclear gene POLG encoding the mitochondrial DNA polymerase gamma have been associated with a MELAS-like phenotype[373].

Diagnostics

The incidence of mitochondrial diseases seems to vary depending on the methodology, geography, and subject group analysed. In fact, several studies reported prevalences of 0.2 per 100,000 in Japan[374] and 18.4 per 100,000 in Finland[375] for MELAS syndrome. However, other studies considering the wide spectrum ranging of MELAS patients (from asymptomatic carriers to severely affected individuals) established that the absolute prevalence of the m.3243A>G mutation can reach 60 per 100,000 individuals in the general population[376].

MELAS syndrome is characterised by normal early development and the absence of symptom after birth. The energy output, although abnormal, is sufficient to meet the body's requirements. However, once the metabolic demands exceed the energy supply available from the defective mitochondria, symptoms make their appearance[377]. The age of onset of the syndrome is variable, ranging from younger than 2 years to older than 60 years, although most patients develop their first symptoms before than 20 years[240,378]. Since the initial description of MELAS syndrome[350], there has been an expansion of the clinical phenotype to include overlap syndromes. In order to distinguish MELAS syndrome from other mitochondrial pathologies, diagnostic criteria were published indicating that the clinical diagnosis of this syndrome is based on the following three invariant criteria: 1) stroke-like episodes before age 40 years, 2) encephalopathy characterized by seizures and/or dementia, and 3) mitochondrial myopathy evident by lactic acidosis and/or ragged-red fibers[379]. More recently, other diagnostic criteria were published by which the diagnosis is considered definitive with at least two category A criteria (headaches with vomiting, seizures, hemiplegia, cortical blindness, and acute focal lesions in neuroimaging) and two category B criteria (high plasma or cerebrospinal fluid (CSF) lactate, mitochondrial abnormalities in muscle biopsy, and a MELAS-related gene mutation)[374]. Diagnosis of MELAS syndrome is, therefore, based in a combination of radiologic images, laboratory and genetic tests, and biopsies[380]:

- ***Radiographic features*.** Stroke-like episodes can be detected using Magnetic resonance (MR) techniques. Even though MR angiography is typically normal, the MR imagining of patients with MELAS show asymmetric lesions of the occipital and parietal lobes that usually fail to correspond to a defined vascular territory, indicating that the stroke-like episodes are nonthrombotic[379]. MR spectroscopy permits *in vivo* evaluation of brain metabolism by detecting abnormalities like a N-acetyl aspartate signal decrease and the accumulation of lactate. There is a general consensus that a lactate peak represents a sensitive metabolic marker of disease[240,381].
- ***Lactate levels analysis*.** One of the nearly absolute findings in MELAS syndrome is the elevation of lactate levels in both the cerebrospinal fluid and the serum. In fact, lactate levels seem to correlate with the degree of neuropsychological and neurologic impairment[382]. Although the serum lactate level remains normal during early stages of the disease, it increases as the disease progresses and is elevated in greater than 90% of patients[240,355,380,383].
- ***Muscle biopsy*.** At histologic level, the examination of muscle tissue can be performed through haematoxylin and eosin staining, Gomori trichrome staining, succinate dehydrogenase (SDH) stain and cytochrome c oxidase (COX) stains. These techniques allow detecting abnormal mitochondrial proliferation or RRFs. At biochemical level, the mutations in MELAS syndrome most commonly disrupt mitochondrial protein synthesis, which leads to decreased activity of the components of the respiratory chain. At least 42% of patients with MELAS syndrome show a decrease in the activity of complex I, followed by 29% with dysfunctions of complex III and 23% in complex IV[239,240,384,385].
- ***Molecular diagnostics*.** The percentage of heteroplasmy for a particular mtDNA mutation may vary widely at biopsy, depending on the specific tissue sampled[240,386]. Blood leukocyte samples for the mutation are not particularly sensitive compared to urinary sediment, skin fibroblasts or buccal mucosa, which carry a higher mutant load[355,387]. Multiple methods based on polymerase chain reaction (PCR) techniques have been reported for detection and quantification of heteroplasmy. Along these, some examples include PCR associated with restriction assays (PCR–restriction fragment length polymorphism) followed by gel electrophoresis and laser densitometric scanning of gel photo[388], PCR with peptide nucleic acid clamp and sequencing[389], PCR with subsequent hybridization using a radioactive allele-specific oligonucleotide probe[390], quantitative real-time PCR with allele-specific primers[391], and PCR with a fluorescence-labelled primer followed by restriction enzyme digestion, separation, and detection by capillary electrophoresis[392]. More recently, interesting advances include the use of pyrosequencing techniques[393], the detection of mutation in a single mitochondria[394], the use of locked nucleic acid modified primers[395] and fluorescence resonance energy transfer technology and melting curve analysis[396].

Clinical Manifestations

Initial symptoms include muscle weakness, exercise intolerance, headaches and vomiting, but with age stroke-like episodes, seizures, and lactic acidosis predominate. Once stroke-like episodes begin, the clinical status of the patient is rapidly aggravated exhibiting multiple defects in numerous organ systems and tissues (Table I2)[385]. Ultimately, patients suffer significant neurologic deterioration and neuromuscular dysfunction that result in severe disability, and premature death. Here, parameters like heteroplasmy load or threshold effect for key organs enter the scene making difficult to determine a prognosis for patients. It is estimated a mean survival time of around 6,5 years from disease onset[240,382].

Frequency	Manifestations
≥90%	Stroke-like episodes
	Dementia
	Epilepsy
	Lactic acidemia
	Ragged red fibers
	Exercise intolerance
75–89%	Hemiparesis
	Cortical vision loss
	Recurrent headaches
	Hearing impairment
	Muscle weakness
50–74%	Peripheral neuropathy
	Learning disability
	Memory impairment
	Recurrent vomiting
	Short stature
25–49%	Basal ganglia calcification
	Myoclonus
	Ataxia
	Episodic altered consciousness
	Gait disturbance
	Depression
	Anxiety
	Psychotic disorders
	Diabetes
<25%	Optic atrophy
	Pigmentary retinopathy
	Progressive external ophthalmoplegia
	Motor developmental delay
	Cardiomyopathy
	Cardiac conduction abnormalities
	Nephropathy
	Vitiligo

Table I2. Overall manifestations of MELAS syndrome. Clinical manifestations of MELAS syndrome organized according to their prevalence. ***Adapted from El-Hattab, A. W. et al (2015)[384].***

- ***Neurological manifestations.*** Stroke-like episodes are one of the canonical features of MELAS patients, which are associated with partially reversible aphasia, cortical vision loss, motor weakness, headaches, altered mental status, and seizures. Neuroimaging studies show an irregular vascular distribution, and hence the term "stroke-like episodes". The neurological dysfunction and the accumulating cortical stroke-like episodes lead to dementia, which affects

intelligence, language, perception, attention, and memory function. Seizures are tremendously frequent and can culminate in epileptic episodes[385,397]. Vomiting can precipitate stroke-like episodes[398]. Sensorineural hearing loss in MELAS syndrome is an early manifestation typically progressive[240]. Peripheral neuropathy is usually a chronic and progressive, sensorimotor, and distal polyneuropathy associated with demyelinating processes[399]. Other neurological manifestations include learning difficulties, memory impairment, myoclonus, ataxia, episodes of altered consciousness and ophthalmological complications including optic atrophy, pigmentary retinopathy, and ophthalmoplegia[239,378]. Finally, depression, bipolar disorder, anxiety, psychosis and personality changes can also appear in MELAS patients[400].

- ***Muscular manifestations.*** MELAS syndrome is characterised by myopathy associated with exercise intolerance and muscle weakness[240]. At histologic level, the examination of muscle tissue can reveal vacuolated muscle fibers with clear surrounding rim by using haematoxylin and eosin staining, and/or RRFs by using the Gomori trichrome staining. RRFs also stain with the succinate dehydrogenase (SDH) stain giving the appearance of ragged blue fibers. Unlike other mitochondrial diseases, most of the RRFs in MELAS stain positively with the cytochrome c oxidase (COX). In MELAS syndrome, the COX stain of muscle tissue can be decreased, normal, or increased which may reflect variable m.3243A>G heteroplasmy in different muscle fibers (**Figure I11**)[384]. In addition, mitochondrial proliferation is typically observed in smooth muscle and endothelial cells with the SDH stain. At biochemical level, analysis of respiratory chain enzymes in muscle extracts usually shows multiple partial defects[239,240,384].

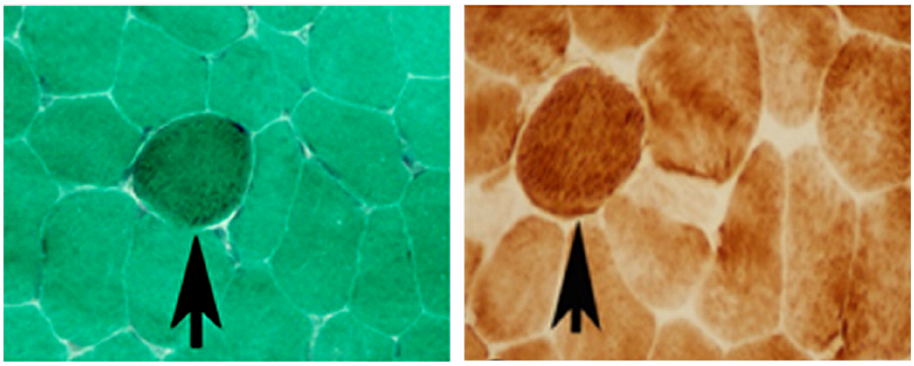

Figure I11. Histopathologic examination of muscle tissues derived from MELAS patients. Arrows indicates ragged red fiber with modified Gomori trichrome and cytochrome c oxidase histochemistry, respectively. ***Adapted from El-Hattab, A. W. et al (2015)[384].***

- ***Lactic acidemia.*** As commented, along with neuropathic and myopathic features, lactic acidemia is other cardinal sign present in affected MELAS individuals. Whereas asymptomatic patients of MELAS syndrome can present normal levels of lactate in serum or cerebrospinal fluid, lactate is often elevated in the majority of affected individuals[239,378].
- ***Cardiac manifestations.*** Cardiac abnormalities like congestive heart failure,

cardiac conduction blockage or hypertrophic cardiomyopathies occur in around 20% of MELAS patients. Non-obstructive concentric hypertrophy[240] and others cardiac conduction abnormalities like Wolff–Parkinson–White syndrome has been also associated with MELAS syndrome[401].

- ***Gastrointestinal manifestations.*** Recurrent or cyclic vomiting is the most common observed gastrointestinal alteration in MELAS syndrome. Diarrhoea, constipation, gastric dysmotility, intestinal pseudo-obstruction, and recurrent pancreatitis have also been reported in MELAS syndrome[240,402].
- ***Endocrine manifestations.*** Diabetes in MELAS syndrome manifests in 30% of individuals and can be type 1 or type 2 in nature. Whereas individuals with type 2 diabetes can initially be treated by diet or sulfonylurea, patients with insulinopenia require insulin treatment[403]. On the other hand, individuals with MELAS syndrome present a shorter stature than their unaffected family members likely due to a growth hormone deficiency, which has occasionally been found in individuals with MELAS syndrome[240,404]. In fact, cases of hypothyroidism, hypogonadotropic hypogonadism, and hypoparathyroidism have been detected in MELAS patients[405].
- ***Other manifestations.*** Renal manifestations of MELAS syndrome include Fanconi proximal tubulopathy, nephrotic range proteinuria, and focal segmental glomerulosclerosis[406]. Pulmonary hypertension has been rarely reported in individuals with MELAS syndrome[407,408]. At dermatological levels, vitiligo and diffuse erythema with reticular pigmentation, are infrequently manifested in MELAS syndrome[409,410]. Finally, chronic anaemia has been also detected in individuals with MELAS syndrome[411].

Pharmacological options

Currently, no curative treatments are available for mitochondrial diseases. In particular for MELAS, no therapeutic protocol has been approved by the Food and Drug Administration (FDA). So far, symptomatic management with mitochondrial cocktails derived from limited clinical trials seem to form the basis of therapeutic care for MELAS patients. In fact, multiple pharmacologic options have been tested, but with differing levels of success. Most treatment strategies for mitochondrial disease have been designed to increase respiratory chain activity and mitigate its dysfunction; and indeed several supplementations, including antioxidants and cofactors, are being used in MELAS syndrome based on limited clinical trials[355,385]. In Table I3 the current treatments, dosage and mechanism for MELAS syndrome are summarised[240,385]. Here below, we highlight some of them:

- ***Coenzyme Q_{10}.*** Since Festenstein and Crane discovered CoQ in 1955[412,413], multiple contributions has been made about its biosynthesis and functions. Coenzyme Q_{10} (CoQ) is a lipid-soluble and mobile molecule present in cell membranes, mainly in the inner mitochondrial membrane where plays a prominent role in the mitochondrial respiratory chain. CoQ is an essential intermediate transferring electrons from complex I and II to complex III resulting in the proton gradient whereby ATP synthase generates ATP. Thus, CoQ participates in every cell to

synthesise energy. In addition to electron carrier, CoQ works as a ROS scavenger[414,415]. CoQ molecule continuously suffers an oxidation–reduction cycle. In its reduced form, the CoQ can lose electrons which are accepted by reactive molecules preventing oxidative damage and lipid peroxidation[416]. The presence of CoQ has been demonstrated in all cell membranes and in blood where it is endued with antioxidant properties[417]. CoQ was also recognized to have a role in stabilisation of the mitochondrial permeability transition pore[418] and an effect on gene expression[419,420]. Moreover, CoQ can stimulate cell growth, inhibit apoptosis, control of thiol groups, form hydrogen peroxide and control of membrane channels[421–423]. Since 1989, multiple CoQ deficiencies have been associated with alterations in MRC and severe manifestations in patients[249,369,414,424–429]. Some studies showed beneficial effects on muscle weakness, fatigability, and lactate level for CoQ in individuals with MELAS syndrome[430,431] and so far, no significant adverse reactions have been reported. Other potential effects of CoQ include a reduction of serum lactate and pyruvate levels, improvement in cardiac conduction defects and eye movements, reduced muscle weakness, improved tolerance and oxygen utilization during exercise, reduced peripheral nerve damage, and improved neurologic function[432]. Molecular mechanisms whereby CoQ induces pleiotropic effects has yet to be completely understood[433]. Recent studies suggested that CoQ might participate in AMPK activation[434–438], however, how CoQ induces AMPK activation is unclear. The dosage ranges between 200-600 mg/day in adults and 2-15 mg/kg/day in paediatric patients[355,439]. Patients taking statins may require higher doses because CoQ biosynthesis is reduced by statins[440]. Interestingly, the ability of CoQ to cross the blood–brain barrier seem to be controversial. Nearly all CoQ supplements enter the bloodstream. But, only CoQ supplements with special formulations have been scientifically shown to enter the mitochondria and cross the blood-brain barrier[441]. On the other hand, its analogue, idebenona, can cross it and improve neurological complications[442,443].

- ***Riboflavin.*** Riboflavin (vitamin B_2) is often considered first-line agents in the treatment of MELAS syndrome[385]. Riboflavin is a precursor of flavin adenine dinucleotide (FAD) and flavin mononucleotide. As prosthetic groups, they are essential for the activity of flavoenzymes including oxidases, reductase and dehydrogenases[444] and function as cofactors in complexes I and II of the MRC[432]. By increasing these substrates, the process of oxidative phosphorylation can be increased to ultimately enhance ATP production[385]. In addition, riboflavin also has antioxidant activity which is mainly derived from its role as a precursor of FAD and reduced glutathione[445], a cofactor of a major antioxidant enzyme, selenium-containing glutathione peroxidase. Oral doses in adult and children range from 50-400 mg/day. Whereas no adverse reaction with doses less than 200 mg/day was

Treatment	Adult Dosage	Pediatric Dosage	Mechanism
L-Arginine	Acute stroke: 500 mg/kg i.v. q6h for 1–3 days Maintenance: 150–300 mg/kg/day p.o. or i.v. in 2–3 divided doses	Same as adult dosage	Vasodilation, increases nitric oxide synthesis
Ascorbic acid (vitamin C)	250–4000 mg/day p.o. in 1–3 divided doses	5 mg/kg/day p.o. in 1–3 divided doses	Antioxidant; improves mitochondrial energy transport
Cytochrome c	6.25 mg i.v. q.d.	No data available	Augments mitochondrial respiratory chain function
Coenzyme Q_{10}	200–600 mg p.o. q.d.	2–15 mg/kg/day p.o. in 2 divided doses	Antioxidant; electron carrier in the mitochondrial respiratory chain
Corticosteroids	Dexamethasone 12–16 mg/day p.o. in 2–4 divided doses Prednisone 2–4 mg/kg p.o. q.d. Methylprednisolone 1 g p.o. q.d.	No data available	Exact mechanism unknown; may stabilize mitochondrial membranes by modulating peroxidation of phospholipids and inhibiting phospholipases
Creatine	20 g/day p.o. for 2 wks followed by 2–10 g/day p.o. in 2 divided doses	100 mg/kg/day p.o. in 2 divided doses	Phosphate donor, regenerates ATP
Idebenone	90–270 mg p.o. q.d.	Same as adult dosage	Antioxidant; electron carrier in the mitochondrial respiratory chain
Levocarnitine	100–1000 mg p.o. or i.v. b.i.d.–t.i.d. (maximum 3 g/day); i.v. infusion: 100–300 mg/kg/day in 4–6 divided doses	50–100 mg/kg/day p.o. or i.v. in 2–3 divided doses (maximum 3 g/day)	Facilitates fatty acid transport into the mitochondria; replaces carnitine stores
Menadione (vitamin K_3)	40–80 mg p.o. q.d.	No data available	Stimulates oxygen utilization in the mitochondria
Nicotinamide (vitamin B_3)	50–500 mg p.o. q.d.	50 mg p.o. q.d.	Cofactor for electron transport in mitochondrial respiratory chain
Riboflavin (vitamin B_2)	50–400 mg p.o. q.d.	Same as adult dosage	Cofactor for electron transport in mitochondrial respiratory chain
Sodium dichloro-acetate	25–50 mg/kg/day p.o. in 2 divided doses	Same as adult dosage	Reduces conversion of pyruvate to lactate
Succinate	6 g p.o. q.d.	No data available	Augments mitochondrial respiratory chain function
Thiamine (vitamin B_1)	50–300 mg p.o. q.d.	Same as adult dosage	Cofactor for electron transport in mitochondrial respiratory chain
Thiocitic acid (α-lipoic acid)	200–600 mg/day p.o. in 3 divided doses	Same as adult dosage	Antioxidant
α-Tocopherol (vitamin E)	400–1200 IU/day p.o. in 1–3 divided doses	1–2 IU/kg/day p.o. in 1–3 divided doses	Scavenges free radicals and maintains membrane integrity by inhibiting lipid peroxidation

Table I3. Pharmacologic Treatment Options for MELAS syndrome. Treatments, dosage,

Treatment	Adverse Effects	Potential Benefits
L-Arginine	i.v. formulation: hypotension, headaches, metabolic acidosis p.o. formulation: nausea, vomiting	May reverse stroke-like symptoms in acute exacerbations; may reduce the frequency and severity of stroke-like episodes with maintenance therapy
Ascorbic acid (vitamin C)	Doses > 3 g/day may cause diarrhea; prolonged high doses may cause kidney stones	Marked improvement in recovery from exercise
Cytochrome c	None reported	May improve fatigue and severity of stroke-like symptoms
Coenzyme Q_{10}	None reported	May improve muscle strength, exercise tolerance, and cognitive function
Corticosteroids	Headache, edema, immunosuppression, glucose intolerance, nausea, vomiting	Benefit in acute phase; may help resolve acute neurologic symptoms
Creatine	Use with caution in patients with renal dysfunction; gastrointestinal distress	May improve muscle strength and exercise tolerance
Idebenone	Gastrointestinal complaints, headache, drowsiness, anxiety, tachycardia	May improve or prevent stroke-like episodes
Levocarnitine	Diarrhea with high oral doses, fishy odor; long-term use of high doses in patients with renal dysfunction can result in accumulation of toxic metabolites	May improve encephalopathy and myopathy
Menadione (vitamin K_3)	May produce hemolytic anemia, kernicterus, and hyperbilirubinemia; contraindicated in newborns, pregnant women, and patients taking warfarin	Symptomatic improvement, increased energy, and improved exercise tolerance
Nicotinamide (vitamin B_3)	Elevated liver function tests, nausea, vomiting, diarrhea, dizziness, headache, flushing	May improve cognitive symptoms and exercise tolerance
Riboflavin (vitamin B_2)	Abdominal pain, nausea and vomiting with high doses (> 200 mg/day)	May improve neurologic symptoms and exercise capacity
Sodium dichloro-acetate	Peripheral neuropathy, liver dysfunction	Prevents development of lactic acidosis
Succinate	None reported	May prevent stroke-like episodes
Thiamine (vitamin B_1)	None reported	May improve neurologic symptoms
Thiocitic acid (α-lipoic acid)	None reported	Improved energy utilization
α-Tocopherol (vitamin E)	None reported	May improve enzyme function or slow oxidative damage

mechanism, adverse effects and potential benefits. ***Adapted from Santa K. M. (2010)[385].***

reported, higher doses can lead to abdominal pain, nausea, and vomiting[295,355,385,432].

- ***AICAR.*** Even though no reported in Table I3 as treatment for MELAS patients, 5-aminoimidazole-4-carboxamide 1-b-D-ribofuranoside (AICAR) is being recently used to increase oxidative metabolism and mitochondrial biogenesis in mice[209,446,447], and presumably might benefit patients of mitochondrial diseases. AICAR is an AMP analogue that activates allosterically AMPK[209]. AICAR is transported into cells by adenosine transporters and metabolized by adenosine kinase to 5-aminoimidazole-4-carboxamide 1-b-D-ribofuranosyl monophosphate (ZMP), which mimics all the effects of AMP on the AMPK system[448]. ZMP then functions like endogenous AMP by binding to the CBS/Bateman domains of γ subunits and promoting allosteric activation of the kinase[449]. The action mechanism of AICAR is similar to that of AMP: it interacts with AMPK through the AMP-binding domain with the formation of hydrogen bonds by the hydroxyl groups of the ribose moiety[450]. Importantly, AICAR does not alter endogenous levels of AMP or ATP[451] but can activate other AMP-sensitive enzymes, including glycogen phosphorylase[446] and fructose-1,6-bisphosphatase[452]. Moreover, due to its potent effect as metabolic modulator, AICAR was reported as prohibited drug by the World Anti-Doping Agency in 2009[453].
- ***Others.*** L-arginine therapy can be beneficial in treatment and prevention of stroke-like episodes. Intravenous infusion or oral supplementation of L-arginine decrease the frequency and severity of stroke-like episodes[454,455]. The therapeutic effect of arginine in stroke-like episodes seems to be related with the increase of nitric oxide availability that improves intracerebral vasodilation and blood flow. Citrulline supplementation to MELAS patients also induces nitric oxide production, therefore, citrulline emerges as possible therapeutic treatment[456]. Creatine is metabolized to phosphocreatine, which is an essential phosphate donor for ATP regeneration in muscle and brain. Creatine monohydrate supplementation seems to increase the strength of high-intensity anaerobic and aerobic activities in individuals with MELAS syndrome and other mitochondrial cytopathies[457]. Other therapies including the combination of creatine monohydrate, CoQ, and lipoic acid resulted in improved muscle strength and lower plasma lactate in MELAS individuals[458]. On the other hand, hearing loss has been treated by surgery with cochlear implants[459]. Traditional anticonvulsant and analgesic drugs can be used for seizures and headaches, respectively. Cardiac manifestation can be treated by standard pharmacologic therapy and diabetes can be managed by dietary modifications with supplementation of insulin if required[384]. Children failing to thrive often need nutrition support and rehabilitation after stroke-like episodes. Regular exercise and training can induce mitochondrial biogenesis and transferring normal mitochondrial templates from satellite cells to mature muscle that may lower the mutation heteroplasmy[384,460].

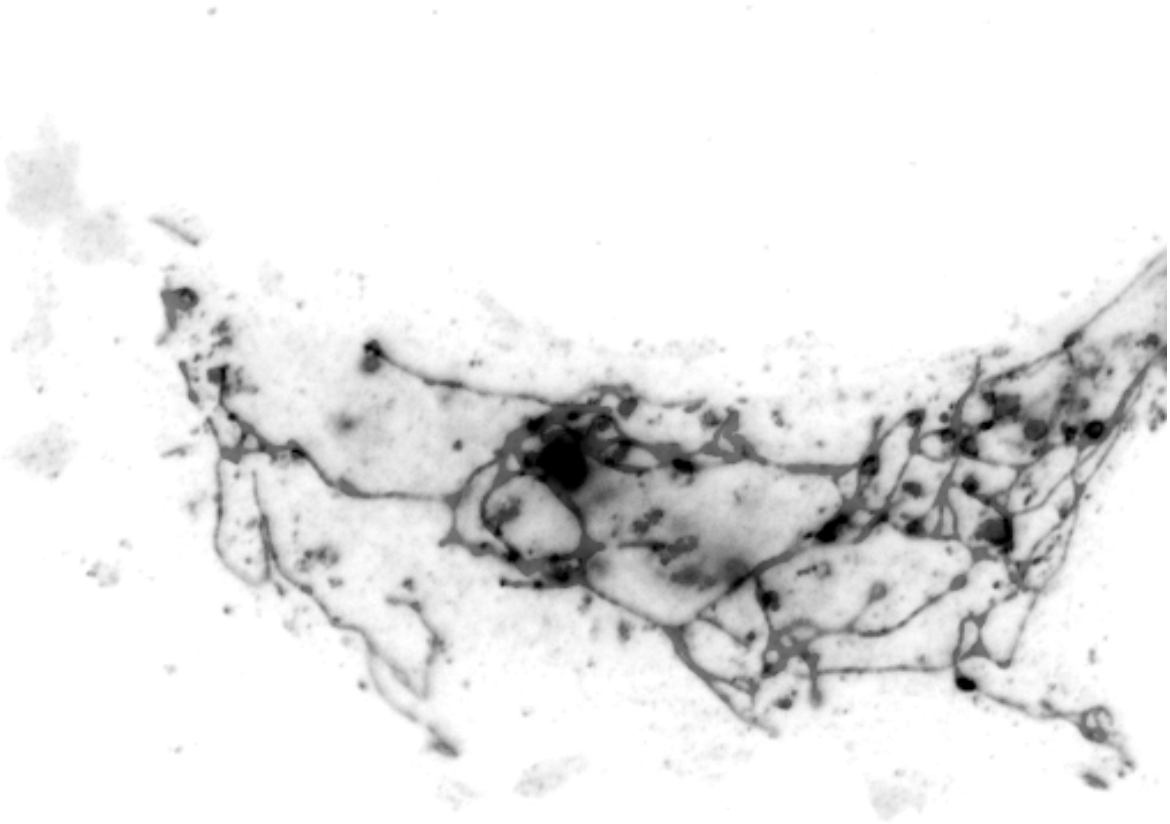

AIMS

AIMS

MELAS is a mitochondrial disease caused mainly by the m.3243A>G mutation in mtDNA. Currently, the molecular mechanisms involved in this disorder are not fully understood. This thesis arises from the pathophysiological differences found in primary fibroblast derived from patients diagnosed with MELAS syndrome. Considering the interest and significance of this differential phenotype, we decided to further explore the physiopathological alterations in MELAS cell lines. Given the low prevalence of the disease and the lack of effective treatment, cellular models of MELAS disease are indispensable tools for both the pathophysiological characterization and the screening of new treatments.

To this end, we proposed the following aims:

1. To characterise and compare the pathophysiology of primary fibroblasts derived from MELAS patients harbouring the m.3243A>G mutation.

2. To evaluate the molecular mechanisms involved in the different patterns of physiopathological alterations in MELAS fibroblasts.

3. To confirm the physiopathological alterations in transmitochondrial cybrids harbouring the m.3243A>G mutation.

4. To set up a screening platform to evaluate the effectiveness of pharmacological compounds for the treatment of MELAS syndrome.

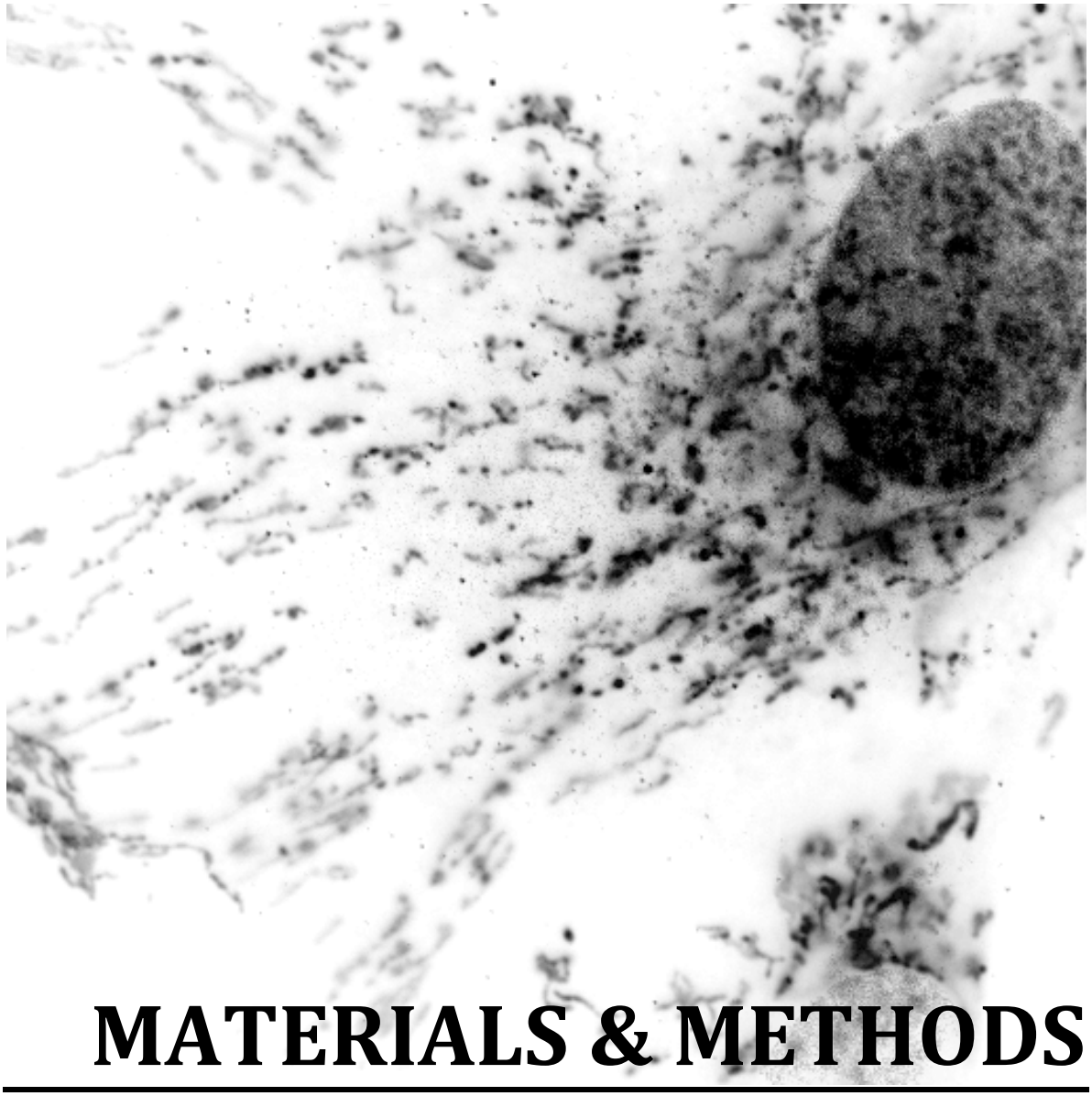

MATERIALS & METHODS

MATERIALS & METHODS

M-I. Reagents

We purchased the following antibodies and chemicals from:

- *BD Biosciences Pharmingen (San Jose, CA, USA):* Anti-cytochrome c antibody.
- *Biosensis (South Australia, Australia):* Anti-hATG12 antibody.
- *Bio-Rad Laboratories Inc. (Hercules, CA, USA):* SDS, Immun Star HRP substrate kit, agarose, Triton X-100, acrylamide/bisacrylamide, running buffer (TGS), transfer buffer (TG), Tween-20 and non fat dry milk.
- *Boehringer Mannheim (Indianapolis, IN, USA):* cocktail of protease inhibitors.
- *Calbiochem-Merck Chemicals Ltd. (Nottingham, UK):* Anti-GAPDH monoclonal antibody, clone 6C5.
- *Cell Signalling Technology (Danvers, MA, USA):* Anti Mn-SOD.
- *EMD, Millipore, (Darmstadt, Germany): Millipore* Immobilon Western Chemiluminescent HRP Substrate.
- *Fermentas (Burlington, Ontario, Canada):* Apa I enzyme.
- *iNtRON Biotechnology (Korea):* Redsafe nucleic acid staining solution.
- *Invitrogen/Molecular Probes (Eugene, OR, USA):* Monoclonal antibodies specific for oxidative phosphorylation, complex III (Core 1 subunit), complex II (30 kDa subunit I), MitoSOX™, NaO, TMRE, MitoTracker® Red CMXRos, JC-1 dye, LysoTracker® Red DND-99, Hoechst 3342, ATP determination kit (A22066), ADP/ATP Ratio Assay Kit (MAK135), NativePAGETM Running Buffer and NativePAGETM Cathode Buffer.
- *Miltenyi Biotec GmbH (Teterow, Germany):* Mitochondria Isolation Kit using magnetic microbeads.
- *Panreac (Barcelona, Spain):* potassium acetate, 2-propanol, ethanol, Sacarose, n-hexane, methanol, n-propanol, lithium perchlorate, sodium chloride, Tris-base, Ammonium persulfate (APS), glacial acetic acid, KOH and KCl.
- *R&D System (Minneapolis, MN, USA):* Anti-phospho-AMPK and Anti-Phospho-PGC-1α AF6650.
- *Santa Cruz Biotechnology (Santa Cruz, CA, USA):* Anti-MAP LC3 (N-20), anti-catalase (H-300), anti-Cathepsin D, anti-PGC-1α, anti-mtTFA, anti-NFR1, anti-ULK1, anti phospho-ULK1 and anti-AMPK.
- *Sigma-Aldrich (St. Louis, MO, USA):* Monoclonal Anti-Actin antibody, Anti-α-tubulin and anti-porin antibodies, FCCP, uridine, riboflavin, compound C, Coenzyme Q_{10}, AICAR, trypsin-EDTA solution, fetal bovine serum (FBS), fenol:cloromormo:IAA solution, trypan blue solution, digitonin, MOPS, EDTA, sodium deoxycholate, TEMED, pounceau reagent, Phosphate-buffered saline (PBS), HEPES, $MgCl_2$, glycerol, EDTA, DTT, PMSF, NaF, sodium orthovanadate, paraformaldehyde, saponin, glutaraldehyde and Na Cacodylate.
- *Vector Laboratories (Burlin-game, CA, USA):* Vectashield mounting medium.

M-II. Fibroblast cultures

Samples from patients and controls were obtained according to the Helsinki Declarations of 1964, as revised in 2001. Cultured fibroblasts were derived from skin biopsies of several healthy donors and five different diagnosed MELAS patients (MELAS 1, MELAS 2, MELAS 3, MELAS A and MELAS B). Genetic analysis were performed and all patients harboured the heteroplasmic m.3243A>G mutation. The heteroplasmy load analysis showed that MELAS 1, MELAS 2 and MELAS 3 harboured higher mutation load than MELAS A and MELAS B fibroblasts (MELAS 1: 17%, MELAS 2: 26%, MELAS 3: 43%, MELAS A: 9% and MELAS B: 4%). We verified that heteroplasmy load did not shift significantly during this work. As controls, age-/sex-matched fibroblasts at similar low passage number were derived from healthy volunteers. Overall, control data were shown as a mean of two control fibroblast cultures. Fibroblasts from the MELAS patient and controls were cultured at 37 °C and 5% CO_2 in DMEM containing 4.5 $g \cdot L^{-1}$ glucose, L-glutamine, and pyruvate supplemented with an antibiotic/antimycotic solution Glucose (GIBCO Life technologies, UK) and 20% fetal bovine serum.

M-III. Construction and culture of transmitochondrial cybrid cell lines

Transmitochondrial cybrids were a gift from Sandra Jackson from Department of Neurology of Medical Faculty Carl Gustav Carus (Dresden University of Technology, Dresden, Germany). Methodology to generate transmitochondrial cybrids is described below. Transmitochondrial MELAS cybrids were generated by fusing enucleated fibroblasts from MELAS patients or controls with 143B osteosarcoma cells which lack mtDNA (rho° cells), using the method described by King and Attardi (1989)[461]. These cells thus possess mtDNA from MELAS patients or controls in a control nuclear background. Both control cybrid cells (100% Wt at nucleotide position 3243) and MELAS cybrid cells harbouring the m.3243A>G mutation (89,6% heteroplasmy at nucleotide position 3243) were cultured at 37 °C and 5% CO_2 in DMEM containing 4.5 $g \cdot L^{-1}$ glucose, supplemented with 5% FBS, 100 $mg \cdot mL^{-1}$ sodium pyruvate, 50 $\mu g \cdot mL^{-1}$ uridine (Sigma-Aldrich, St. Louis, MO, USA) and 1% antibiotic/antimycotic solution (PAA Laboratories GmbH, Austria). We verified that the heteroplasmy load in MELAS cybrids did not shift significantly during the study.

M-IV. Treatments

During the conduction of this thesis, both fibroblasts and transmitochondrial cybrids were used to test the effect of several drugs on pathophysiological parameters (60 nM riboflavin, 100 μM CoQ_{10} and 100 μM AICAR). No confluent fibroblast cultures were exposed to these drugs at 37 °C during 1 week whereas the cybrid cells were incubated during 48 hours. The pharmacological inhibition of AMPK was achieved with 10 μM compound C 24 hours before collecting cells and the pharmacological blockage of autophagic flux was achieved with 100 nM bafilomycin A1. In cybrids, to make more evident the mitochondrial defects and discard compensatory effects by other pathways, during treatments they were cultured in a glucose-restricted medium

using DMEM 2,5 g·L^{-1} Glucose (GIBCO Life technologies, UK) supplemented with 2% FBS.

M-V. Measurement of mutant heteroplasmy

Heteroplasmy was determined by PCR-RFLP. DNA was extracted from fibroblasts and cybrids using standard methods. Cellular pellets were lysed in 1% SDS buffer at 65 °C for 30 minutes. DNA was extracted using fenol:cloromormo:IAA solution. The aqueous upper phase was extracted and DNA was precipitated by adding 5 M potassium acetate and 2-propanol. After precipitation, DNA was washed with ethanol and dried in a speed-vac system (Savant SPD111V, Thermo Scientific). Finally, DNA was diluted in TE buffer and quantified in a NanoDrop instrument (Thermo Scientific, Waltham, MA, USA). DNA amplification was performed by using the following primers pair:

Reverse primer: 5'-AGTAATGTTGATAGTAGAAT-3'
Forward primer: 5'-ATTTATTAATGCAAACAGTA-3'

PCR conditions for all reactions were 94 °C for 5 minutes, 35 cycles with denaturation at 94 °C for 35 seconds, annealing at 55 °C for 35 seconds and elongation at 72 °C for 1 minute; 1 cycle at 72 °C for 7 minutes, and a final hold at 4°C. After PCR, the amplicon was digested with Apa I enzyme (Fermentas, Burlington, Ontario, Canada) for 5 hours at 37 °C and DNA fragments were separated in 1% agarose gel. Gels stained with RedSafe nucleic acid staining solution (iNtRON Biotechnology, INC., Korea) and placed on a UV light transilluminator. Digested products were visualized and analysed by using ImageJ software.

M-VI. Proliferation assay

Cells were seeded in 6-well 35 mm plates. Several pictures of different 20X-fields were taken by using a conventional microscope. Cells were counted by using ImageJ software before and after treatments in order to analyse cell growth. To measure proliferation rate, we seed a known initial number of cells (N_0) and after treatment, cells were harvested and quantified (N) by using a conventional Neubauer counter chamber. Cell viability was assessed by trypan blue exclusion. Proliferation rate (n) was calculated by using the formula $N=N_0x2^n$. Results are expressed as mean ± SD.

M-VII. Lysosomal content assay

Cells were cultured in 6-well 35 mm plate until confluence and incubated for 30 minutes with 100 nM LysoTracker® Red DND-99 (Invitrogen/Molecular Probes), a fluorophore which is concentrated in cell acidic vacuoles. After incubation cells were then washed twice with PBS and harvested by trypsinization. The emitted red fluorescence was measured by flow cytometry (FACScalibur™, BD Biosciences, San Jose, CA, USA). Results are expressed as mean ± SD.

M-VIII. Measurement of intracellular generation of reactive oxygen species (ROS)

Mitochondrial superoxide is generated as a by-product of oxidative phosphorylation. In an otherwise tightly coupled electron transport chain, approximately 1–3% of mitochondrial oxygen consumed is incompletely reduced; those "leaky" electrons can quickly interact with molecular oxygen to form superoxide anion, the predominant ROS in mitochondria.[22–25] Increases in cellular superoxide production have been implicated in cardiovascular diseases, including hypertension, atherosclerosis, and diabetes-associated vascular injuries,[25–27] as well as in neurodegenerative diseases such as Parkinson's, Alzheimer's, and amyotrophic lateral sclerosis.[22,28–31]

Since it is assumed that mitochondria serve as intracellular source of ROS, flow cytometric analysis of the intracellular generation of ROS was performed by using MitoSOX™ Red mitochondrial superoxide indicator (Invitrogen/Molecular Probes, Eugene, OR, USA), which is a novel fluorogenic dye for highly selective detection of superoxide in the mitochondria of live cells. MitoSOX™ Red reagent is live-cell permeant and is rapidly and selectively targeted to the mitochondria. Once in the mitochondria, MitoSOX™ Red reagent is oxidized by superoxide and exhibits red fluorescence. MitoSOX™ Red reagent is readily oxidized by superoxide but not by other ROS– or RNS–generating systems, and oxidation of the probe is prevented by superoxide dismutase.

Cells were cultured in 6-well 35 mm plates and, at confluence, incubated with 5 μM MitoSOX™ Red for 30 minutes at 37°C. After incubation cells were harvested by trypsinization, washed twice with fresh medium and analysed by flow cytometry (FACScalibur™, BD Biosciences, San Jose, CA, USA). As MitoSOX™ Red has mitochondrial localization, ROS levels were expressed relative to the mitochondrial mass (ROS signal/NAO signal). Results are expressed as mean ± SD.

M-IX. ATP assays

ATP levels were quantified in two different ways: Total ATP amount and ATP/ADP ratio. Firstly, ATP was measured by using a kit for quantitative determination of ATP (Molecular Probes, OR, USA). Samples were lysed and measured in a Tuner Designs Luminometer TD 20/20 (Sunnyvale, CA, USA) by adding 10% homogenate volume to Reaction buffer (1X Component E, 1 mM DTT, 0.5 mM D-luciferin, 1.25 mg/ml luciferase). Background luminescence was always subtracted. First, a standard curve was generated using a series of increasing ATP concentrations, and secondly experimental samples were measured. The amounts of ATP were calculated extrapolating the bioluminescent signals in the standard curve.

Moreover, ATP/ADP ratio was obtained by using another luciferase-based assay, according to the adapted instructions of the manufacturer (ADP/ATP Ratio Assay Kit, Sigma-Aldrich). The assay involves two steps. First, the working reagent lyses cells to release ATP and ADP. In the presence of luciferase, ATP immediately reacts with the substrate D-luciferin to produce light. The light intensity is a direct measure of the intracellular ATP concentration. To do so, culture medium was replaced by ATP

reagent (assay buffer, substract, co-substract, ATP enzyme) for 1 minute at room temperature and RLU (relative light units) was then measured on the luminometer (RLU_A). In the second step, the ADP will be converted to ATP through an enzyme reaction. This newly formed ATP then reacts with the D-luciferin as in the first step. The second light intensity measured represents the total ADP and ATP concentration in the sample. Due to this, after RLU_A measure, the same samples were incubated for 10 minutes and background was measured (RLU_B). Immediately after this, ADP reagent was added and after 1 minute, luminescence was again read (RLU_C). Finally, ATP/ADP ratio was calculated as $RLU_A/(RLU_C-RLU_B)$. Results are expressed as mean ± SD.

M-X. Mitochondrial membrane potential determination

To estimate mitochondrial membrane potential ($\Delta\Psi_m$), control and MELAS fibroblasts were exposed to tetramethylrhodamine ethyl ester (TMRE) (Molecular Probes; Invitrogen, Carlsbad, CA, USA). Approximately 1×10^6 cells were incubated with 100 nM TMRE for 20 min at 37°C, trypsinized, washed twice with PBS, resuspended in 500 µl of PBS, and analysed by flow cytometry (FACScalibur™, BD Biosciences, San Jose, CA, USA). In addition of TMRE, MitoTracker® Red CMXRos (Invitrogen/Molecular Probes) was also used in order to measure $\Delta\Psi_m$. Thus, cells were cultured in 6-well 35 mm plates until confluence. Then, cells were treated for 30 minutes with 100 nM MitoTracker reagent and after incubation cells were harvested, washed with PBS and analysed by flow cytometry. Results are expressed as mean ± SD.

Because depolarized or inactive mitochondria decrease membrane potential and fail to sequester TMRE, we verify our results by using 5,5', 6,6'-tetrachloro-1,1'3,3'-tetraethylbenzimidazolecarbocyanine iodide (JC-1; Molecular Probes, Inc., Eugene, OR). This cyanine dye accumulates in the mitochondrial matrix under the influence of the $\Delta\Psi_m$ and forms J-aggregates, which have a characteristic absorption and emission spectra. Healthy cells with functional mitochondria contain red JC-1 aggregates and are detectable in the FL2 channel, and unhealthy cells with collapsed mitochondria contain mainly green JC-1 monomers and are detectable in the FL1 channel. For flow cytometry, control and MELAS fibroblasts were seeded in 6-wells plate. At confluence, cells were incubated with 0.5 µM JC-1 for 30 minutes. As a positive control for reduction of $\Delta\Psi_m$, a sample treated with the uncoupling agent carbonyl cyanide m-chlorophenylhydrazone (cyanide; 100 mM; Sigma) before labelling with JC-1. After the JC-1 was removed, cells were washed with PBS, harvested by trypsinization, and resuspended in PBS. The amount of JC-1 retained by 10,000 cells per sample was measured at 530 nm (FL1 channel) and 590 nm (FL2 channel) with a flow cytometer (FACScalibur™, BD Biosciences, San Jose, CA, USA). The ratiometric measurement between red and green fluorescence was evaluated to determine $\Delta\Psi_m$ and its behaviour. Results are expressed as mean ± SD.

Finally, to confirm the results of the TMRE, MitoTracker assays and JC-1, cells were treated with MitoTracker® Red CMXRos at the same concentration and

immunostaining was performed. Samples were visualized using a DeltaVision system (Applied Precision; Issaquah, WA, USA) with an Olympus IX-71 microscope.

M-XI. Mitochondrial respiratory chain enzyme activities

Activities of NADH:coenzyme Q1 oxidoreductase (complex I), Succinate dehydrogenase (complex II), cytochrome c oxidase (complex IV), ubiquinol:cytochrome c oxidoreductase (complex III), NADH: cytochrome c reductase (complex I + III), succinate:cytochrome *c* reductase (complex II + III) were determined in cell extracts using spectrophotometric methods previously described[462,463]. Results are expressed as units of activity (U)/citrate synthase activity (CS) (mean ± standard deviation). Proteins of fibroblasts homogenates were determined by the Bradford procedure[464].

Digitonisation

To measure MRC activities on *In vitro* samples, mitochondrial complexes need a proper lipid context to work. To achieve so, a digitonisation step is performed. Thus, samples were lysed by using Buffer A (20 mM MOPS + 0.25 M Sacarose), and 0.2 mg/ml digitonin was added in the same proportion. Samples were picked on ice for 5 minutes and centrifuged for 3 minutes at 5000 g. While the supernatant was discarded, pellet was resuspended in Buffer B (20 mM MOPS + 0.25 M Sacarose + 1 mM EDTA). After 5 minutes more on ice, a 10,000 g centrifugation for 3 minutes was performed and supernatant was discarded. Finally, the pellet was resuspended in 10 mM Buffer KP pH 7.4.

Citrate Synthase

Coefficient (ε) = 13.6 $mM^{-1}cm^{-1}$ λ = 412 nm Temperature = 30 °C

0.75 M Tris-HCl pH 8	100 µl	75 mM
1 mM DTNB	100 µl	100 µM
1% Triton	100 µl	0.1%
7 mg/ml Acetyl CoA	50 µl	350 µg/ml
Homogenate	5 µl	
Distilled water	595 µl	
Agitation and incubation for 2 minutes at 30 °C.		
10 mM Oxalacetate	50 µl	0.5 mM

New agitation and incubation for 30 seconds before measuring wavelength for 2 minutes. Slope (Absorbance per minute after adding oxalacetate) was used to calculate U/l with the following formula: (slope x 1000)/ε/homogenate volume (ml). To obtain specific activity to divide by protein concentration (mg/ml).

Complex I – NADH:coenzyme Q1 oxidoreductase

Coefficient (ε) = 6.81 $mM^{-1}cm^{-1}$ λ = 340 nm Temperature = 30 °C

40 mM Buffer KP pH 8	500 µl	20 mM
1 mM NADH	200 µl	0.2 mM
50 mM NaN_3	20 µl	1 mM
1% BSA-EDTA	100 µl	
Homogenate	50 µl	
Distilled water	120 µl	

Samples were agitated and incubated for 30 seconds and baseline absorbance was measured for 2 minutes.

10 mM CoQ_1	10 µl	100 µM

Agitation and incubation for 2 minutes at 30 °C.

0.25 mM Rotenone	20 µl	5 µM

Finally, samples were newly agitated and incubated for 30 seconds before measuring absorbance for 2 minutes at 30 °C. Rotenone inhibition should rise by 80%. Slope after rotenone inhibition was used to calculate the U/l activity: (Slope x 100 x 0.8 -rotenone inhibition-)/ε/homogenate volume (ml). Specific activity was calculated dividing U/l by protein concentration (mg/ml). To calculate for unit of Citrate synthase, U/l was divided for U/l of Citrate synthase analysis and multiplying by 100.

Complex II – Succinate Dehydrogenase (SDH)

Coefficient (ε) = 19 $mM^{-1}cm^{-1}$ λ = 600 nm Temperature = 30 °C

100 mM Buffer KP pH 7	500 µl	50 mM
30 mM KCN	50 µl	1.5 mM
1 mM DCPIP	100 µl	0.1 mM
Homogenate	40 µl	
Distilled water	210 µl	

Agitation and incubation for 2 minutes at 30 °C.

320 mM Succinate	100 µl	32 mM

Agitation of cuvette, make blank and incubation for 30 seconds before measuring baseline for 2 minutes at 30 °C.

CoQ_1 10 mM	5 µl	50 µM

Finally, samples were newly agitated and incubated for 30 seconds before measuring absorbance for 2 minutes at 30° C.

To calculate SDH activity, the highest slope after adding succinate was used: Slope x 1000 /ε/homogenate volume (ml).

To calculate Complex II activity: the highest slope after adding CoQ_1 was used: Slope x 1000/ε/homogenate volume (ml). Specific activity was calculated dividing U/l by protein concentration (mg/ml). To calculate for unit of Citrate synthase, U/l was divided for U/l of Citrate synthase analysis and multiplying by 100.

Complex III – Ubiquinol:cytochrome c oxidoreductase

Coefficient (ε) = 21 $mM^{-1}cm^{-1}$ λ = 550 nm Temperature = 30 °C

100 mM Buffer KP pH 7.5	500 µl	50 mM
50 mM NaN_3	40 µl	2 mM
1%BSA-EDTA	100 µl	
1 mM Cytochrome c	50 µl	50 µM
± 1 mg/ml Antimycin A	10 µl	50 µM
Distilled water	285 µl (295 µl for non antimycin added)	
10 mM DBH_2	5 µl	50 µM

Agitation of cuvette, make blank and incubation for 30 seconds before measuring baseline for 2 minutes at 30 °C.

Homogenate 10 µl

Finally, samples were newly agitated and incubated for 30 seconds before measuring absorbance for 2 minutes at 30 °C.

To calculate U/l Complex III activity, the difference between the highest slopes before and after adding antimycin was required: Slopes-difference x 1000/ε/homogenate volume (ml). Specific activity was calculated dividing U/l by protein concentration (mg/ml). To calculate for unit of Citrate synthase, U/l was divided for U/l of Citrate synthase analysis and multiplying by 100.

Complex IV – cytochrome c oxidase

Coefficient (ε) = 21 $mM^{-1}cm^{-1}$ λ = 550 nm Temperature = 38 °C

100 mM Buffer KP pH 7	100 µl	10 mM
Reduced 800 µM cytochrome c	100 µl	80 µM
Distilled water	770 µl	

Samples were agitated and incubated for 2 minutes at 38 °C.

Homogenate 30 µl

Samples were newly agitated and absorbance was measured for 2 minutes.

To calculate U/l Complex IV activity, the highest slope for measuring was chosen: Slope x 1000/ε/homogenate volume (ml). Before and after adding antimycin were required: Slope difference x 1000/ε/homogenate volume (ml). Specific activity was calculated dividing U/l by protein concentration (mg/ml). To calculate for unit of Citrate synthase, U/l was divided for U/l of Citrate synthase analysis and multiplying by 100.

Complex I+III – NADH: cytochrome c reductase

Coefficient (ε) = 21 $mM^{-1}cm^{-1}$ λ = 550 nm Temperature = 30 °C

100 mM Buffer KP pH 7.5	550 µl	55 mM
1 mM Cytochrome c	100 µl	100 µM
30 mM KCN	30 µl	900 µM
Homogenate	40 µl	

Distilled water 180 µl
Samples were shaken and incubated for 30 seconds. Baseline was then measured for 2 minutes at 30 °C.
1 mM NADH 100 µl
Samples were newly agitated and absorbance was measured for 2 minutes.
To calculate U/l Complex I+III activity, the highest slope for measuring was chosen: Slope x 1000/ε/homogenate volume (ml). Specific activity was calculated dividing U/l by protein concentration (mg/ml). To calculate for unit of Citrate synthase, U/l was divided for U/l of Citrate synthase analysis and multiplying by 100.

Complex II+III – Succinate:cytochrome c reductase

Coefficient (ε) = 21 $mM^{-1}cm^{-1}$ λ = 550 nm Temperature = 30 °C

100 mM Buffer KP pH 7.5	550 µl	55 mM
1 mM Cytochrome c	100 µl	100 µM
30 mM KCN	30 µl	900 µM
Homogenate	40 µl	
Distilled water	180 µl	

Samples were shaken and incubated for 30 seconds. Baseline was then measured for 2 minutes at 30 °C.
Succinate 30 mM 100 µl
Samples were newly agitated and absorbance was measured for 2 minutes.
To calculate U/l Complex II+III activity, the highest slope for measuring was chosen: Slope x 1000/ε/homogenate volume (ml). Specific activity was calculated dividing U/l by protein concentration (mg/ml). To calculate for unit of Citrate synthase, U/l was divided for U/l of Citrate synthase analysis and multiplying by 100.

M-XII. CoQ determination

Cell samples were lysed with 1% SDS and a mixture of ethanol:isopropanol (95:5). In order to recover CoQ, hexane was added and several centrifugations were performed at 1000 g for 5 minutes at 4°C. The upper phases from three extractions were recovered and dried using a rotary evaporator (BÜCHI, Switzerland). Lipid extracts were suspended in ethanol, dried in a speed-vac system (Savant SPD111V, Thermo Scientific) and stored at -20°C up to the HPLC analysis. Lipid components were separated by a Beckmann 166–126 HPLC system equipped with a 15-cm Kromasil C-18 column in a column oven set to 40°C, with a flow rate of 1 ml/minute and a mobile phase containing 65:35 methanol/isopropanol and 1.42 mM lithium perchlorate. CoQ levels were analysed with ultraviolet (System Gold 168), electrochemical (Coulochem III ESA) or radioactivity (Radioflow Detector LB 509, Berthod Technologies) based detectors as necessary. Coenzyme Q_9 (CoQ_9) was used as an internal standard and CoQ content was expressed as pmol/mg protein[99].

M-XIII. Mitochondrial mass

To measure mitochondrial mass we follow-up two strategies. First, mitochondrial mass was determined by flow cytometry by using Nonyl-Acridine orange (NAO)[465] as a probe, which specifically binds to cardiolipin and it is used to estimate mitochondrial mass. This lipid constitutes about 20% of the total lipid composition in mitochondria[10].

Cells were seeded in 6-well 35 mm plates up to confluence and were stained with 10 μM NAO for 10 minutes at 37°C in the dark. After staining, cells were washed with PBS, collected and analysed by flow cytometry (FACScalibur™, BD Biosciences, San Jose, CA, USA). However, it has been reported that NAO fluorescence is dependent upon mitochondrial membrane potential[466]. To determine whether NAO binding was dependent on mitochondrial potential, NAO fluorescence was determined in the absence and presence of the uncoupler FCCP (1μM).

On the other hand, mitochondrial mass was estimated by measuring citrate synthase activity. Cellular homogenates were incubated for 2 minutes with a solution 75 mM Tris-HCl pH 8, 1 mM DTNB, 0.1% Triton X-100 and 350 mg/ml acetyl CoA. After incubation, 500 μM oxaloacetate was added. The increase in absorbance was used to calculate citrate synthase activity[462,467]. Slope (Absorbance per minute after adding oxalacetate) was used to calculate U/l with the following formula: (slope x 1000)/ε/homogenate volume (ml). To obtain the specific activity is needed to divide by protein concentration (mg/ml).

M-XIV. Immunoblotting assay

Western blotting was performed by using standard methods. Samples were lysed with different lysis buffer according to our porpoises: for membrane proteins by using RIPA buffer [50 mM Tris-HCl, 150 mM sodium chloride, 1.0% Triton X-100, 0.5% sodium deoxycholate, 0.1% SDS, pH 8.0] and for cytoplasmic proteins by using a standard lysis buffer (50 mM Tris-HCl, 1% Triton X-100, 150 mM sodium chloride, pH 8.5). Proteins were quantified by Bradford assay[464] and separated in SDS-PAGE gels (12.5% acrylamide/bisacrylamide, 0.375 M Tris-HCl pH 8.8, 0.10% SDS, 0.10% TEMED and 0.10% APS) at 120 V (or 35 mA per gel) in running buffer TGS (25 mM Tris, 190 mM glycine, 0.1% SDS, pH 8.3). Transference of proteins to nitrocellulose membrane (Hybond-ECL, Amerscham Biosciences) was performed with a Trans-Blot SD Semi-Dry system (Bio-Rad, USA) at 25V for 1 hour using transfer buffer TG (25 mM Tris, 190 mM glycine, 20% methanol, pH 8.3). After transference, Pounceau staining was performed to check the transfer quality. 0.2% Pounceau S in 5% glacial acetic acid for 2 minutes was used to stain and three washes with 0.05% T-TBS to rinse off. Blocking step was performed with 5% non-fat dry milk in 0.05% T-TBS (blocking buffer) at room temperature for 1 hour. Membranes were incubated with primary antibody at the appropriate dilution (1:200-1:1000) in blocking buffer with gentle agitation overnight at 4°C. Three washes with 0.05% T-TBS were performed to remove the unbound antibody and afterwards species appropriate HRP-conjugated secondary antibody (1:2500) in blocking buffer was then used to detect the protein of

interest with gentle agitation for 1-2 hours at room temperature. Finally, three washes more were performed with 0.05% T-TBS and proteins of interest were identified using the Immun Star HRP substrate kit (Bio-Rad Laboratories Inc., Hercules, CA, USA) or Millipore Immobilon Western Chemiluminescent HRP Substrate (EMD, Millipore, Darmstadt, Germany). ChemiDoc™ MP System was used to visualise signals in membranes.

M-XV. Blue-native PAGE (BN-PAGE) and Immunoblotting

Functional pure mitochondria from control and MELAS fibroblasts were isolated by a Mitochondria Isolation Kit using magnetic microbeads (Miltenyi Biotec GmbH, Teterow, Germany). Cells were partially lysed and mitochondria were magnetically labelled with Anti-TOM22 Microbeads. The monoclonal anti-TOM22 antibody specifically binds to the translocase of outer mitochondrial membrane 22 (TOM22) of human mitochondria. Then, the labelled cell lysate was loaded onto a MACS Column, which was placed in the magnetic field of a MACS Separator. The magnetically-labelled mitochondria are retained within the column. The unlabelled organelles and cell components run through. After removing the column from the magnetic field, the magnetically retained mitochondria can be eluted. The BN-PAGE system was used for separation of mitochondrial respiratory complexes on 4–16% polyacrylamide gradient gels; 20 mg of the total solubilized protein were electrophoresed for 90 min at 150 V in NativePAGETM Running Buffer and NativePAGETM Cathode Buffer. Proteins were electro-transferred onto a nitrocellulose membrane for 1 h at 25 V. We used monoclonal antibodies for complex I (39 kDa subunit), complex II (70 kDa subunit), complex III (core 2 subunit), complex IV (COX II subunit) and complex V (aF1F0-ATPase) diluted 1:1000 (Molecular Probes, Invitrogen). An antibody against porin, a housekeeping mitochondrial protein, was used as loading control. The secondary antibody was monoclonal anti-mouse IgG horseradish (Amersham Biosciences) diluted 1:1000. Immun Star HRP substrate kit (Bio-Rad Laboratories Inc.) was used to detect the proteins according to the manufacturer's instructions.

M-XVI. Cell fractionation and isolation of nuclear proteins

Cells were grown in several T-175 flasks for having large amounts of cells. After treatments, cells were pelleted and washed using buffer A (10 mM HEPES-KOH pH 7.9, 15 mM $MgCl_2$, 10 mM KCl). Then, cells were centrifuged 5 minutes at 13,000 rpm at 4 °C. While supernatant was discarded (cytoplasmic proteins), the pellet was resuspended in buffer B (20 mM Hepes-KOH pH 7.9, 1.5 mM $MgCl_2$, 25% glycerol, 0.2 mM EDTA, 420mM NaCl) and incubated 20 minutes on ice. Buffer A and B were supplemented with 1 mM DTT, 0.5 mM PMSF, 1 mM NaF and 1 mM sodium orthovanadate. Finally, we centrifuged the solution for 2 minutes at 13,000 rpm and nuclear proteins (supernatant) were collected. Nuclear proteins were frozen in liquid nitrogen and stored as aliquots at -80 °C until further analysis.

M-XVII. Immunofluorescence microscopy

Cells were grown on 18x18 mm glass coverslips (Thermo Scientific™ Gold Seal™, Waltham, MA, USA). After treatments, cells were rinsed once with PBS, fixed in 3.8% paraformaldehyde for 5 minutes at room temperature, and permeabilised with 0.1% saponin for 5 minutes. Glass coverslips were then incubated with primary antibodies diluted 1:100 in 0.05% T-PBS. After incubation, three washes were performed with 0.05% T-PBS and then incubated with secondary antibodies diluted 1:100 in 0.05% T-PBS. The samples were incubated for 1 hour at 37°C. Coverslips were then rinsed with T-PBS, incubated for 10 minutes with 1mg·mL^{-1} Hoechst 33342 and washed with PBS three times more. Finally, the coverslips were mounted onto microscope slides using Vectashield Mounting Medium (Vector Laboratories, Burlingame, CA, USA) and analysed using an upright fluorescence microscope (Leica DMRE, Leica Microsystems GmbH, Wetzlar, Germany). Deconvolution studies and 3D projections were performed using a DeltaVision system (Applied Precision; Issaquah, WA, USA) with an Olympus IX-71 microscope.

M-XVIII. Mitophagy analysis

Cells were cultured in 6-well 35 mm plates on 18x18 mm glass coverslips (Thermo Scientific™ Gold Seal™, Waltham, MA, USA) and, at confluence, mitophagy analysis was performed by standard immunofluorescence techniques by using LC3B (autophagosome marker) and cytochrome c (mitochondrial marker) as antibodies. Colocalisated signal of LC3B/cytochrome c proteins was assessed by using DeltaVision software and calculating the Pearson´s coefficient of correlation. Positive punctate (positive LC3B/cytochrome c) were considered when Pearson´s coefficient of correlations were higher than 0.75. Mitophagic cells are scored when more of 10 puncta are observed per cell. Samples were visualised using a DeltaVision system (Applied Precision; Issaquah, WA, USA) with an Olympus IX-71 microscope. Results are expressed as mean ± SD.

M-XIX. Mitochondrial morphology assessment

After staining of mitochondria with MitoTracker, mitochondrial size and shape were quantified by ImageJ (NIH) software. Mitochondria that were longer than 0.5 μm were defined as tubular mitochondria. To assure accuracy in the scoring process, mitochondrial size and shape were determined and analysed independently by two investigators. More than 200 clearly identifiable mitochondria from 50 cells per experiment, randomly selected, were measured in three independent experiments.

M-XX. Electron microscopy

Electron microscopy was performed using a protocol previously described by our group[99]. Fibroblasts were fixed for 15 min in the culture plates with 2% glutaraldehyde in culture medium and then for 30 minutes in Buffer A (2% glutaraldehyde, 0.1 M Na Cacodylate/HCl, pH 7.4). Cells were then washed three times with Buffer B (0.2 M Na Cacodylate/HCl, pH 7.4) for 10 minutes and then post-fixed with Buffer C (1% OsO_4, 0.15M NaCacodylate/HCl, pH 7.4) for 30 minutes. After

dehydration in increasing concentrations of ethanol, 5 min for each step: 30, 50, 70 and 95%, impregnation steps and inclusion were performed in Epon and finally polymerized at 60°C for 48 hour. 60–80 nm sections were obtained using an ultramicrotome RMC-MTX (Tucson, Arizona, USA), and contrasted with uranyl acetate and lead citrate. Observations were performed on a Philips CM-10 transmission electron microscope.

M-XXI. Statistical analysis

All results are expressed as mean ± SD, unless stated otherwise. The measurements were statistically analysed using Student's t-test for comparing two groups and ANOVA for more than two groups. Overall, P-values of less than 0.05 were considered significant. Specifically, $^{*}P < 0.05$; significance of MELAS respect to control fibroblasts. $^{b}P < 0.01$; significance of MELAS A and MELAS B fibroblasts respect to MELAS 1 and MELAS 2 fibroblasts. $^{\#}P < 0.05$ and $^{\#\#}P < 0.01$; significance between the presence and absence of riboflavin, AICAR or CoQ treatment. $^{\$}P < 0.05$, $^{\$\$}P < 0.01$ and $^{\$\$\$}P < 0.001$; significance between the presence and absence of bafilomycin A1 or compound C.

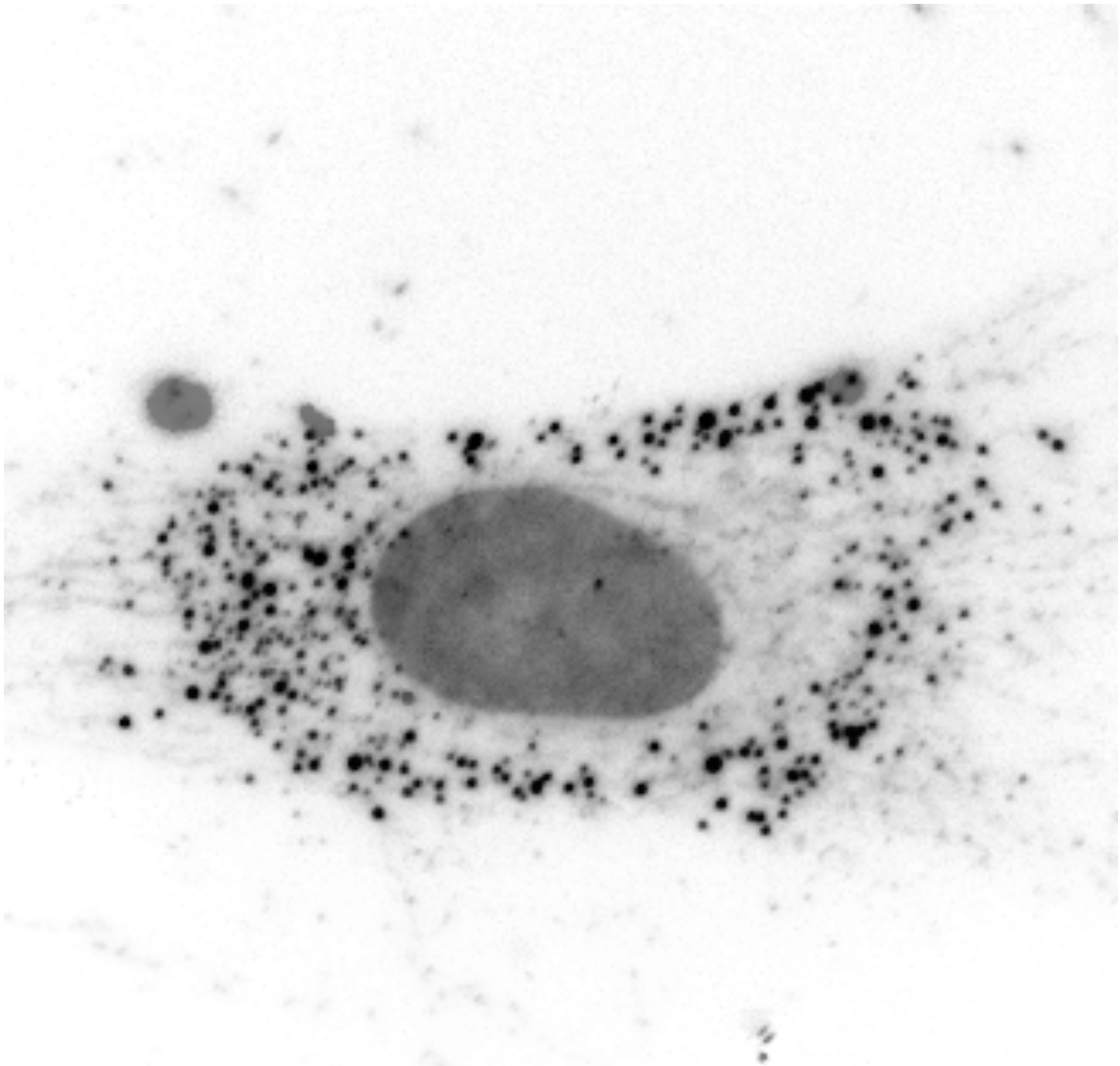

RESULTS

RESULTS

R-I. Characterisation of mitochondrial dysfunction in fibroblasts derived from MELAS patients

In the last years, primary cultures of dermal fibroblasts derived from patients are being extensively used to study several disorders. Fibroblasts are one of easiest types of cells to grow in culture and are amenable to a wide variety of manipulations. Furthermore, its capacity to manifest physiopathological alterations associated with the disease, the homogeny of cell culture, the low-cost methodology and the possibility of tightly control the physicochemical and the physiological environment in which the cells growth, make fibroblasts an attractive biological model. Although the results obtained from fibroblasts assays may not support direct correlations for the treatment of patients, they can allow the characterization of the molecular mechanisms underlying the diseases and provide important clues to understanding the clinical phenotype of the patients.

In this Results subsection, skin fibroblast derived from three MELAS patients (MELAS 1, MELAS 2 and MELAS 3) were used for unravelling the pathophysiology of the disease. All MELAS fibroblasts harboured the heteroplasmic m.3243A>G mutation. The mutational load was quantified by PCR-RFLP resulting in 17% for MELAS 1, 26% for MELAS 2 and 43% for MELAS 3 (**Figure R1**). Heteroplasmy loads were continuously followed-up during the conduction of this work to rule out any potential changes in the percentage of mutated mtDNA.

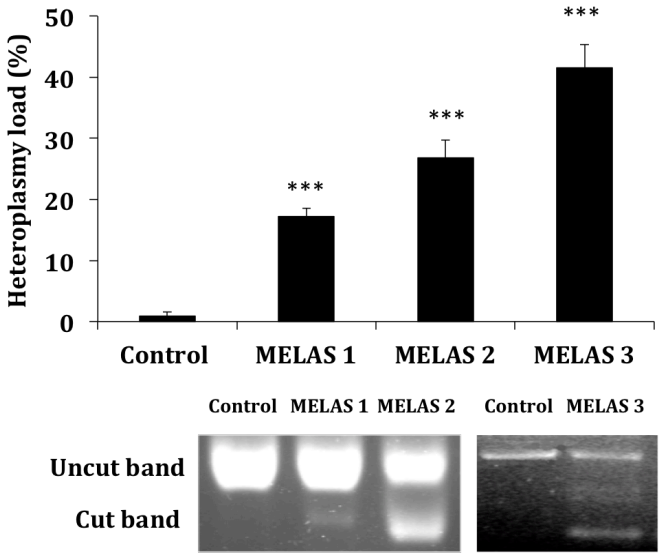

Figure R1. Heteroplasmy load in MELAS 1, MELAS 2 and MELAS 3 fibroblasts. Heteroplasmy loads were determined by PCR-RFLP assay. Results are expressed as mean ± SD. Significance of MELAS respect to control fibroblasts was represented as $^{***}P < 0.001$.

In order to test cellular homeostasis in MELAS fibroblasts, several parameters were analysed such as growth rate, ATP levels, mitochondrial respiratory chain activities, coenzyme Q_{10} content, reactive oxygen species levels or mitochondrial membrane potential.

First, proliferation assays showed decreased growth rates in the three MELAS fibroblasts cell lines suggesting a lack of the optimum cellular conditions for cell division. Growth rate was notably decreased in MELAS 1, MELAS 2 and MELAS 3 by 54%, 34% and 20%, respectively (**Figure R2**).

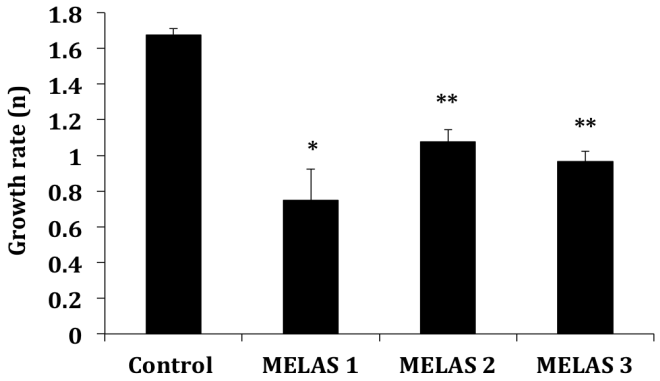

Figure R2. Proliferation rate in MELAS 1, MELAS 2 and MELAS 3 fibroblasts. Growth rate was determined by quantifying the number of cells after a week respect to initial ones. Results are expressed as mean ± SD. Significance of MELAS respect to control fibroblasts was represented as $^{*}P < 0.05$ and $^{**}P < 0.01$.

As low proliferation rate could be explained as a lack of energy production to support proper cell division, we determined the bioenergetics status of MELAS cultures. Mitochondria are the main energy-producing organelles of eukaryotic cells through ATP generation. Some mutations in the mtDNA have been reported to cause impairment of ATP synthesis[468,469]. Accordingly, we measured ATP/ADP levels in MELAS fibroblast cultures. ATP/ADP levels were significantly decreased by 45-60% in the three MELAS cell lines respect to controls. (**Figure R3**).

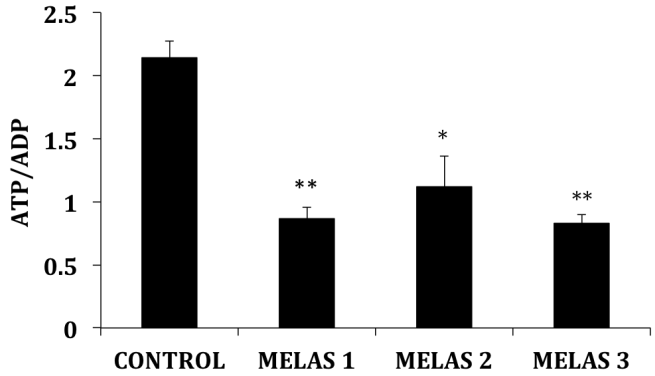

Figure R3. ATP/ADP levels in MELAS 1, MELAS 2 and MELAS 3 fibroblasts. ATP/ADP ratio was determined by using a luciferase-based assay. Results are expressed as mean ± SD. Significance of MELAS respect to control fibroblasts was represented as $^{*}P < 0.05$ and $^{**}P < 0.01$.

Low growth rate and energy deficiency could easily be associated with defects in the energy production system of mitochondria. The ultimately responsible for ATP production in mitochondria is the mitochondrial respiratory chain (MRC)[17–20]. As defects in some subunit of these complexes may impair ATP production, mitochondrial electron transport and mitochondrial homeostasis, we therefore examined the mitochondrial protein expression levels of several subunits of MRC complexes. Overall, as shown in **Figure R4**, MELAS 1 and MELAS 2 showed a significant reduction in mitochondrial protein expression levels. Complex I was decreased by 40%, complex II by 75%, complex III by 70% and complex IV by 73%.

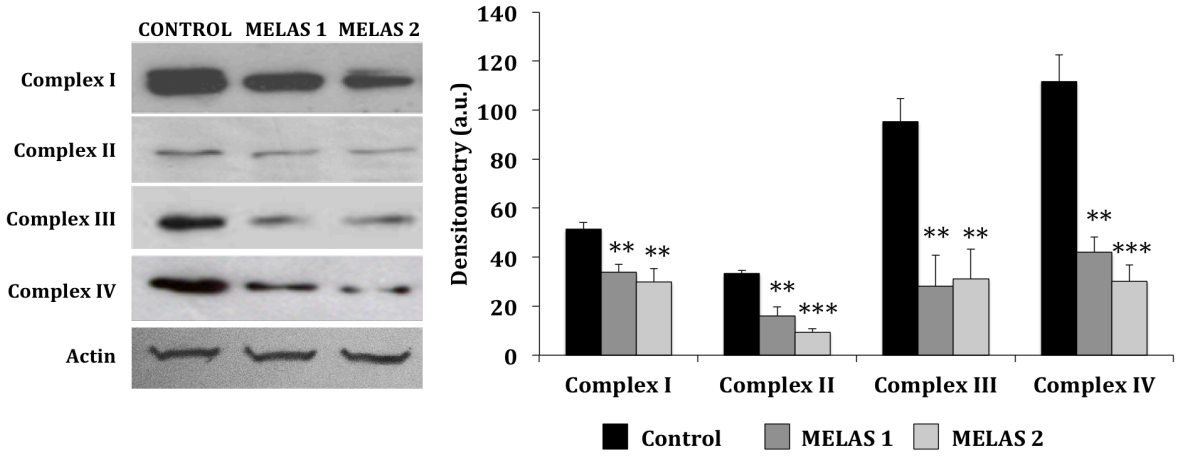

Figure R4. MRC protein analysis of MELAS 1 and MELAS 2 fibroblasts. Western blotting of MRC proteins was performed by using standard methods. Protein extracts (50 µg) were separated on a 12.5% SDS polyacrylamide gel and immunostained with antibodies against complex I (ND1), complex II (30 KDa subunit), complex III (core 1 subunit) and complex IV (subunit 1). Actin was used as loading control. Densitometry of Western blotting was performed by using the ImageJ software. Results are expressed as mean ± SD. Significance of MELAS respect to control fibroblasts was represented as $^{**}P < 0.01$ and $^{***}P < 0.001$.

To test whether reduced mitochondrial protein expression levels had an effect on mitochondrial function, we next measured respiratory chain enzyme activity in control and MELAS fibroblasts. The activity of all MRC complexes was significantly reduced in MELAS 1 and MELAS 2 fibroblasts. Complex IV activity, the most altered, was reduced by 73%. Complex I activity was reduced by 60% respect to control values in both MELAS fibroblasts. Complex II activity was reduced by 50% respect to control values. Complex I+III activity and complex II+III were reduced by 35% and 60% in MELAS fibroblasts respectively. Complex III activity was reduced by 65% in MELAS compared to control (**Figure R5**). These results support previous publications that have documented a reduction in MRC enzymatic activities in MELAS cells. Most of the literature reports a decrease in complex I and IV activities[470–472], but also there are publications describing alterations of complex II[473] or complex III activities[474].

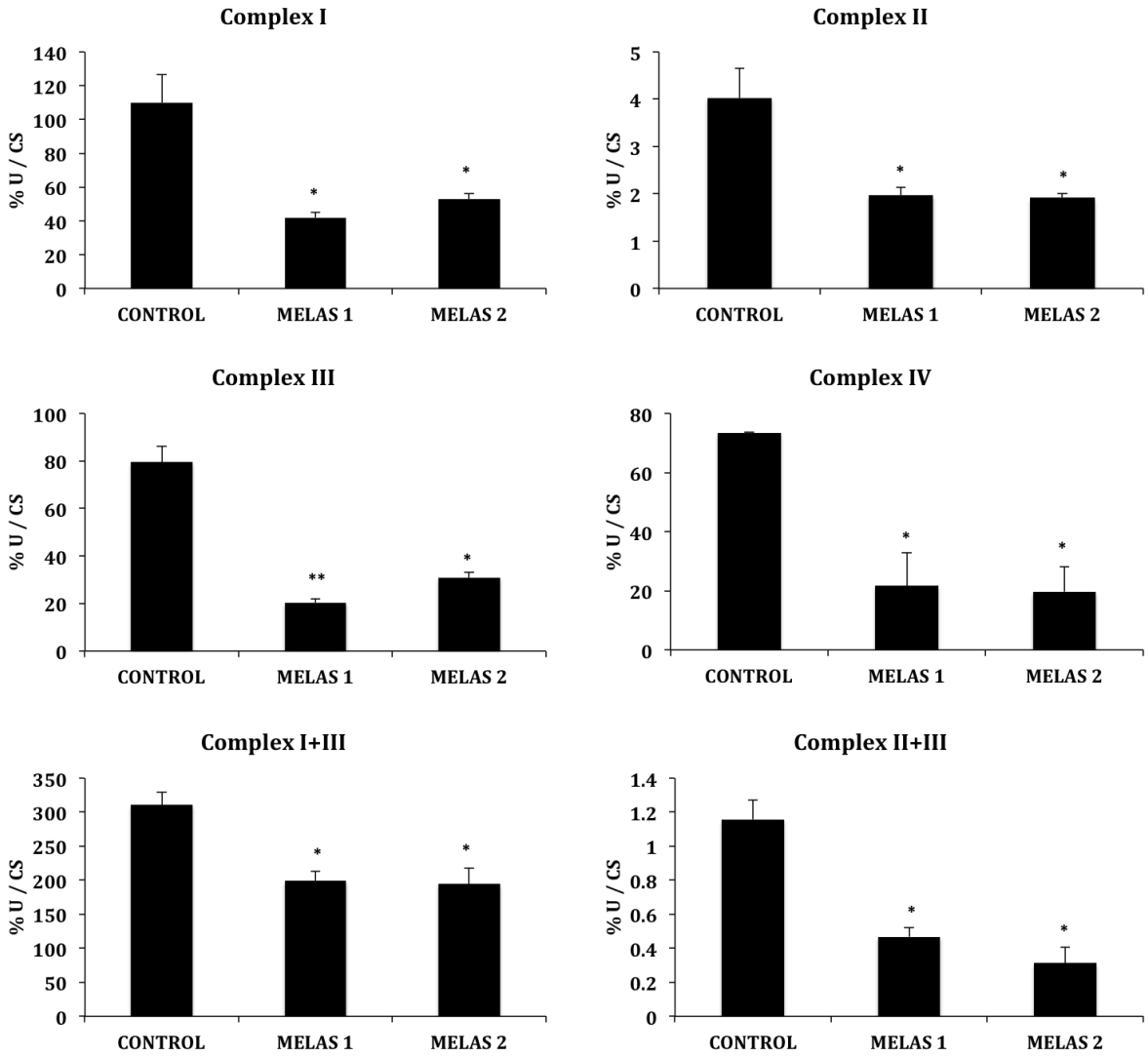

Figure R5. MRC activity analysis of MELAS 1 and MELAS 2 fibroblasts. Activities of mitochondrial respiratory complexes [NADH:coenzyme Q1 oxidoreductase (complex I), Succinate dehydrogenase (complex II), Ubiquinol:cytochrome c oxidoreductase (complex III), Cytochrome c oxidase (complex IV), NADH: cytochrome c reductase (Complex I+III), Succinate:cytochrome c reductase (Complex II+III)] were measured using spectrophotometric methods. For the control cells the data are the means ± SD for experiments on two different control cell lines. Data represent the mean ± SD of three separate experiments. Results are expressed as % U/CS (mean ± SD). Significance of MELAS respect to control fibroblasts was represented as $^{*}P<0.05$ and $^{**}P<0.01$.

Coenzyme Q_{10} (CoQ) is an essential electron and proton carrier in MRC that transports electrons from complexes I and II to complex III[18]. As multiple CoQ deficiencies have been associated with alterations in MRC and severe phenotypic manifestations in patients[249,369,414,424–429], we therefore assessed CoQ levels in MELAS fibroblasts. We found CoQ levels decreased by 50% respect to control fibroblasts (**Figure R6**). These results indicated that MELAS 1, MELAS 2 and MELAS 3 fibroblasts showed CoQ deficiency.

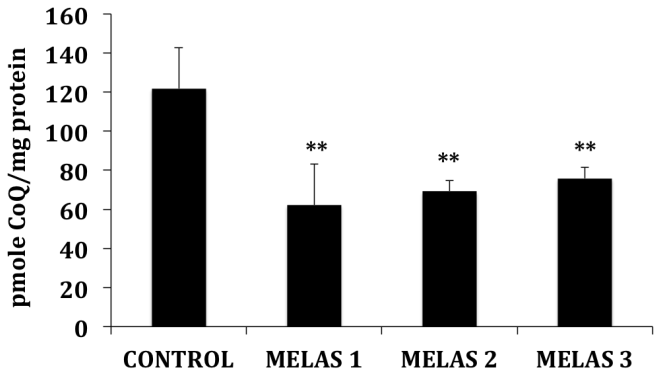

Figure R6. CoQ levels in MELAS 1, MELAS 2 and MELAS 3 fibroblasts. CoQ levels were measured by using HPLC as described in Materials & Methods. The results were expressed in pmole CoQ/mg protein. Data are expressed as mean ± SD of three separate experiments. Significance of MELAS respect to control fibroblasts was represented as $^{**}P < 0.01$.

As the mitochondrial energy-production system in MELAS 1, MELAS 2 and MELAS 3 fibroblasts seems to be markedly impaired, we wondered whether these alterations could be associated with selective degradation of dysfunctional mitochondria. Different theories about induction of selective autophagy for mitochondrial clearance have been proposed. Recent works point to ROS[98], mitochondrial depolarisation[53] and mitochondrial permeability transition (MPT)[97] as triggers for selective mitochondrial degradation. First, we examined superoxide levels in control and MELAS cultures by flow cytometry by using MitoSOX as a mitochondrial superoxide sensor. All MELAS fibroblasts showed increased ROS levels, reaching a 7-fold increase in MELAS 2 fibroblasts compared to controls (**Figure R7**). These results suggest increased ROS production or that the antioxidant defence system could be altered in MELAS fibroblasts.

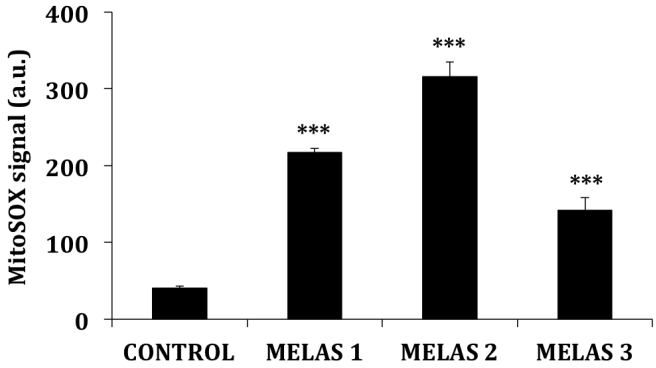

Figure R7. ROS levels in MELAS 1, MELAS 2 and MELAS 3 fibroblasts. ROS levels were quantified by using MitoSOX as a probe. Flow cytometry signal was measured from FL3 channel and represented as mean fluorescence intensity ± SD. Data represent results of three separate experiments. Significance of MELAS respect to control fibroblasts was represented as $^{***}P < 0.001$.

Next, we analysed mitochondrial polarisation in control and MELAS fibroblasts. Mitochondrial membrane potential ($\Delta\Psi_m$) is usually a good marker of proper

mitochondrial function, and mitochondrial depolarisation is a well-known signal of mitochondrial dysfunction that promotes mitophagy activation[475,476]. We measured $\Delta\Psi_m$ by flow cytometry using several probes such as MitoTracker Red CMXRos or TMRE. All the probes showed similar results. We found that $\Delta\Psi_m$ was reduced by 50-60% in MELAS 1, MELAS 2 and MELAS 3 fibroblasts cell lines respect to control fibroblasts (**Figure R8**).

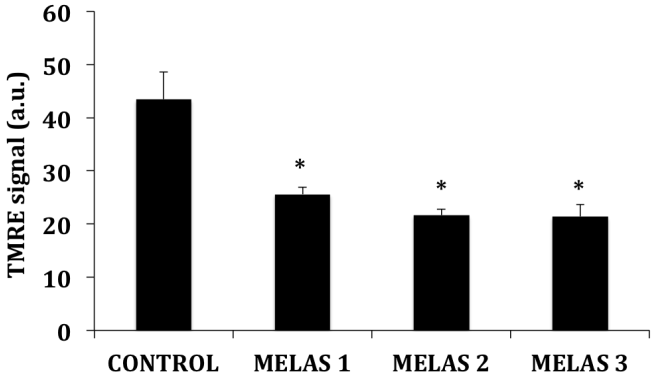

Figure R8. $\Delta\Psi_m$ levels in MELAS 1, MELAS 2 and MELAS 3 fibroblasts. Mitochondrial membrane potential was quantified by using TMRE as a probe. Fluorescence signal was measured from FL3 channel by using flow cytometry and represented as mean ± SD. Data represent results of three separate experiments. Significance of MELAS respect to control fibroblasts was represented as $^*P < 0.05$.

To confirm that changes in $\Delta\Psi_m$ were indeed the results of mitochondrial polarisation and not caused by alterations in mitochondrial mass or proliferation, individual mitochondria were examined in control and MELAS fibroblasts by fluorescence microscopy. MitoTracker and cytochrome c staining confirmed the presence of depolarised mitochondria in MELAS fibroblasts cell lines (**Figure R9**). Whereas control fibroblasts showed a normal polarised mitochondrial tubular network, two populations of mitochondria with different polarisation degree were observed in MELAS fibroblasts: a poor population of tubular mitochondria with high polarisation and another smaller rounded and fragmented one with low polarisation.

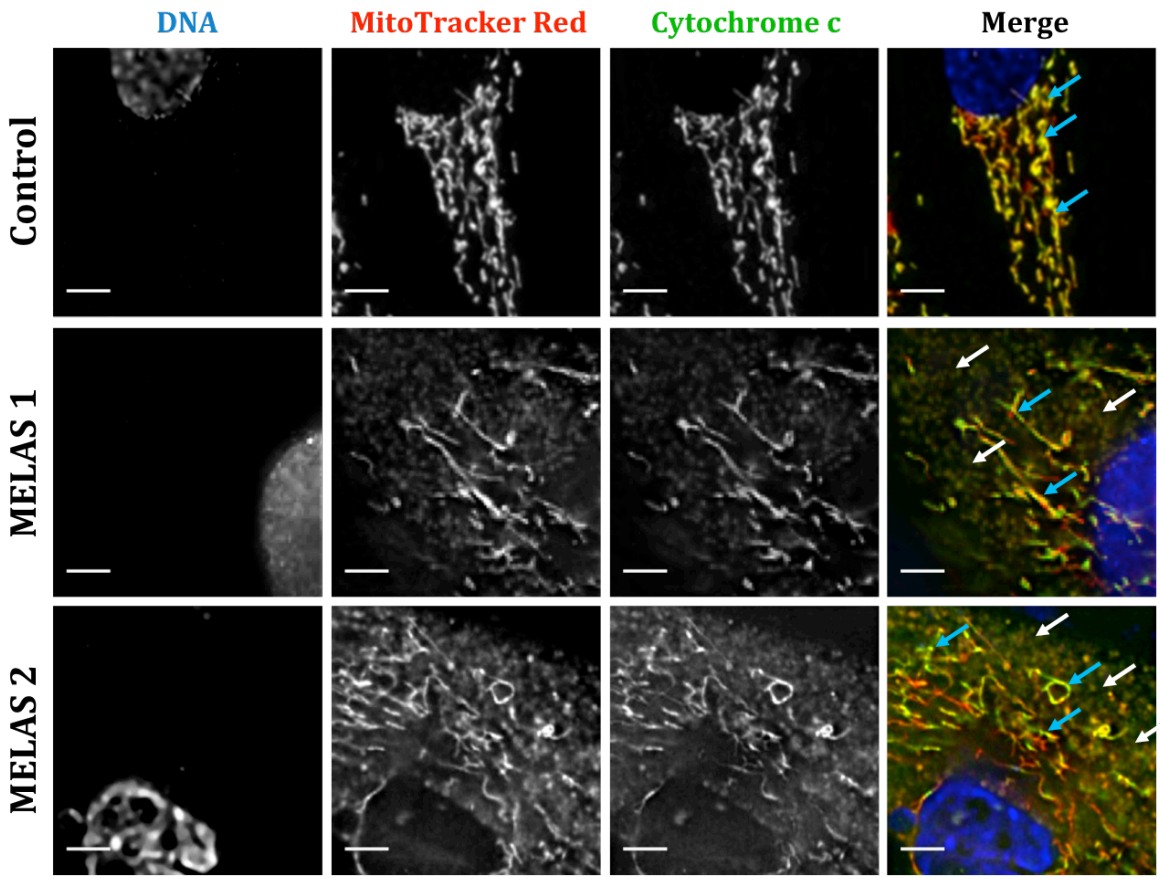

Figure R9. Cytochrome c and MitoTracker Red staining of mitochondria in MELAS 1 and MELAS 2 fibroblasts. Colocalisation of MitoTracker Red and Cytochrome c signal in mitochondria revealed specificity of MitoTracker to dyed mitochondria. Two relevant populations of mitochondria were found in MELAS fibroblasts: a smaller rounded and fragmented one (white arrows) with low polarisation degree and another tubular with high polarisation (cyan arrows). [Scale bar = 5 μm].

Lysosomal content is usually increased when autophagy is activated, so we quantified the amount of acidic vesicles using LysoTracker Red staining and flow cytometry analysis. Lysosomal content was significantly increased in MELAS fibroblasts cell lines respect to control fibroblasts (**Figure R10**).

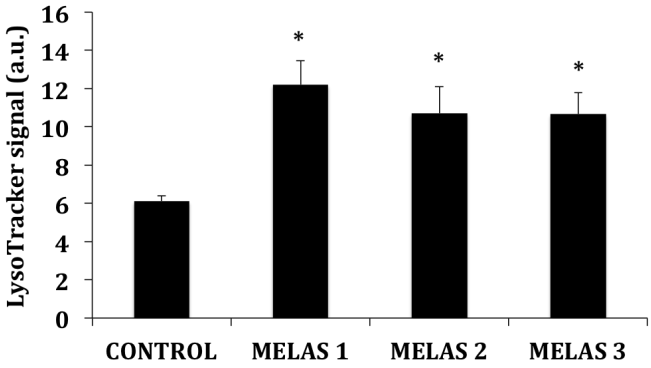

Figure R10. Acidic vacuoles levels in MELAS 1, MELAS 2 and MELAS 3 fibroblasts. Quantification of acidic vacuoles in control and MELAS fibroblasts was performed by LysoTracker staining and flow cytometry analysis. Results are expressed as mean fluorescence intensity (FL3 channel) ± SD of three separate experiments. Significance of MELAS respect to control fibroblasts was represented as $^{*}P < 0.05$.

Given that mitophagy requires the autophagy machinery to engulf damaged mitochondria, we next determined protein expression levels of well-known autophagic proteins such as conjugated ATG12-ATG5 and LC3B-II. As shown in **Figure R11**, ATG12-ATG5 and LC3B-II protein expression levels were higher in MELAS fibroblasts than in control cells, suggesting autophagy activation.

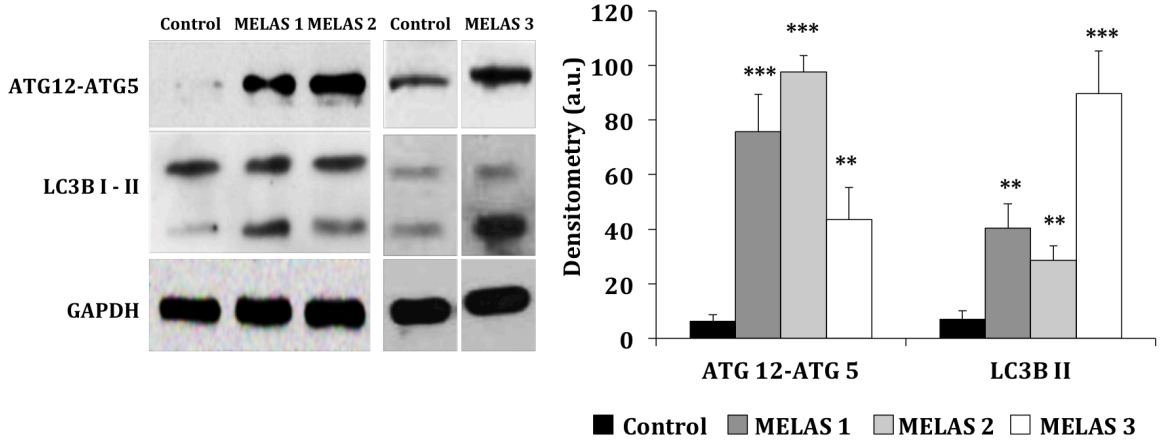

Figure R11. Protein expression of autophagic proteins in MELAS 1, MELAS 2 and MELAS 3 fibroblasts. Protein expression levels of LC3B and ATG12 were determined in control and MELAS fibroblasts cultures by Western blotting. The ATG12 band represents the Atg12-Atg5 conjugated form (55 kDa). Densitometry analysis of Western blotting was performed by using ImageJ software. GAPDH was used as a loading control. Data represent the mean ± SD of three separate experiments. Significance of MELAS respect to control fibroblasts was represented as $^{**}P < 0.01$ and $^{***}P < 0.001$.

Finally, to confirm whether mitochondria were selectively degraded by mitophagy in MELAS fibroblasts, we followed several methodological approaches recently published by our lab[100,101]. Mitophagy was detected by labelling cytochrome c as a mitochondrial protein and LC3B as an autophagosome associated protein. MELAS 1,

MELAS 2 and MELAS 3 fibroblasts frequently showed massive mitochondrial degradation and a poor tubular mitochondrial network (**Figure R12**).

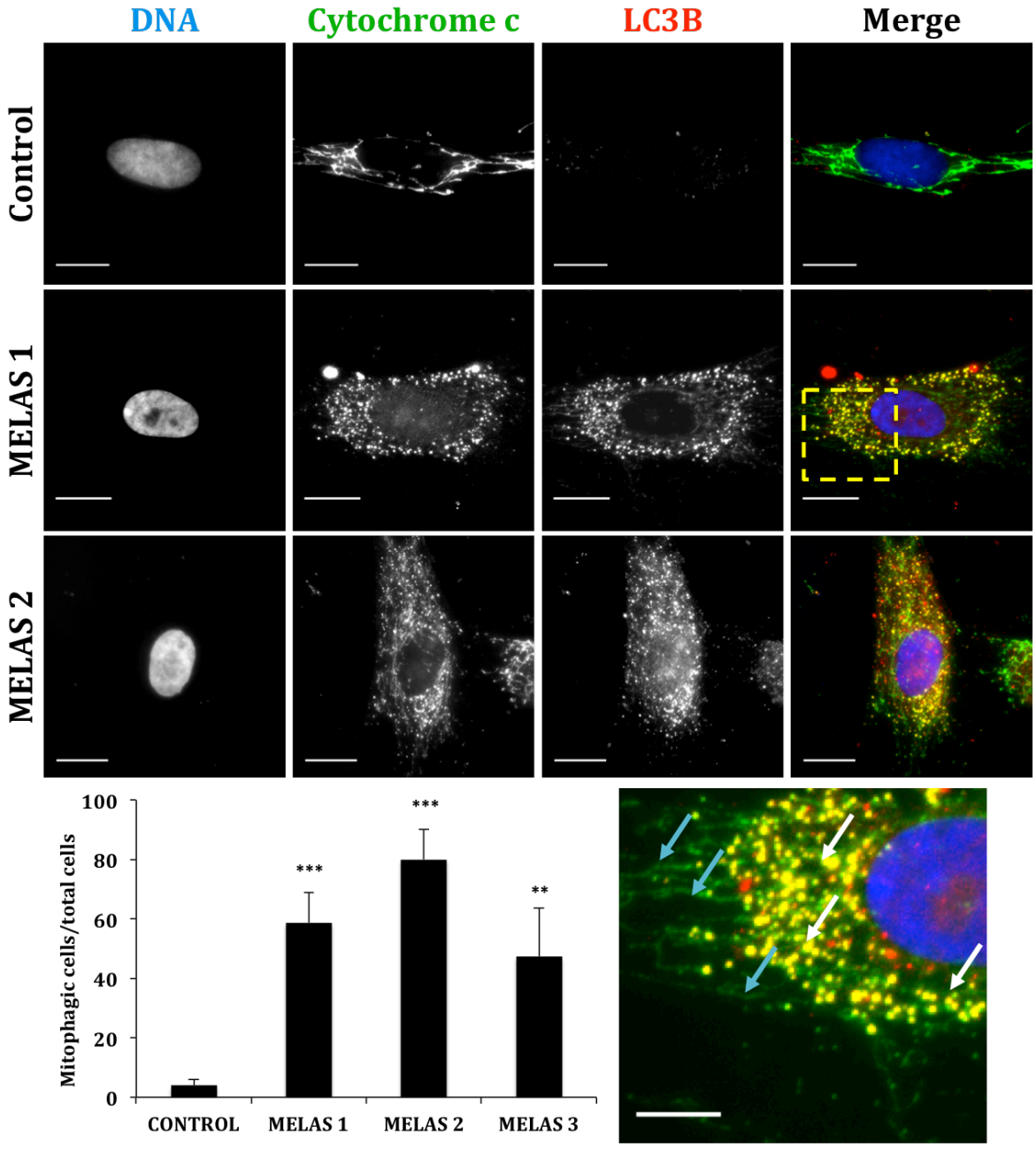

Figure R12. Mitophagy analysis in MELAS 1, MELAS 2 and MELAS 3 fibroblasts. Immunostaining of cytochrome c (mitochondrial marker) and LC3B (autophagosome marker) was performed to visualise degrading mitochondria (punctate) in control and MELAS fibroblasts. Magnification of MELAS 1 fibroblasts shows two populations of mitochondria: a smaller rounded and fragmented one (white arrows) with high cytochrome c/LC3B colocalisation degree and another tubular with low cytochrome c/LC3B colocalisation degree (cyan arrows). To quantify mitophagy, a positive mitophagic cell was scored when more of 10 puncta were observed per cell. Data represent the mean ± SD of three separate experiments. Significance of MELAS respect to control fibroblasts was represented as $^{**}P < 0.01$ and $^{***}P < 0.001$. [Scale bar = 10 μm and = 5 μm in magnified MELAS 1 picture].

Colocalisation of cytochrome c/LC3B signal was found in all MELAS cell lines indicating a general activation of the selective degradation of mitochondria. Whereas small rounded and fragmented mitochondria (white arrows) showed a high colocalisation between mitochondrial and autophagic markers, the tubular network (cyan arrows) revealed low colocalisation.

Mitophagy activation in MELAS fibroblasts was also confirmed by electron microscopy (**Figure R13**). Laminar bodies and autophagosomes with membrane structures resembling mitochondria were present in all MELAS fibroblasts (white arrows).

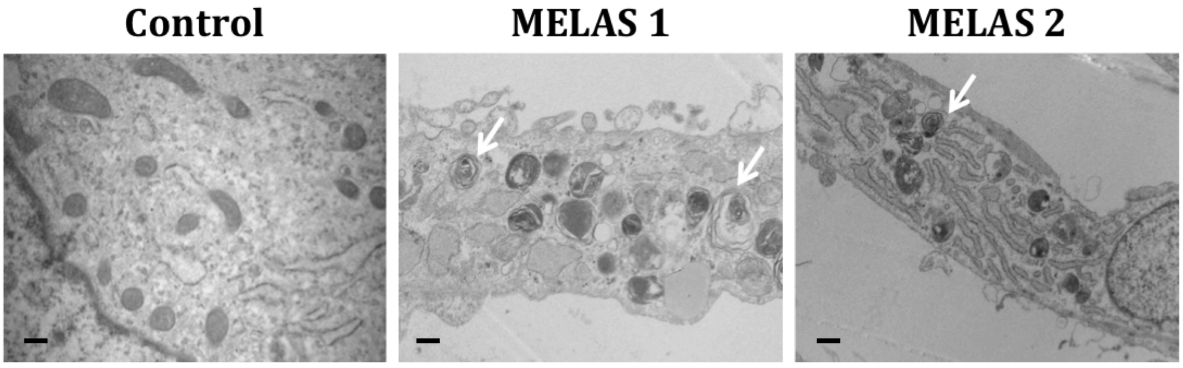

Figure R13. Electron microscopy of MELAS 1 and MELAS 2 fibroblasts. Mitophagy activation was detected by using electron microscopy [Scale bar = 2 μm].

In addition, as Parkin seems to have a fundamental role in the selective recognition of impaired mitochondria by the mitophagic machinery[104,110,477], we next examined Parkin translocation to mitochondria in MELAS fibroblasts. As is shown in **Figure R14**, we found a high colocalisation between Parkin signal and depolarised mitochondria suggesting Parkin translocation to small rounded mitochondria.

In summary, MELAS 1, MELAS 2 and MELAS 3 fibroblasts showed severe pathophysiological alterations characterised by mitochondrial dysfunction and defects in MRC function accompanied by mitophagy activation.

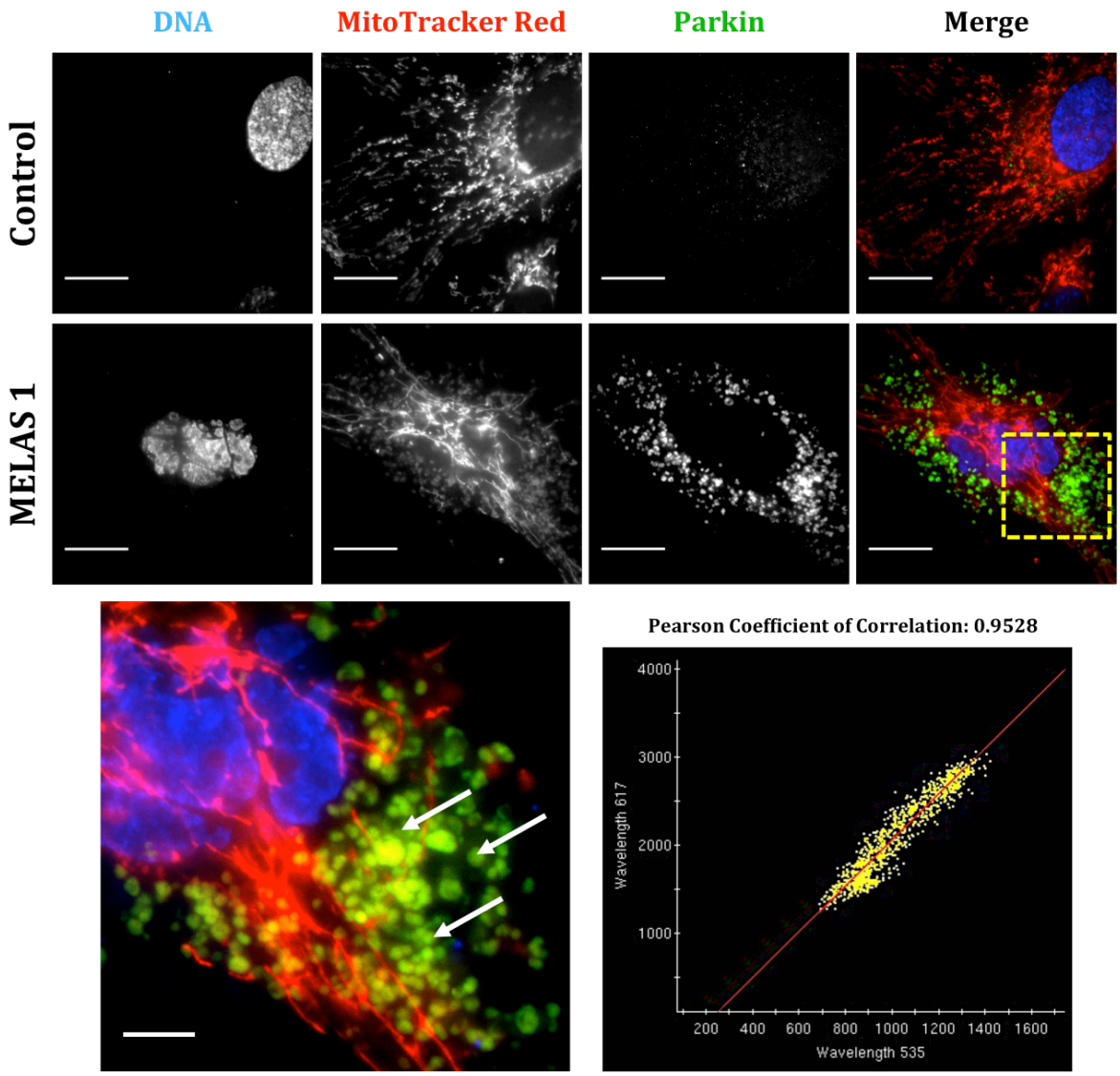

Figure R14. Parkin translocation to depolarized mitochondria in MELAS 1 fibroblasts. Immufluorescence microscopy of MitoTracker RED and Parkin was performed as described in Materials & Methods. Magnification of a small area of MELAS 1 fibroblasts showing translocated Parkin into small, rounded depolarized mitochondria (white arrow). Colocalisation analysis of Parkin and depolarized mitochondria resulted in a high colocalisation (Pearson coefficient of correlation ~ 0.95). [Scale bar = 10 μm and = 5 μm in magnified picture].

R-II. Differential pathophysiology in fibroblasts derived from MELAS patients

Interestingly for our purposes, the expansion of our studies to other fibroblast cell lines derived from several MELAS patients revealed a differential pathophysiological severity among MELAS fibroblasts cell lines. In this Result subsection, two new MELAS cultures were included, MELAS A and MELAS B, which harboured the same heteroplasmic m.3243A>G mutation. The mutational load was quantified by PCR-RFLP resulting in 9% for MELAS A and 4% for MELAS B. Therefore, MELAS A and MELAS B showed significantly reduced heteroplasmy levels respect to MELAS 1 and MELAS 2, with 17 and 26% respectively (**Figure R15**). All mutational loads were continuously followed-up during the conduction of this thesis and no significant change was observed.

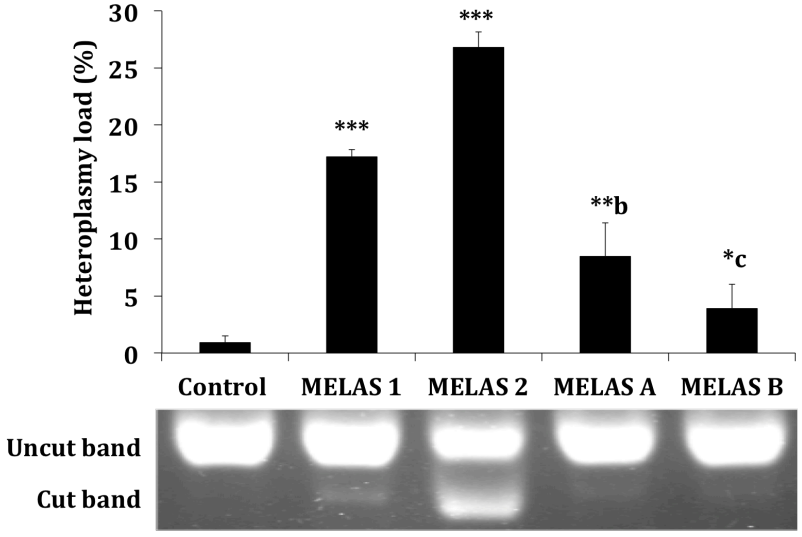

Figure R15. Heteroplasmy load in MELAS 1, MELAS 2, MELAS A and MELAS B fibroblasts. Heteroplasmy loads were determined by PCR-RFLP assay. Results are expressed as mean ± SD. Significance of MELAS respect to control fibroblasts was represented as $^{*}P < 0.05$, $^{**}P < 0.01$ and $^{***}P < 0.001$. Significance of MELAS A and B respect to MELAS 1 and 2 fibroblasts was represented as $^{b}P < 0.01$ and $^{c}P < 0.001$.

As in the previous Results subsection, the pathophysiological behaviour of MELAS A and MELAS B was analysed by determining the proliferation rate, ATP and ADP levels, respiratory chain enzyme activities, CoQ levels and ROS production, as main indicators of mitochondrial function. For comparative purposes, we show the results found in MELAS 1, MELAS 2, MELAS A and MELAS B fibroblasts.

Proliferation rate assays showed two clear patterns of growth in MELAS fibroblasts. Unlike decreased growth rates in MELAS 1 and 2, proliferation rates in MELAS A and MELAS B were near to control values (**Figure R16**) reflecting a substantial difference in the proliferation capacity between both groups of MELAS fibroblasts.

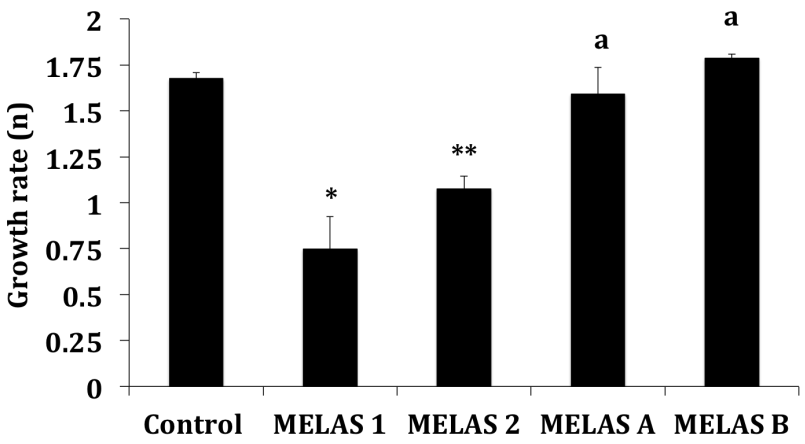

Figure R16. Proliferation rate in MELAS 1, MELAS 2, MELAS A and MELAS B fibroblasts. Growth rate was determined by quantifying the number of cells after a week respect to initial ones. Results are expressed as mean ± SD. Significance of MELAS respect to control fibroblasts was represented as $^{*}P < 0.05$ and $^{**}P < 0.01$. Significance of MELAS A and B respect to MELAS 1 and 2 fibroblasts was represented as $^{a}P < 0.05$.

Next, the evaluation of the bioenergetic state of MELAS A and MELAS B was determined by measuring ATP/ADP ratios. MELAS A and MELAS B showed ATP/ADP ratios near to control levels and notably increased respect to MELAS 1 and MELAS 2 (**Figure R17**).

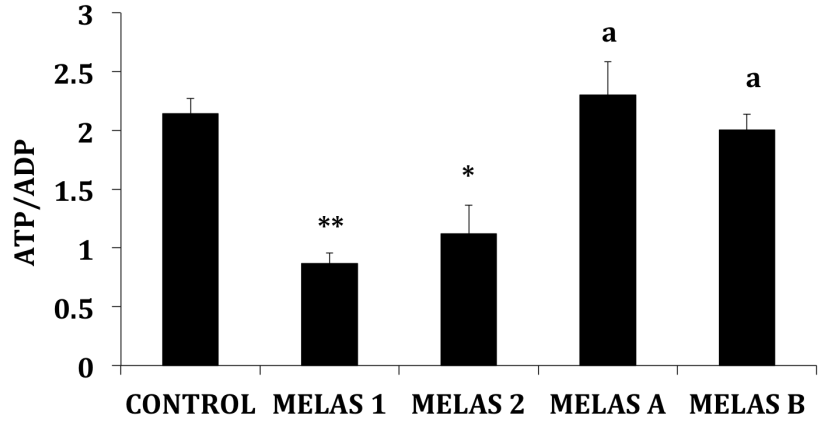

Figure R17. ATP/ADP levels in MELAS 1, MELAS 2, MELAS A and MELAS B fibroblasts. ATP/ADP ratio was determined by using a luciferase-based assay. Results are expressed as mean ± SD. Significance of MELAS respect to control fibroblasts was represented as $^{*}P < 0.05$ and $^{**}P < 0.01$. Significance of MELAS A and B respect to MELAS 1 and 2 fibroblasts was represented as $^{a}P < 0.05$.

In order to test the possibility of mitochondrial dysfunction in MELAS A and MELAS B fibroblasts, we next analysed mitochondrial protein expression levels by immunoblotting. As shown in **Figure R18**, MELAS A and MELAS B showed no significant reductions in mitochondrial protein expression levels, while MELAS 1 and MELAS 2 showed decreased protein expression levels of mitochondrial complexes.

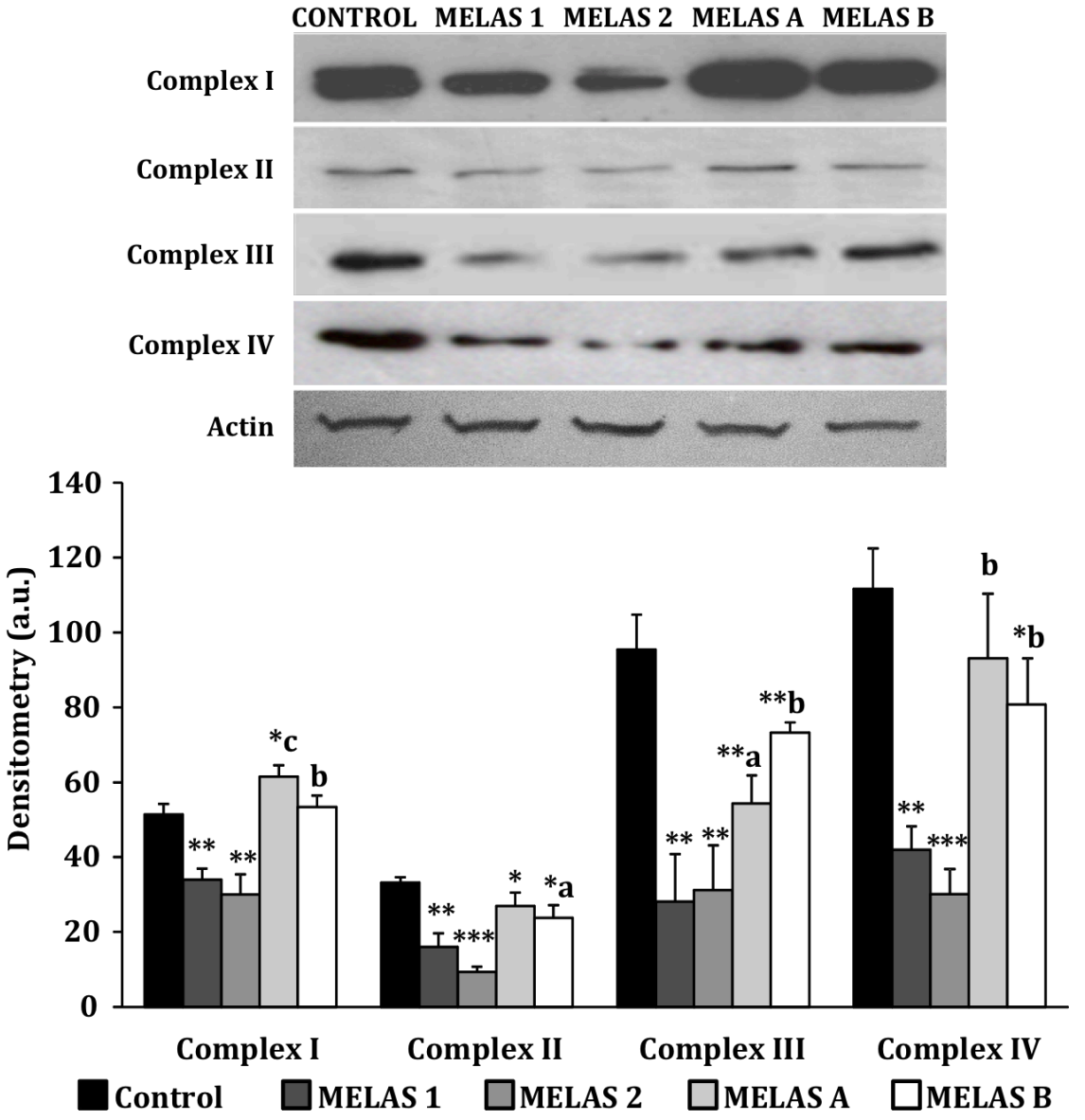

Figure R18. MRC protein analysis of MELAS 1, MELAS 2, MELAS A and MELAS B fibroblasts. Western blotting of MRC proteins was performed by using standard methods. Protein extracts (50 µg) were separated on a 12.5% SDS polyacrylamide gel and immunostained with antibodies against complex I (ND1), complex II (30 kDa subunit), complex III (core 1 subunit) and complex IV (subunit 1). Actin was used as loading control. Densitometry of Western blotting was performed using the ImageJ software. Results are expressed as mean ± SD. Significance of MELAS respect to control fibroblasts was represented as $^{*}P < 0.05$ and $^{**}P < 0.01$ and $^{***}P < 0.001$. Significance of MELAS A and B respect to MELAS 1 and 2 fibroblasts was represented as $^{a}P < 0.05$, $^{b}P < 0.01$ and $^{c}P < 0.001$.

In addition, we also measured the respiratory chain enzymes activities in MELAS A and MELAS B. The activities of all mitochondrial respiratory chain complexes showed levels close to Control, or even higher (**Figure R19**). These results seem to indicate the absence of a detectable mitochondrial dysfunction in MELAS A and MELAS B.

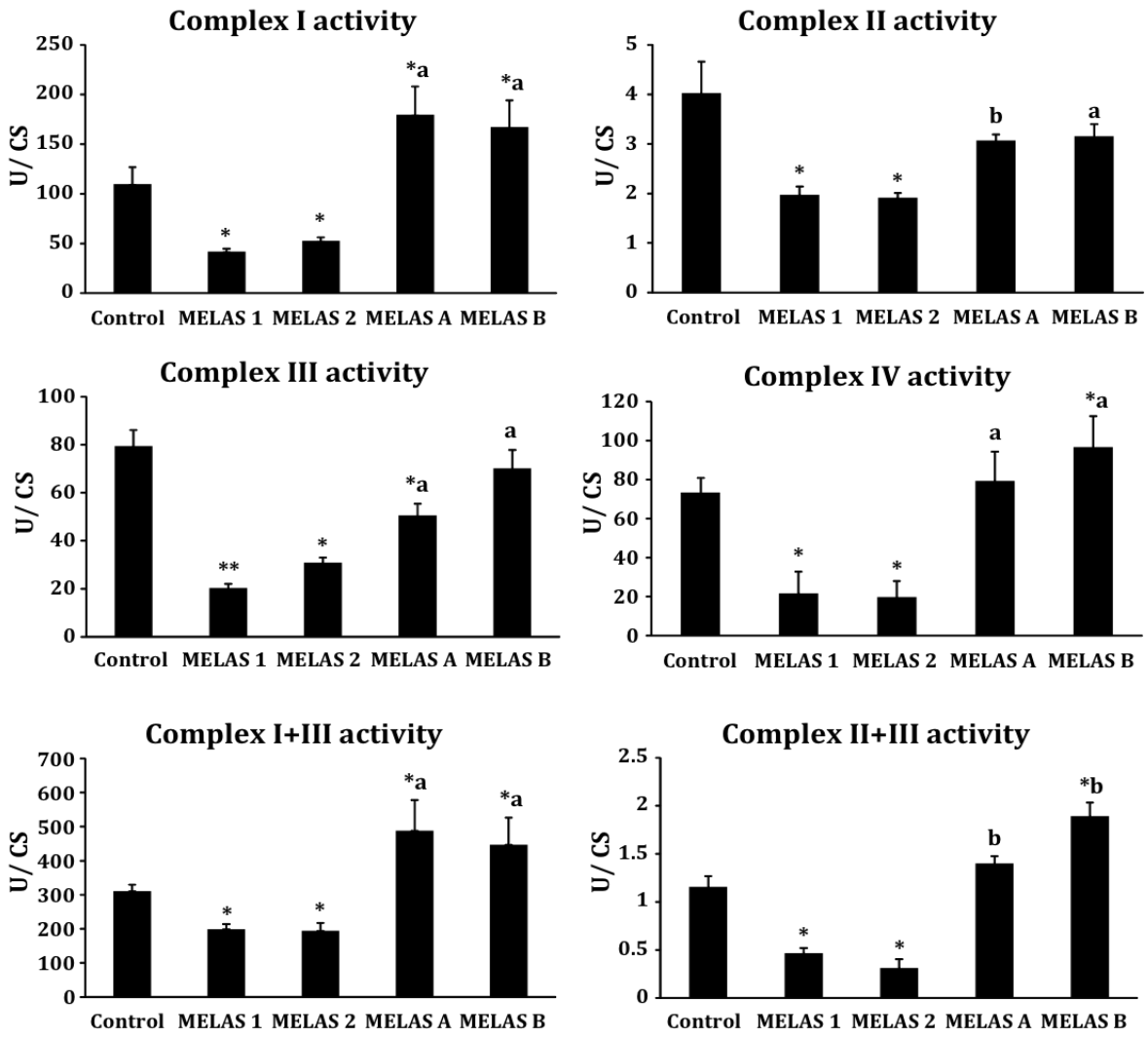

Figure R19. MRC activity analysis of MELAS 1, MELAS 2, MELAS A and MELAS B fibroblasts. Activities of mitochondrial respiratory complexes [NADH:coenzyme Q1 oxidoreductase (complex I), Succinate dehydrogenase (complex II), Ubiquinol:cytochrome c oxidoreductase (complex III), Cytochrome c oxidase (complex IV), NADH: cytochrome c reductase (Complex I+III), Succinate:cytochrome c reductase (Complex II+III)] were measured using spectrophotometric methods. For the control cells the data are the means ± SD for experiments on two different control cell lines. Data represent the mean ± SD of three separate experiments. Results are expressed as % U/CS (mean ± SD). Significance of MELAS respect to control fibroblasts was represented as $^{*}P < 0.05$ and $^{**}P < 0.01$. Significance of MELAS A and B respect to MELAS 1 and 2 fibroblasts was represented as $^{a}P < 0.05$ and $^{b}P < 0.01$.

The analysis of CoQ levels in MELAS A and MELAS B resulted in significant differences respect to MELAS 1 and MELAS 2 fibroblasts. Unlike drastic reductions in MELAS 1 and MELAS 2 fibroblasts, CoQ levels in MELAS A and MELAS B fibroblasts were increased from 1.7 to 2.7-fold, respectively (**Figure R20**). These data indicate that MELAS A or MELAS B are not CoQ deficient. These results are in agreement with previous publications that reported high CoQ content and complex II+III activity in skeletal muscle and fibroblasts derived from patients presenting encephalopathy, ataxia, and lactic acidosis[478].

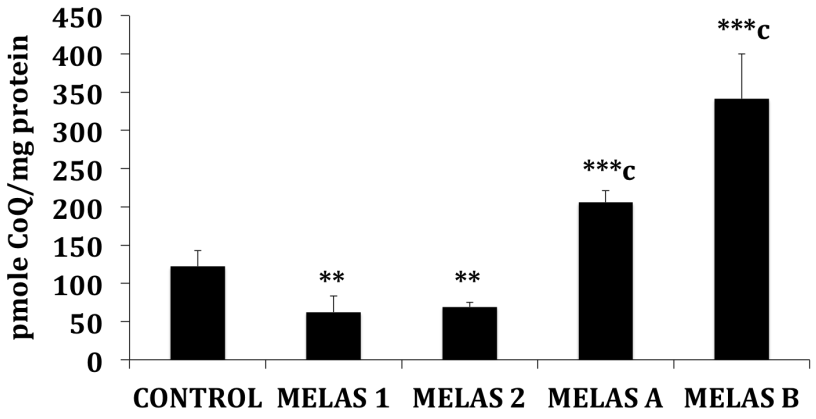

Figure R20. CoQ levels in MELAS 1, MELAS 2, MELAS A and MELAS B fibroblasts. CoQ levels were measured by using HPLC as described in Materials & Methods. The results were expressed in pmole CoQ/mg protein. Data are expressed as mean ± SD of three separate experiments. Significance of MELAS respect to control fibroblasts was represented as $^{**}P < 0.01$ and $^{***}P < 0.001$. Significance of MELAS A and B respect to MELAS 1 and 2 fibroblasts was represented as $^{c}P<0.001$.

Since in the previous Results subsection we found severe alterations caused by mitochondrial dysfunction (high ROS levels and mitochondrial depolarisation) in MELAS fibroblasts, we next examined ROS levels and mitochondrial polarisation in MELAS A and MELAS B cultures. The analysis of ROS, by using MitoSOX as a mitochondrial superoxide sensor in MELAS A and MELAS B, resulted in values near to control and significantly decreased compared to MELAS 1 and MELAS 2 (**Figure R21**). These results suggest that mitochondrial dysfunction severity and the proper activation of the enzymatic antioxidant system might participate in the differential pathophysiology observed in these four MELAS cell lines.

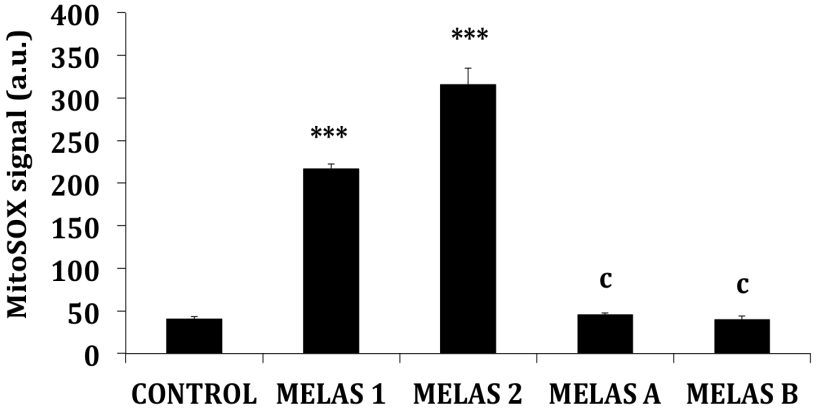

Figure R21. ROS levels in MELAS 1, MELAS 2, MELAS A and MELAS B fibroblasts. ROS levels were quantified by using MitoSOX as a probe. Flow cytometry signal was measured from FL3 channel and represented as mean fluorescence intensity ± SD. Data represent results of three separate experiments. Significance of MELAS respect to control fibroblasts was represented as $^{***}P<0.001$. Significance of MELAS A and B respect to MELAS 1 and 2 fibroblasts was represented as $^{c}P < 0.001$.

As noted above, in addition to increased ROS, mitochondria depolarization can also trigger selective degradation of mitochondria by mitophagy. Therefore, we analysed mitochondrial polarisation degree in control and MELAS A and MELAS B fibroblasts. We measured $\Delta\Psi_m$ by flow cytometry using several probes such as MitoTracker Red CMXRos and TMRE with similar outcomes. We found that $\Delta\Psi_m$ was reduced by 50-60% in the four MELAS fibroblasts cell lines respect to control fibroblasts (**Figure R22**). No significant differences were found in $\Delta\Psi_m$ between both groups of MELAS fibroblasts.

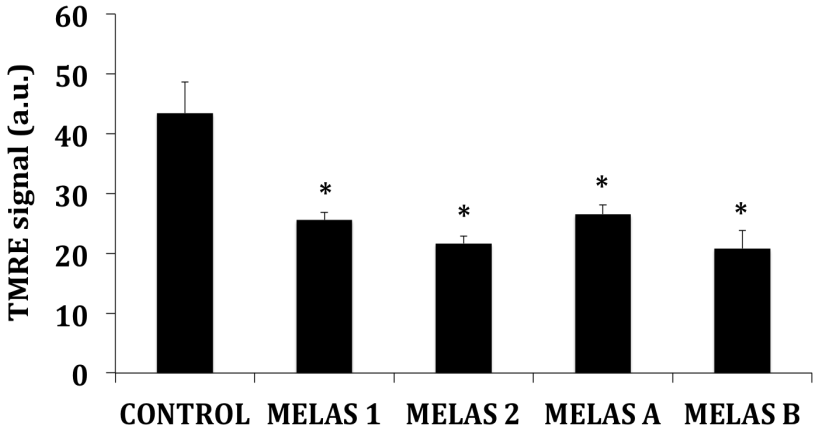

Figure R 22. $\Delta\Psi_m$ levels in MELAS 1, MELAS 2, MELAS A and MELAS B fibroblasts. Mitochondrial membrane potential was quantified by using TMRE as a probe. Florescence signal was measured from FL3 channel by using flow cytometry and represented as mean ± SD. Data represent results of three separate experiments. Significance of MELAS respect to control fibroblasts was represented as $^*P < 0.05$.

Since depolarized or inactive mitochondria decrease membrane potential and fail to sequester probes such as TMRE or MitoTracker, we verify our results by using JC-1 as a ratiometric probe. The analysis by flow cytometry is shown in **Figure R23**. We found high levels of green fluorescence signal associated with depolarised mitochondria in all MELAS fibroblasts respect to Control. However, the main red fluorescence signal, which is related to polarised mitochondria, presented lower levels than Control. These data support previous results in which the analysis of $\Delta\Psi_m$ revealed low levels in all MELAS fibroblasts. The percentage of depolarised mitochondria (green FL1 channel) and polarised mitochondria (red FL2 channel) is plotted in **Figure R23**. MELAS 1 and MELAS 2 fibroblasts presented a significantly reduced signal of polarised mitochondria compared with MELAS A and MELAS B. As an example, we show the graph of the flow cytometry analysis, in which we can observed as the MELAS A's red peak suffered a shift to the right compared to MELAS 1 that suggests an increase of the amount of polarised mitochondria.

The ratio of red to green fluorescence is dependent only on the mitochondrial membrane potential and not on the other factors such as plasma membrane potential, mitochondrial size, shape, and density that might affect a single component fluorescence signal such as red fluorescence. Thus, the JC1-aggregates/JC-1 monomers

ratio was estimated for control and MELAS fibroblasts. Whereas all MELAS fibroblasts presented lower ratios than Control, MELAS A and MELAS B presented significantly higher ratios than MELAS 1 and MELAS 2. Altogether, these ratiometric measurements showed significant differences that provided evidences of the presence of two populations of mitochondria which were unequally distributed in MELAS 1 and MELAS 2 respect to MELAS A and MELAS B.

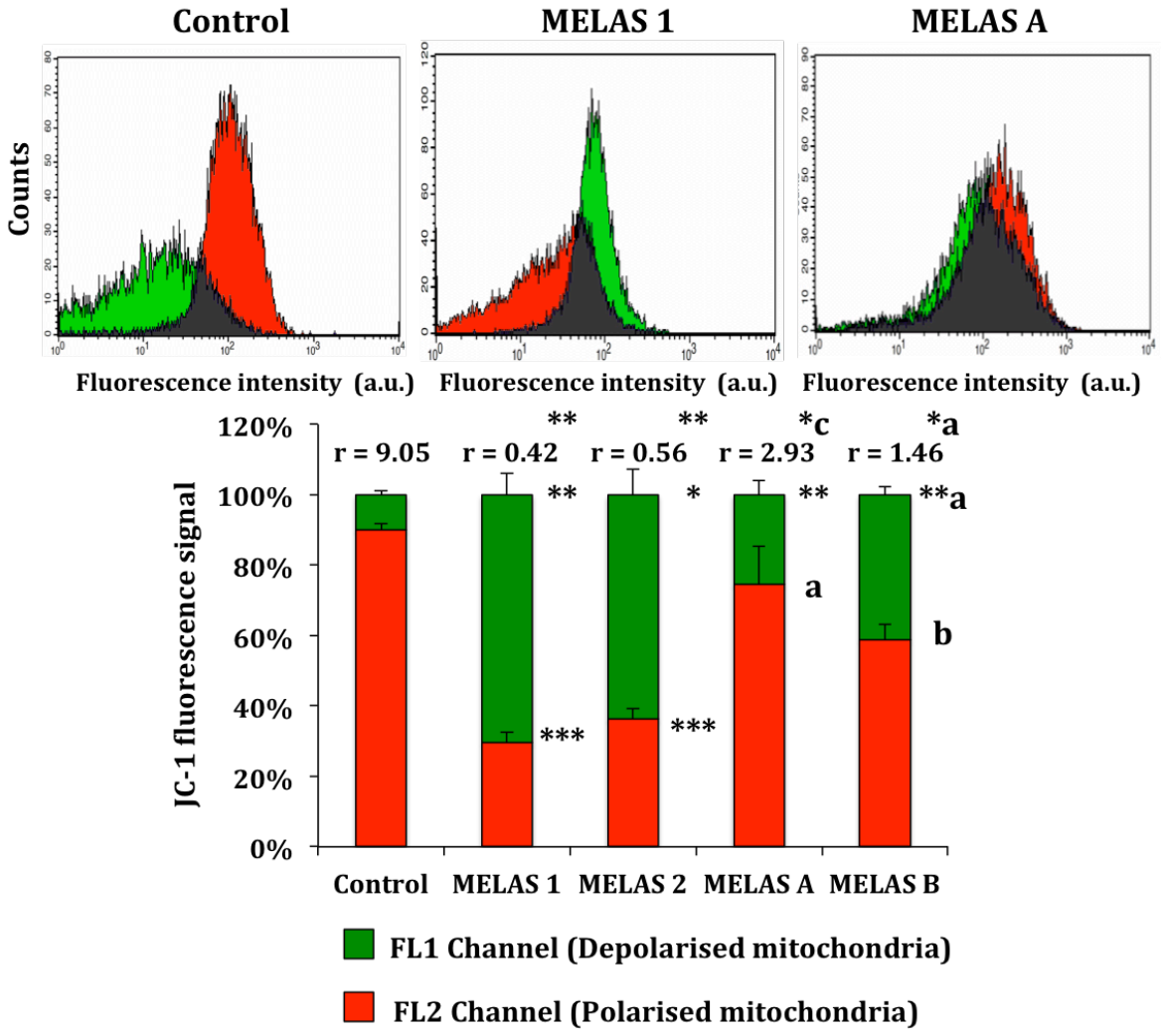

Figure R23. Analysis of mitochondrial membrane potential by using JC-1 as a ratiometric probe in MELAS fibroblasts. Green and red fluorescence signals were measured by flow cytometry in control and MELAS fibroblasts by using JC-1 as a probe. Whereas green signal (FL1 channel) was associated to JC-1 monomers and dissipated mitochondrial potential, red signal (FL2 channel) represents the J-aggregated form of JC-1, which indicates the intact mitochondrial membrane potential. JC-1 fluorescence of 10,000 events were plotted to control, MELAS 1 and MELAS A fibroblasts (a.u.; arbitrary units). The stacked bar graph shows the percentage of main JC-1 fluorescence. Ratio between both signals (FL2/FL1 signals) was estimated. Significance of MELAS respect to control fibroblasts was represented as $^{*}P < 0.05$, $^{**}P < 0.01$ and $^{***}P < 0.001$. Significance of MELAS A and B respect to MELAS 1 and 2 fibroblasts was represented as $^{a}P < 0.05$, $^{b}P < 0.01$ and $^{c}P < 0.001$.

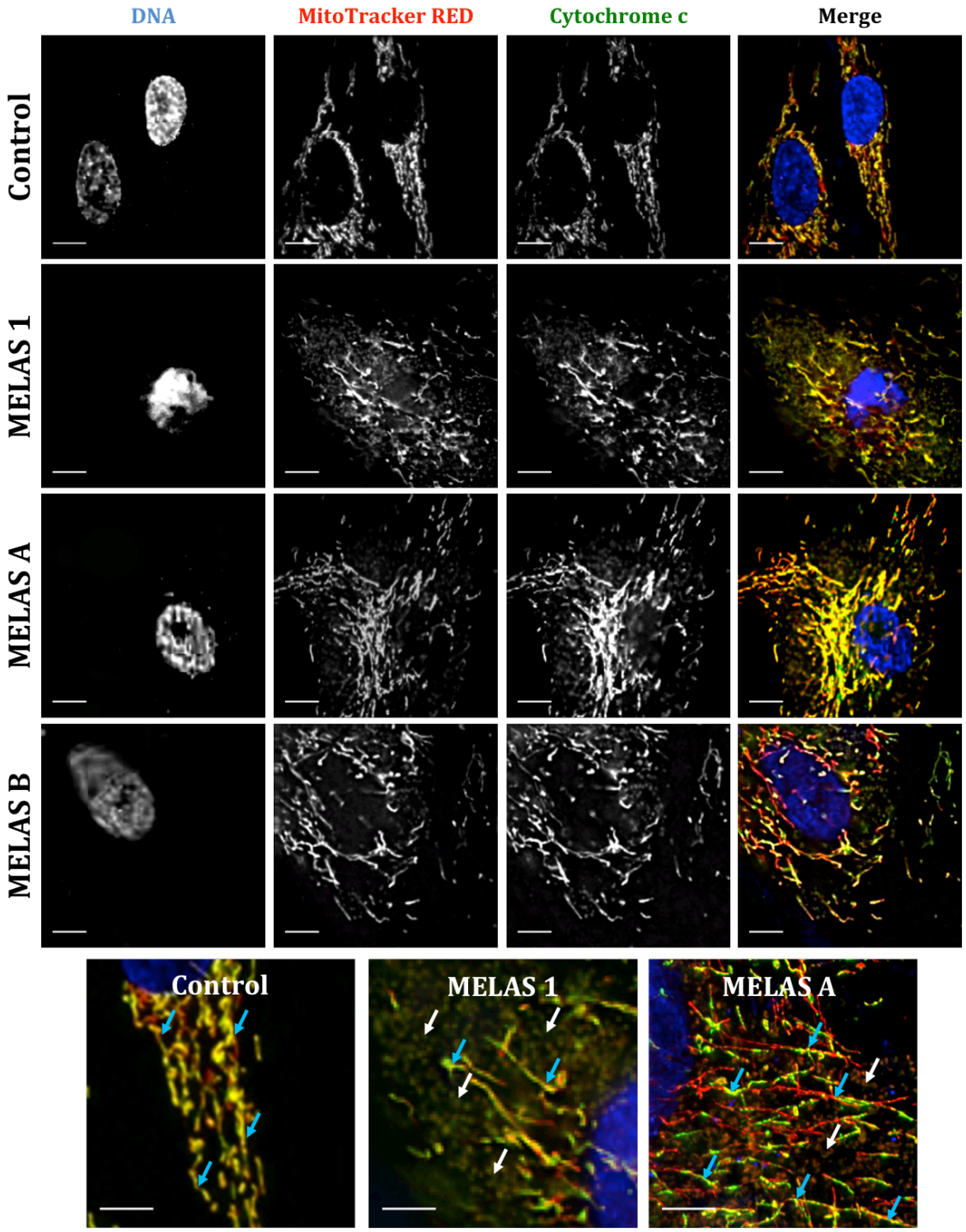

Figure R24. Cytochrome c and MitoTracker Red staining of mitochondria in MELAS 1, MELAS 2, MELAS A and MELAS B fibroblasts. Colocalisation of MitoTracker Red and Cytochrome c signal in mitochondria revealed specificity of MitoTracker to dyed mitochondria. Two relevant populations of mitochondria were found in MELAS fibroblasts: a smaller rounded and fragmented one with low polarisation degree (white arrows) and another tubular with high polarisation degree (cyan arrows). [Scale bar = 10 μm and = 5 μm in magnified picture].

These data were confirmed through examination of individual mitochondria in control and MELAS fibroblasts by fluorescence microscopy. MitoTracker Red CMXRos and cytochrome c staining confirmed the presence of an abundant population of depolarized mitochondria in the four MELAS fibroblasts cell lines analysed (**Figure R24**). However, not only did we find depolarised mitochondria in MELAS fibroblasts, but we also detected polarised tubular ones, which were particularly rich in MELAS A and MELAS B cultures. As shown in magnified pictures, MELAS 1 and MELAS A fibroblasts presented mitochondria with different polarization levels as indicated with white (low polarization) and cyan arrows (high polarization).

To confirm these results and quantify both populations of mitochondria (polarised and depolarised), mitochondrial morphology was assessed by imaging analysis from MitoTracker Red staining pictures as described in Materials and Methods. Results confirmed our previous observations about mitochondrial distribution. The tubular mitochondria population in MELAS A and MELAS B was significantly larger than in MELAS 1 and MELAS 2; whereas the population of small fragmented mitochondria was present in all MELAS fibroblasts without significant differences between them (**Figure R25**).

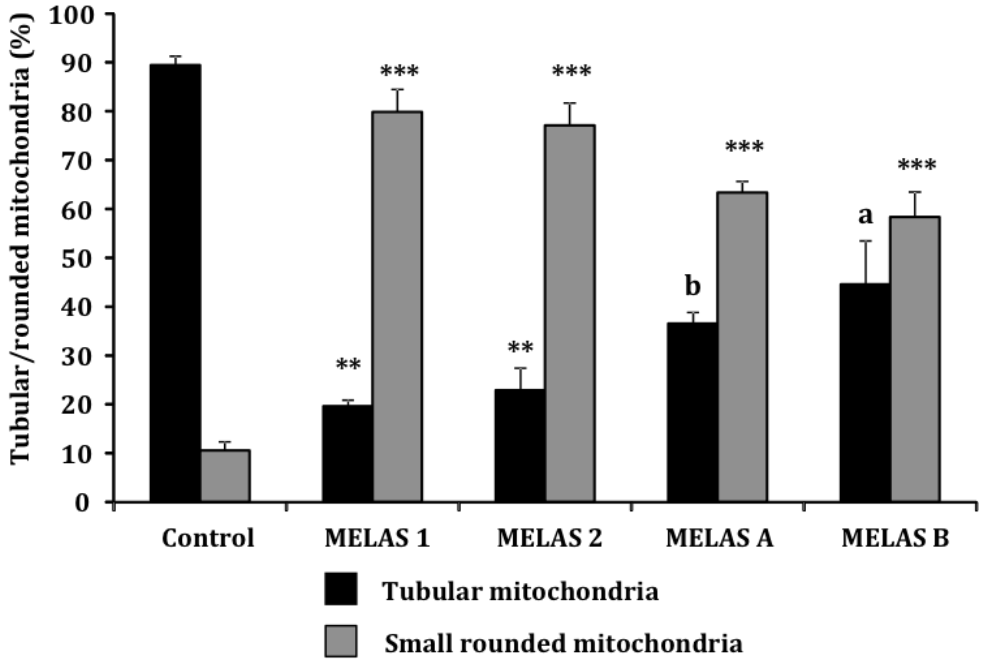

Figure R 25. Mitochondrial morphology assessment in MELAS 1, MELAS 2, MELAS A and MELAS B fibroblasts. Tubular and rounded mitochondria were quantified from MitoTracker Red stained samples. More than 200 clearly identifiable mitochondria from 50 cells per experiment, randomly selected, were measured in three independent experiments. Mitochondria that were longer than 0.5 μm were defined as tubular mitochondria and small fragmented ones were scored as small rounded ones. Results are shown as percentage (%) ± SD. Significance of MELAS respect to control fibroblasts was represented as $^{**}P < 0.01$ and $^{***}P < 0.001$. Significance of MELAS A and B respect to MELAS 1 and 2 fibroblasts was represented as $^{a}P < 0.05$ and $^{b}P < 0.01$.

Although generally MELAS A and MELAS B showed low levels of free radicals, decreased $\Delta\Psi_m$ could trigger the selective degradation of mitochondria in these cultures. In order to check whether depolarised potential was sufficient stimulus to induce mitophagy in MELAS A and MELAS B, we assessed mitophagic activation in MELAS A and MELAS B fibroblasts as well as in MELAS 1 and MELAS 2.

First, we assessed autophagic activation in MELAS fibroblasts. As in the previous subsection, we first quantified the amount of acidic vesicles using LysoTracker Red staining and flow cytometry analysis. Lysosomal content was significantly increased in the four MELAS fibroblasts cell lines respect to control fibroblasts (**Figure R26**). No significant differences were found between MELAS 1-2 and MELAS A-B.

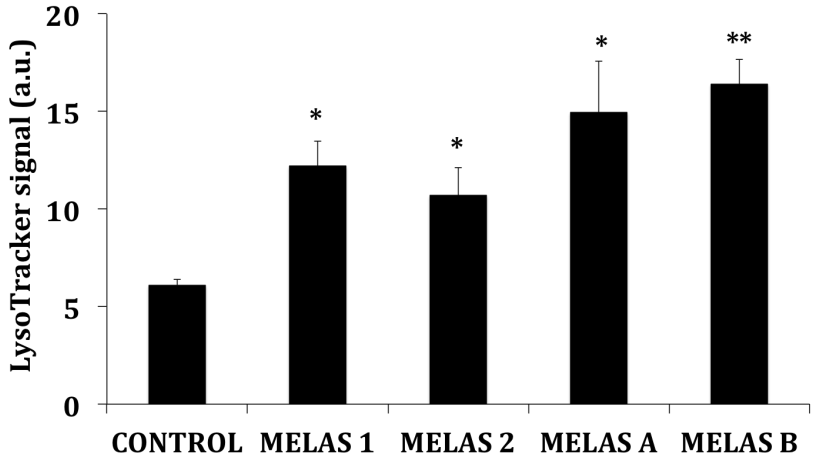

Figure R26. Lysosomal content in MELAS 1, MELAS 2, MELAS A and MELAS B fibroblasts. Quantification of acidic vacuoles in control and MELAS fibroblasts was performed by LysoTracker staining and flow cytometry analysis. Results are expressed as mean fluorescence intensity (FL3 channel) ± SD of three separate experiments. Significance of MELAS respect to control fibroblasts was represented as $^{*}P < 0.05$ and $^{**}P < 0.01$.

As previously mentioned, given that mitophagy needs the autophagy machinery, once again we determined the protein expression levels of well-known autophagic proteins such as the conjugated ATG12-ATG5 and LC3B-II. As shown in **Figure R27**, ATG12-ATG5 and LC3B-II protein expression levels were higher in all MELAS fibroblasts than in control cells suggesting autophagy up-regulation.

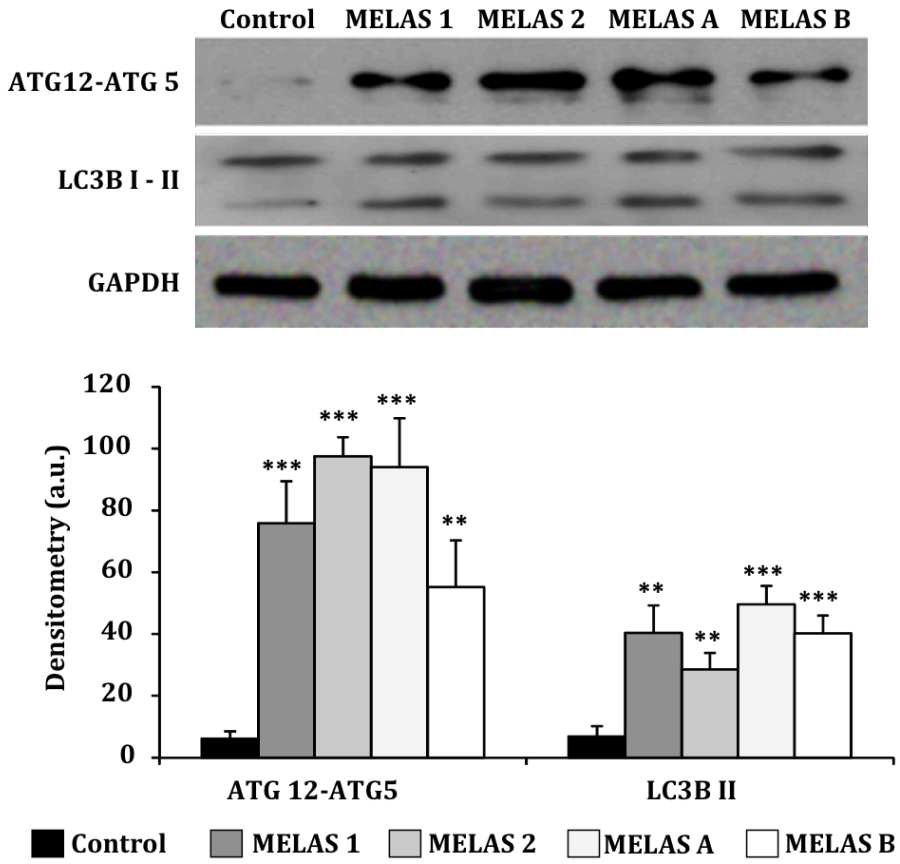

Figure R27. Protein expression of autophagic proteins in MELAS 1, MELAS 2, MELAS A and MELAS B fibroblasts. Protein expression levels of LC3B and ATG12 were determined in control and MELAS fibroblasts cultures by Western blotting. The ATG12 band represents the Atg12-Atg5 conjugated form (55 kDa). Densitometry analysis of Western blotting was performed by using ImageJ software. GAPDH was used as a loading control. Data represent the mean ± SD of three separate experiments. Significance of MELAS respect to control fibroblasts was represented as $^{**}P < 0.01$ and $^{***}P < 0.001$.

Since all MELAS 1, MELAS 2, MELAS A and MELAS B presented high levels of autophagic activation compared to control, we checked whether mitochondria were selectively degraded by mitophagy in MELAS A and MELAS B fibroblasts as well as in MELAS 1, MELAS 2 and MELAS 3 cultures. Mitophagic events, detected by colocalisation of LC3B with cytochrome c, were increased in the four MELAS fibroblast cell lines (**Figure R28**).

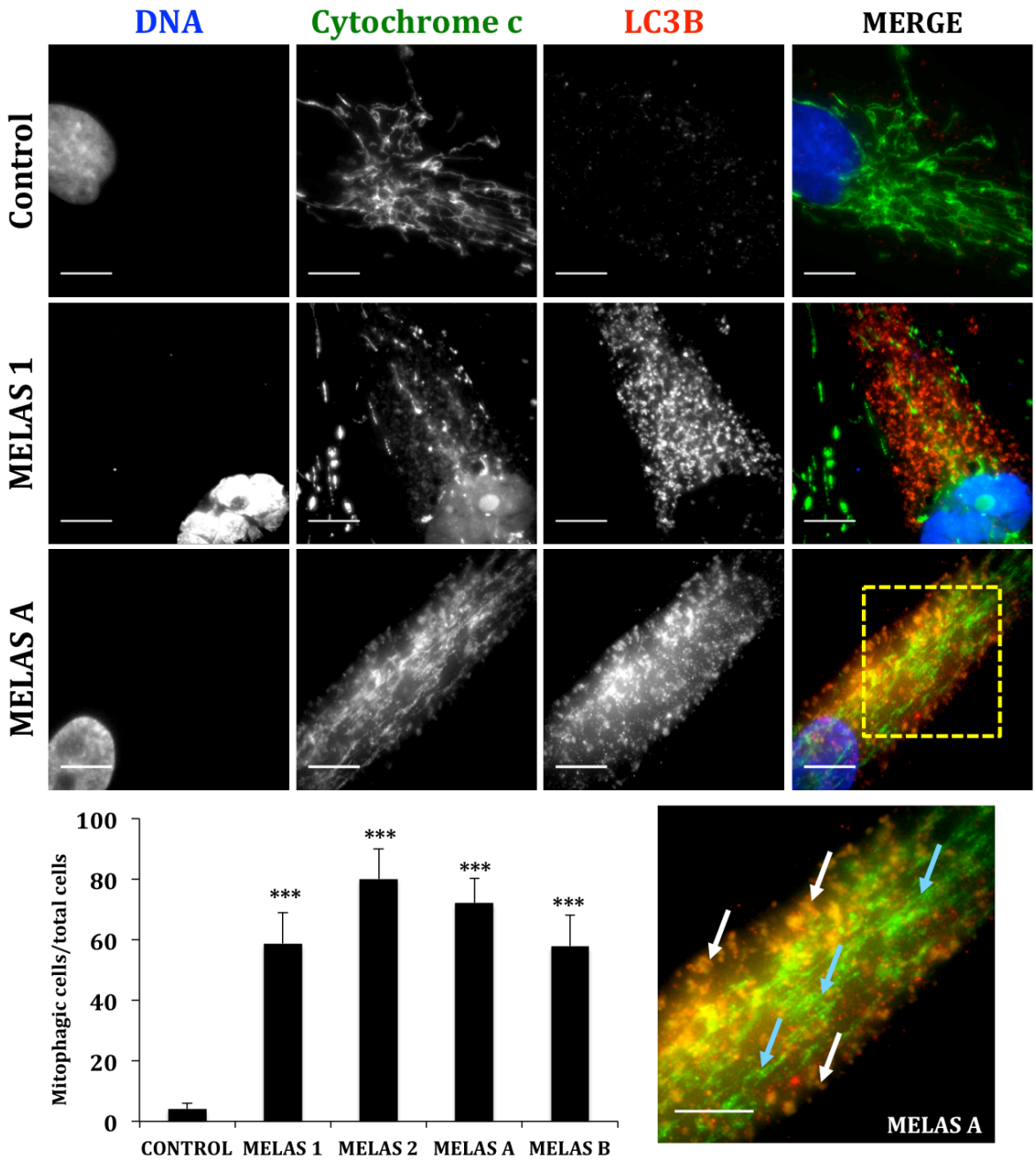

Figure R28. Mitophagy analysis in MELAS 1, MELAS 2, MELAS A and MELAS B fibroblasts. Immunostaining of cytochrome c (mitochondrial marker) and LC3B (autophagosome marker) was performed to visualise degrading mitochondria (punctate) in control and MELAS fibroblasts. Magnification of MELAS A fibroblasts revealed two populations of mitochondria: a smaller rounded and fragmented one with high cytochrome c/LC3B colocalisation degree (white arrows) and another tubular with low cytochrome c/LC3B colocalisation degree (cyan arrows). To quantify mitophagy a positive mitophagic cell was scored when more of 10 puncta were observed per cell. Data represent the mean ± SD of three separate experiments. Significance of MELAS respect to control fibroblasts was represented as $^{***}P < 0.001$. [Scale bar = 10 µm and =5 µm in magnified picture].

Altogether, these results suggest that all MELAS fibroblasts show mitophagy activation. Strikingly, the high levels of mitochondrial degradation had no effect on ATP levels in MELAS A and MELAS B, which might presumably activate a compensatory response. This differential behaviour between MELAS 1-2 and MELAS A-B could be due to their different mutational load. Indeed, MELAS 1 and MELAS 2 with a higher mutation load presented a more severe pathological phenotype. Rather, MELAS A and MELAS B cultures with a lower mutational load did not manifest the same severe alterations. Therefore, the in-depth characterisation of MELAS A and MELAS B cell lines could provide new insights for unravelling the different phenotypes found in MELAS syndrome.

R-III. Mitochondrial biogenesis as a compensatory mechanism in MELAS fibroblasts

Both MELAS groups, MELAS 1-2 and MELAS A-B, showed substantial differences respect to their pathophysiological alterations. The analysis of heteroplasmy load resulted in slight differences between both groups, which could explain the different pathophysiological severity in MELAS fibroblasts. However, when $\Delta\Psi_m$ and mitophagy were further explored, we observed clear differences in the population of mitochondria. In particular, a richer proliferating mitochondrial network was found in MELAS A and MELAS B compared with network found in MELAS 1 and MELAS 2 fibroblasts. The analysis of $\Delta\Psi_m$ by using JC-1 already pointed out an unequal proportion of polarised and depolarised mitochondria in MELAS 1-2 respect to MELAS A-B (**Figure R23**). Furthermore, mitochondrial morphology analysis definitively supported these results because MELAS A and MELAS B fibroblasts showed a larger amount of tubular mitochondrial network than MELAS 1 and MELAS 2 fibroblasts (**Figure R25**).

Taking these results into account, we then hypothesized that mitochondrial biogenesis might be properly activated in MELAS A and MELAS B fibroblasts to compensate mitochondrial degradation and bioenergetics deficit. By contrast, this compensatory mechanism might be less efficient or absent in MELAS 1 and MELAS 2 fibroblasts.

In order to verify our hypothesis, we then explored mitochondrial biogenesis in control and MELAS fibroblasts. Mitochondrial biogenesis include two distinct processes, the mitochondrial proliferation and the differentiation whereby mitochondria get their structural and functional characteristics[479]. Therefore, mitochondrial biogenesis involves an increase of mitochondrial mass and, consequently, an increase in the functional activity of these organelles. To check whether mitochondrial biogenesis is up-regulated in MELAS A and MELAS B, we measured mitochondrial mass by determining the amount of cardiolipin in mitochondrial membranes. This lipid constitutes about 20% of the total lipid composition in mitochondria[10]. The determination of cardiolipin was measured by using nonyl acridine orange (NaO) as a probe[465] in presence of an uncoupling agent (FCCP) to avoid the dependence of this probe on mitochondrial potential. We found that mitochondrial mass was reduced by 50% in MELAS 1 and MELAS 2 fibroblasts respect to control fibroblasts. Conversely, mitochondrial mass was significantly higher in MELAS A and MELAS B respect to MELAS 1 and MELAS 2 (**Figure R29**).

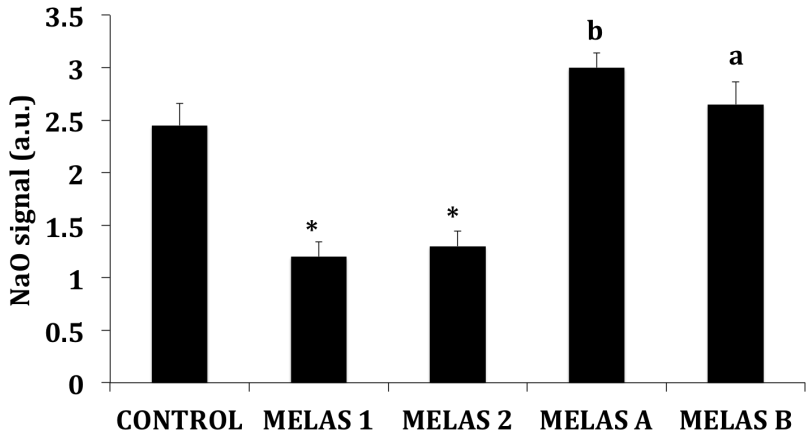

Figure R29. Mitochondrial mass measurement in MELAS 1, MELAS 2, MELAS A and MELAS B fibroblasts. Mitochondrial mass was determined quantifying the amount of cardiolipin in control and MELAS cells by flow cytometry after staining with Nonyl-Acridine Orange (NaO). Results are expressed as mean ± SD. Significance of MELAS respect to control fibroblasts was represented as $^{*}P < 0.05$. Significance of MELAS A and MELAS B respect to MELAS 1 and MELAS 2 fibroblasts was represented as $^{a}P < 0.05$ and $^{b}P < 0.01$.

Mitochondrial mass was also assessed by determining citrate synthase activity, a mitochondrial matrix enzyme whose activity correlates with mitochondrial mass[480]. As shown in **Figure R30**, citrate synthase activity was significantly reduced by 50% in MELAS 1 and 65% in MELAS 2 fibroblasts. On the contrary, citrate synthase activity was near to control values in MELAS A and MELAS B fibroblasts. These results support the hypothesis that mitochondrial proliferation might be compensating the mitochondrial elimination in MELAS A and MELAS B but not in MELAS 1 and MELAS 2 fibroblasts.

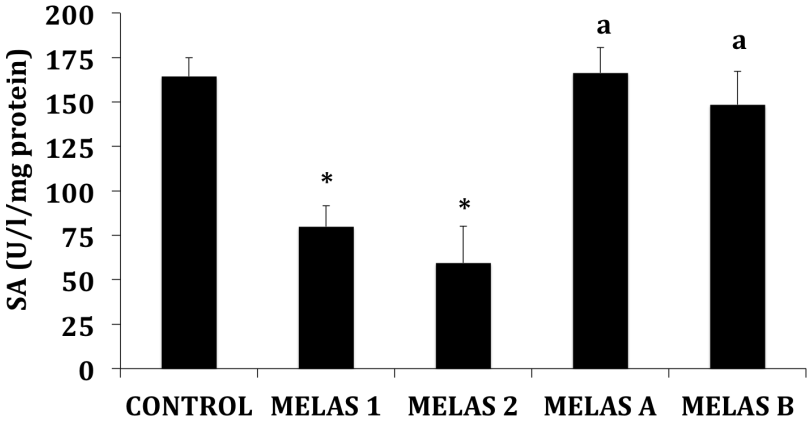

Figure R 30. Mitochondrial activity measurement in MELAS 1, MELAS 2, MELAS A and MELAS B fibroblasts. Mitochondrial activity was measured by citrate synthase specific activity (SA) expressed as activity units (U)/l/mg protein in control and MELAS fibroblasts. Results are expressed as mean ± SD. Significance of MELAS respect to control fibroblasts was represented as $^{*}P < 0.05$. Significance of MELAS A and MELAS B respect to MELAS 1 and MELAS 2 fibroblasts was represented as $^{a}P < 0.05$.

To confirm these findings, we examined protein levels of well-known activators of mitochondrial proliferation. Mitochondrial biogenesis activation involves the engagement of many proteins, among which play a prominent role peroxisome proliferator-activated receptor gamma coactivator 1 alpha (PGC-1α), nuclear respiratory factor 1 (NRF-1) and mitochondrial transcriptional factor A (mtTFA). These three proteins generate a signalling cascade that triggers *de novo* synthesis of mitochondria. In particular, PGC-1α binds to and coactives the transcriptional function of NRF1 on the promoter for mtTFA directly regulating mitochondrial DNA replication and transcription[143].

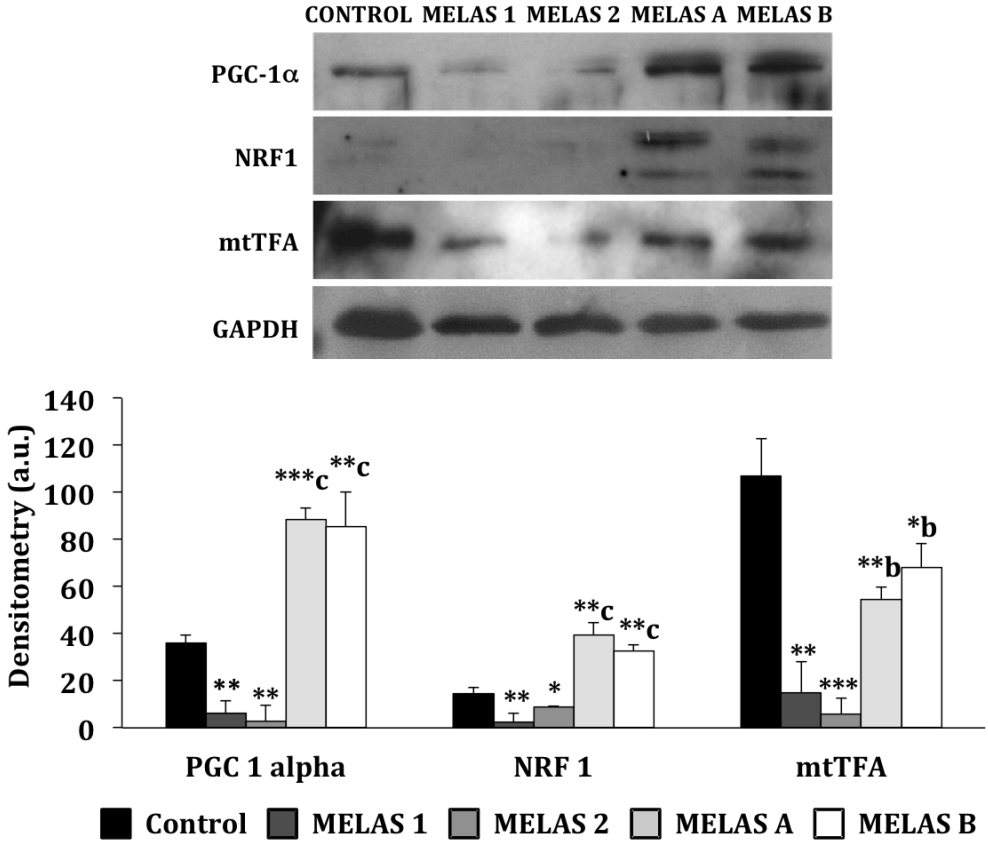

Figure R31. Mitochondrial biogenesis protein expression in MELAS 1, MELAS 2, MELAS A and MELAS B fibroblasts. Western blotting of regulatory proteins involved in mitochondrial biogenesis (PGC-1 alpha, NRF1, mtTFA) was performed with control and MELAS protein samples. GAPDH was used as loading control. Densitometry (a.u., arbitrary units) of Western blotting was performed by using ImageJ software. Results are expressed as mean ± SD. Significance of MELAS respect to control fibroblasts was represented as $^{*}P < 0.05$, $^{**}P < 0.01$ and $^{***}P < 0.001$. Significance of MELAS A and MELAS B respect to MELAS 1 and MELAS 2 fibroblasts was represented as $^{b}P < 0.01$ and $^{c}P < 0.001$.

Thus, the expression levels of PGC-1α, NRF-1 and mtTFA were significantly decreased for MELAS 1 and MELAS 2 fibroblasts whereas they were notably increased for MELAS A and MELAS B fibroblasts (**Figure R31**). PGC-1α and NRF-1 protein expression levels in MELAS A and MELAS B were even higher than in control

fibroblasts. The expression levels of mtTFA in MELAS A and MELA B were increased respect to MELAS 1 and MELAS 2 but not higher than control levels.

These results support the hypothesis that high expression levels of proteins involved in mitochondrial biogenesis were necessary to maintain high mitochondria mass for compensating mitochondrial loss by mitophagy in MELAS A and MELAS B fibroblasts. However, this compensatory mechanism seems not to be efficiently activated in MELAS 1 and MELAS 2 fibroblasts.

R-IV. Differential activation of 5'AMP-activated protein kinase in MELAS fibroblasts

Once shown that mitochondrial biogenesis is differentially activated in MELAS fibroblasts, most of our efforts were focused mainly on exploring this differential activation. Current literature reports that mitochondrial biogenesis is directly and indirectly regulated by the transcription factor PGC-1α[141,481]. As mentioned above, MELAS A and MELAS B presented more mitochondrial mass than MELAS 1 and MELAS 2 associated with a differential protein expression of PGC1-α, NRF-1 and mtTFA (**Figures R29**, **R30** and **R31**). Even though there are many studies reported about mitochondrial biogenesis regulation[155,156,160,189,482–493], how this process is differentially activated in fibroblasts derived from patients with mitochondrial disease is unknown.

In order to unravel how mitochondrial biogenesis is differentially misregulated in MELAS cultures, we focused in PGC-1α, one of the master regulators of this process. Given that the activity of PGC-1α and, hence of mitochondrial biogenesis, is regulated by direct phosphorylation of AMPK[156], we wondered whether AMPK might be involved in the differential activation of mitochondrial biogenesis in MELAS fibroblasts. AMPK is activated in response to cellular stress situations as ATP depletion[494] or high ROS levels[199–202]. Interestingly for our purposes, as shown in **Figure R17** and **R21**, both ATP and ROS production were dysregulated in MELAS 1 and MELAS 2, whereas were close to control in MELAS A and MELAS B. Consequently, we next checked AMPK activation in MELAS fibroblasts. Specifically, we explore the phosphorylation state of AMPK, since activation of AMPK requires phosphorylation of threonine 172 within the catalytic α subunit[495]. Phospho-AMPK/total-AMPK ratio was increased in MELAS A and MELAS B but not in MELAS 1 and MELAS 2. In fact a decrease by 35-40% in MELAS 1 and MELAS 2 was found respect to MELAS A and MELAS B fibroblasts.

In addition, we examined the protein expression levels of several proteins involved in ROS scavenging such as catalase, which seems to redirect to damaged mitochondria[496], a mitochondrial manganese superoxide dismutase (Mn SOD) and an eminently cytoplasmic antioxidant enzyme like copper- and zinc-containing superoxide dismutase (Cu-Zn SOD)[497]. Whereas protein expression of the cytoplasmic Cu-Zn SOD showed high levels in all of MELAS fibroblasts compared with control fibroblasts, catalase and mitochondrial Mn SOD were increased only in MELAS A and MELAS B fibroblasts (**Figure R32**). On the contrary, the expression levels of catalase and Mn SOD were dramatically decreased in MELAS 1 and MELAS 2 respect to control fibroblasts. This result is particularly interesting as both manganese superoxide dismutase and catalase have been related to AMPK-induced ROS defence system[498].

Altogether, these results suggest a deficient AMPK and antioxidant defence activation in MELAS 1 and MELAS 2 fibroblasts with the most severe phenotype.

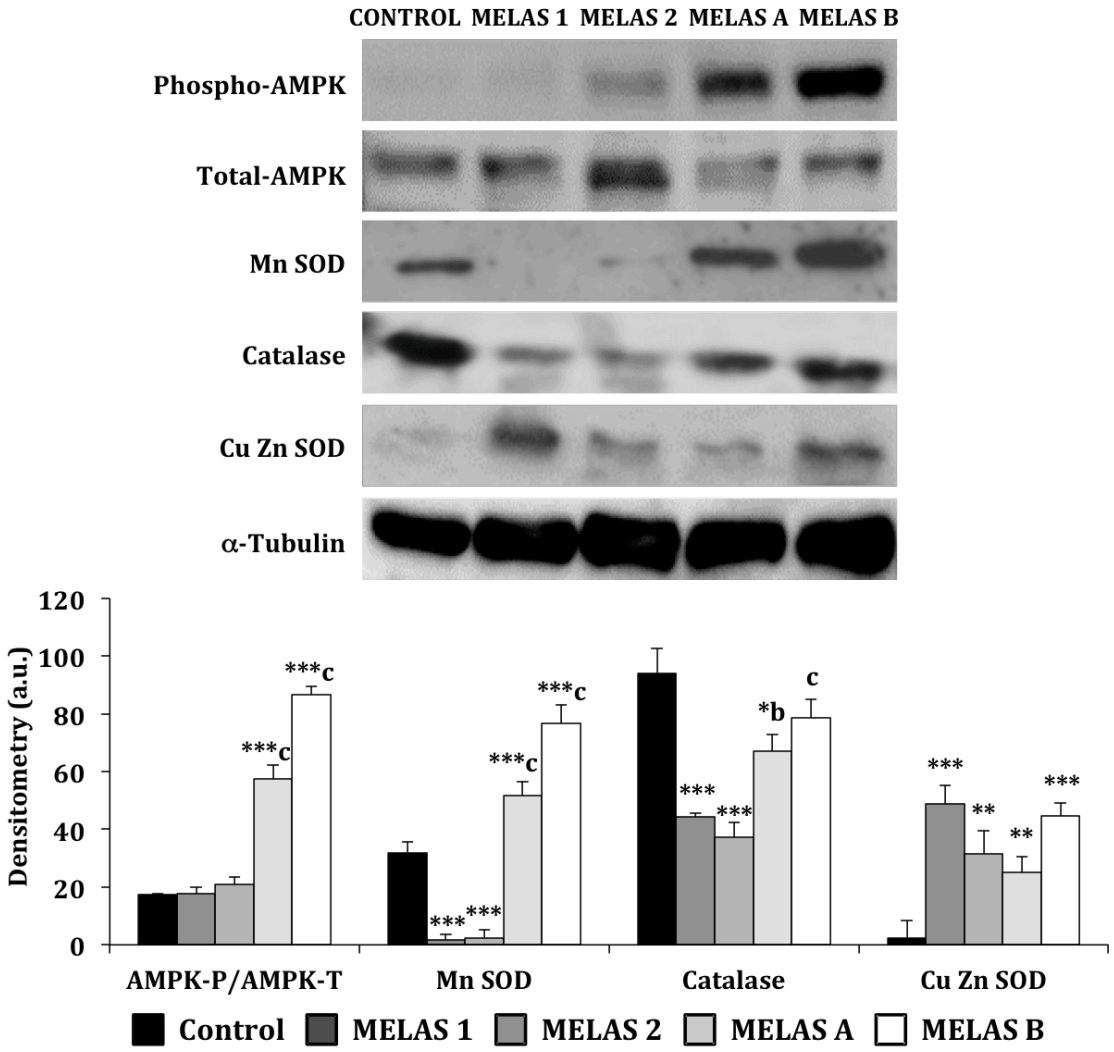

Figure R32. Antioxidant defence system response and AMPK activation in MELAS fibroblasts. Western blotting of phosphorylated and total AMP-activated protein kinase, Mn SOD, catalase and Cu-Zn SOD were performed according to standard methods. Densitometry (a.u., arbitrary units) of Western blotting was performed by using the ImageJ software. α-tubulin was used as loading control. Results are expressed as mean ± SD. $^{*}P < 0.05$, $^{**}P < 0.01$ and $^{***}P < 0.001$, significance of MELAS respect to control fibroblasts; $^{b}P < 0.01$ and $^{c}P < 0.001$ significance of MELAS A and MELAS B fibroblasts respect to MELAS 1 and MELAS 2 fibroblasts.

R-V. Pharmacological stimulation of AMPK pathway through AICAR and Coenzyme Q_{10} treatments in MELAS fibroblasts

So far, our studies indicated that MELAS 1 and MELAS 2 fibroblasts presented a severe phenotype concomitant with high heteroplasmy load and mitochondrial dysfunction. In addition to impaired energy production system, MELAS 1 and MELAS 2 fibroblasts were associated with high ROS production and decreased mitochondrial mass. On the other hand, the same pathophysiological studies indicated that MELAS A and MELAS B fibroblasts resulted in low levels of ROS, high ATP production and increased mitochondrial mass. Our findings suggest that AMPK might be insensitive to high free radicals and low levels of ATP (which mainly trigger its activation) in MELAS 1 and MELAS 2[192–198,494].

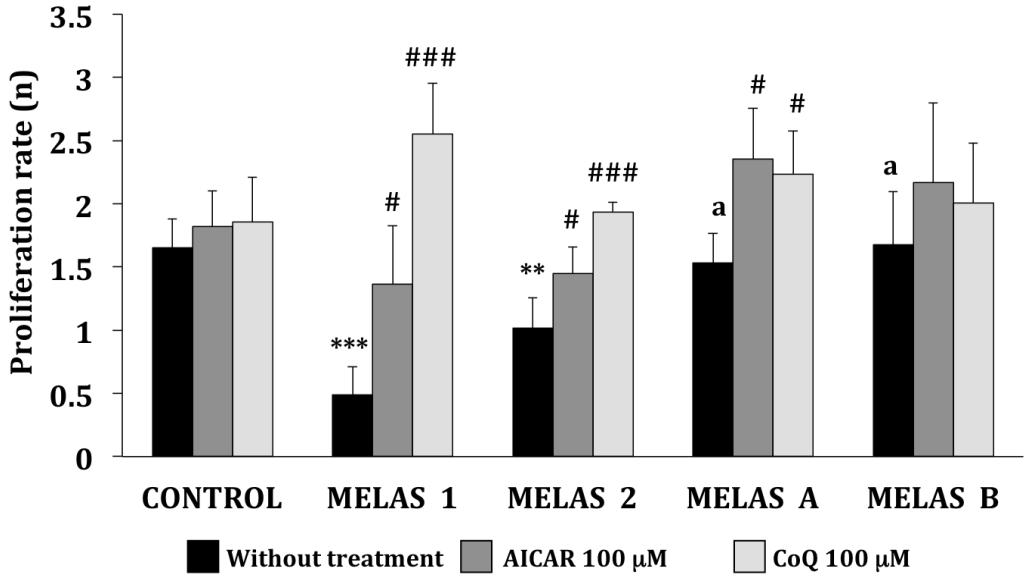

Figure R33. Effect of AICAR or CoQ treatment on proliferation rate in MELAS fibroblasts. Proliferation rate was analysed by counting viable cells after treatments as described in Materials and Methods. Results are expressed as mean ± SD. $^{**}P < 0.01$ and $^{***}P < 0.001$; significance of MELAS respect to control fibroblasts. $^{a}P < 0.01$; significance of MELAS A and MELAS B fibroblasts respect to MELAS 1 and MELAS 2 fibroblasts. $^{\#}P < 0.05$ and $^{\#\#\#}P < 0.001$; significance of MELAS fibroblasts after treatment respect to without treatment conditions.

In light of the possible role of AMPK on the differential pathophysiology observed in MELAS fibroblasts, we studied the effectiveness of its activation by AICAR and Coenzyme Q_{10} treatments. As previously noted, AMPK acts as a metabolic regulator that is activated in situations of low energy availability (low ATP/ADP ratios). AICAR is an AMP analogue that activates allosterically AMPK[209]. On the other hand, although less known as AMPK activator, Coenzyme Q_{10} (CoQ) plays a prominent role in the mitochondrial respiratory chain transferring electrons from complex I and II to complex III resulting in the proton gradient whereby ATP synthase generates ATP.

Recent studies also suggest that CoQ might participate in AMPK activation[434–438]. However, how CoQ induces AMPK activation is unclear.

In order to unravel how AMPK stimulation can influence on MELAS pathophysiology, control and MELAS fibroblast were treated with 100 μM AICAR or 100 μM CoQ for a week. After treatments, the pathophysiological parameters were re-analysed. Proliferation rate of MELAS 1 and MELAS 2 fibroblasts was notably increased after AICAR or CoQ treatments (**Figure R33**). Especially, the proliferation rate of MELAS 1 fibroblasts treated with CoQ was the most prominent with a 5-fold increase.

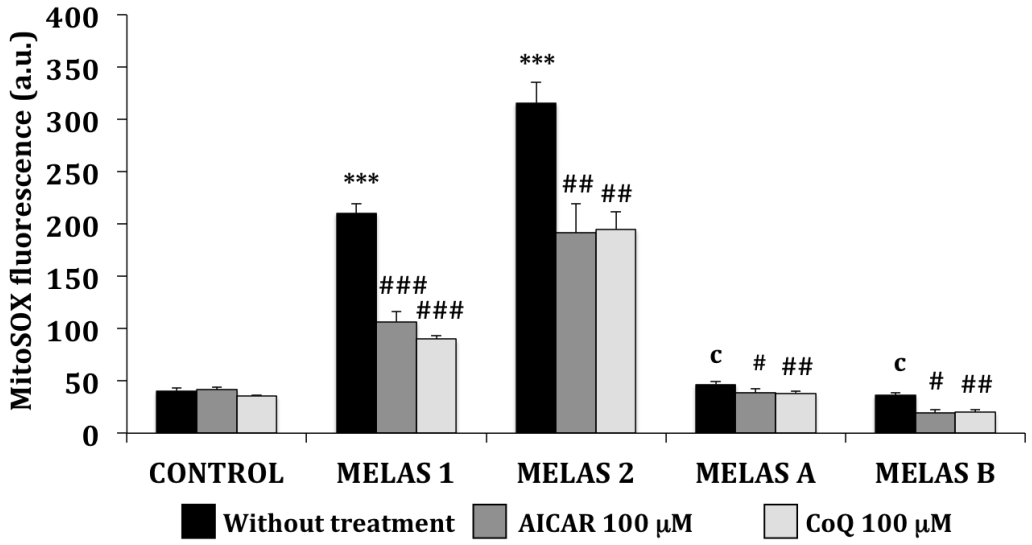

Figure R34. Effect of AICAR or CoQ treatment on ROS levels in MELAS fibroblasts. ROS levels were measured by MitoSOX staining. 10,000 events were analysed by flow cytometry. Results are shown as mean ± SD. $^{***}P < 0.001$; significance of MELAS respect to control fibroblasts. $^{c}P < 0.001$; significance of MELAS A and MELAS B fibroblasts respect to MELAS 1 and MELAS 2 fibroblasts. $^{\#}P < 0.05$, $^{\#\#}P < 0.01$ and $^{\#\#\#}P<0.001$; significance of MELAS fibroblasts after treatment respect to without treatment conditions.

Before treatments, ROS levels in MELAS 1 and MELAS 2 fibroblasts were higher than control and even, than the other MELAS cultures (MELAS A and MELAS B). The inclusion of AICAR or CoQ in the culture medium had no effect on the levels of superoxide in control cultures, but was associated with a considerable reduction in superoxide levels in all MELAS cultures, especially in MELAS 1 fibroblasts where a decrease of 50% was achieved (**Figure R34**).

After AICAR and CoQ treatments, mitophagy activation was measured as in previous Results subsections. Supplementation of the medium with AICAR and CoQ was also effective in decreasing autophagolysosome accumulation in the four MELAS cell lines (**Figure R35**). The major decrease was achieved in MELAS 1 fibroblasts, reaching an 85% reduction of cells containing mitophagic punctate (positive colocalisation of LC3B and cytochrome c).

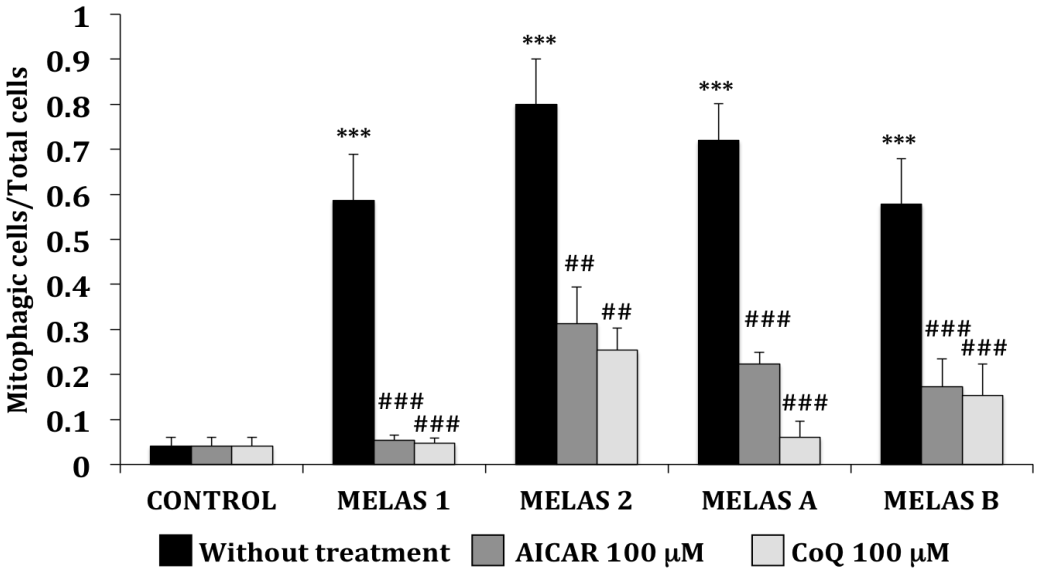

Figure R35. Effect of AICAR or CoQ treatment on mitophagic events in MELAS 1, MELAS 2, MELAS A and MELAS B fibroblasts. Immunostaining of cytochrome c (mitochondrial marker) and LC3B (autophagosome marker) was performed to explore degrading mitochondria (punctate) in control and MELAS fibroblasts after AICAR or CoQ treatments. To quantify mitophagy a positive mitophagic cell was scored when more of 10 puncta were observed per cell. Data represent the mean ± SD of three separate experiments. Significance of MELAS respect to control fibroblasts was represented as $^{***}P < 0.001$. Significance of MELAS fibroblasts after treatment respect to without treatment conditions was represented as $^{##}P < 0.01$ and $^{###}P<0.001$.

In addition, AICAR or CoQ treatments were effective increasing mitochondrial mass in MELAS 1 fibroblasts determined by measuring citrate synthase activity (**Figure R36**). This increase supports the hypothesis that mitochondrial biogenesis might be directly stimulated with AMPK activation.

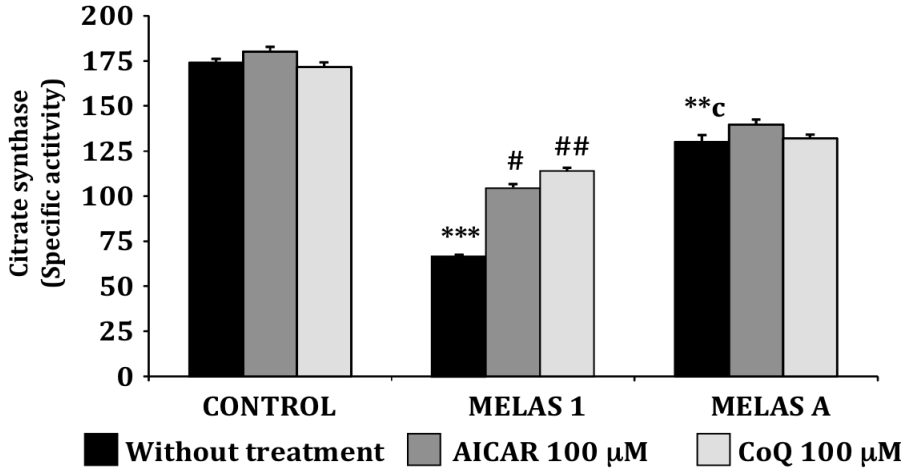

Figure R36. Effect of AICAR or CoQ treatment on mitochondrial activity in MELAS fibroblasts. Mitochondrial mass was measured by citrate synthase activity following described methods. Results are shown as mean ± SD. $^{**}P < 0.01$ and $^{***}P < 0.001$; significance of MELAS respect to control fibroblasts. $^{c}P < 0.01$; significance of MELAS A and MELAS B fibroblasts respect to MELAS 1 and MELAS 2 fibroblasts. $^{#}P < 0.05$ and $^{##}P < 0.01$; significance of MELAS fibroblasts after treatment respect to without treatment conditions.

These results suggest that both AICAR and CoQ treatments improved the pathophysiological alterations in MELAS fibroblasts, especially in those cases with a more severe phenotype (MELAS 1 and MELAS 2).

To further explore the effect of AICAR and CoQ treatments, we focused in the most severe phenotype, MELAS 1 fibroblasts, which showed extreme alterations in the pathophysiological parameters analysed. We examined the expression levels by Western blotting of several key proteins involved in cellular signalling pathways such as mitochondrial biogenesis (PGC-1α), enzymatic antioxidant defence (Mn SOD and catalase), regulators of both pathways (as AMPK) and autophagosome accumulation (LC3B) (**Figure R37**).

PGC-1α, Mn SOD, catalase, and AMPK protein expression levels were decreased in MELAS 1 fibroblasts respect to control levels. The expression levels of Mn SOD and phospho-AMPK were the most affected with a 96% and 82% reduction, respectively. Catalase and PGC-1α protein expression levels were reduced by 45% and 65%, respectively. AICAR or CoQ treatments completely restored PGC-1α, Mn SOD and catalase protein expression levels. The analysis of AMPK revealed extra bands in presence of AICAR or CoQ supplementation, which might be extra-phosphorylated forms of AMPK.

As shown in **Figure 37**, AICAR and CoQ treatments, both putative AMPK activators, reduced the levels of LC3B-II, a well-known marker of autophagy and autophagosome accumulation. Given that AMPK activation has been described to activate autophagy and autophagic flux[499], our results could come into conflict with the reported literature. However, we can speculate that the reduction of LC3B-II band found after treatments could be due to acceleration of the autophagic flux and, as a consequence, a reduction of autophagosomes accumulation. Thus, we wondered whether autophagic flux was altered in MELAS fibroblasts and whether AICAR and CoQ could stimulate it.

As previously shown, the analysis of ATG12-ATG5 and LC3B-II protein expression in all MELAS fibroblasts resulted in high levels of autophagic proteins suggesting autophagy up-regulation. This accumulation could indicate either autophagic activation or a blockage of downstream steps in autophagy, as well as inefficient fusion or decreased lysosomal degradation[372,500]. To check for autophagosome maturation and autophagic flux in MELAS fibroblasts, we used bafilomycin A1, a specific inhibitor of vacuolar H^+ -ATPases and a blocker of autophagosome-lysosome fusion[94,136]. Control, MELAS 1 and MELAS B fibroblasts were incubated for 12 hours with 100 nM bafilomycin A1 (**Figure R38**).

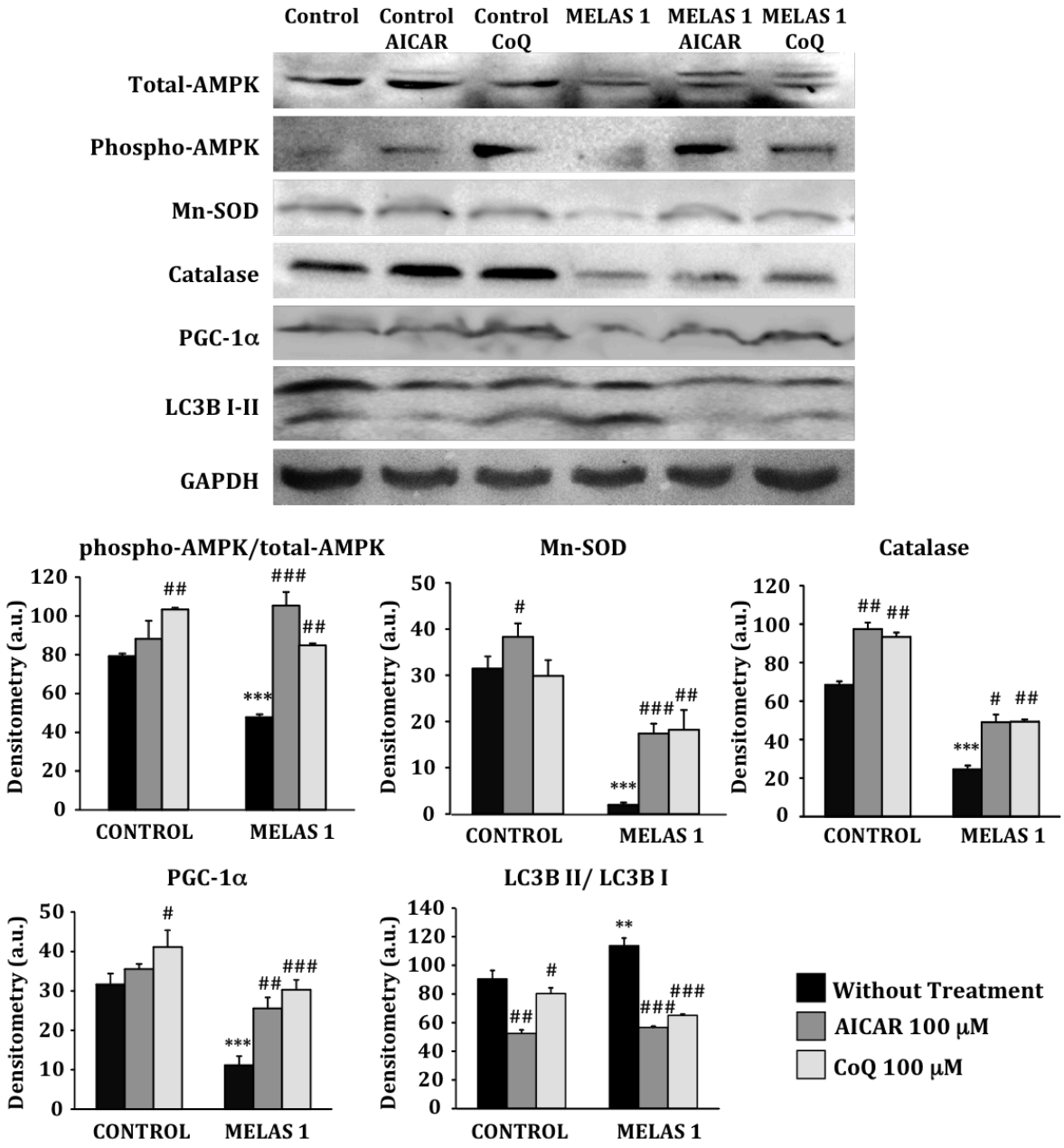

Figure R37. Effect of AICAR or CoQ treatment on AMPK activation, enzymatic antioxidant system, PGC-1 alpha and LC3B expression levels in MELAS 1 fibroblasts. Control and MELAS 1 fibroblasts, the most severe phenotype found, were treated with 100 μM AICAR or 100 μM CoQ for one week. Western blotting of phospho-AMPK, total-AMPK, Mn SOD, Catalase, PGC-1 alpha and LC3B were performed as described in Materials & Methods. GAPDH was used as loading control and densitometries (a.u., arbitrary units) were performed by using ImageJ software. All results were expressed as mean ± SD of three independent experiments. $^{**}P < 0.01$ and $^{***}P < 0.001$; significance of MELAS respect to control fibroblasts. $^{\#}P < 0.05$, $^{\#\#}P < 0.01$ and $^{\#\#\#}P < 0.001$; significance between the presence or absence of AICAR or CoQ treatment.

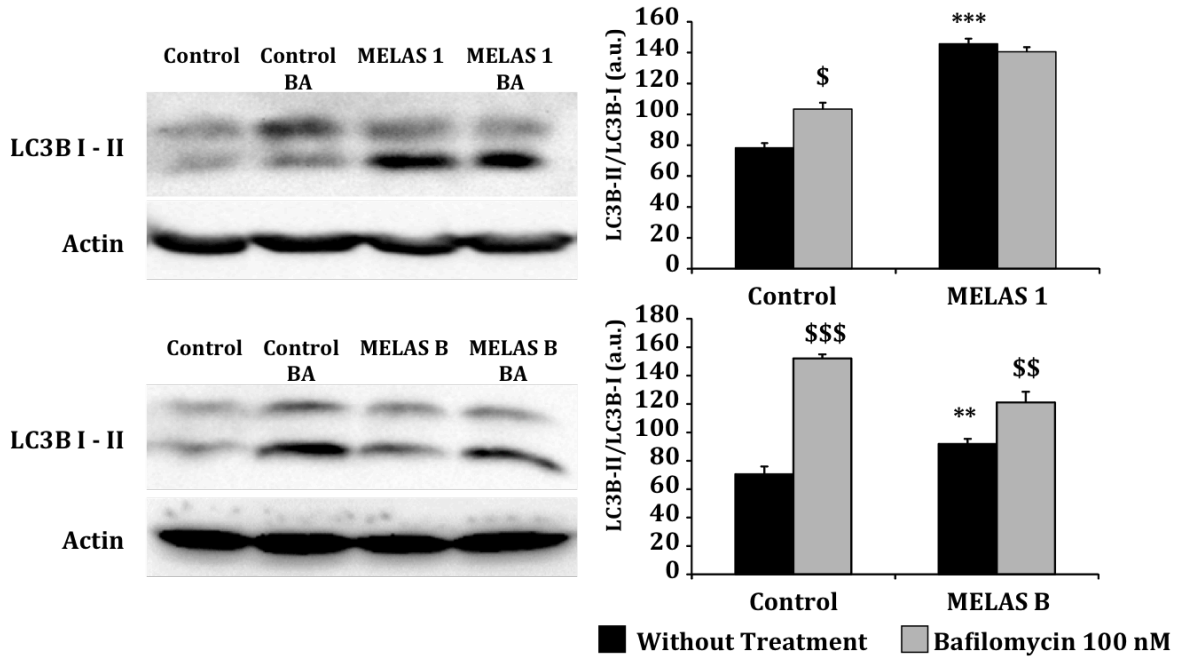

Figure R38. Autophagic flux analysis in MELAS 1 and MELAS B fibroblasts. Autophagic flux in control, MELAS 1 and MELAS B fibroblasts was determined by determination of LC3B II expression levels in the presence and absence of bafilomycin A1 (BA). Control and MELAS fibroblasts were incubated with 100 nM bafilomycin A1 for 12 h. Total cellular extracts were analysed by immunoblotting with antibodies against LC3B. Actin was used as a loading control. Densitometry of LC3B II was performed by using ImageJ software. Data are represented as mean ± SD of three separate experiments. $^{**}P < 0.01$ and $^{***}P < 0.001$; significance of MELAS respect to control fibroblasts. $^{\$}P < 0.05$, $^{\$\$}P < 0.01$ and $^{\$\$\$}P < 0.001$; significance between presence and absence of bafilomycin A1 treatment.

As expected, bafilomycin A1 treatment in control fibroblast cells led to a significant increase in the LC3B II/LC3 B I ratio, suggesting that autophagic flux is normal in control cells. However, bafilomycin A1 treatment in MELAS 1 fibroblasts had no effect on LC3B II/LC3B I ratio, indicating that autophagic flux was severely impaired in MELAS 1 fibroblasts with high heteroplasmy load. In contrast, bafilomycin A1 treatment in MELAS B fibroblasts had a slight effect on LC3B II/LC3B I ratio, indicating that autophagic flux was moderately impaired in MELAS B fibroblasts, which were harbouring low heteroplasmy load. These alterations in autophagic flux support the same differential pattern observed up to now, that is, MELAS 1 and MELAS 2 show more pathophysiological alterations than MELAS A and MELAS B.

In order to test whether AICAR or CoQ treatments were reducing autophagolysome accumulation by increasing autophagic flux, we assessed protein expression of LC3B in control and MELAS 1 fibroblasts, which showed impaired autophagic flux. Thus, control and MELAS 1 fibroblasts pre-treated with AICAR or CoQ were incubated for the last 12 hours with the autophagic flux blocker and LC3B II expression levels were examined by Western blotting (**Figure R39**).

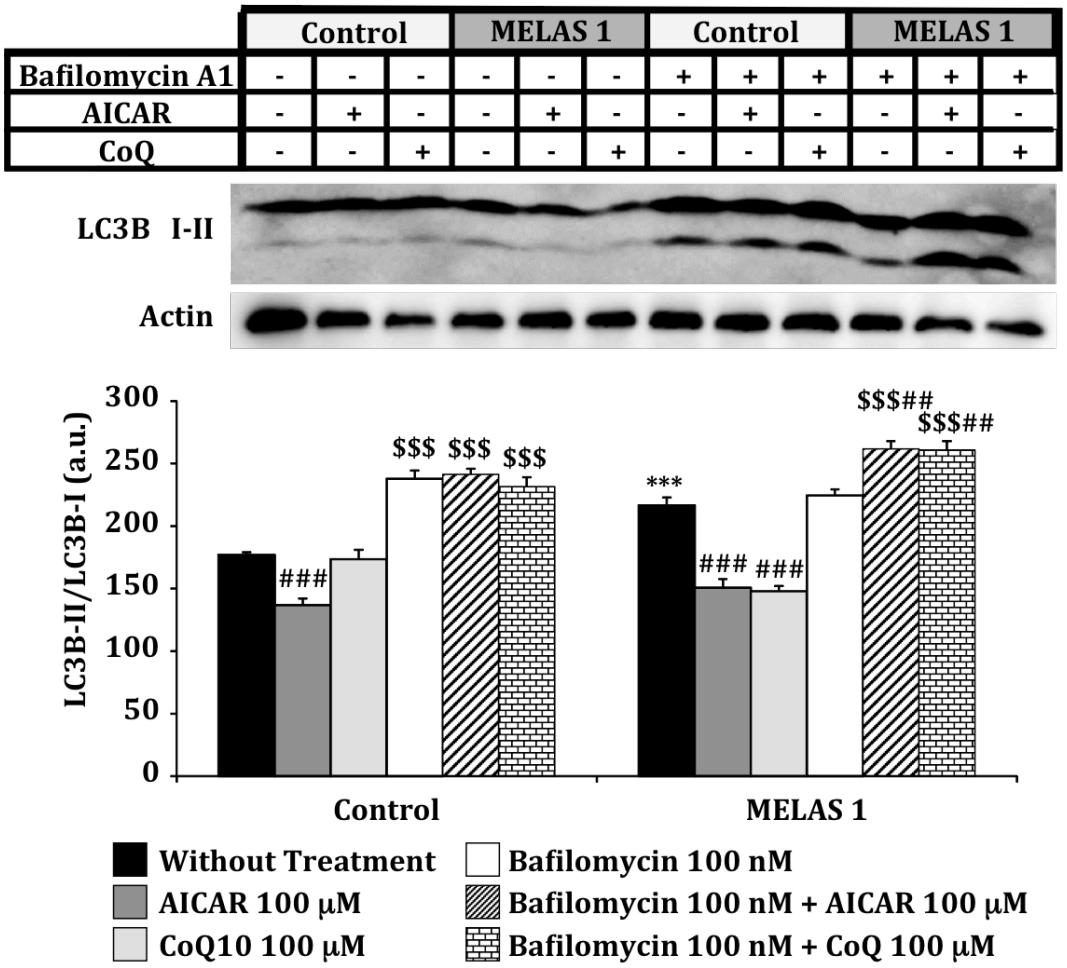

Figure R39. Effect of AICAR and CoQ treatment on autophagic flux in MELAS 1 fibroblasts. Control and MELAS 1 fibroblasts were pre-treated with 100 μM AICAR or 100 μM CoQ for 1 week. 12 hours before harvesting, cells were treated with 100 nM bafilomycin A1. Total cellular extracts were analysed by immunoblotting with antibodies against LC3B. Actin was used as a loading control. Densitometry of Western blotting was performed by using ImageJ software. All results were expressed as mean ± SD of three independent experiments. $^{***}P < 0.001$; significance of MELAS 1 respect to control fibroblasts. $^{\#\#}P < 0.01$ and $^{\#\#\#}P < 0.001$; significance between the presence and absence of AICAR or CoQ treatment. $^{\$\$\$}P < 0.001$; significance between the presence and absence of bafilomycin A1 (BA) in pre-treated fibroblasts.

Bafilomycin A1 incubation induced a significant increase on LC3-II expression levels of AICAR or CoQ-treated control and MELAS 1 fibroblasts. These results suggested that autophagic flux was indeed increased by AICAR or CoQ treatments.

Finally, to confirm that both AICAR and CoQ were able to increase the expression levels and activation of autophagy via AMPK, we explored one of the direct down-stream target of AMPK, ULK1, which is an activator of autophagy required for proper autophagic flux[501]. After AICAR or CoQ treatments, we found in control and MELAS 1 fibroblasts increased levels of phosphorylated ULK1, the active form of ULK1, concomitant with AMPK phosphorylation (**Figure R40**). Altogether, these data

support the hypothesis that AICAR and CoQ treatment reduce autophagosome accumulation in MELAS cells by increasing autophagy clearance.

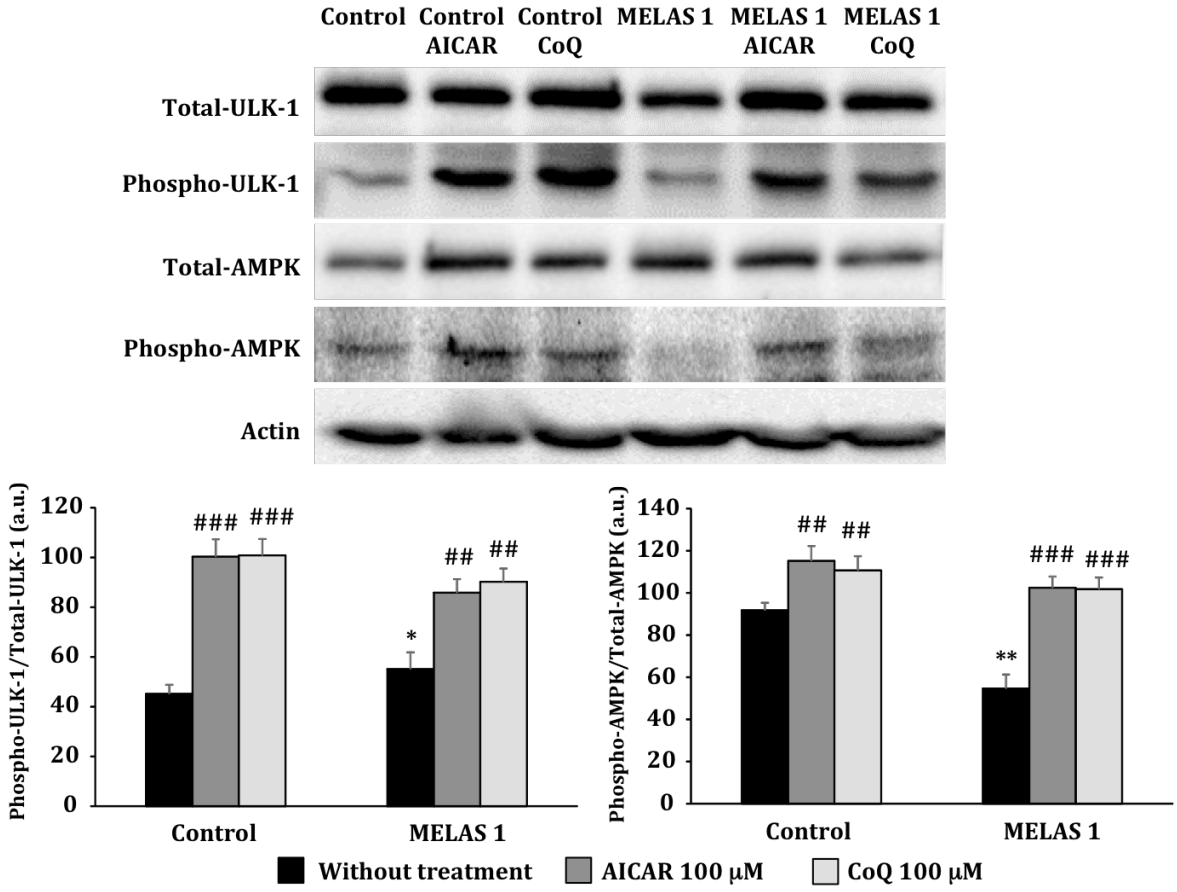

Figure R40. Effect of AICAR and CoQ treatments on ULK-1 and AMPK activation in MELAS 1 fibroblasts. Control and MELAS 1 fibroblasts were treated with 100 μM AICAR or 100 μM CoQ for 1 week. Western blottings of phospho-AMPK, total-AMPK, phospho-ULK1, total-ULK1 were performed as described in Materials & Methods. Actin levels were used as loading control. Densitometry was performed by using ImageJ software. Results were expressed as mean ± SD. *P<0.05 and **P < 0.01; significance of MELAS 1 respect to control fibroblasts. ##P < 0.01 and ###P < 0.001; significance between the presence and absence of AICAR or CoQ treatment.

R-VI. AICAR or CoQ treatments induces nuclear sublocalisation of phospho-PGC-1 alpha mediated by AMPK activation

In addition to enhancing autophagic flux and ameliorating pathophysiological parameters, AMPK stimulation by AICAR and CoQ treatments induced mitochondrial biogenesis in MELAS fibroblasts. Here, we wondered about how mitochondrial biogenesis is activated in MELAS fibroblast through AMPK activators. It is known that PGC-1α, essential regulator of mitochondrial biogenesis, is activated by AMPK. AMPK activation increases the expression of PGC-1α mRNA[502] and also its activation by direct phosphorylation[156]. On the other hand, there are evidences of nuclear PGC-1α translocation when it is phosphorylated[174]. Therefore, the subcellular localization of PGC-1α seems to have great importance for the functional activation of pathways such as mitochondrial biogenesis. Consequently, we analysed the subcellular localization of phospho-PGC-1α (active form) by immunostaining and fluorescence microscopy examination in the four MELAS fibroblasts cell lines (**Figure R41**).

Phospho-PGC-1α predominantly showed cytoplasmic localization in MELAS 1 and MELAS 2 fibroblasts whereas a major presence of phospho-PGC-1α in nuclei was observed in control, MELAS A and MELAS B fibroblasts. Likewise, we wondered about the effects of AICAR and CoQ treatments on phospho-PGC-1α sublocalisation. Thus, we also quantified phospho-PGC-1α nuclear foci before and after treating for a week with AICAR or CoQ. We observed that phospho-PGC-1α nuclear foci were significantly increased in control and all MELAS fibroblasts after treatments, including MELAS 1 and MELAS 2 cultures, which showed few nuclear PGC-1α foci before treatments. These results suggest that AMPK stimulation by AICAR or CoQ can control the nuclear localisation of phospho-PGC-1α.

In order to assess the role of AMPK in PGC-1α nuclear translocation after AICAR or CoQ treatment, we quantified nuclear phospho-PGC-1α foci in the presence or absence of compound C, a selective small-molecule inhibitor of AMPK[213] (**Figure R42**). Phospho-PGC-1α nuclear foci were increased after AICAR or CoQ treatments, however, in presence of compound C this increase was attenuated in case of MELAS A and, practically absence in MELAS 1.

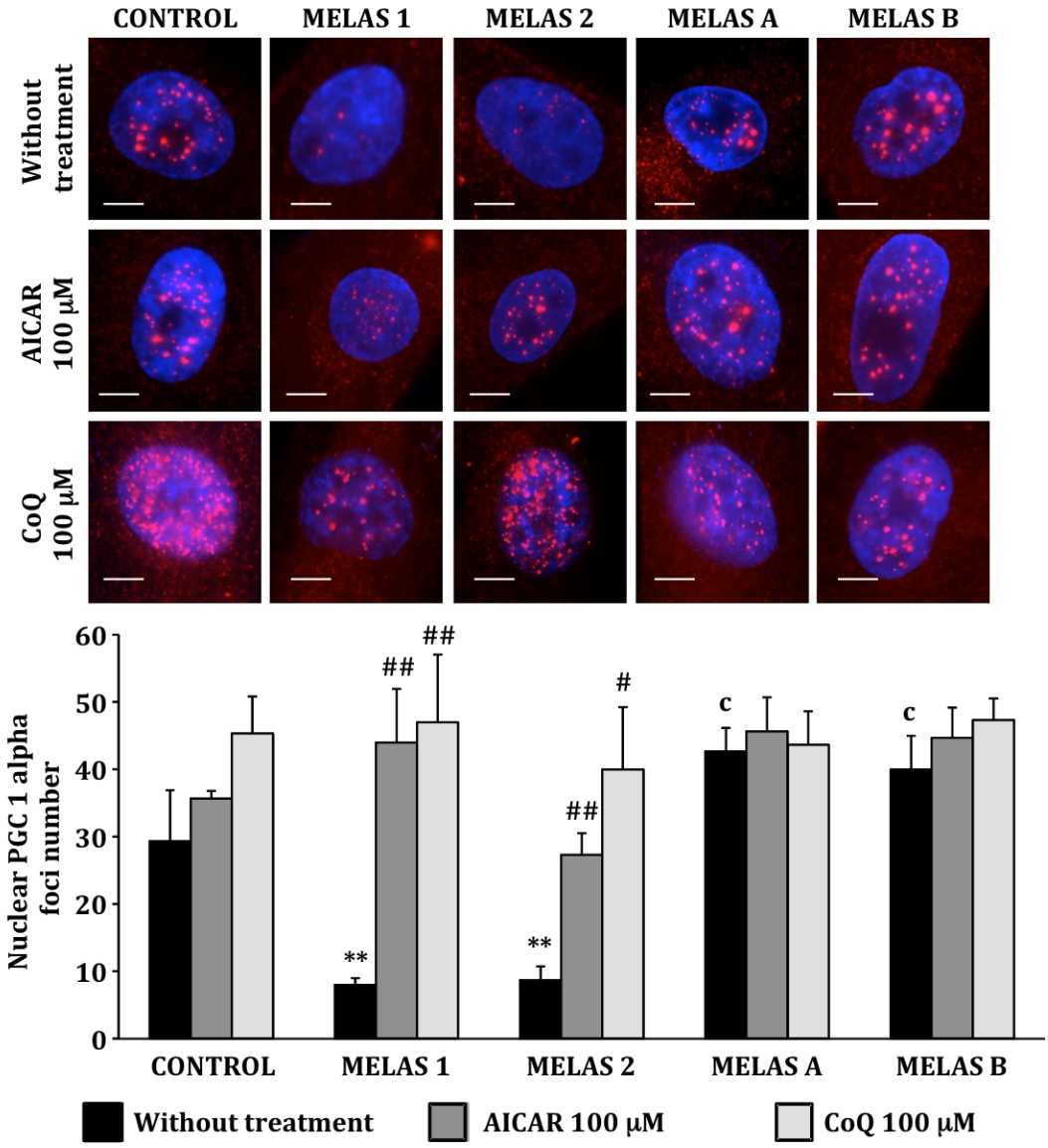

Figure R41. Effect of AICAR and CoQ treatment on nuclear PGC - 1 alpha sublocalisation in MELAS fibroblasts. Control, MELAS 1, MELAS 2, MELAS A and MELAS B fibroblasts were treated with 100 μM AICAR or 100 μM CoQ for 1 week. Immunostaining of phospho - PGC - 1 alpha (red) and DNA (blue) were performed according to described methods and visualized by fluorescence microscopy. Quantification of fluorescent phospho-PGC – 1 alpha foci in the nuclei was performed by using ImageJ software. More than 100 randomly selected cells were analysed for each experimental condition. Results are expressed as mean ± SD of three independent experiments. $^{**}P < 0.01$; significance of MELAS respect to control fibroblasts. $^{c}P < 0.001$; significance of MELAS A and MELAS B fibroblasts respect to MELAS 1 and MELAS 2 fibroblasts. $^{\#}P < 0.05$ and $^{\#\#}P < 0.01$; significance between the presence and absence of AICAR or CoQ treatment. [Scale bar = 5 μm].

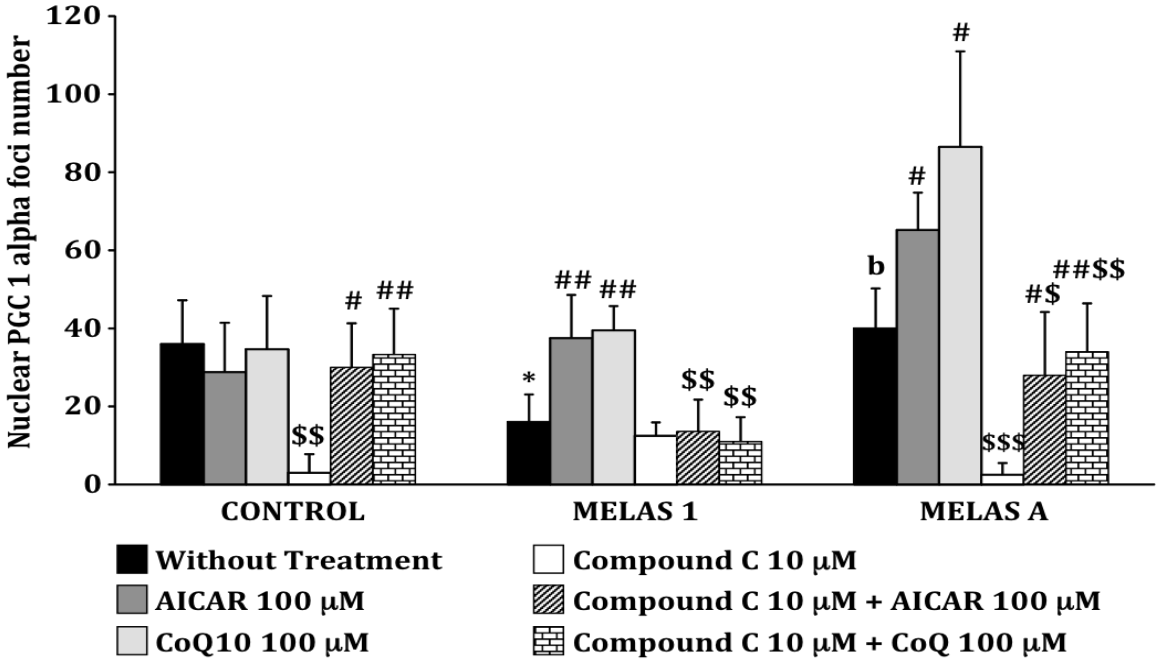

Figure R42. Effect of AMPK inhibition on nuclear PGC – 1 alpha localization in MELAS 1 and MELAS A fibroblasts. Control and MELAS 1 and MELAS A fibroblasts were treated with 100 μM AICAR or 100 μM CoQ for 1 week in the presence and absence of 10 μM compound C, an AMPK inhibitor. Nuclear phospho-PGC – 1 alpha foci were counted by using ImageJ software. More than 100 randomly selected cells were analysed for each experimental condition. Results are expressed as mean ± SD. $^{*}P < 0.05$; significance of MELAS respect to control fibroblasts. $^{b}P < 0.01$; significance of MELAS A and MELAS B fibroblasts respect to MELAS 1 and MELAS 2 fibroblasts. $^{\#}P < 0.05$ and $^{\#\#}P < 0.01$; significance between the presence and absence of AICAR or CoQ treatment. $^{\$}P < 0.05$, $^{\$\$}P < 0.01$ and $^{\$\$\$}P < 0.001$; significance between the presence and absence of compound C.

These results were confirmed by subcellular fractionation techniques and the evaluation of phospho-PGC-1α expression levels in the nuclear fraction by Western blotting (**Figure R43**). As shown, phospho-PGC-1α increased in nuclear fractions after AICAR and CoQ treatments, especially in the case of MELAS 1 fibroblasts that showed low levels before treatment. Supplementation of medium with compound C at the same time that AMPK activators resulted in attenuated increases of phospho-PGC-1α in MELAS A and a drastic reduction of signal in MELAS 1 fibroblasts.

Taken together these data suggest that PGC-1α nuclear translocation is impaired in MELAS 1 and MELAS 2 fibroblasts, and CoQ or AICAR treatments increase nuclear phospho-PGC1-α foci, possibly through AMPK activation. Once in the nucleus, phospho-PGC-1α is supposed to active mitochondrial biogenesis and thus compensate the deleterious defects of increased mitophagy.

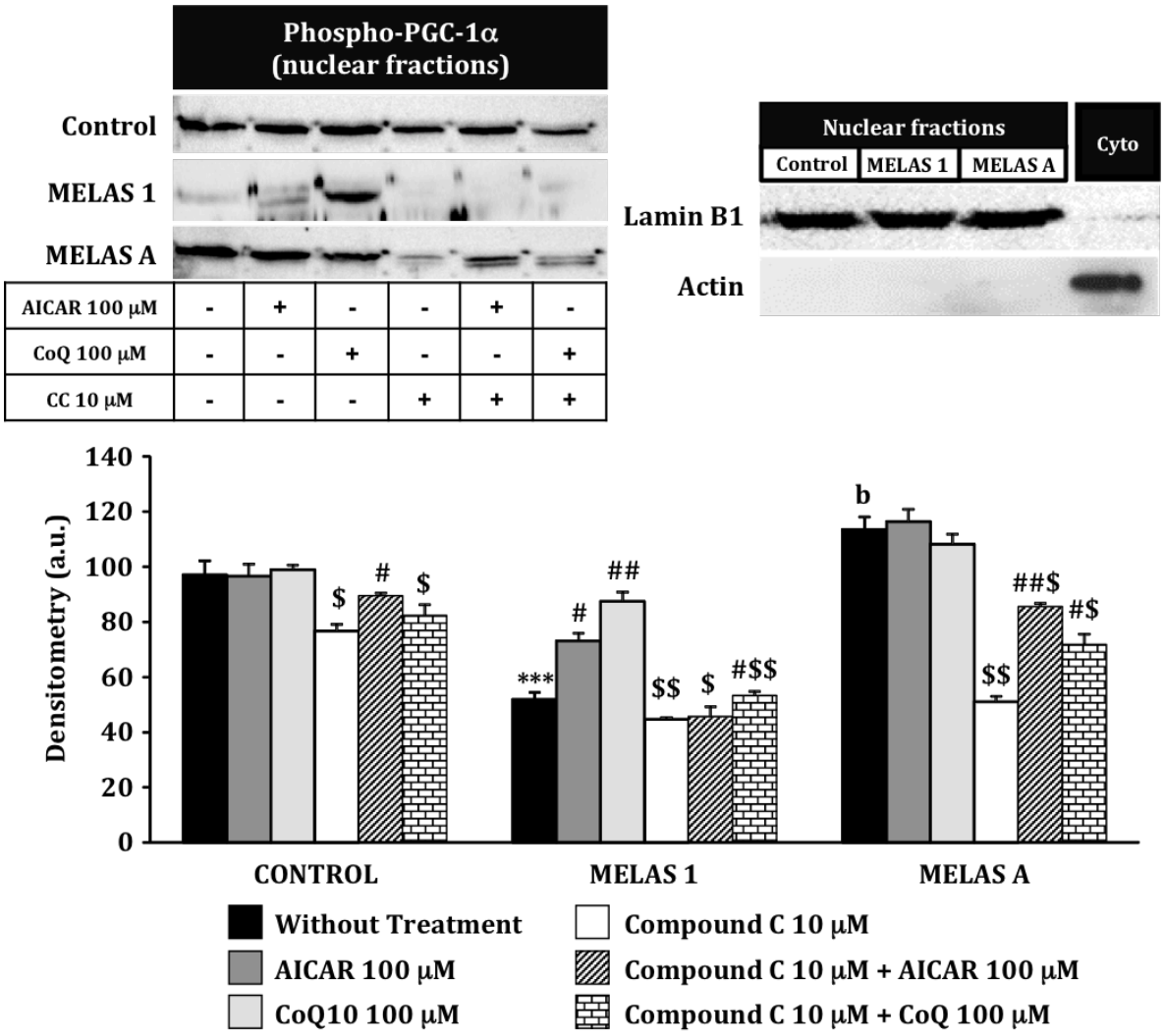

Figure R43. Effect of AMPK inhibition on nuclear PGC – 1 alpha localization in MELAS 1 and MELAS A fibroblasts nuclear fractions. Control and MELAS 1 and MELAS A fibroblasts were treated with 100 μM AICAR or 100 μM CoQ for one week in the presence and absence of 10 μM compound C, an AMPK inhibitor. Subcellular fractioning was performed as described in Materials & Methods to isolate nuclear fractions. Phospho-PGC – 1 alpha was analysed on nuclear fractions by Western blotting. The purity of the nuclear fraction of control and MELAS fibroblasts was validated by Western blotting analysis of a "house-keeper" marker protein (Lamin B1) specific for the nuclear compartment. Actin was used as cytosolic marker to check the cytosolic fraction (Cyto) as purification control. Densitometry (a.u., arbitrary units) was performed by using ImageJ software. Results are expressed as mean ± SD. $^{***}P < 0.001$; significance of MELAS respect to control fibroblasts. $^{b}P < 0.01$; significance of MELAS A fibroblasts respect to MELAS 1 fibroblasts. $^{\#}P < 0.05$ and $^{\#\#}P < 0.01$; significance between the presence and absence of AICAR or CoQ treatment. $^{\$}P < 0.05$ and $^{\$\$}P < 0.01$; significance between the presence and absence of compound C.

R-VII. AICAR and CoQ also restored pathophysiological alterations in MELAS cybrids harbouring a 90% heteroplasmy load.

Our findings indicated that differential pathophysiology observed in MELAS fibroblasts could be related to heteroplasmy load. Fibroblasts with the most severe phenotypes harboured higher mutational loads (MELAS 1: 17%, MELAS 2: 26% and MELAS 3: 43%) than fibroblasts with less severe alterations (MELAS A: 9% and MELAS B: 4%). In order to definitively associate pathophysiological severity to heteroplasmy load, we decided to extend our observations to a transmitochondrial MELAS cybrid cell line harbouring an extremely high heteroplasmy level (90 %). Transmitochondrial cybrid cell lines are indispensable tools in mitochondrial investigation for providing a controlled nuclear background in which to study the molecular mechanisms by which mutations in mtDNA impair cellular function[100,101,461,503–505]. This model is particularly interesting given that subtle changes in mtDNA heteroplasmic genotype can have profound effects on the nuclear gene expression state[506]. Therefore, in addition to relating pathophysiology and heteroplasmy, we can discard putative compensatory effects of the nuclear context by analysing this MELAS cybrids.

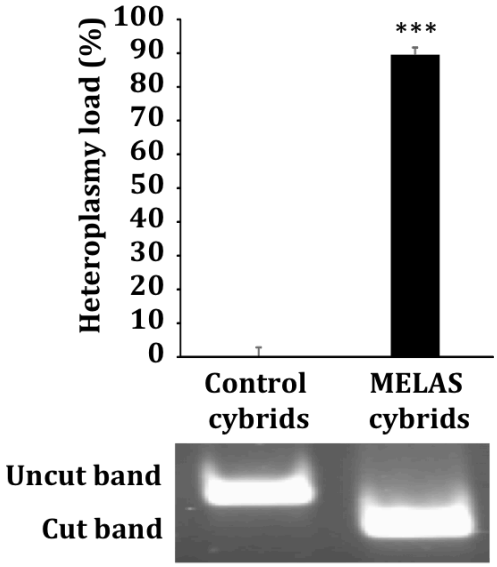

Figure R44. Heteroplasmy load in transmitochondrial MELAS cybrids. Heteroplasmy load was determined by PCR-RFLP assay. Results are expressed as mean ± SD. Significance of MELAS respect to control cybrids was represented as $^{***}P < 0.001$.

Thus, we explored several pathophysiological parameters in transmitochondrial cybrid cells harbouring the same MELAS mutation (m.3243A>G) to confirm that AICAR and CoQ treatments were also effective on MELAS cybrids, independently of the nuclear context. First, we performed a heteroplasmy analysis to verify the mutational load of these MELAS cybrids. We confirmed that MELAS cybrids harboured an extremely high heteroplasmy load close to 90 % (89.6%) (**Figure R44**).

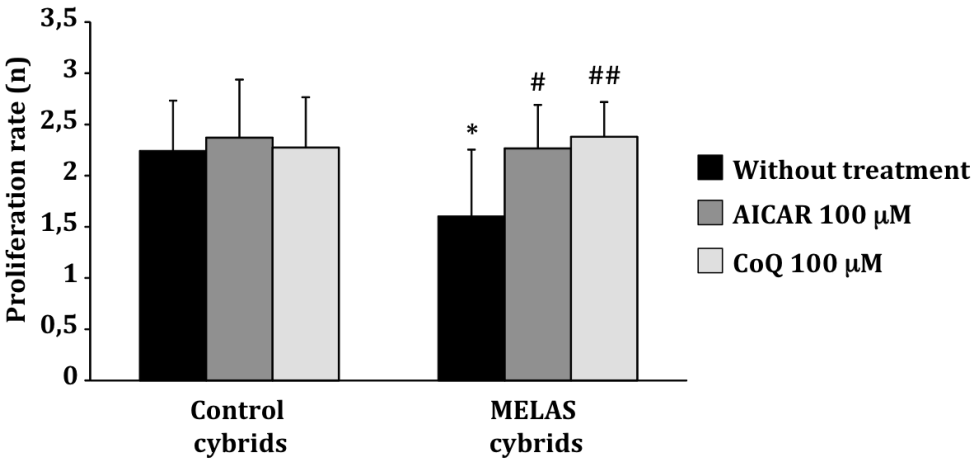

Figure R45. Proliferation rate in transmitochondrial MELAS cybrids. Effect of AICAR or CoQ on proliferation rate in control and transmitochondrial MELAS cybrids was analysed by counting viable cells after treatment as described in Materials & Methods. Results are expressed as mean ± SD. Significance of MELAS cybrids respect to control cybrids was represented as $^{*}P < 0.05$. Significance between the presence and absence of AICAR or CoQ treatment was represented as $^{\#}P < 0.05$ and $^{\#\#}P < 0.01$.

Because of tumour origin and high mutational load of cybrids, cellular metabolism is supposed to switch from a predominantly oxidative to glycolytic metabolism[506], which could mask mitochondrial dysfunction. To reduce glycolytic metabolism, induce respiration and make more evident the mitochondrial defects, transmitochondrial cybrids were cultured in glucose-restricted conditions as described in Materials and Methods. Then, we examined growth rate, ATP production and expression levels of LC3B and PGC-1α in control and MELAS cybrids clones. Likewise, we examined the effectiveness of AICAR and CoQ on these parameters. Growth rate of MELAS cybrids was decreased respect to control cybrids by 30% and restored by 100 μM AICAR or 100 μM CoQ treatments significantly (**Figure R45**).

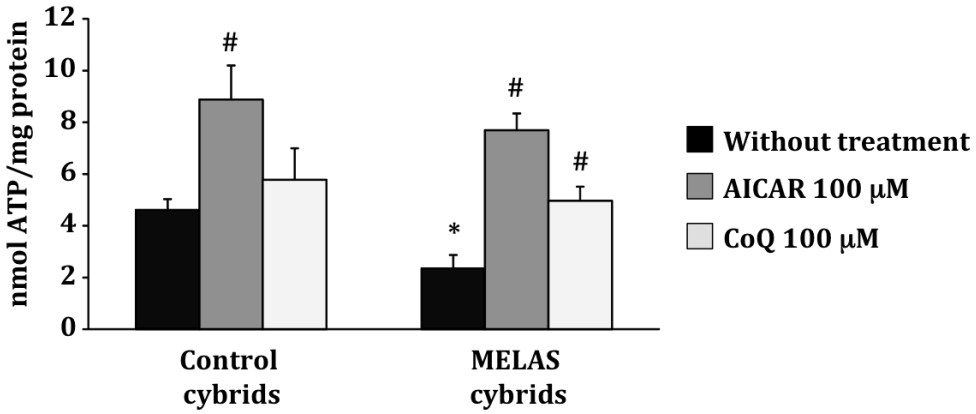

Figure R46. ATP production in transmitochondrial MELAS cybrids. Effect of AICAR or CoQ treatment on ATP levels in control and MELAS cybrids was determined by using a luciferase-based assay. Results are expressed as nmole ATP/mg protein units (mean ± SD). Significance of MELAS respect to control cybrids was represented as $^{*}P < 0.05$. Significance between the presence and absence of AICAR or CoQ treatment was represented as $^{\#}P < 0.05$.

In the same way, we found significantly decreased ATP levels in MELAS cybrids suggesting energy depletion in MELAS cybrids. AICAR or CoQ treatments restored these values up to control levels (**Figure R46**).

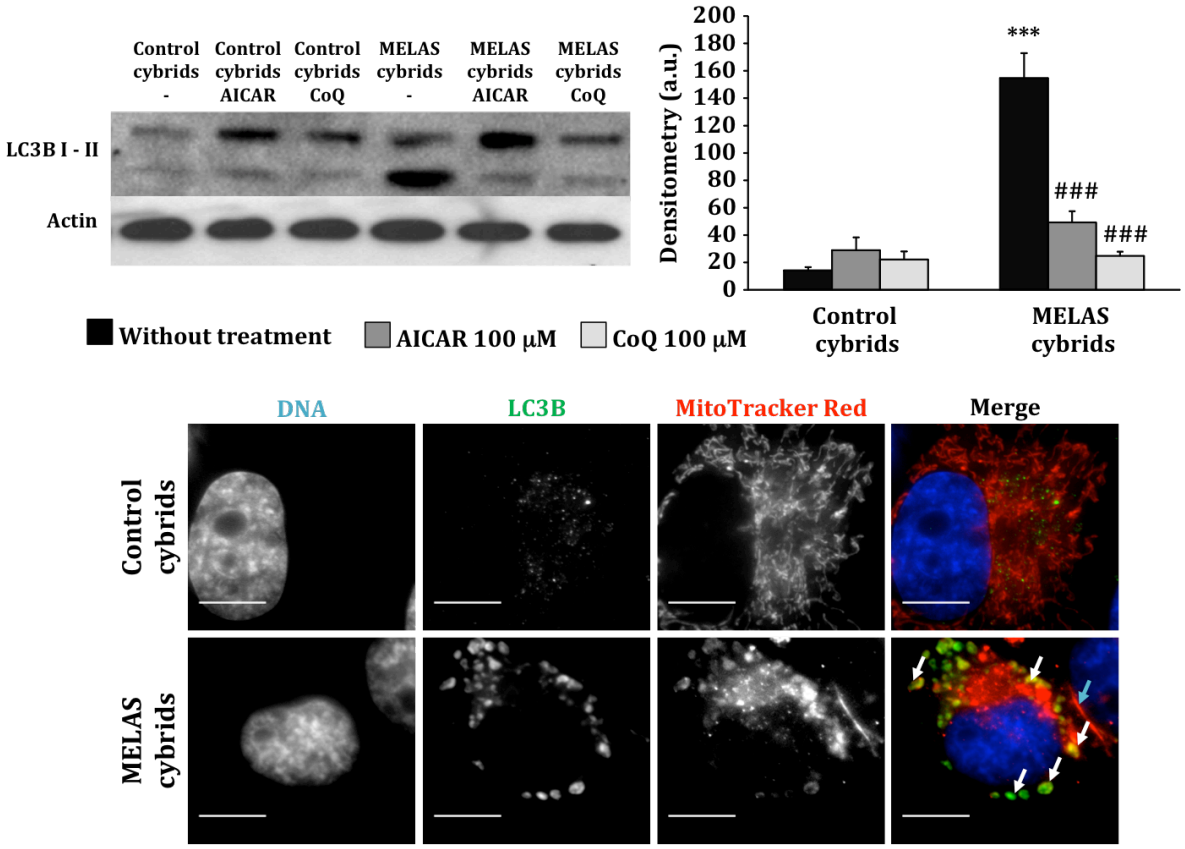

Figure R47. Autophagy and mitophagy in transmitochondrial MELAS cybrids. Effect of AICAR or CoQ treatment on protein expression levels of LC3B was measured by Western blotting analysis. Densitometry is shown representing data as mean ± SD of three separate experiments. Significance of MELAS cybrids respect to control cybrids was represented as $^{***}P < 0.001$. Significance between the presence and absence of AICAR or CoQ treatment was represented as $^{###}P < 0.001$. Immunostaining of cytochrome c (mitochondrial marker) and LC3B (autophagosome marker) was performed to visualise degrading mitochondria (white arrows) in Control and MELAS cybrids. [Scale bar = 10 μm].

The protein expression levels of LC3B were analysed by using Western blotting techniques. High levels of LC3B suggested enhanced autophagy and possible selective mitochondrial degradation phenomena as later confirmed in **Figure R47**. Therefore, mitophagy activation was also demonstrated in transmitochondrial MELAS cybrids as a consequence of the mutation in mtDNA and not the product of a concomitant nuclear gene defect.

Since AICAR and CoQ treatments restored control levels of protein expression of LC3B, we related these results with increased autophagic flux observed in MELAS

fibroblasts. As shown in **Figure R48**, AICAR and CoQ were also able to increase autophagic flux in MELAS cybrids.

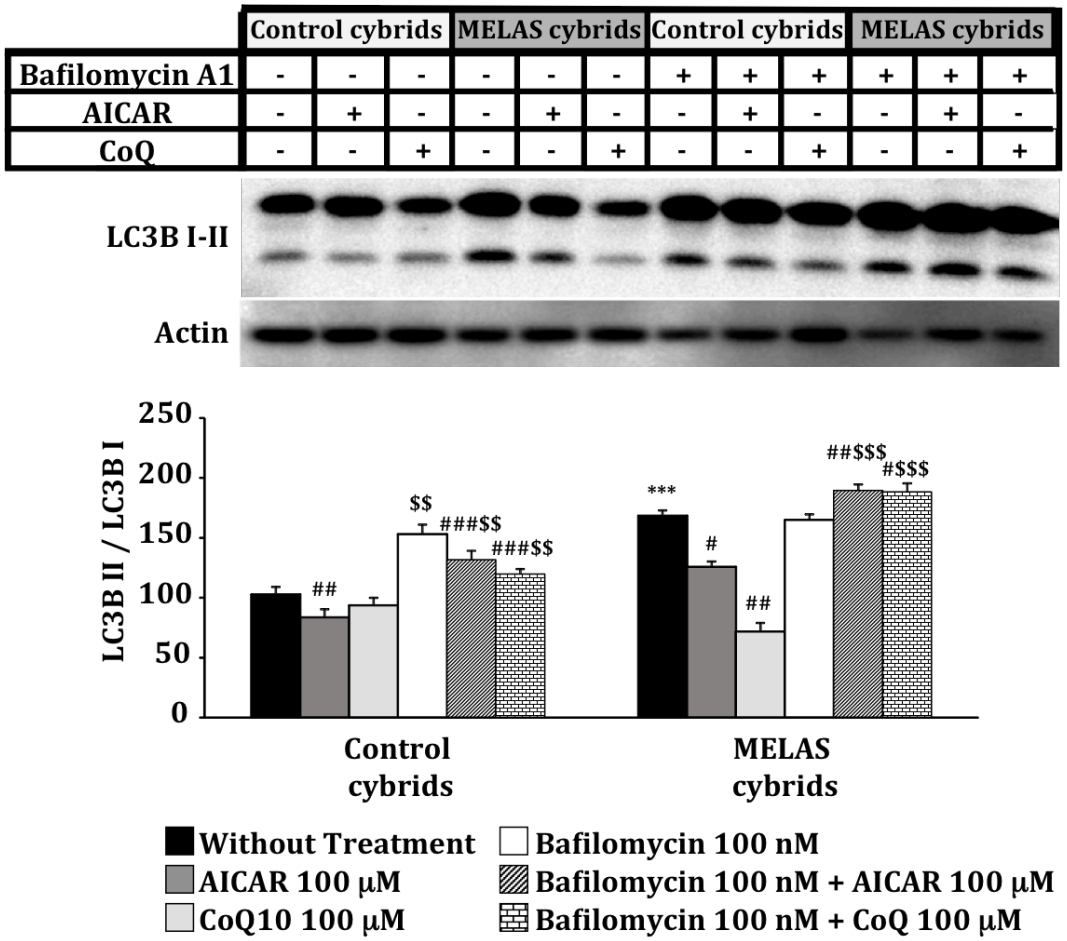

Figure R48. Effect of AICAR and CoQ treatment on autophagic flux in transmitochondrial MELAS cybrids. Control and MELAS cybrids were pre-treated with 100 μM AICAR or 100 μM CoQ for 48 hours. 12 hours before harvesting, cells were treated with 100 nM bafilomycin A1. Total cellular extracts were analysed by immunoblotting with antibodies against LC3B. Actin was used as a loading control. Densitometry of Western blotting was performed by using ImageJ software and results were expressed as mean ± SD of three independent experiments. $^{***}P < 0.001$; significance of MELAS respect to control cybrids. $^{\#}P < 0.05$, $^{\#\#}P < 0.01$ and $^{\#\#\#}P < 0.001$; significance between the presence and absence of AICAR or CoQ treatment. $^{\$\$}P < 0.01$ and $^{\$\$\$}P < 0.001$; significance between the presence and absence of bafilomycin A1 (BA) in pre-treated cybrids.

The analysis of PGC-1α reported similar results. As in the case of fibroblasts, low levels of phospho-PGC1-α were found in MELAS cybrids compared to control cybrids, and they were restored under AICAR or CoQ supplementation. These results were also concomitant with mislocalisation of phospho-PGC-1α, which was relocated to nuclei after AICAR and CoQ treatments (**Figure R49**).

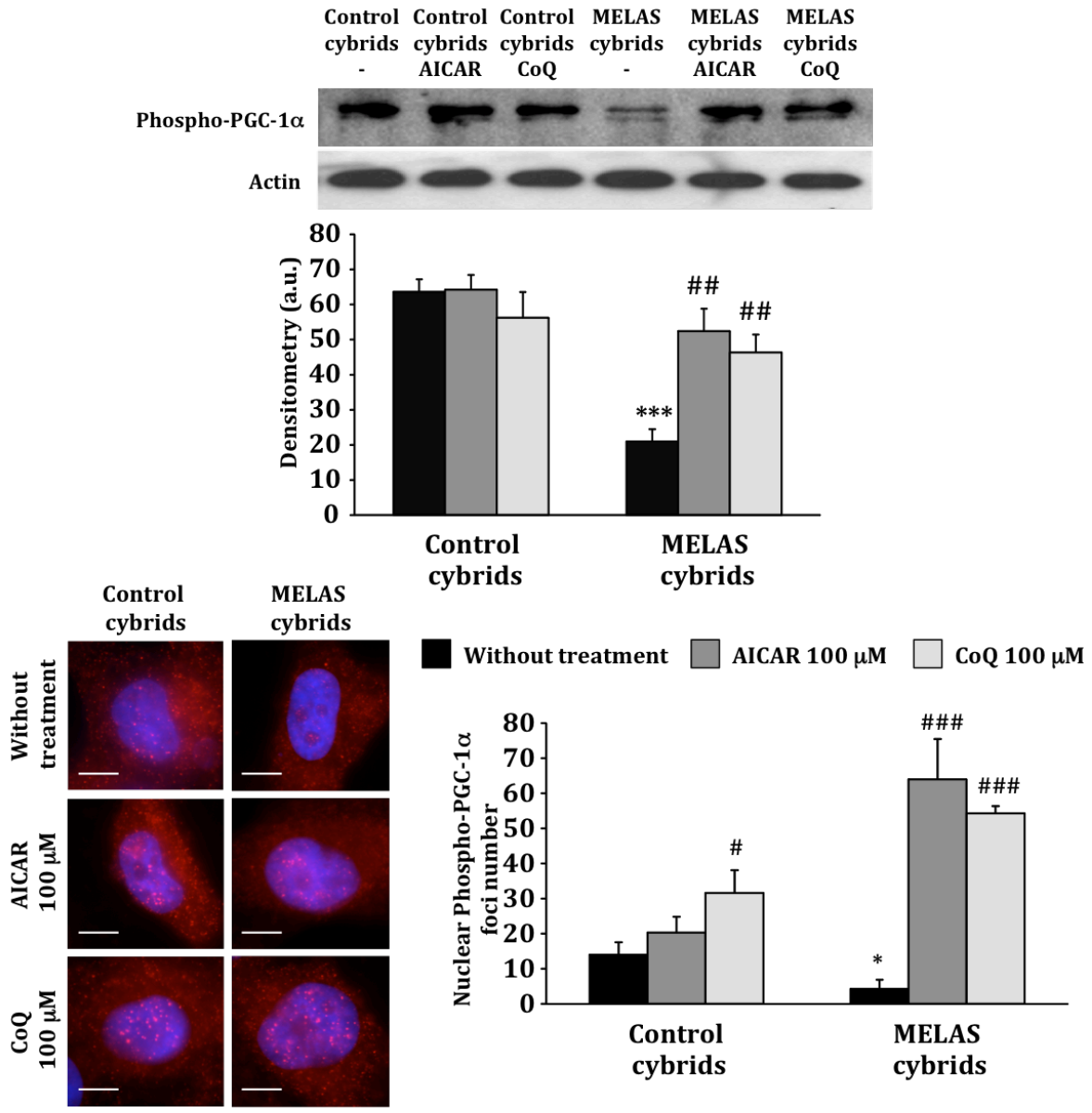

Figure R49. Effect of AICAR and CoQ treatment on phospho-PGC – 1 alpha in transmitochondrial MELAS cybrids. Control and MELAS cybrids were treated with 100 μM AICAR or 100 μM CoQ for 48 hours. Total cellular extracts were analysed by immunoblotting with antibody against Phospho-PGC – 1 alpha. Actin was used as a loading control. Densitometry of Western blotting was performed by using ImageJ software. Representative images of the subcellular localisation of phospho-PGC – 1 alpha (red) in control and MELAS cybrids was examined by fluorescence microscopy. Quantification of nuclear phospho-PGC – 1 alpha foci was performed by using ImageJ software. More than 100 randomly selected cells were analysed for each experimental condition. All results were expressed as mean ± SD of three independent experiments. $^{*}P < 0.05$ and $^{***}P < 0.001$; significance of MELAS respect to control cybrids. $^{\#}P < 0.05$, $^{\#\#}P < 0.01$ and $^{\#\#\#}P < 0.001$; significance between the presence and absence of AICAR or CoQ treatment. [Scale bar = 5 μm].

Previously in this work, PGC-1α activation in MELAS fibroblasts has been strongly associated to mitochondrial biogenesis and AMPK activation. To further investigate

whether the effect of AICAR and CoQ on AMPK activation and mitochondrial biogenesis is also extensible for MELAS cybrids, we analysed AMPK phosphorylation and mitochondrial mass measured by citrate synthase activity in transmitochondrial cybrids after treatments. As expected, AMPK activation was increased after AICAR or CoQ treatments (**Figure R50**). However, in presence of compound C, AMPK phosphorylation was only partially increased.

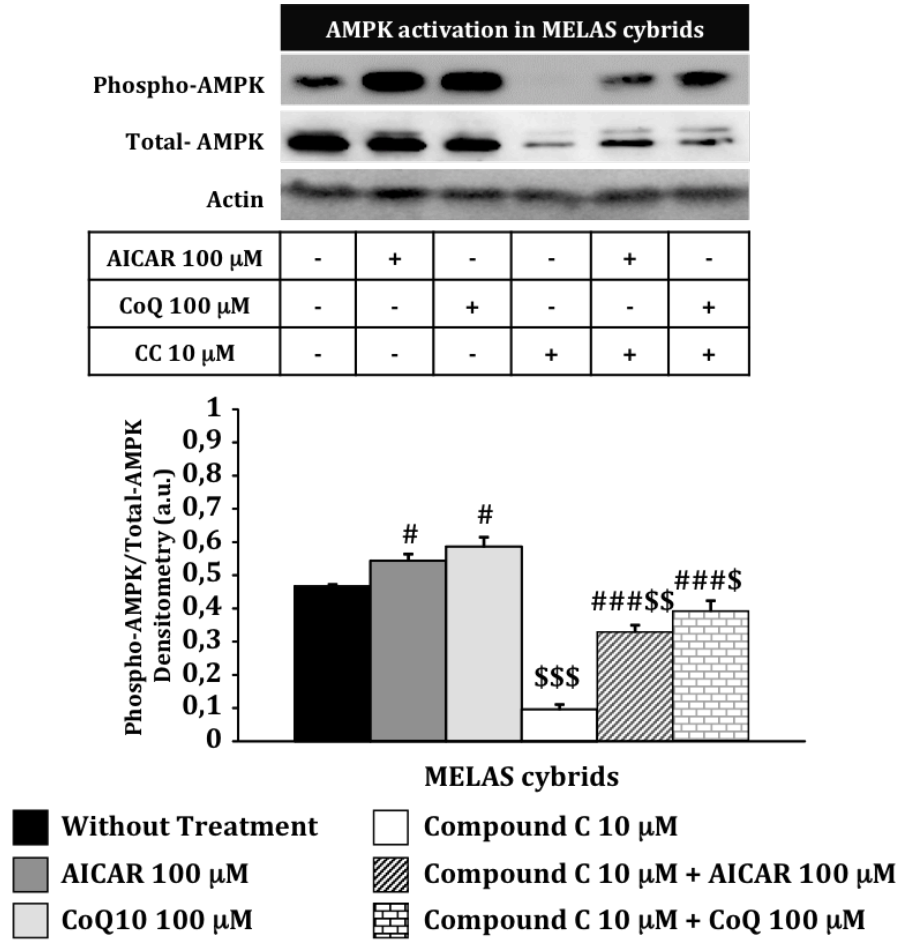

Figure R50. Effect of AICAR and CoQ treatments on AMPK activation in absence of AMPK activation in transmitochondrial MELAS cybrids. Control and MELAS cybrids were treated with 100 μM AICAR or 100 μM CoQ for 48 hours in presence and absence of 10 μM compound C, an AMPK inhibitor. AMPK activation was assessed by Western blotting by using antibodies against the total and phosphorylated form of AMPK. Actin was used as a loading control. Densitometry of Western blotting was performed by using ImageJ software and all results were expressed as mean ± SD. $^{\#}P<0.05$ and $^{\#\#\#}P<0.001$; significance between the presence and absence of AICAR or CoQ treatment. $^{\$}P < 0.05$, $^{\$\$}P < 0.01$ and $^{\$\$\$}P < 0.001$; significance between the presence and absence of compound C.

Mitochondrial mass measured by citrate synthase activity was significantly reduced in transmitochondrial MELAS cybrids (**Figure R51**). AICAR and CoQ treatment restored citrate synthase activity except in cases where compound C prevented AMPK

activation. These results strongly indicate that mitochondrial dysfunction shown by MELAS cybrids could be mediated by alteration in AMPK activation.

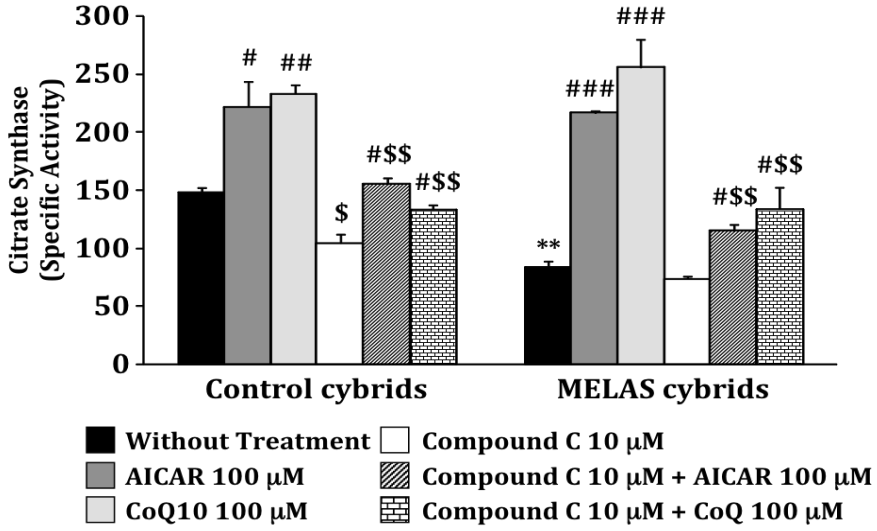

Figure R51. Effect of AICAR or CoQ treatment on mitochondrial biogenesis measured by citrate synthase activity in absence of AMPK activation in transmitochondrial MELAS cybrids. Control and MELAS cybrids were treated with 100 μM AICAR or 100 μM CoQ for 48 hours in presence and absence of 10 μM compound C, an AMPK inhibitor. Results are expressed as mean ± SD. Significance of MELAS respect to control cybrids was represented as $^{**}P < 0.01$. Significance between the presence and absence of AICAR or CoQ treatment was represented as $^{\#}P < 0.05$, $^{\#\#}P < 0.01$ and $^{\#\#\#}P < 0.001$. Significance between the presence and absence of compound C was represented as $^{\$}P < 0.05$ and $^{\$\$}P < 0.01$.

As AMPK activation seems to regulate mitochondrial biogenesis activation, we wondered whether sublocalisation of phospho-PGC-1α is also compromised in absence of AMPK activation. Once again, we prevented AMPK activation by using compound C during AICAR or CoQ treatments and we found that phospho-PGC-1α localisation was increased in nuclei after AICAR or CoQ treatments, but notably decreased when combined AMPK stimulators with the AMPK inhibitor (**Figure R52**).

Altogether, our findings indicated that MELAS cybrids with extremely high heteroplasmy also reproduced severe pathophysiological alterations such as reduced proliferation rate, ATP production, mitochondrial mass or nuclear PGC-1α foci. Furthermore, these results also support the hypothesis that observed alterations are a direct result of the mitochondrial m.3243A>G mutation and not a consequence of nuclear defects. Definitively, these alterations can be ameliorated by both AICAR and CoQ treatments or prevented by compound C suggesting that this rescue is mediated, at least partially, by AMPK activation. Therefore, AMPK thus becomes a cornerstone upon which mitochondrial biogenesis and mitophagy activation can regulate the pathophysiological state of MELAS cells. Our therapeutic approaches with fibroblasts and transmitochondrial cybrids reinforce the usefulness of AICAR and Coenzyme Q_{10} as treatments opening multiple possibilities to screen the effectiveness of a huge set of untested pharmacological drugs.

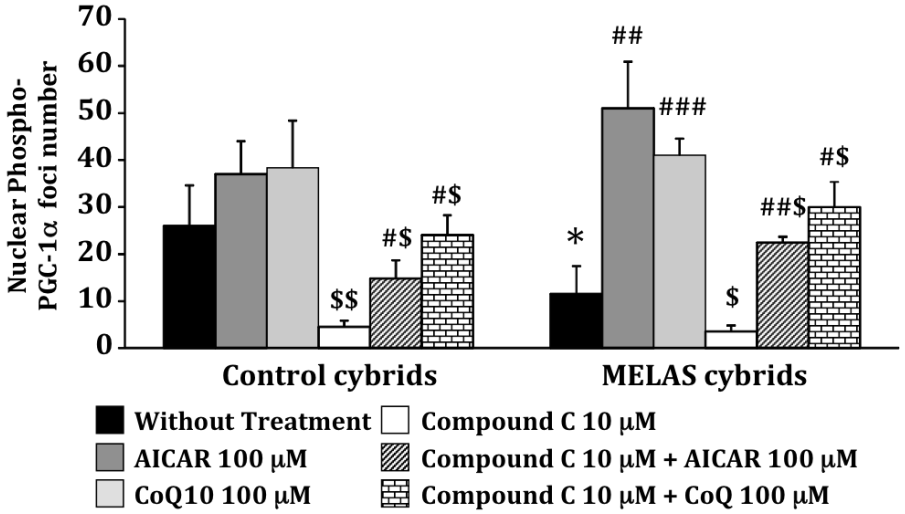

Figure R52. Effect of AICAR or CoQ treatments on the sublocalisation of phospho-PGC – 1 alpha in absence of AMPK activation in transmitochondrial MELAS cybrids. Control and MELAS cybrids were treated with 100 μM AICAR or 100 μM CoQ in presence and absence of 10 μM compound C, an AMPK inhibitor. Quantification of nuclear phospho-PGC – 1 alpha foci was performed by using ImageJ software. More than 100 randomly selected cells were analysed for each experimental condition. Results are expressed as mean ± SD. Significance of MELAS respect to control cybrids was represented as $^{*}P < 0.05$. Significance between the presence and absence of AICAR or CoQ treatments was represented as $^{\#}P < 0.05$, $^{\#\#}P < 0.01$ and $^{\#\#\#}P<0.001$. Significance between the presence and absence of compound C was represented as $^{\$}P < 0.05$ and $^{\$\$}P < 0.01$.

R-VIII. Transmitochondrial cybrids and patient-derived fibroblasts as a platform to validate the effectiveness of pre-screened drugs for MELAS syndrome

Currently, no consensus criteria exist for treating MELAS syndrome or mitochondrial dysfunction in other diseases due to the fact that few consistent results have been achieved with current therapies[355]. As commented in Introduction, some of the most used therapeutic approaches in treating MELAS syndrome have been adopted through isolated case reports or limited clinical trials.

In previous Results subsections, our results confirmed that AICAR and Coenzyme Q_{10} are effective pharmacological treatments for MELAS syndrome at cellular level. Both AICAR and Coenzyme Q_{10} ameliorated many physiopathological alterations such as defective respiratory activities, toxic levels of ROS or energy depletion in fibroblasts derived from MELAS patients and transmitochondrial cybrids with the m.3243A>G MELAS mutation. Our results and other recent works demonstrate the usefulness and the potential of primary cultures of fibroblasts and cybrids to study mitochondrial disorders. Therefore, we propose the use of these cellular models for the screening and validation of pharmacological drugs selected from *in silico* studies or massive pre-screening analysis.

In previous studies, our group used a strain of *Saccharomyces cerevisiae* harbouring the A14G mutation equivalent to the human m.3243A > G mutation as a cellular model in the search for effective drugs for the treatment of MELAS disease[507,508]. From this preliminary screening, 60 nM riboflavin and 100 μM Coenzyme Q_{10} resulted in the most efficient drugs in restoring the respiratory defect in the mutant yeast[101]. Both riboflavin and coenzyme Q_{10} are often considered first-line agents in the treatment of MELAS syndrome since no significant adverse reactions have been reported at low doses[295,355,385,432,439]. As already introduced above, riboflavin is an essential cofactor in complexes I and II of the MRC[432] that shows antioxidant activity derived from its role as a precursor of FAD[445]. On the other hand, CoQ functions as an essential electron transporter in the MRC and also acts as an potent antioxidant that can protect from oxidative damage[509].

Along this work, we have demonstrated that MELAS cybrids and fibroblasts share common pathological characteristics, especially when mutational load is substantially high. In this section, we propose the use of transmitochondrial cybrids and fibroblasts derived from MELAS patients with high heteroplasmy load for the evaluation of pre-screened selected drugs. Therefore, we used the transmitochondrial cybrids harbouring 90% heteroplasmy, and a MELAS fibroblast cell line (MELAS 3) with 43% of heteroplasmy.

Due to its tumour origin, cybrids growth fast, avoiding the main handicap of the use of fibroblasts derived from patients, the low growth rate. Therefore, the initial use of transmitochondrial cybrids allows us to quickly screen a large amount of drugs (in treatments of 48 hours) to finally select particular candidates for evaluation in

fibroblasts (in treatments of 1 week), a cellular model that in theory can reflect better MELAS patient phenotype.

In order to check the screening potential of cybrids and fibroblasts, first, we tested the selected treatments of 60 nM riboflavin and 100 μM CoQ for 48 hours in transmitochondrial MELAS cybrids. CoQ was used as a positive control since its effects on cybrids in the pathophysiological parameters was already shown above. Therefore, as in previous Results subsections, we studied several physiopathological parameters such as proliferation rate, ATP production, mitochondrial respiratory capacity and ROS levels (**Figure R53**).

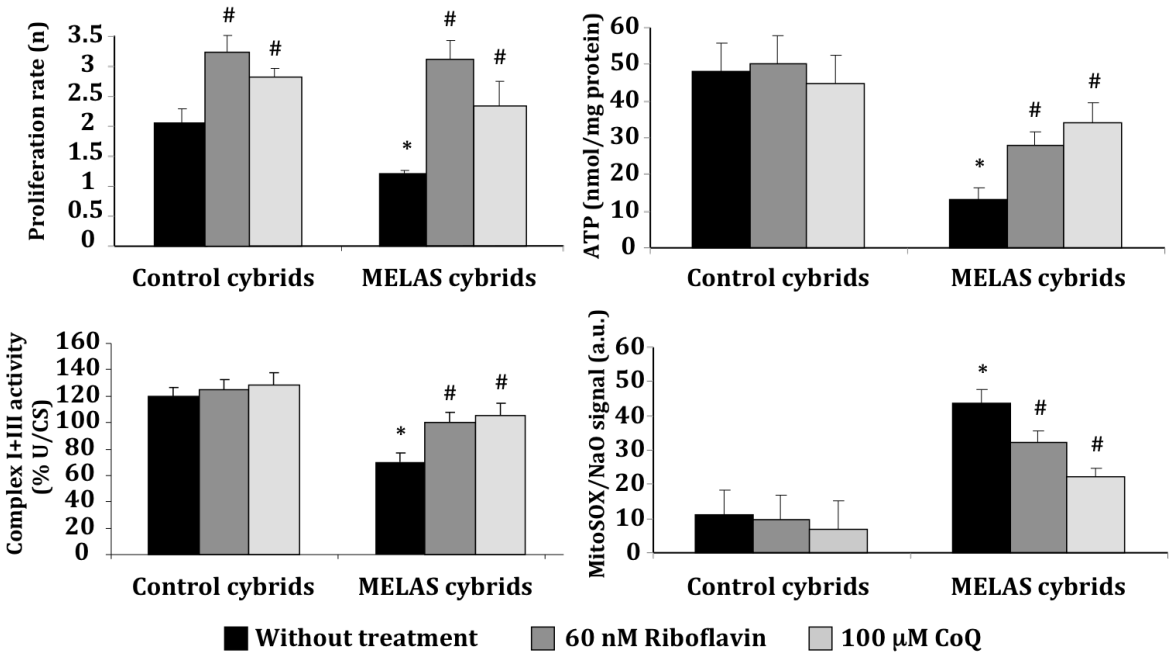

Figure R53. Effect of riboflavin and CoQ treatments on pathophysiological parameters in transmitochondrial MELAS cybrids. Control and MELAS cybrids were cultured in the absence or presence of 60 nM riboflavin or 100 μM CoQ for 48 hours. Cellular proliferation rate, ATP production, complexes I + II activity and ROS levels were determined as described in Materials & Methods. In complexes I + III activity, results were expressed as mean ± SD expressed in units (U) per citrate synthase (CS) units. Overall, data in arbitrary units (a.u.) represent the mean ± SD of three separate experiments. $^{*}P < 0.05$; significance of MELAS respect to control cybrids. $^{\#}P < 0.05$; significance between the presence and absence of riboflavin or CoQ.

Cellular proliferation rate was significantly reduced in MELAS cybrids when compared with control; and both treatments significantly increased the proliferation rate of MELAS and control cybrids. Likewise, ATP levels were reduced in the MELAS cybrids compared with the control cybrids. Treatments with riboflavin had no effect on ATP levels in control cybrids, but resulted in increased ATP levels in MELAS cybrid cells indicating that both treatments restored partially the bioenergetic status of the MELAS cybrids. In fact, the activity of complexes I + III, significantly reduced in the MELAS cybrids before treatments, was definitively restored by riboflavin supplementation.

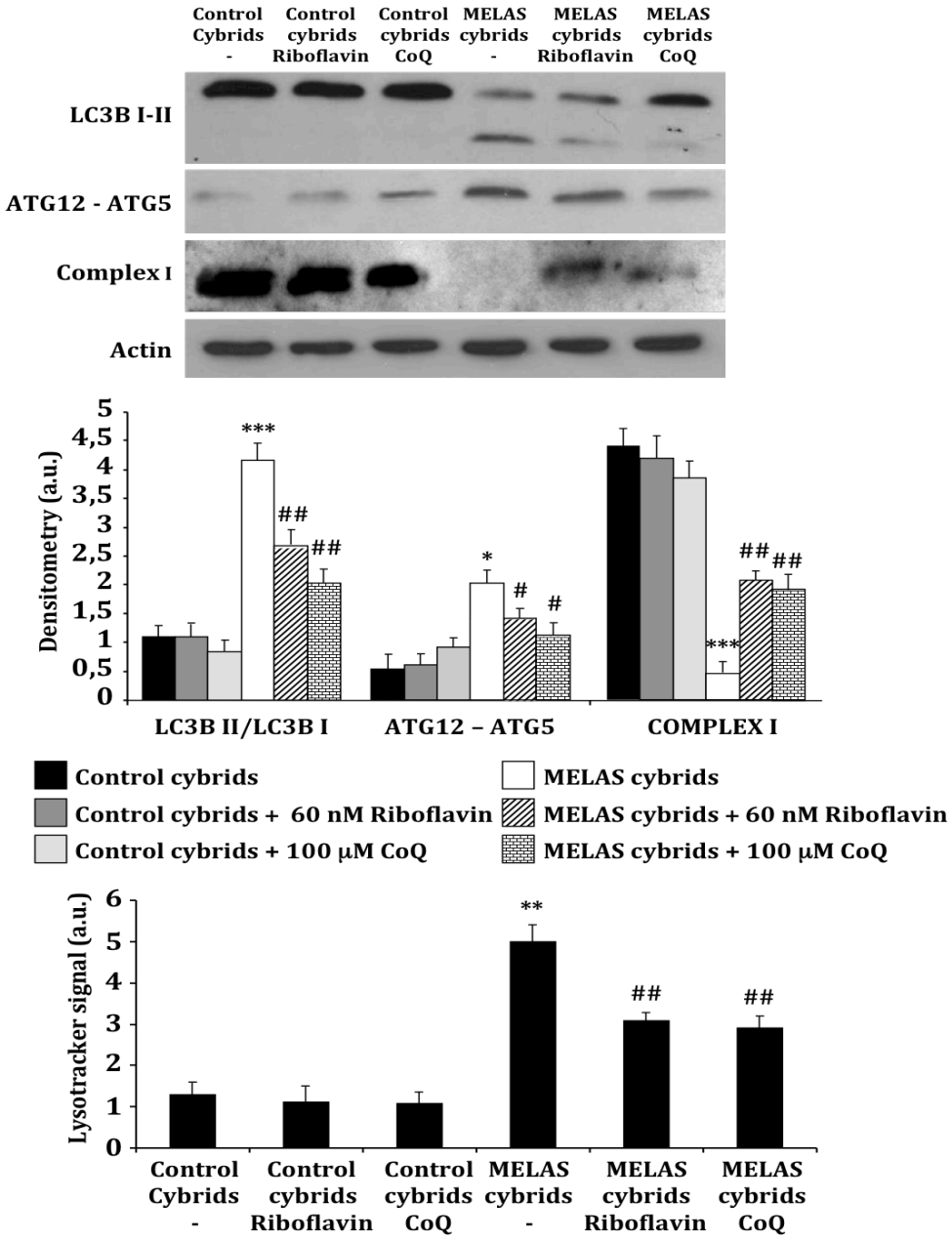

Figure R54. Effect of riboflavin and CoQ treatments on autophagic markers in transmitochondrial MELAS cybrids. Control and MELAS cybrids were cultured for 48 hours in the presence or absence of 60 nM riboflavin or 100 μM CoQ. Acidic vacuoles were quantified by LysoTracker staining and analysed by flow cytometry. Protein expression levels of LC3B-I (upper band) and LC3-II (lower band), ATG12-ATG5 and complex I (30 kDa subunit) was determined in control and MELAS cybrid cultures by Western blotting. Actin was used as a loading control. Densitometry was performed by using ImageJ software. Data in arbitrary units (a.u.) represent the mean ± SD of three separate experiments. $^{*}P < 0.05$, $^{**}P < 0.01$ and $^{***}P < 0.001$; significance between control and MELAS cybrids. $^{\#}P < 0.05$ and $^{\#\#}P < 0.01$; significance between the presence and the absence of riboflavin or CoQ.

We next examined mitochondrial ROS levels in control and MELAS cybrids by using MitoSOX Red and flow cytometry as described in Material and Methods. At the same time, the mitochondrial mass was estimated with NAO, and the ratio of MitoSOX signal to NAO fluorescence was determined. An approximate 3-fold increase was detected in mitochondrial ROS production of MELAS cybrids. The inclusion of riboflavin in the culture medium induced a considerable reduction in ROS levels, although they were not fully restored to control values in these cells. Therefore, in addition to CoQ, riboflavin resulted in positive effects on proliferation rate, ROS generation and bioenergetic status of transmitochondrial MELAS cybrids.

On the other hand, as AICAR and CoQ induced autophagic flux and reduced LC3B – II levels in fibroblasts and MELAS cybrids, we next checked the effectiveness of riboflavin in decreasing autophagic markers (**Figure R54**).

As previously done, we explored the conversion of LC3B-I to LC3-II, since the amount of the latter is closely correlated with the number of autophagosomes. We found a significant 4-fold increase in the ratio of LC3-II to LC3-I in MELAS cybrids when compared with control cybrids. Likewise, the amount of ATG12-ATG5 was also increased 3-fold in MELAS cybrids, which indicates an increase of autophagic machinery. Moreover, LysoTracker staining intensity was determined as a way to quantify acidic vesicles in cells, which are associated to autophagy and presence of autophagolysosomes. The LysoTracker mean intensity resulted in an approximate 3-fold increase in the MELAS cybrid clone compared to control cybrids (**Figure R54**). Supplementation of the culture medium with 60 nM riboflavin resulted in a significant decrease in the levels of LC3-II, ATG12-ATG5 and acidic vesicles, which could be presumably due to the induction of autophagic flux as in the case of AICAR and CoQ treatments, supporting the hypothesis of autophagosomes could be being cleared after these treatments. In agreement with the results of complex I + III activity shown in **Figure R53**, we found that protein expression of the 30 kDa subunit of complex I of the mitochondrial respiratory chain (MRC) was also reduced in the MELAS cybrid. Supplementation with riboflavin partially restored its expression levels as well.

Given clear evidences of improvement of the autophagy levels after treatments (**Figure R54**), we wondered whether riboflavin was also able to reduced selective degradation of mitochondria. Thus, we next examined colocalisation of LC3B and cytochrome c in MELAS cybrids (**Figure R55**). Whereas in control cybrids mitochondria did not co-localise with LC3B, in MELAS cybrids co-localization of cytochrome c and LC3B was clear. Treatment with riboflavin resulted in a significant reduction of the colocalisation between mitochondria and autophagosomes, supporting our previous results with AICAR and CoQ treatments.

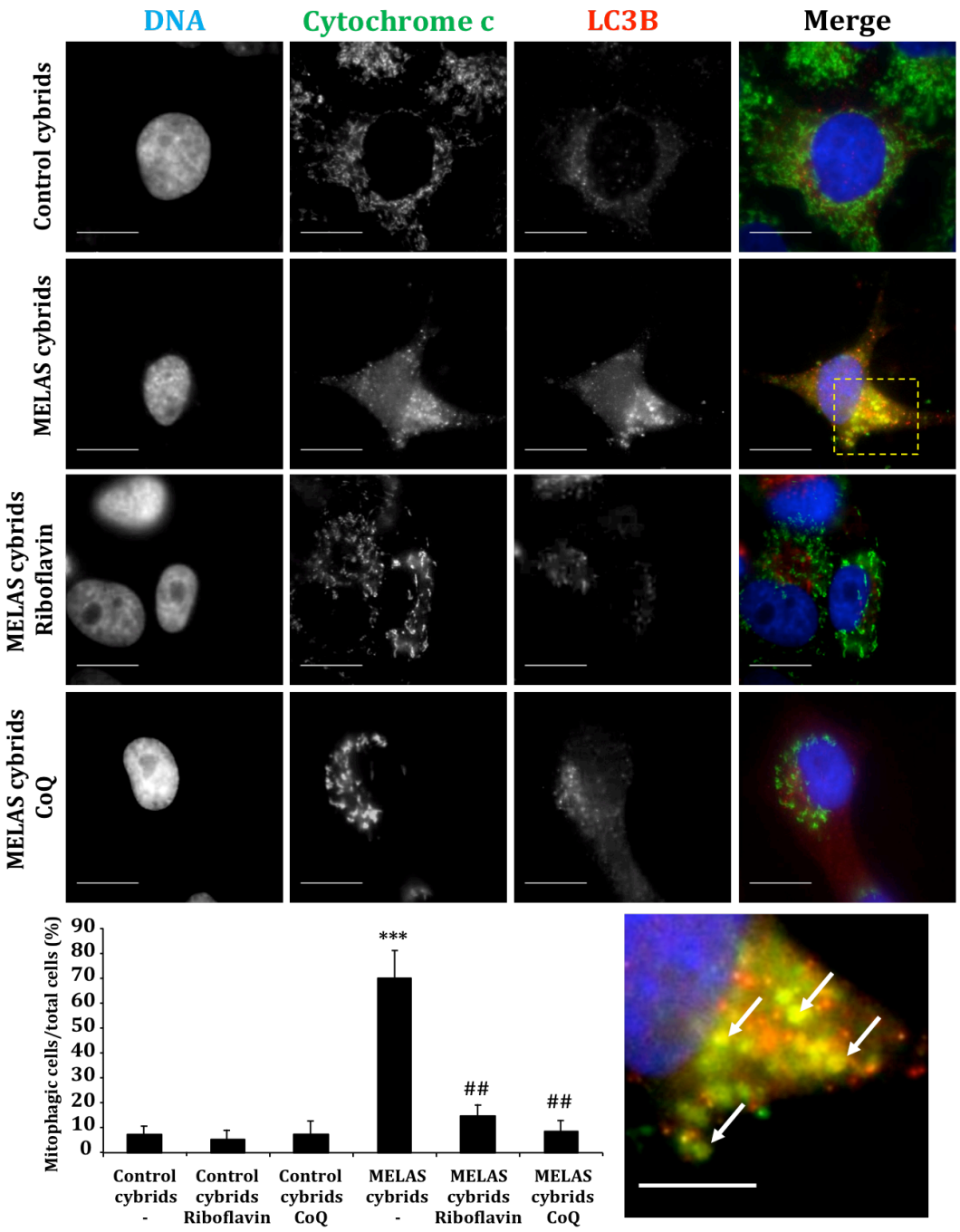

Figure R55. Effect of riboflavin and CoQ treatments on selective mitochondrial degradation in transmitochondrial MELAS cybrids. After 60 nM riboflavin and 100 μM CoQ treatments, control and MELAS cybrids were immunostained with anti-LC3B (autophagosome marker) and cytochrome c (mitochondrial marker) to visualise degrading mitochondria (punctate) in control and MELAS cybrids. To quantify mitophagy, a positive mitophagic cell was scored when more than 10 puncta (white arrows) were observed per cell. Data represent the mean ± SD of three separate experiments. $^{***}P < 0.001$; significance between control and MELAS cybrids. $^{\#\#}P < 0.01$; significance between the presence and the absence of riboflavin or CoQ. [Scale bar = 10 μm and = 5 μm in magnified picture].

Once proven that riboflavin considerably ameliorated pathophysiological alterations in transmitochondrial MELAS cybrids after only 48 hours of treatment, now we extend the evaluation to MELAS fibroblasts, a cellular model with a much lower growth rate capacity but that can reflect better patient pathophysiology. Although the culture of fibroblast present some disadvantages such as low growth and fast senescence, the opportunity of working in an almost personalized manner for each patient becomes an attractive approach. Here below, we evaluated riboflavin and CoQ treatments in a MELAS primary fibroblast culture, MELAS 3, which showed the highest heteroplasmy load of the MELAS fibroblasts under study, 43%.

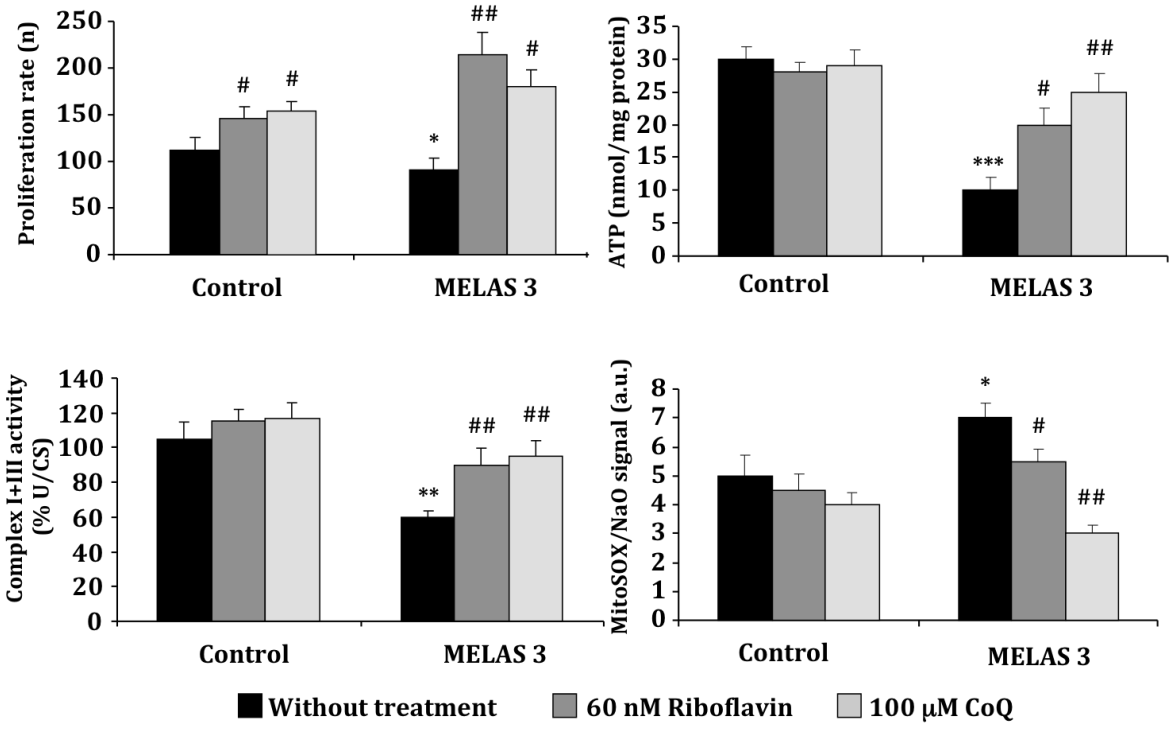

Figure R56. Effect of riboflavin and CoQ treatments on pathophysiological parameters in MELAS 3 fibroblasts. Control and MELAS 3 fibroblasts were cultured in the absence or presence of 60 nM riboflavin or 100 μM CoQ for a week. Cellular proliferation rate, ATP production, complexes I+III activity and ROS levels were determined as described in Materials & Methods. In complexes I+III activity, results were expressed as mean ± SD expressed in units (U) per citrate synthase (CS) units. Overall, data in arbitrary units (a.u.) represent the mean ± SD of three separate experiments. $^{*}P < 0.05$, $^{**}P < 0.01$ and $^{***}P < 0.001$; significance of MELAS respect to control cybrids. $^{\#}P < 0.05$ and $^{\#\#}P < 0.01$; significance between the presence and absence of riboflavin or CoQ.

First, control and MELAS 3 fibroblasts were treated with the same dose used in cybrids, 60 nM riboflavin and 100 μM CoQ, but in spite of 48 hours, treatments in fibroblasts lasted 1 week. Proliferation rate analysis showed decreased growth rate for MELAS 3 fibroblasts compared with control fibroblasts. None of these agents had a significant effect on the proliferation rate of control fibroblasts. However, supplementation in MELAS fibroblasts significantly increased this growth rate to

control values. To determine whether riboflavin or CoQ had an effect on improving cellular bioenergetics, we determined their effect on intracellular ATP levels and complex I+III activity in control and MELAS 3 fibroblasts. As expected, ATP levels and Complex I+III activity were significantly decreased in MELAS 3 fibroblasts, and treatments with either 60 nM riboflavin or 100 μM CoQ caused a substantial increase in its bioenergetics capacity (**Figure R56**). As done with cybrids, we also examined superoxide levels in control and MELAS fibroblasts by flow cytometry using MitoSOX Red as a probe. ROS production was notably increased in MELAS 3 fibroblasts and was reduced after a week of riboflavin and CoQ treatments.

Next, we wondered whether autophagy and, in particular, mitophagy activation also occurred in MELAS 3 culture as happened with other MELAS cultures studied. To determine whether increased mitochondrial degradation was activated in MELAS 3 fibroblasts, we first quantified levels of acidic vacuoles by the use of LysoTracker staining coupled with flow cytometry analysis. Acidic vacuoles were significantly increased in MELAS 3 fibroblasts when compared with control fibroblasts (**Figure R57**). In the same manner than CoQ, riboflavin resulted quite effective by reducing lysosome content. Once again, as a marker of autophagic activity, we also explored the conversion of LC3B-I to LC3-II. Results indicated a 5-fold increase in the amount of LC3-II in MELAS 3 fibroblast culture compared with control fibroblasts. This significant increase in LC3-II conversion in MELAS 3 fibroblasts indicated that autophagosome formation is enhanced in these cells as well as the rest of MELAS cultures. Supplementation with riboflavin or CoQ treatments achieved a 50% decrease in the levels of LC3-II in these cultures. Additionally, the study of ATG12-ATG5 protein levels reported similar results than LC3B.

Next, we performed a double staining immunodetection with antibodies against LC3B and cytochrome c to confirm presence of mitophagy activation in MELAS 3 fibroblasts. Whereas in control fibroblasts a rich tubular mitochondrial network negative for LC3B staining was observed, in the MELAS 3 fibroblasts we identified two mitochondria populations: few normal tubular mitochondria negative for LC3B along with many small rounded and fragmented mitochondria positive for LC3B (**Figure R58**). These results suggested the presence of autophagosome engulfing mitochondria (positive LC3/cytochrome c punctate) as observed in other MELAS fibroblasts studied along this thesis. Riboflavin and CoQ treatment resulted in drastic reductions of engulfed mitochondria.

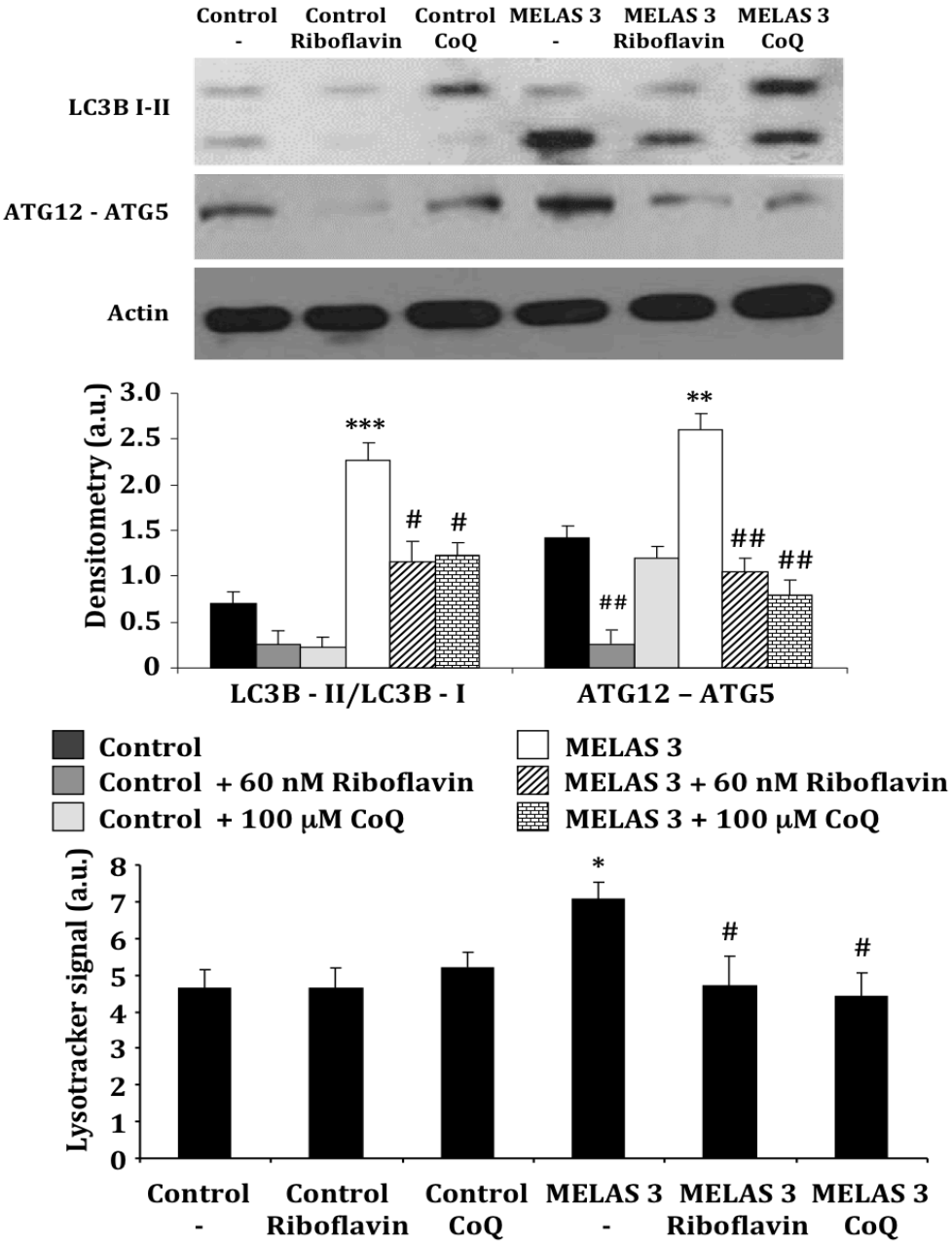

Figure R57. Effect of riboflavin and CoQ treatments on autophagic markers in MELAS 3 fibroblasts. Control and MELAS 3 fibroblasts were cultured in the absence or presence of 60 nM riboflavin or 100 μM CoQ for a week. Quantification of acidic vacuoles by LysoTracker staining and flow cytometry analysis. Protein expression of LC3 and Atg12-atg5 conjugated form. Actin was used as loading control. Densitometry was performed using the ImageJ software. Overall, data in arbitrary units (a.u.) represent the mean ± SD of three separate experiments. $^{*}P < 0.05$, $^{**}P < 0.01$ and $^{***}P < 0.001$; significance of MELAS respect to control cybrids. $^{\#}P < 0.05$ and $^{\#\#}P < 0.01$; significance between the presence and absence of riboflavin or CoQ.

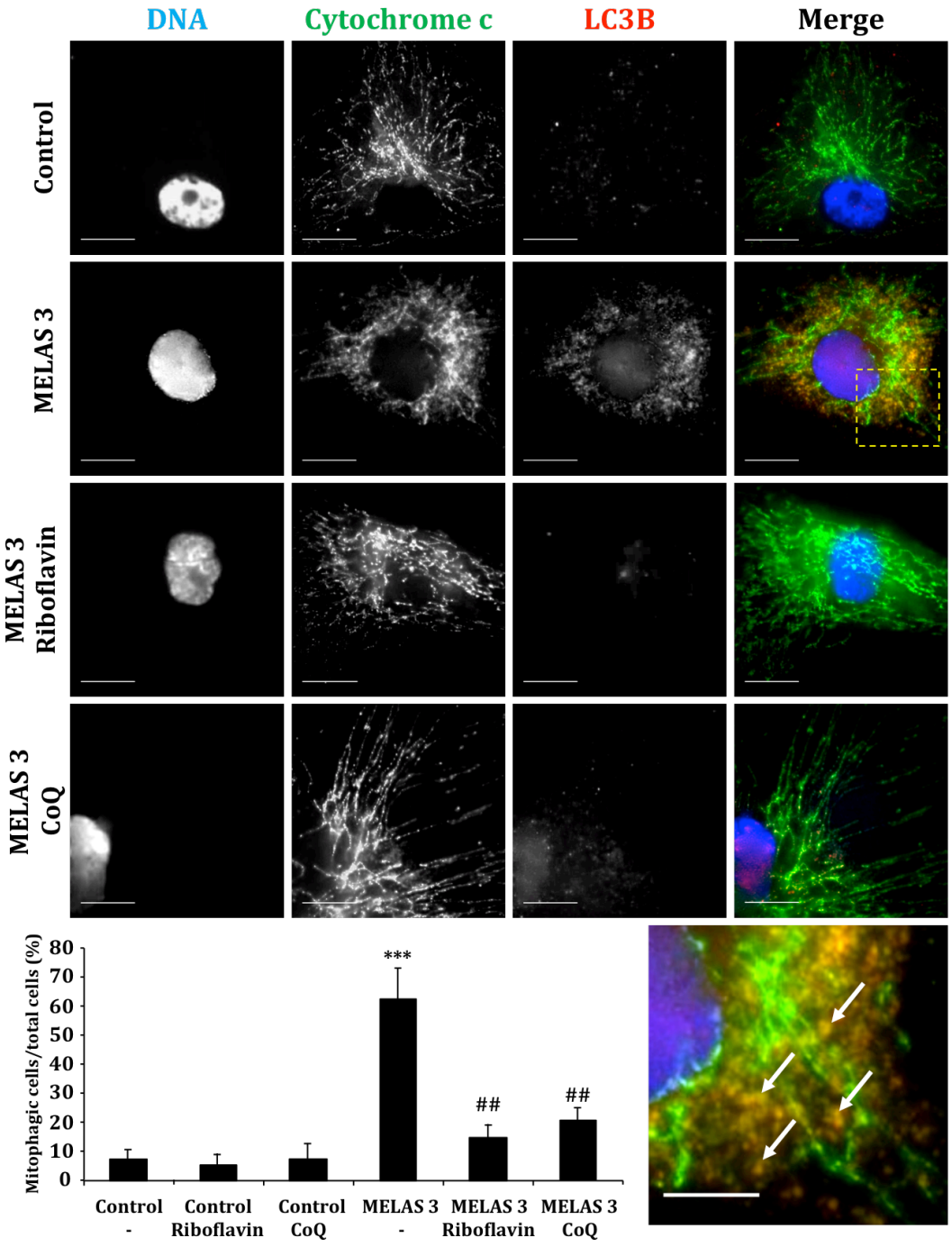

Figure R58. Effect of riboflavin and CoQ treatments on selective mitochondrial degradation in MELAS 3 fibroblasts. After 60 nM riboflavin and 100 μM CoQ treatments, control and MELAS 3 fibroblasts were immunostained with anti-LC3B (autophagosome marker) and cytochrome c (mitochondrial marker) to visualise degrading mitochondria (punctate) in control and MELAS cybrids. To quantify mitophagy, a positive mitophagic cell was scored when more than 10 puncta (white arrows) were observed per cell. Data represent the mean ± SD of three separate experiments. $^{***}P < 0.001$; significance between control and MELAS cybrids. $^{\#\#}P < 0.01$; significance between the presence and the absence of riboflavin or CoQ. [Scale bar = 10 μm and = 5 μm in magnified picture].

Curiously, as found in the other MELAS fibroblasts with high heteroplasmy (MELAS 1 and MELAS 2), enhanced mitophagy in MELAS 3 cells was concomitant with a significant decrease in protein expression for both nuclear and mitochondrial encoded subunits of MRC complexes (**Figure R59**): 30 KDa subunit of complex I (nuclear encoded), the 30 KDa subunit of complex II (nuclear encoded), the core I subunit of complex III (nuclear encoded) and the COX II subunit of complex IV (mtDNA encoded) showed reduced protein levels than control fibroblasts. Treatments with 60 nM riboflavin or 100 μM CoQ were able to partially restore mitochondrial protein expression levels.

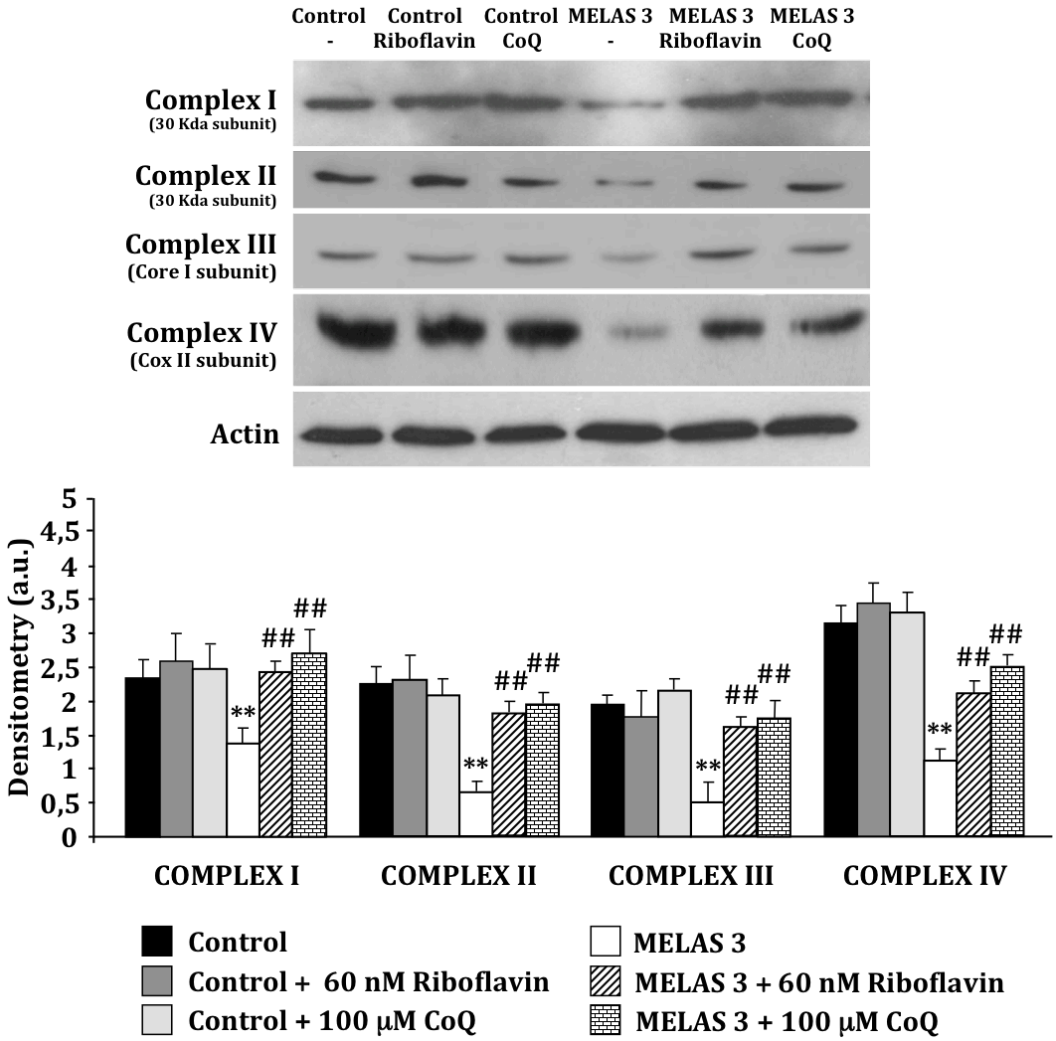

Figure R59. Mitochondrial protein expression levels in MELAS 3 fibroblasts. Western blot analysis of mitochondrial respiratory chain proteins -complex I (30Kda subunit), complex II (30 KDa subunit), complex III (core 1 subunit), complex IV (COX II subunit)- of control and MELAS 3 fibroblasts incubated with 60 nM riboflavin or 100 μM CoQ for 1 week. Actin was used as loading control. Densitometry of Western blotting was performed using ImageJ software. Data in arbitrary units (a.u.) represent the mean ± SD of three separate experiments. $^{**}P < 0.01$ between control and MELAS fibroblasts. $^{\#\#}P < 0.01$, between the presence and the absence of riboflavin or CoQ.

Given the substantial reduction of MRC proteins observed in MELAS 1, MELAS 2 and MELAS 3, all of them with high heteroplasmy load, we wondered about the reasons for this drastic decrease. We can speculate that a massive selective degradation of mitochondria might diminish mitochondrial mass, and as a consequence to induce a drastic reduction in MRC proteins. Riboflavin or CoQ increased the amount of MRC proteins, but it is unclear the molecular mechanism involved in this process. The role of other mitochondrial players in structural stability of the mitochondrial complexes[510–513] might shed some light on the functional role of riboflavin or CoQ on this matter.

To explore whether riboflavin or CoQ were able to increase stability and assembly of complexes, we isolated mitochondria from MELAS 3 culture by magnetically labelling with anti-TOM22 (translocase of outer mitochondrial membrane 22) microbeads and magnetic separation. This method isolates intact mitochondria and, contrary to whole cell lysate analysis, avoids the influence of mitophagy on the evaluation of mitochondrial complexes assembly. Analysis of mitochondrial respiratory complexes by BN-PAGE revealed in MELAS 3 fibroblasts an almost complete absence of fully assembled complex I, only trace amounts of fully assembled complexes IV and V, and normal levels of complex III (**Figure R60**). Curiously, complex II, which has four subunits entirely encoded by nuclear genes, was increased in MELAS 3 intact mitochondria. This result could easily be interpreted as an increased transcription of nuclear-encoded mitochondrial proteins to compensate deficient mitochondrial activity. Treatments for 1 week with 60 nM riboflavin or 100 μM CoQ resulted in a significant increase in fully assembled complexes I, IV and V in MELAS fibroblasts 3 supporting the role of riboflavin and CoQ as agents that promote proper complexes assembling.

Altogether, these results suggest that cellular models such as transmitochondrial cybrids and fibroblasts derived from MELAS patients could be suitable for screening and validating pre-screened or new drug candidates for MELAS disease. In these assays, we observed that riboflavin or CoQ effectively improved the viability and pathophysiology of MELAS cell models confirming our expectations since these drugs are used clinically in the treatment of MELAS patients[385]. As no difference was detected between the response to treatments in MELAS 3 fibroblasts with 43% of heteroplasmy and MELAS cybrids with 90% of heteroplasmy, these models, at least with this heteroplasmy, seem to behave similarly regarding the pathophysiological parameters analysed. Likewise, in anterior subsections AICAR and CoQ treatments also ameliorated severe pathophysiological alterations in MELAS 1 and MELAS 2 fibroblasts, both cell lines harbouring high heteroplasmy load as well. Therefore, MELAS patient-derived fibroblasts showing severe physiopathology and harbouring high heteroplasmy, seem suitable models for testing the effects of treatments for MELAS patients.

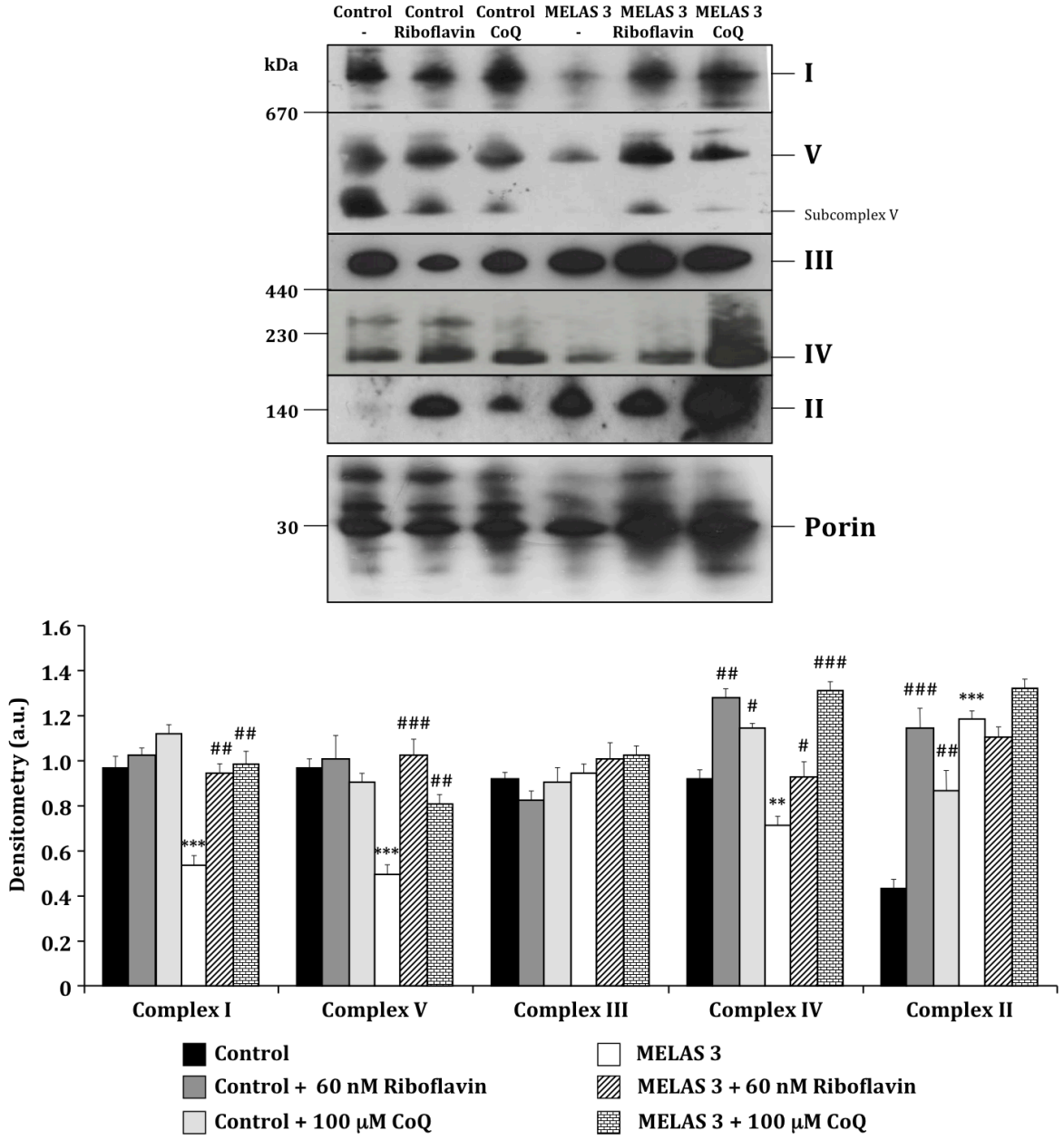

Figure R60. Effect of riboflavin and CoQ treatments on assembly of mitochondrial complexes in MELAS 3 fibroblasts. Control and MELAS 3 fibroblasts were treated with 60 nM riboflavin or 100 μM CoQ for a week. Intact mitochondria were isolated as described in Materials & Methods and analysed by BN-PAGE. The blots were incubated with antibodies against specific native subunits of mitochondrial complexes (I–V). An antibody against porin, housekeeping mitochondrial protein, was used as loading control. 'Subcomplex V' indicates the presence of partially assembled complexes V in MELAS 3 fibroblasts. Densitometry of mitochondrial complexes signal normalized by porin was performed by using ImageJ software. Data in arbitrary units (a.u.) represent the mean ± SD of two blots. $^{**}P < 0.01$ and $^{***}P < 0.001$; significance between control and MELAS 3 fibroblasts. $^{\#}P < 0.05$, $^{\#\#}P < 0.01$ and $^{\#\#\#}P < 0.001$; significance between the presence and the absence of riboflavin or CoQ.

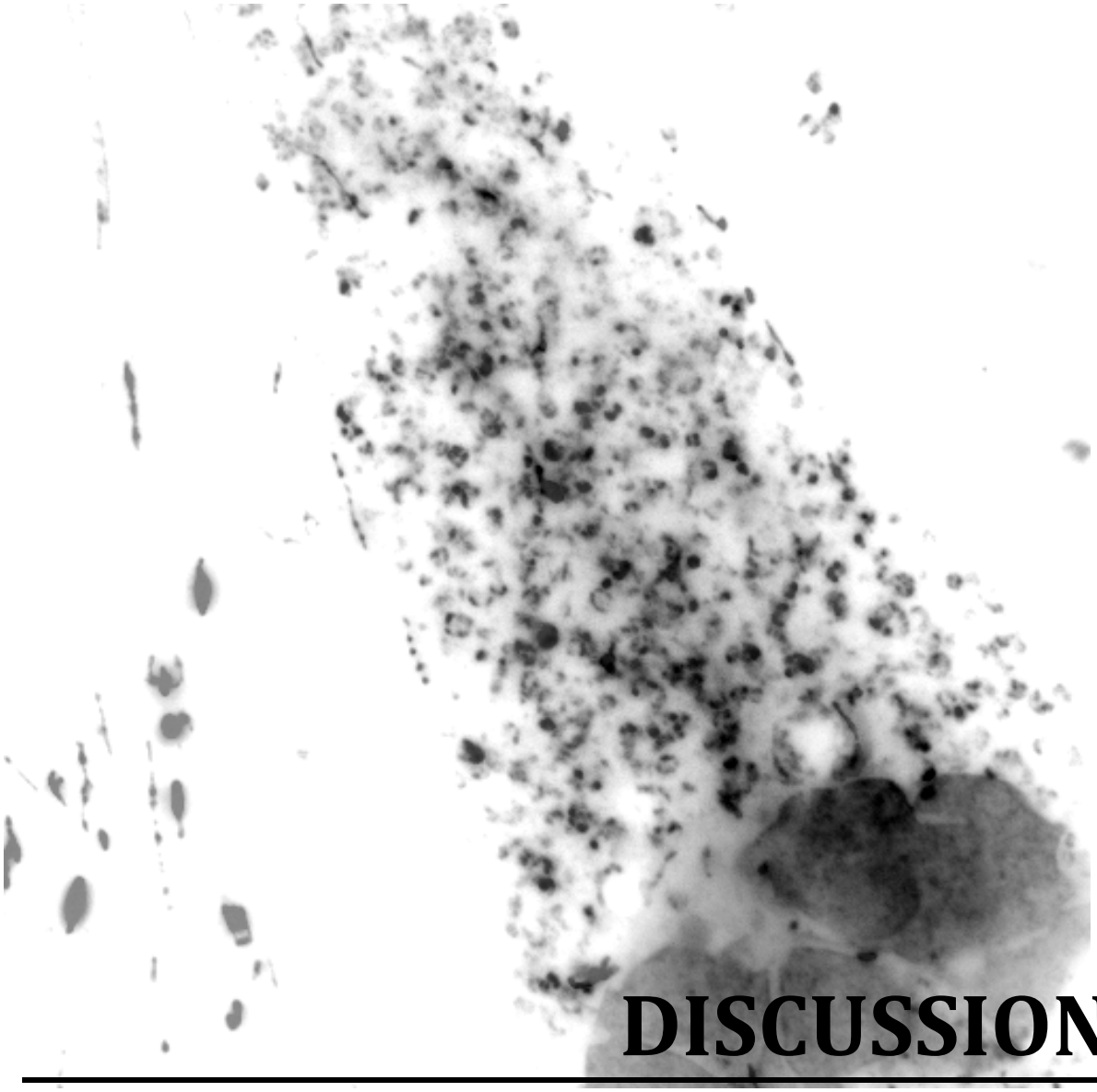

DISCUSSION

DISCUSSION

MELAS syndrome is a genetically heterogeneous mitochondrial disorder with multifaceted manifestations. MELAS syndrome is associated in about 80% of cases with a mutation at position 3243 in the mitochondrial gene MTTL1, encoding mitochondrial tRNA leucine 1 (m.3243A>G), although other mutations have also been described[240]. Given the difficulty in accessing to large cohorts of MELAS patients, most of the progress and therapeutic approaches for managing patients are based in isolated case reports or limited clinical trials with little or no consensual benefits. Here, we propose the use of the cellular models for studying pathophysiological mechanisms of the disease and the screening of pharmacological compounds for MELAS treatment. During the conduction of this thesis, we have performed the pathophysiological characterisation of primary dermal fibroblasts derived from five MELAS patients carrying the m.3243A>G mutation (MELAS 1, MELAS 2, MELAS 3, MELAS A and MELAS B). Our findings revealed that MELAS fibroblasts showed different degrees of pathophysiological alterations severity. We found significant differences in pathophysiological parameters such as growth rate, ATP/ADP ratio, CoQ levels, ROS production, activation of the enzymatic antioxidant system, MRC activities, autophagic flux and mitophagy activation, and mitochondrial biogenesis associated with PGC-1α, NRF1 and mtTFA regulation and AMPK activation. Two groups were clearly differenced according to the severity on these parameters: a first group with severe alterations (MELAS 1, MELAS 2 and MELAS 3), and a second group with slight or no alterations (MELAS A and MELAS B). The severity of these alterations was correlated with the mutational load of MELAS fibroblasts. Thus, MELAS fibroblasts with a more severe phenotype showed higher levels of heteroplasmy (MELAS 1: 17%, MELAS 2: 26%, MELAS 3: 43%) than MELAS fibroblasts with less pathophysiological alterations (MELAS A: 9% and MELAS B: 4%). Interestingly, MELAS syndrome shows a wide range of clinical phenotypes: from patients with the whole spectrum of symptoms to asymptomatic individuals. This wide variety of phenotypes has been associated with heteroplasmy load and the tissue affected. Indeed, heteroplasmy seems to correlate with oxygen uptake and workload, resting plasma lactate, and muscle morphology abnormalities in individuals with MELAS syndrome. Interestingly, the threshold of muscle mutation load seems to be about 50%[361], by 40% lower than found *in vitro* (90%)[274]. This differential behaviour is not limited to MELAS syndrome, but also other point mtDNA mutations has been previously found to show correlation between heteroplasmy load and clinical progression of mitochondrial disorders. Thus, the same m.8993T>G mutation may develop a subacute or chronic disease in young adults (NARP) when the degree of heteroplasmy is around 70%, and a rapidly progressive encephalopathy of infancy or childhood (Leigh syndrome) when the mutational load is close to 90%[237,388]. According to our findings, this phenotypic diversity in patients of mitochondrial diseases is also manifested in primary fibroblast. In this thesis, we report a different degree of pathophysiological alterations in MELAS fibroblasts depending on the

heteroplasmy load. In particular, our findings showed that low heteroplasmy load (around 20%) was sufficient to cause pathophysiological alterations *in vitro*.

To gain further insight into MELAS pathophysiology, we confirmed the relationship between the presence of severe pathophysiological alterations and high mutational load by using MELAS transmitochondrial cybrids harbouring the m.3243A>G mutation with an extremely high heteroplasmy load of m.3243A>G mutation (90%). Furthermore, results indicated that pathophysiological alterations were a consequence of the mutation in mtDNA and not the product of a concomitant nuclear gene defect. Altogether, our results suggest that the threshold for mutant load at which pathophysiological alterations emerge in fibroblasts carrying the 3243A>G mutation may be much lower than previously believed.

Our findings suggested a critical balance between mitophagy and mitochondrial biogenesis in MELAS fibroblasts. Both mitophagy and mitochondrial biogenesis are critical processes that regulate mitochondrial content and preserve cell homeostasis. The tight regulation between these pathways is crucial for cellular adaptation in response to cellular stress and other intracellular or environmental insults. Interestingly, dysregulation between mitochondrial biogenesis and mitophagy has been involved in progressive development of numerous conditions. In fact, excessive mitophagy in the absence of mitochondrial biogenesis may also contribute to defective mitochondrial function, subsequent cell death and neuronal loss[514].

We found that whereas mitophagy was activated in all MELAS cell lines, mitochondrial biogenesis was only up-regulated in some of them, MELAS A and MELAS B, precisely those cell lines that showed less pathophysiological alterations. Mitochondrial proliferation may help to ameliorate respiratory defects[515] by mitigating the energy depletion caused by degradation of dysfunctional mitochondria found in MELAS fibroblasts. These results support previous work at which the up-regulation of mitochondrial biogenesis avoids the penetrance of mitochondrial diseases such as in Leber's hereditary optic neuropathy (LHON)[277]. Thus, mitochondrial biogenesis might work as a compensatory mechanism in response to increased ROS production, reduced ATP levels and mitophagic degradation.

Mitochondrial biogenesis activation seems to be mediated by AMPK protein, which directly phosphorylates PGC-1α and, hence regulates mitochondrial biogenesis[156]. According to our results, mitochondrial biogenesis was accompanied by AMPK activation since the analysis of AMPK phosphorylation resulted in significant high phospho-AMPK/total-AMPK ratios (activation) in MELAS A and MELAS B when compared to MELAS 1 and MELAS 2 fibroblasts, which showed low AMPK activation. This differential activation of AMPK suggested an insufficient or deficient activity of AMPK in the most severe phenotypes of MELAS 1 and MELAS 2 fibroblasts. In light of these data, recent literature comes into conflict with our results. AMPK is a kinase well conserved through evolution[516] that acts as an energy sensor of the cell and works as a key regulator of mitochondrial biogenesis[146]. Functionally, AMPK activates pathways such as glycolysis and amino acid oxidation for ATP production, while concurrently inhibits energy-dependent pathways such as biosynthesis of fatty acids and

gluconeogenesis[517]. This energy reprograming is activated by a decrease of the ATP/ADP ratio[179,180] or in response to elevated mitochondrial ROS[518]. In fact, it has been shown that skin fibroblasts with MERRF syndrome, another mitochondrial disease caused by mutations in mitochondrial tRNAs, produced high level of mitochondrial ROS associated with AMPK activation[519]. By contrast, our results revealed that at least MELAS 1 and MELAS 2 fibroblasts showed low ATP/ADP ratios and high ROS production, which were concomitant with low levels of AMPK activation.

But, why AMPK is not properly activated in MELAS 1 and MELAS 2 fibroblasts? Currently, the mechanism to explain AMPK insensitivity is unknown. We can speculate that these more severe phenotypes are caused by decreased sensitivity of AMPK activation as it has been reported during aging[520] and mitochondrial-related diseases as fibromyalgia[521]. This loss of sensitivity of AMPK might be due to the impairment of the kinase by the continuous activation of the pathway through the high cellular stress generated by the high mutational load. The lack of a proper AMPK activation under circumstances of bioenergetics imbalance and cellular stress might aggravate oxidative stress and reduce autophagic clearance and, as a result, MELAS cells show a more severe phenotype. By contrast, in response to oxidative stress, AMPK is properly activated in MELAS A and MELAS B fibroblasts and trigger adaptive responses for cell survival[522]. Thus, AMPK performs the direct phosphorylation of PGC-1α and FOXO3a, which in turn augment mitochondrial biogenesis (e.g., up-regulation of mtTFA, NFR1, and NFR2) and the antioxidant defence system response (e.g., the up-regulation of Mn SOD and catalase). Therefore, we hypothesize that reduced phosphorylation of AMPK is responsible for impaired autophagy flux, poor compensatory response to mitophagy and increased oxidative stress, which in turn impairs the bioenergetics state of MELAS fibroblasts leading to a more severe phenotype.

In addition to affecting on antioxidant defence, AMPK has other effects on mitochondrial parameters as mitochondrial fusion and fission[523–525]. Thus, a gain-of-function mutation in AMPK has been reported to increase the expression of mitochondrial fusion/fission proteins such as Mfn2, OPA1 and Drp1 in skeletal muscle[526], which implicates AMPK in the regulation of mitochondrial dynamics and mitochondrial quality control processes. Furthermore, AMPK activation can stimulate autophagy and autophagic flux[205,527], and consequently reduce autophagolysosome accumulation in cellular contexts of increased mitophagy. All together these responses suggest that activation of AMPK plays an essential role in the up-regulation of mitochondrial biogenesis, antioxidant enzymes and autophagic flux, as the adaptive and compensatory responses to mitochondrial dysfunction for the survival of affected cells.

Considering the incapacity of the most severe phenotypes (MELAS 1 and MELAS 2) to activate the compensatory response through AMPK pathway, AMPK pathway was stimulated by supplementation with AICAR and coenzyme Q_{10} (CoQ), two reported AMPK inducers[209,434–438,448]. By AICAR and CoQ treatments, the pathological alterations of MELAS 1 and MELAS 2 fibroblasts were restored. The mechanism by which AICAR actives AMPK seem to be currently understood. It is known that AICAR

mimics the effects of AMP on AMPK promoting its allosteric activation by phosphorylation[209,448–450]. By contrast, how CoQ is able to induce AMPK phosphorylation has still not been elucidated. CoQ is a lipid-soluble that plays a prominent role in the mitochondrial respiratory chain[413,528]. The non-protein nature of CoQ makes impossible any direct kinase activity on AMPK, however, its antioxidant activity on ROS might be involved[414,415]. ROS/RNS are well recognised for playing a "two-faced" role as both deleterious and beneficial species. At low/moderate concentrations, ROS involves the regulation of a number of cellular signalling pathways to protect the cells against oxidative stress and re-establish "redox homeostasis"[529,530]. In particular, oxidative modifications of AMPK, such as cysteine oxidation in α- and β- subunits, induce an allosteric rearrangement of the AMPK αβγ heterotrimer, thereby facilitating AMP-mediated activation of the kinase domain[530–532]. By contrast, overproduction of ROS/RNS can generate damage on cell structure including membranes, proteins and DNA. Oxidative attack can induces either a loss of function, a gain of function, or a switch to a different function. In fact, it has been reported that reactive nitrogen species, such as nitric oxide (NO) can reduced AMPK phosphorylation[533] and, therefore reduce the anti-oxidative stress response as well as other downstream pathways. An excessive and/or sustained increase in ROS production has been implicated in the pathogenesis of cancer, diabetes mellitus, atherosclerosis, neurodegenerative diseases and other disorders[534]. Furthermore, excessive ROS production has been implicated in mtDNA mutations, ageing, and cell death[529,535]. Altogether, we can speculate that CoQ might indirectly active AMPK by reducing ROS levels up to low enough values for allowing AMPK activation by low ATP/ADP ratios. On the other hand, it has been reported that CoQ induces an increase in cytoplasmic calcium concentrations, which may activate Ca2+/calmodulin-dependent protein kinase kinase (CaMKK), an upstream AMPK activator. Either inhibition or knockdown CaMKK blocked CoQ-induced AMPK phosphorylation, suggesting the involvement of calcium in CoQ-mediated AMPK signalling[437]. CoQ also increased the expression of PGC-1α at both the mRNA and protein levels. Knock down of AMPK with siRNA or pharmacological inhibition of AMPK by using compound C also blocked CoQ-induced expression of PGC-1α, indicating that AMPK plays a critical role in PGC-1α induction by CoQ[437]. Recently, it has been proposed that CoQ may activate Sirt1 and PGC-1α by increasing cyclic adenosine monophosphate (cAMP) levels that, in turn, activate AMPK[536].

A major challenge in mitochondrial diseases, and MELAS disease in particular, is the moderate effectiveness of pharmacological therapies; in this sense, AMPK activators such as AICAR and CoQ have been demonstrated to provide new therapeutic opportunities. Particularly, coenzyme Q_{10} treatment can be an invaluable treatment for MELAS patients with secondary CoQ deficiencies. According to our results, low CoQ levels can also function as a biochemical marker of poor AMPK-dependent compensatory response in MELAS fibroblasts. Benefits for CoQ supplementation include: increase in mitochondrial electron transport and ATP production, improvement of antioxidant protection, beneficial alteration in redox signalling, and mitochondrial permeability transition pore stabilization that may protect against autophagy and apoptosis[537]. Our study suggests that CoQ deficiency is the result of

increased mitophagy without proper compensatory response by mitochondrial biogenesis as it is seen in MELAS 1 and MELAS 2 fibroblasts. Therefore, CoQ treatment could be effective by alleviating the deficiency itself and by increasing mitochondrial biogenesis, the enzymatic antioxidant system response and autophagy clearance through AMPK activation (**Figure D1**).

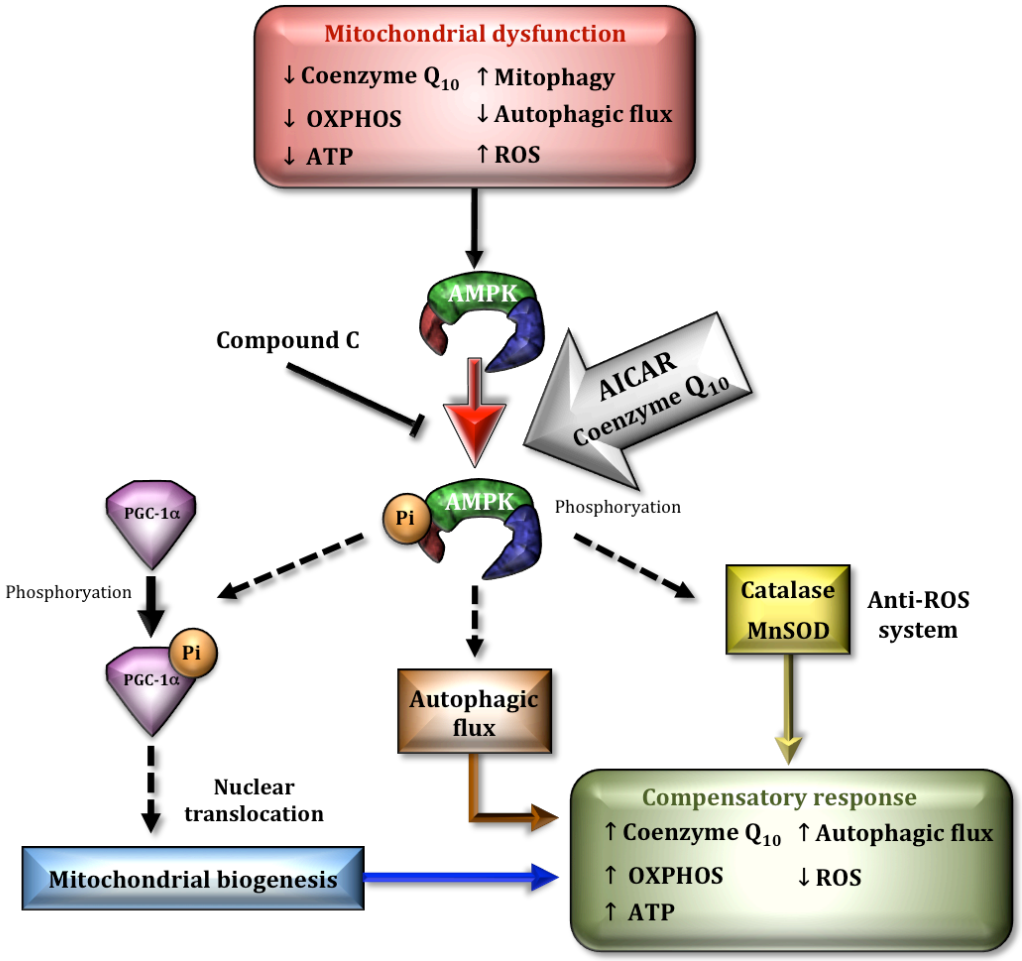

Figure D1. Scheme of pathophysiological alterations in MELAS fibroblasts and the effect of AICAR or CoQ treatment on AMPK activation.

Given the relationship between the most severe MELAS phenotypes and AMPK insensitivity, and the pathophysiological improvement after AMPK stimulation with activators such as AICAR and CoQ, we suggest that AMPK activation signalling pathway is worthy of further investigation in relation to the pathophysiology of MELAS disease. In addition, considering AMPK a potential therapeutic target, it is imperative to investigate whether AMPK activators such as AICAR or CoQ or others, as resveratrol, are beneficial to patients with mitochondrial diseases in general and MELAS disease in particular. A deeper understanding of the signalling cascade induced by AMPK activation and its tissue-specific regulation may provide new targets for the treatment of mitochondrial dysfunction related diseases.

On the other hand, AICAR and CoQ treatment induced AMPK activation and increased nuclear PGC-1α translocation associated with increased mitochondrial biogenesis. There are evidences of nuclear PGC-1α translocation when is phosphorylated by other proteins as Protein kinase A (PKA). It seems that PGC-1α is a protein whose subcellular localization is in the nucleus but is actively interacting with nuclear transporters like CRM1 in order to be exported to the cytoplasm. Phosphorylation of PGC-1α by PKA prevents nuclear export and increases PGC-1α in the nucleus[174], where is supposed to activate downstream pathways like mitochondrial biogenesis. Although our results pointed a clear increase in nuclear phopho-PGC1α foci observed by immunostaining assays and nuclear fractioning, further studies should be performed because nuclear acetylated PGC-1α foci have been also demonstrated to be involved in the repression of PGC-1α. Acetylation of PGC-1α by GCN5 acetyltransferase complex results in a transcriptionally inactive protein that re-localizes from the promoter of regulated genes to nuclear foci[487]. Therefore, further investigations need to be performed in this matter.

Currently, treatment for MELAS syndrome includes various pharmacologic options, as well as lifestyle modifications such as diet and exercise programs[385]. However, evaluation of the effectiveness of the various treatment options is complicated by the relative rarity of the disease, the diverse phenotypes associated, and the unpredictable clinical course. The lack of clear evidence in favour of any one therapy or combination of them and the progressive nature of the syndrome make extremely difficult to find new therapeutic options. Furthermore, the low frequency of the disease makes clinical trials challenging, leaving case reports as the main source of knowledge and guidance for medical practitioners. Moreover, many of the available clinical trials include patients with multiple types of mitochondrial disorders, making even more complicated to extrapolate the results to MELAS patients. Therefore, studies that include larger numbers of patients and well-defined outcomes are needed to clarify the potential role of pharmacotherapy for MELAS syndrome[380]. A variety of pharmacologic options, mostly nutritional supplements and vitamins, have been tried with differing levels of success. Most treatment options focus on increasing respiratory chain activity by administering antioxidants, respiratory chain substrates, and cofactors that augment the production or utilization of ATP[385].

During this thesis, we have developed a screening platform formed by cybrid and fibroblast cell models of MELAS disease to search for effective drugs for the treatment of this disorder. In particular, we propose the use of these cellular models for the screening and validation of pharmacological drugs previously selected from *in silico* studies or massive screening analysis. Computational analysis of databases of drugs can provide a long list of putative beneficial compounds for several disorders. Computer-aided drug discovery/design methods have played a major role in the development of therapeutically important small molecules for over three decades[538]. However, these computer-based approaches ultimately select drugs that need to be tested in more complex models. Recently, several organism models have been proposed as screening platforms for drug discovery in rare diseases. *Drosophila melanogaster* has been used to perform a long-scale pharmacological screening *in vivo*

to search for beneficial drugs in myotonic dystrophy type 1 (DM1)[539]. On the other hand, *S. cerevisiae* is also an excellent model system for drug discovery[540]. As proposed by our group[101], a yeast strain with the homologue mutation of human m.3243A>G mutation can be initially used in the search for effective drugs for the treatment of MELAS[507,508]. In this thesis, biochemical studies of transmitochondrial cybrids and fibroblasts with high heteroplasmy load provided a wealth of information for understanding the pathophysiological changes present in these diseases[285,461,541]. We found that riboflavin and CoQ were able to restore all the pathological alterations found in cybrid models and patient-derived fibroblasts (including mitochondrial protein synthesis and respiratory complexes assembly), validating the usefulness of the cellular models in screening candidate drugs for the treatment of human respiratory chain disorders. Therefore, these cellular models with high mutational load in are very effective in order to find the molecular mechanisms of mitochondrial disease and the screening of different treatments that suppress or enhance the pathophysiological alterations detected.

Despite the fact that in general CoQ and riboflavin treatments have produced mixed results, both drugs are considered a first-line therapy for patients with MELAS syndrome because no significant adverse reactions have been reported[355,439]. Indeed, CoQ supplementation is frequently employed in patients with mitochondrial disorders in the absence of a specific therapy and particularly in MELAS, mainly in primary and secondary coenzyme Q deficiencies. While in primary CoQ deficiency the effect of this therapy is clearly established[542], in secondary forms, contradicting results have been reported[295]. However, the high frequency of secondary CoQ deficiency among patients with mitochondrial myopathy[543] and the relative safety of the treatment, provide a rationale for the future study of the effects of oral CoQ supplementation in patients with mitochondrial disorders, especially if a CoQ deficiency is detected, regardless of the precise genetic aetiology.

According to our findings, the heteroplasmy load and AMPK activation seem crucial parameters that should be considered in the search for popper models of MELAS disease. Inappropriate AMPK activation led to impaired autophagic flux, autophagolysosome accumulation, inadequate antioxidant defence, deficient compensatory mitochondrial biogenesis and the expression of a more severe phenotype in MELAS fibroblasts with high mutational load. In those fibroblasts, AMPK re-activation by AICAR or CoQ was capable of compensating most of the pathophysiological alterations. By contrast, fibroblasts with low heteroplasmy load and compensated pathophysiological parameters can mask the effect of drugs. Indeed, this response was precisely noted in MELAS A and MELAS B fibroblasts. Therefore, we suggest that a previous analysis of parameters such as AMPK activation and heteroplasmy in MELAS cellular models is imperative to perform to a suitable screening.

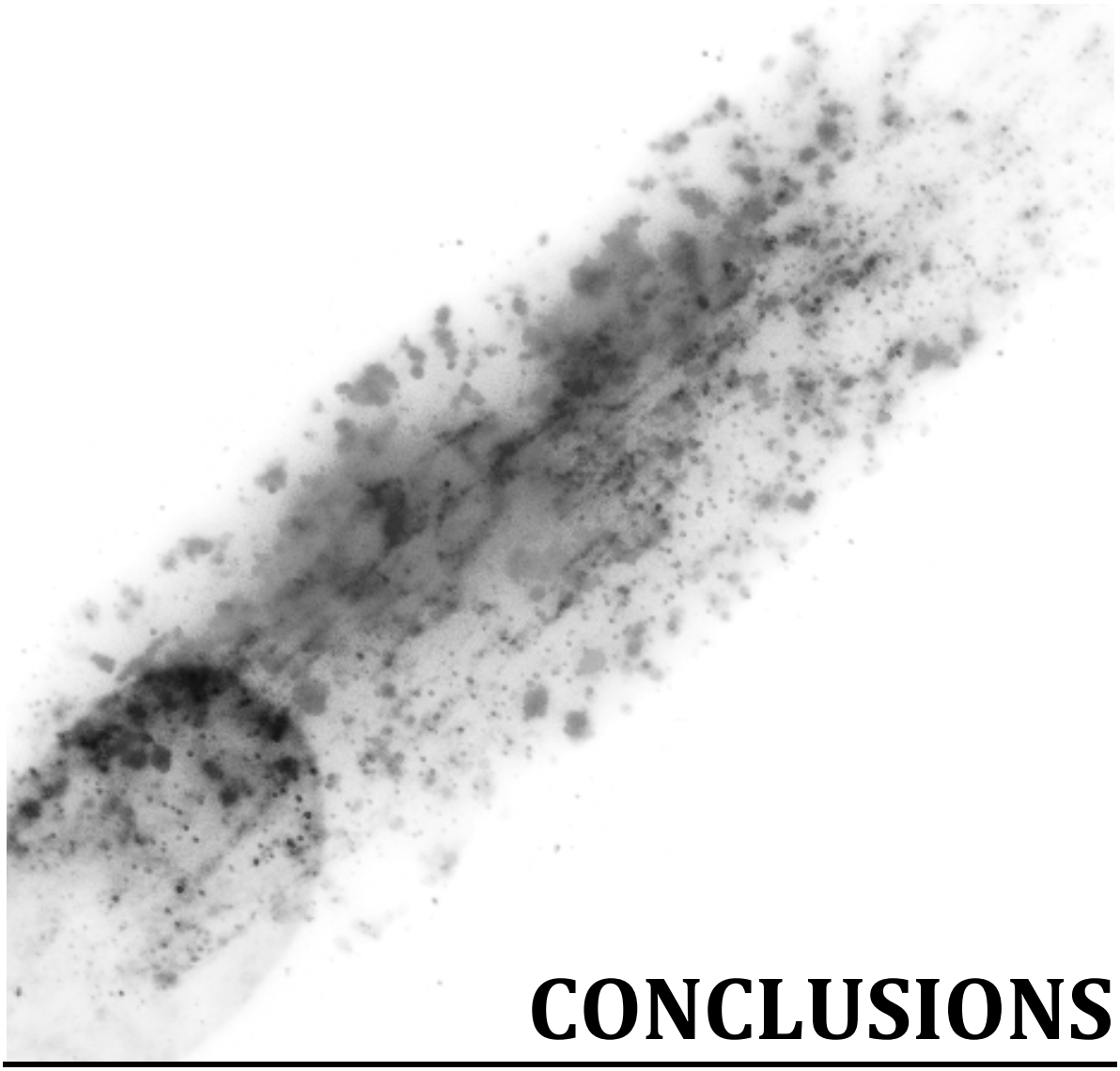

CONCLUSIONS

CONCLUSIONS

1. The pathophysiological alterations of primary fibroblasts derived from MELAS patients show different degrees of severity.

2. Mitochondrial biogenesis and mitophagy balance determines the phenotype of MELAS fibroblasts. Mitochondrial biogenesis works as a compensatory mechanism in response to degradation of dysfunctional mitochondria by mitophagy.

3. Heteroplasmy load and AMPK activation determine the severity of pathophysiological alterations in MELAS fibroblasts. Both, high mutational load and AMPK dysregulation aggravate the bioenergetics state of MELAS fibroblasts leading to a more severe phenotype.

4. AICAR or CoQ treatment stimulate AMPK activation and restore pathophysiological alterations in MELAS fibroblasts with the most severe phenotype.

5. AICAR and CoQ treatment enhance nuclear Phospho-PGC-1α translocation and hence, stimulate mitochondrial biogenesis through AMPK activation.

6. Transmitochondrial MELAS cybrids with high heteroplasmy load manifest severe pathophysiological alterations that were reverted by AICAR or Coenzyme Q_{10} treatment.

7. Screening platforms using transmitochondrial cybrids and fibroblasts with high heteroplasmy load and severe pathophysiological alterations are suitable for validating pharmacological compounds for the treatment of MELAS disease. Supplementation with riboflavin as well as CoQ improved the viability and pathophysiology of MELAS cells models.

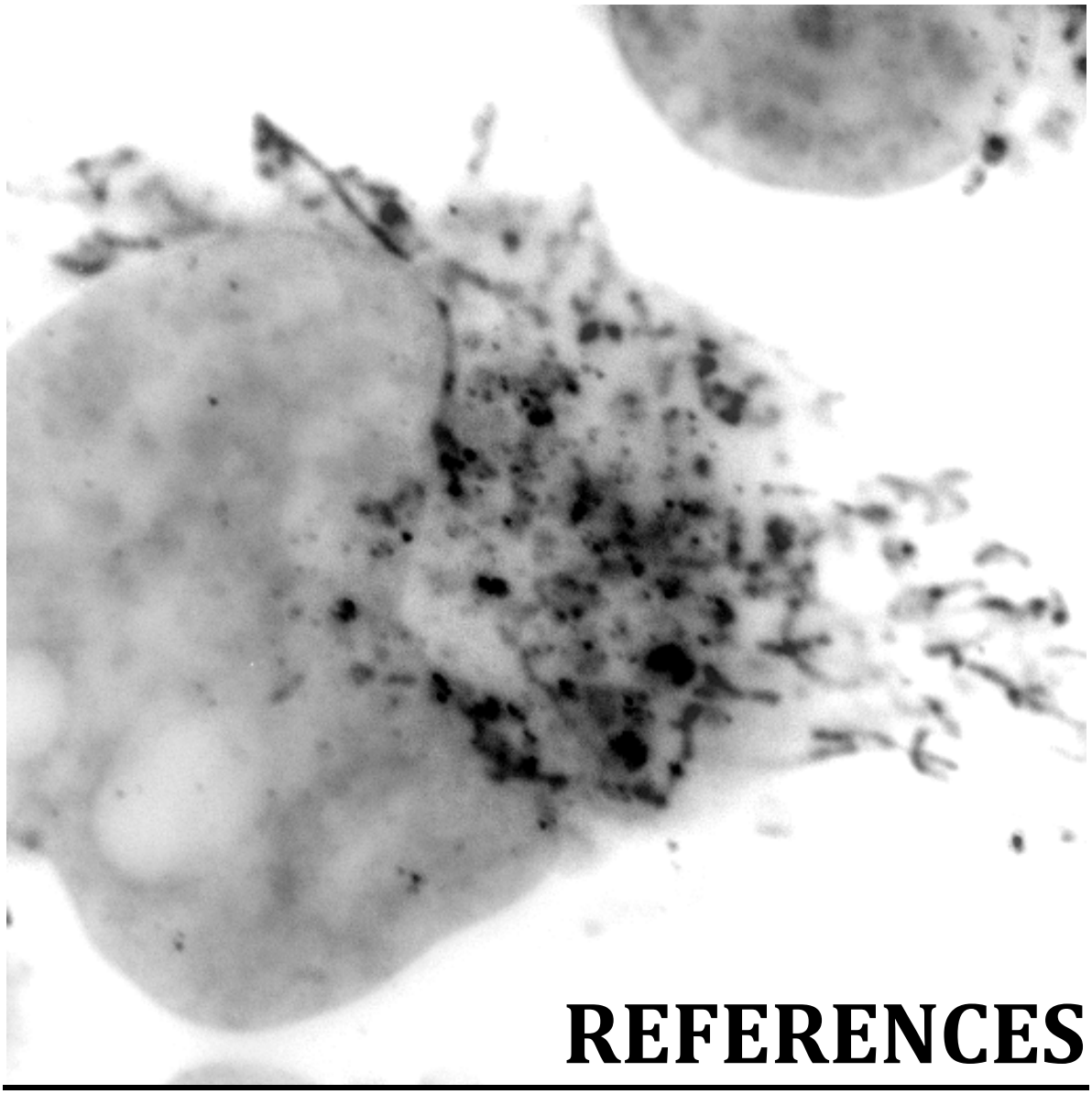

REFERENCES

REFERENCES

1. Margulis, L. Symbiotic theory of the origin of eukaryotic organelles; criteria for proof. *Symposia of the Society for Experimental Biology* 21–38 (1975).

2. Margulis, L. & Bermudes, D. Symbiosis as a mechanism of evolution: status of cell symbiosis theory. *Symbiosis (Philadelphia, Pa.)* **1,** 101–124 (1985).

3. Andersson, S. G. & Kurland, C. G. Origins of mitochondria and hydrogenosomes. *Current Opinion in Microbiology* **2,** 535–541 (1999).

4. DiMauro, S. Mitochondrial DNA medicine. *Bioscience reports* **27,** 5–9 (2007).

5. Chen, L. B. Mitochondrial membrane potential in living cells. *Annual review of cell biology* **4,** 155–81 (1988).

6. Alberts, B. *et al. Molecular Biology of the Cell*. *4th Edition, New York* (2002).

7. Neupert, W. & Herrmann, J. M. Translocation of proteins into mitochondria. *Annual review of biochemistry* **76,** 723–749 (2007).

8. Hayashi, T., Rizzuto, R., Hajnoczky, G. & Su, T. P. MAM: more than just a housekeeper. *Trends in Cell Biology* **19,** 81–88 (2009).

9. Rappaport, L., Oliviero, P. & Samuel, J. L. Cytoskeleton and mitochondrial morphology and function. *Molecular and cellular biochemistry* **184,** 101–105 (1998).

10. McMillin, J. B. & Dowhan, W. Cardiolipin and apoptosis. *Biochimica et Biophysica Acta - Molecular and Cell Biology of Lipids* **1585,** 97–107 (2002).

11. Herrmann, J. M. & Neupert, W. Protein transport into mitochondria. *Current Opinion in Microbiology* **3,** 210–214 (2000).

12. Stowe, D. F. & Camara, A. K. S. Mitochondrial reactive oxygen species production in excitable cells: modulators of mitochondrial and cell function. *Antioxidants & redox signaling* **11,** 1373–1414 (2009).

13. Chipuk, J. E., Bouchier-Hayes, L. & Green, D. R. Mitochondrial outer membrane permeabilization during apoptosis: the innocent bystander scenario. *Cell death and differentiation* **13,** 1396–1402 (2006).

14. Green, D. R. Apoptotic pathways: the roads to ruin. *Cell* **94,** 695–8 (1998).

15. Hajnóczky, G. *et al.* Mitochondrial calcium signalling and cell death: approaches for assessing the role of mitochondrial Ca2+ uptake in apoptosis. *Cell calcium* **40,** 553–60

16. Greaves, L. C. & Taylor, R. W. Mitochondrial DNA mutations in human disease. *IUBMB life* **58,** 143–151 (2006).

17. Lenaz, G. & Genova, M. L. Kinetics of integrated electron transfer in the mitochondrial respiratory chain: random collisions vs. solid state electron channeling. *American journal of physiology. Cell physiology* **292,** C1221–C1239 (2007).

18. Lenaz, G., Fato, R., Formiggini, G. & Genova, M. L. The role of Coenzyme Q in mitochondrial electron transport. *Mitochondrion* **7,** (2007).

19. Vonck, J. & Schäfer, E. Supramolecular organization of protein complexes in the mitochondrial inner membrane. *Biochimica et biophysica acta* **1793,** 117–124 (2009).

20. Acin-Perez, R. & Enriquez, J. A. The function of the respiratory supercomplexes: the plasticity model. *Biochimica et biophysica acta* **1837,** 444–50 (2014).

21. Ozawa, T., Tanaka, M., Suzuki, H. & Nishikimi, M. Structure and function of mitochondria: their organization and disorders. *Brain & development* **9,** 76–81 (1987).

22. Batandier, C., Fontaine, E., Kériel, C. & Leverve, X. M. Determination of mitochondrial reactive oxygen species: methodological aspects. *Journal of cellular and molecular medicine* **6,** 175–87

23. Kudin, A. P., Bimpong-Buta, N. Y.-B., Vielhaber, S., Elger, C. E. & Kunz, W. S. Characterization of superoxide-producing sites in isolated brain mitochondria. *The Journal of biological chemistry* **279,** 4127–35 (2004).

24. Liu, Y., Fiskum, G. & Schubert, D. Generation of reactive oxygen species by the mitochondrial electron transport chain. *Journal of neurochemistry* **80,** 780–7 (2002).

25. Gauuan, P. J. F. *et al.* Superoxide dismutase mimetics: synthesis and structure-activity relationship study of MnTBAP analogues. *Bioorganic & medicinal chemistry* **10,** 3013–21 (2002).

26. Zhang, D. X., Zou, A.-P. & Li, P.-L. Ceramide-induced activation of NADPH oxidase and endothelial dysfunction in small coronary arteries. *American journal of physiology. Heart and circulatory physiology* **284,** H605–12 (2003).

27. De Bilbao, F. *et al.* Resistance to cerebral ischemic injury in UCP2 knockout mice: evidence for a role of UCP2 as a regulator of mitochondrial glutathione levels. *Journal of neurochemistry* **89,** 1283–92 (2004).

28. Beckman, J. S., Estévez, A. G., Crow, J. P. & Barbeito, L. Superoxide dismutase and the death of motoneurons in ALS. *Trends in neurosciences* **24,** S15–20 (2001).

29. Estévez, A. G. *et al.* Nitric oxide and superoxide contribute to motor neuron apoptosis induced by trophic factor deprivation. *The Journal of neuroscience : the official journal of the Society for Neuroscience* **18,** 923–31 (1998).

30. Rego, A. C. & Oliveira, C. R. Mitochondrial dysfunction and reactive oxygen species in excitotoxicity and apoptosis: implications for the pathogenesis of neurodegenerative diseases. *Neurochemical research* **28,** 1563–74 (2003).

31. Tieu, K., Ischiropoulos, H. & Przedborski, S. Nitric oxide and reactive oxygen species in Parkinson's disease. *IUBMB life* **55,** 329–35 (2003).

32. NASS, M. M. & NASS, S. INTRAMITOCHONDRIAL FIBERS WITH DNA CHARACTERISTICS. I. FIXATION AND. *The Journal of cell biology* **19,** 593–611 (1963).

33. Schatz, G., Haslbrunner, E. & Tuppy, H. Deoxyribonucleic acid associated with yeast mitochondria. *Biochemical and Biophysical Research Communications* **15,** 127–132 (1964).

34. Wiesner, R. J., Rüegg, J. C. & Morano, I. Counting target molecules by exponential polymerase chain reaction: copy number of mitochondrial DNA in rat tissues. *Biochemical and biophysical research communications* **183,** 553–559 (1992).

35. Anderson, S. *et al.* Sequence and organization of the human mitochondrial genome. *Nature* **290,** 457–465 (1981).

36. Diaz, F. & Moraes, C. T. Mitochondrial biogenesis and turnover. *Cell Calcium* **44,** 24–35 (2008).

37. Kaufman, B. A. *et al.* In organello formaldehyde crosslinking of proteins to mtDNA: identification of bifunctional proteins. *Proceedings of the National Academy of Sciences of the United States of America* **97,** 7772–7777 (2000).

38. Chang, D. D. & Clayton, D. A. Priming of human mitochondrial DNA replication occurs at the light-strand promoter. *Proceedings of the National Academy of Sciences of the United States of America* **82,** 351–355 (1985).

39. Clayton, D. A. Replication of animal mitochondrial DNA. *Cell* **28,** 693–705 (1982).

40. Brown, T. A., Cecconi, C., Tkachuk, A. N., Bustamante, C. & Clayton, D. A. Replication of mitochondrial DNA occurs by strand displacement with alternative light-strand origins, not via a strand-coupled mechanism. *Genes and Development* **19,** 2466–2476 (2005).

41. Holt, I. J., Lorimer, H. E. & Jacobs, H. T. Coupled leading- and lagging-strand synthesis of mammalian mitochondrial DNA. *Cell* **100,** 515–524 (2000).

42. Montoya, J., Christianson, T., Levens, D., Rabinowitz, M. & Attardi, G. Identification of initiation sites for heavy-strand and light-strand transcription in human mitochondrial DNA. *Proceedings of the National Academy of Sciences of the United States of America* **79,** 7195–7199 (1982).

43. Montoya, J., Gaines, G. L. & Attardi, G. The pattern of transcription of the human mitochondrial rRNA genes reveals two overlapping transcription units. *Cell* **34,** 151–159 (1983).

44. Taanman, J. W. The mitochondrial genome: structure, transcription, translation and replication. *Biochimica et biophysica acta* **1410,** 103–123 (1999).

45. Martin, M., Cho, J., Cesare, A. J., Griffith, J. D. & Attardi, G. Termination factor-mediated DNA loop between termination and initiation sites drives mitochondrial rRNA synthesis. *Cell* **123,** 1227–1240 (2005).

46. Christian, B. E. & Spremulli, L. L. Mechanism of protein biosynthesis in mammalian mitochondria. *Biochimica et biophysica acta* **1819,** 1035–54

47. Odintsova, M. S. & Iurina, N. P. Mitochondrial ribosomes. *Biokhimiia (Moscow, Russia)* **42,** 1347–1360 (1977).

48. Liao, H. X. & Spremulli, L. L. Identification and initial characterization of translational initiation factor 2 from bovine mitochondria. *Journal of Biological Chemistry* **265,** 13618–13622 (1990).

49. Spremulli, L. L., Coursey, A., Navratil, T. & Hunter, S. E. Initiation and elongation factors in mammalian mitochondrial protein biosynthesis. *Progress in nucleic acid research and molecular biology* **77,** 211–61 (2004).

50. Rorbach, J. *et al.* The human mitochondrial ribosome recycling factor is essential for cell viability. *Nucleic Acids Research* **36,** 5787–5799 (2008).

51. Parra, V. *et al.* The complex interplay between mitochondrial dynamics and cardiac metabolism. in *Journal of Bioenergetics and Biomembranes* **43,** 47–51 (2011).

52. Westermann, B. Merging mitochondria matters. Cellular role and molecular machinery of mitochondrial fusion. *EMBO Reports* **3,** 527–531 (2002).

53. Twig, G. *et al.* Fission and selective fusion govern mitochondrial segregation and elimination by autophagy. *The EMBO journal* **27,** 433–446 (2008).

54. Ni, H.-M., Williams, J. A. & Ding, W.-X. Mitochondrial dynamics and mitochondrial quality control. *Redox biology* **4,** 6–13 (2015).

55. Nakada, K., Inoue, K. & Hayashi, J. Interaction theory of mammalian mitochondria. *Biochemical and biophysical research communications* **288,** 743–746 (2001).

56. Menzies, R. A. & Gold, P. H. The turnover of mitochondria in a variety of tissues of young adult and aged rats. *Journal of Biological Chemistry* **246,** 2425–2429 (1971).

57. Smirnova, E., Griparic, L., Shurland, D. L. & van der Bliek, A. M. Dynamin-related protein Drp1 is required for mitochondrial division in mammalian cells. *Molecular biology of the cell* **12,** 2245–2256 (2001).

58. James, D. I., Parone, P. A., Mattenberger, Y. & Martinou, J. C. hFis1, a novel component of the mammalian mitochondrial fission machinery. *Journal of Biological Chemistry* **278,** 36373–36379 (2003).

59. Van der Bliek, A. M., Shen, Q. & Kawajiri, S. Mechanisms of mitochondrial fission and fusion. *Cold Spring Harbor Perspectives in Biology* **5,** (2013).

60. Chan, D. C. Mitochondria: Dynamic Organelles in Disease, Aging, and Development. *Cell* **125,** 1241–1252 (2006).

61. Yu, T., Robotham, J. L. & Yoon, Y. Increased production of reactive oxygen species in hyperglycemic conditions requires dynamic change of mitochondrial morphology. *Proceedings of the National Academy of Sciences of the United States of America* **103,** 2653–2658 (2006).

62. Lee, Y., Jeong, S.-Y., Karbowski, M., Smith, C. L. & Youle, R. J. Roles of the mammalian mitochondrial fission and fusion mediators Fis1, Drp1, and Opa1 in apoptosis. *Molecular biology of the cell* **15,** 5001–5011 (2004).

63. Chen, H. *et al.* Mitofusins Mfn1 and Mfn2 coordinately regulate mitochondrial fusion and are essential for embryonic development. *Journal of Cell Biology* **160,** 189–200 (2003).

64. Legros, F., Lombès, A., Frachon, P. & Rojo, M. Mitochondrial fusion in human cells is efficient, requires the inner membrane potential, and is mediated by mitofusins. *Molecular biology of the cell* **13,** 4343–4354 (2002).

65. Meeusen, S. *et al.* Mitochondrial Inner-Membrane Fusion and Crista Maintenance Requires the Dynamin-Related GTPase Mgm1. *Cell* **127,** 383–395 (2006).

66. Olichon, A. *et al.* The human dynamin-related protein OPA1 is anchored to the mitochondrial inner membrane facing the inter-membrane space. *FEBS Letters* **523,** 171–176 (2002).

67. Cipolat, S., Martins de Brito, O., Dal Zilio, B. & Scorrano, L. OPA1 requires mitofusin 1 to promote mitochondrial fusion. *Proceedings of the National Academy of Sciences of the United States of America* **101,** 15927–15932 (2004).

68. Griparic, L., Kanazawa, T. & Van Der Bliek, A. M. Regulation of the mitochondrial dynamin-like protein Opa1 by proteolytic cleavage. *Journal of Cell Biology* **178,** 757–764 (2007).

69. Ishihara, N., Fujita, Y., Oka, T. & Mihara, K. Regulation of mitochondrial morphology through proteolytic cleavage of OPA1. *The EMBO journal* **25,** 2966–2977 (2006).

70. Baricault, L. *et al.* OPA1 cleavage depends on decreased mitochondrial ATP level and bivalent metals. *Experimental Cell Research* **313,** 3800–3808 (2007).

71. Guillery, O. *et al.* Metalloprotease-mediated OPA1 processing is modulated by the mitochondrial membrane potential. *Biology of the cell / under the auspices of the European Cell Biology Organization* **100,** 315–325 (2008).

72. Duvezin-Caubet, S. *et al.* Proteolytic processing of OPA1 links mitochondrial dysfunction to alterations in mitochondrial morphology. *Journal of Biological Chemistry* **281,** 37972–37979 (2006).

73. Song, M. *et al.* Super-suppression of mitochondrial reactive oxygen species signaling impairs compensatory autophagy in primary mitophagic cardiomyopathy. *Circulation Research* **115,** 348–353 (2014).

74. Kim, N. C. *et al.* VCP is essential for mitochondrial quality control by PINK1/Parkin and this function is impaired by VCP mutations. *Neuron* **78,** 65–80 (2013).

75. Winklhofer, K. F. Parkin and mitochondrial quality control: Toward assembling the puzzle. *Trends in Cell Biology* **24,** 332–341 (2014).

76. Kim, I., Rodriguez-Enriquez, S. & Lemasters, J. J. Selective degradation of mitochondria by mitophagy. *Archives of Biochemistry and Biophysics* **462,** 245–253 (2007).

77. Krysko, D. V. *et al.* Emerging role of damage-associated molecular patterns derived from mitochondria in inflammation. *Trends in Immunology* **32,** 157–164 (2011).

78. Kirkinezos, I. G. & Moraes, C. T. Reactive oxygen species and mitochondrial diseases. *Seminars in cell & developmental biology* **12,** 449–457 (2001).

79. Bender, T., Lewrenz, I., Franken, S., Baitzel, C. & Voos, W. Mitochondrial enzymes are protected from stress-induced aggregation by mitochondrial chaperones and the Pim1/LON protease. *Molecular biology of the cell* **22,** 541–554 (2011).

80. Leonhard, K. *et al.* Membrane protein degradation by AAA proteases in mitochondria: extraction of substrates from either membrane surface. *Molecular cell* **5,** 629–638 (2000).

81. ASHFORD, T. P. & PORTER, K. R. Cytoplasmic components in hepatic cell lysosomes. *The Journal of cell biology* **12,** 198–202 (1962).

82. Lemasters, J. J. Selective mitochondrial autophagy, or mitophagy, as a targeted defense against oxidative stress, mitochondrial dysfunction, and aging. *Rejuvenation research* **8,** 3–5 (2005).

83. Ravikumar, B., Moreau, K., Jahreiss, L., Puri, C. & Rubinsztein, D. C. Plasma membrane contributes to the formation of pre-autophagosomal structures. *Nature cell biology* **12,** 747–757 (2010).

84. Axe, E. L. *et al.* Autophagosome formation from membrane compartments enriched in phosphatidylinositol 3-phosphate and dynamically connected to the endoplasmic reticulum. *Journal of Cell Biology* **182,** 685–701 (2008).

85. Hamasaki, M. & Yoshimori, T. Where do they come from? Insights into autophagosome formation. *FEBS Letters* **584,** 1296–1301 (2010).

86. Klionsky, D. J. *et al.* A comprehensive glossary of autophagy-related molecules and processes (2 nd edition). *Autophagy* **7,** 1273–1294 (2011).

87. Homma, K., Suzuki, K. & Sugawara, H. The autophagy database: An all-inclusive information resource on autophagy that provides nourishment for research. *Nucleic Acids Research* **39,** (2011).

88. Pattingre, S., Espert, L., Biard-Piechaczyk, M. & Codogno, P. Regulation of macroautophagy by mTOR and Beclin 1 complexes. *Biochimie* **90,** 313–323 (2008).

89. Todde, V., Veenhuis, M. & van der Klei, I. J. Autophagy: Principles and significance in health and disease. *Biochimica et Biophysica Acta - Molecular Basis of Disease* **1792,** 3–13 (2009).

90. Kundu, M. & Thompson, C. B. Autophagy: basic principles and relevance to disease. *Annual review of pathology* **3,** 427–455 (2008).

91. Reggiori, F. Membrane Origin for Autophagy. *Current Topics in Developmental Biology* **74,** 1–30 (2006).

92. Nishida, Y. *et al.* Discovery of Atg5/Atg7-independent alternative macroautophagy. *Nature* **461,** 654–658 (2009).

93. Zhang, J. Teaching the basics of autophagy and mitophagy to redox biologists – mechanisms and experimental approaches. *Redox Biology* **4,** 242–59 (2015).

94. Yamamoto, A. *et al.* Bafilomycin A1 prevents maturation of autophagic vacuoles by inhibiting fusion between autophagosomes and lysosomes in rat hepatoma cell line, H-4-II-E cells. *Cell structure and function* **23,** 33–42 (1998).

95. Ehses, S. *et al.* Regulation of OPA1 processing and mitochondrial fusion by m-AAA protease isoenzymes and OMA1. *Journal of Cell Biology* **187,** 1023–1036 (2009).

96. Cohen, M. M. J., Leboucher, G. P., Livnat-Levanon, N., Glickman, M. H. & Weissman, A. M. Ubiquitin-proteasome-dependent degradation of a mitofusin, a critical regulator of mitochondrial fusion. *Molecular biology of the cell* **19,** 2457–2464 (2008).

97. Lemasters, J. J. Modulation of mitochondrial membrane permeability in pathogenesis, autophagy and control of metabolism. in *Journal of Gastroenterology and Hepatology (Australia)* **22,** S31–7 (2007).

98. Scherz-Shouval, R. & Elazar, Z. ROS, mitochondria and the regulation of autophagy. *Trends in Cell Biology* **17,** 422–427 (2007).

99. Rodríguez-Hernández, Á. *et al.* Coenzyme Q deficiency triggers mitochondria degradation by mitophagy. *Autophagy* **5,** 19–32 (2009).

100. Cotán, D. *et al.* Secondary coenzyme Q10 deficiency triggers mitochondria degradation by mitophagy in MELAS fibroblasts. *The FASEB journal : official publication of the Federation of American Societies for Experimental Biology* **25,** 2669–2687 (2011).

101. Garrido-Maraver, J. *et al.* Screening of effective pharmacological treatments for MELAS syndrome using yeasts, fibroblasts and cybrid models of the disease. *British Journal of Pharmacology* **167,** 1311–28 (2012).

102. Jin, S. M. *et al.* Mitochondrial membrane potential regulates PINK1 import and proteolytic destabilization by PARL. *Journal of Cell Biology* **191,** 933–942 (2010).

103. Jin, S. M. & Youle, R. J. PINK1- and Parkin-mediated mitophagy at a glance. *Journal of cell science* **125,** 795–9 (2012).

104. Narendra, D. P. *et al.* PINK1 is selectively stabilized on impaired mitochondria to activate Parkin. *PLoS Biology* **8,** (2010).

105. Narendra, D., Tanaka, A., Suen, D. F. & Youle, R. J. Parkin is recruited selectively to impaired mitochondria and promotes their autophagy. *Journal of Cell Biology* **183,** 795–803 (2008).

106. Greene, A. W. *et al.* Mitochondrial processing peptidase regulates PINK1 processing, import and Parkin recruitment. *EMBO reports* **13,** 378–385 (2012).

107. Iguchi, M. *et al.* Parkin-catalyzed ubiquitin-ester transfer is triggered by PINK1-dependent phosphorylation. *Journal of Biological Chemistry* **288,** 22019–22032 (2013).

108. Chen, Y. & Dorn, G. W. PINK1-phosphorylated mitofusin 2 is a Parkin receptor for culling damaged mitochondria. *Science (New York, N.Y.)* **340,** 471–5 (2013).

109. Wang, X. *et al.* PINK1 and Parkin target miro for phosphorylation and degradation to arrest mitochondrial motility. *Cell* **147,** 893–906 (2011).

110. Geisler, S. *et al.* PINK1/Parkin-mediated mitophagy is dependent on VDAC1 and p62/SQSTM1. *Nature cell biology* **12,** 119–131 (2010).

111. Kirkin, V. *et al.* A Role for NBR1 in Autophagosomal Degradation of Ubiquitinated Substrates. *Molecular Cell* **33,** 505–516 (2009).

112. Pankiv, S. *et al.* p62/SQSTM1 binds directly to Atg8/LC3 to facilitate degradation of ubiquitinated protein aggregates by autophagy*[S]. *Journal of Biological Chemistry* **282,** 24131–24145 (2007).

113. Orvedahl, A. *et al.* Image-based genome-wide siRNA screen identifies selective autophagy factors. *Nature* **480,** 113–117 (2011).

114. Van Humbeeck, C., Cornelissen, T. & Vandenberghe, W. Ambra1: A Parkin-binding protein involved in mitophagy. *Autophagy* **7,** 1555–1556 (2011).

115. Strappazzon, F. *et al.* Mitochondrial BCL-2 inhibits AMBRA1-induced autophagy. *The EMBO journal* **30,** 1195–1208 (2011).

116. Kane, L. A. *et al.* PINK1 phosphorylates ubiquitin to activate parkin E3 ubiquitin ligase activity. *Journal of Cell Biology* **205,** 143–153 (2014).

117. Kazlauskaite, A. *et al.* Phosphorylation of Parkin at Serine65 is essential for activation: elaboration of a Miro1 substrate-based assay of Parkin E3 ligase activity. *Open biology* **4,** 130213 (2014).

118. Novak, I. *et al.* Nix is a selective autophagy receptor for mitochondrial clearance. *EMBO reports* **11,** 45–51 (2010).

119. Chakrama, F. Z. *et al.* GABARAPL1 (GEC1) associates with autophagic vesicles. *Autophagy* **6,** 495–505 (2010).

120. Lee, Y., Lee, H.-Y., Hanna, R. A. & Gustafsson, A. B. Mitochondrial autophagy by Bnip3 involves Drp1-mediated mitochondrial fission and recruitment of Parkin in cardiac myocytes. *AJP: Heart and Circulatory Physiology* **301,** H1924–H1931 (2011).

121. Liu, L. *et al.* Mitochondrial outer-membrane protein FUNDC1 mediates hypoxia-induced mitophagy in mammalian cells. *Nature Cell Biology* **14,** 177–185 (2012).

122. Russell, R. C., Yuan, H.-X. & Guan, K.-L. Autophagy regulation by nutrient signaling. *Cell research* **24,** 42–57 (2014).

123. Zhang, J. *et al.* A tuberous sclerosis complex signalling node at the peroxisome regulates mTORC1 and autophagy in response to ROS. *Nature cell biology* **15,** 1186–96 (2013).

124. Shen, H.-M. & Mizushima, N. At the end of the autophagic road: an emerging understanding of lysosomal functions in autophagy. *Trends in biochemical sciences* **39,** 61–71 (2014).

125. Dunlop, E. A. & Tee, A. R. mTOR and autophagy: A dynamic relationship governed by nutrients and energy. *Seminars in Cell & Developmental Biology* **36,** 121–129 (2014).

126. Dunlop, E. a & Tee, A. R. The kinase triad, AMPK, mTORC1 and ULK1, maintains energy and nutrient homoeostasis. *Biochemical Society transactions* **41,** 939–43 (2013).

127. Zhao, M. & Klionsky, D. J. AMPK-dependent phosphorylation of ULK1 induces autophagy. *Cell Metabolism* **13,** 119–120 (2011).

128. Alers, S., Loffler, A. S., Wesselborg, S. & Stork, B. Role of AMPK-mTOR-Ulk1/2 in the Regulation of Autophagy: Cross Talk, Shortcuts, and Feedbacks. *Molecular and Cellular Biology* **32,** 2–11 (2012).

129. Yuan, H.-X., Russell, R. C. & Guan, K.-L. Regulation of PIK3C3/VPS34 complexes by MTOR in nutrient stress-induced autophagy. *Autophagy* **9,** 1983–95 (2013).

130. Martina, J. A., Chen, Y., Gucek, M. & Puertollano, R. MTORC1 functions as a transcriptional regulator of autophagy by preventing nuclear transport of TFEB. *Autophagy* **8,** 903–914 (2012).

131. Kabeya, Y. *et al.* Erratum: LC3, a mammalian homolog of yeast Apg8p, is localized in autophagosome membranes after processing (EMBO Journal (2000) 19 (5720-5728)). *EMBO Journal* **22,** 4577 (2003).

132. Klionsky, D. J. *et al.* Guidelines for the use and interpretation of assays for monitoring autophagy. *Autophagy* **8,** 445–544 (2012).

133. Fass, E., Shvets, E., Degani, I., Hirschberg, K. & Elazar, Z. Microtubules support production of starvation-induced autophagosomes but not their targeting and fusion with lysosomes. *Journal of Biological Chemistry* **281,** 36303–36316 (2006).

134. Zhang, X., Chen, S., Huang, K. & Le, W. Why should autophagic flux be assessed? *Acta pharmacologica Sinica* **34,** 595–9 (2013).

135. Ju, J. S., Varadhachary, A. S., Miller, S. E. & Weihl, C. C. Quantitation of 'autophagic flux' in mature skeletal muscle. *Autophagy* **6,** 929–935 (2010).

136. Klionsky, D. J., Elazar, Z., Seglen, P. O. & Rubinsztein, D. C. Does bafilomycin A1 block the fusion of autophagosomes with lysosomes? *Autophagy* **4,** 849–850 (2008).

137. Tanida, I., Minematsu-Ikeguchi, N., Ueno, T. & Kominami, E. Lysosomal turnover, but not a cellular level, of endogenous LC3 is a marker for autophagy. *Autophagy* **1,** 84–91 (2005).

138. Lenka, N., Vijayasarathy, C., Mullick, J. & Avadhani, N. G. Structural organization and transcription regulation of nuclear genes encoding the mammalian cytochrome c oxidase complex. *Prog Nucleic Acid Res Mol Biol* **61,** 309–344 (1998).

139. Scarpulla, R. C. Nuclear activators and coactivators in mammalian mitochondrial biogenesis. *Biochimica et Biophysica Acta - Gene Structure and Expression* **1576,** 1–14 (2002).

140. Roy, D., Felty, Q., Narayan, S. & Jayakar, P. Signature of mitochondria of steroidal hormones-dependent normal and cancer cells: potential molecular targets for cancer therapy. *Frontiers in bioscience : a journal and virtual library* **12,** 154–173 (2007).

141. Puigserver, P. *et al.* A cold-inducible coactivator of nuclear receptors linked to adaptive thermogenesis. *Cell* **92,** 829–39 (1998).

142. Virbasius, J. V & Scarpulla, R. C. Activation of the human mitochondrial transcription factor A gene by nuclear respiratory factors: a potential regulatory link between nuclear and mitochondrial gene expression in organelle biogenesis. *Proceedings of the National Academy of Sciences of the United States of America* **91,** 1309–13 (1994).

143. Wu, Z. *et al.* Mechanisms controlling mitochondrial biogenesis and respiration through the thermogenic coactivator PGC-1. *Cell* **98,** 115–124 (1999).

144. Ventura-Clapier, R., Garnier, A. & Veksler, V. Transcriptional control of mitochondrial biogenesis: The central role of PGC-1α. *Cardiovascular Research* **79,** 208–217 (2008).

145. Meirhaeghe, A. *et al.* Characterization of the human, mouse and rat PGC1 beta (peroxisome-proliferator-activated receptor-gamma co-activator 1 beta) gene in vitro and in vivo. *The Biochemical journal* **373,** 155–65 (2003).

146. Jornayvaz, F. R. & Shulman, G. I. Regulation of mitochondrial biogenesis. *Essays in biochemistry* **47,** 69–84 (2010).

147. PAUL, M. H. & SPERLING, E. Cyclophorase system. XXIII. Correlation of cyclophorase activity and mitochondrial density in striated muscle. *Proceedings of the Society for Experimental Biology and Medicine. Society for Experimental Biology and Medicine (New York, N.Y.)* **79,** 352–4 (1952).

148. Holloszy, J. O. Biochemical adaptations in muscle. Effects of exercise on mitochondrial oxygen uptake and respiratory enzyme activity in skeletal muscle. *The Journal of biological chemistry* **242,** 2278–82 (1967).

149. Gollnick, P. D., Armstrong, R. B., Saubert, C. W., Piehl, K. & Saltin, B. Enzyme activity and fiber composition in skeletal muscle of untrained and trained men. *Journal of applied physiology* **33,** 312–9 (1972).

150. Hoppeler, H., Lüthi, P., Claassen, H., Weibel, E. R. & Howald, H. The ultrastructure of the normal human skeletal muscle. A morphometric analysis on untrained men, women and well-trained orienteers. *Pflügers Archiv : European journal of physiology* **344,** 217–32 (1973).

151. Fink, W. J., Costill, D. L. & Pollock, M. L. Submaximal and maximal working capacity of elite distance runners. Part II. Muscle fiber composition and enzyme activities. *Annals of the New York Academy of Sciences* **301,** 323–327 (1977).

152. Holloszy, J. O. & Booth, F. W. Biochemical adaptations to endurance exercise in muscle. *Annual review of physiology* **38,** 273–91 (1976).

153. Freyssenet, D., Di Carlo, M. & Hood, D. A. Calcium-dependent regulation of cytochrome c gene expression in skeletal muscle cells. Identification of a protein kinase c-dependent pathway. *J Biol Chem* **274,** 9305–9311 (1999).

154. Wright, D. C., Geiger, P. C., Han, D.-H., Jones, T. E. & Holloszy, J. O. Calcium induces increases in peroxisome proliferator-activated receptor gamma coactivator-1alpha and mitochondrial biogenesis by a pathway leading to p38 mitogen-activated protein kinase activation. *The Journal of biological chemistry* **282,** 18793–18799 (2007).

155. Puigserver, P. *et al.* Cytokine stimulation of energy expenditure through p38 MAP kinase activation of PPARgamma coactivator-1. *Molecular cell* **8,** 971–982 (2001).

156. Jäger, S., Handschin, C., St-Pierre, J. & Spiegelman, B. M. AMP-activated protein kinase (AMPK) action in skeletal muscle via direct phosphorylation of PGC-1alpha. *Proceedings of the National Academy of Sciences of the United States of America* **104,** 12017–22 (2007).

157. Akimoto, T. *et al.* Exercise stimulates Pgc-1alpha transcription in skeletal muscle through activation of the p38 MAPK pathway. *The Journal of biological chemistry* **280,** 19587–19593 (2005).

158. Cao, W. *et al.* p38 mitogen-activated protein kinase is the central regulator of cyclic AMP-dependent transcription of the brown fat uncoupling protein 1 gene. *Molecular and cellular biology* **24,** 3057–3067 (2004).

159. Wu, Z. *et al.* Transducer of regulated CREB-binding proteins (TORCs) induce PGC-1alpha transcription and mitochondrial biogenesis in muscle cells. *Proceedings of the National Academy of Sciences of the United States of America* **103,** 14379–14384 (2006).

160. Gerhart-Hines, Z. *et al.* Metabolic control of muscle mitochondrial function and fatty acid oxidation through SIRT1/PGC-1alpha. *The EMBO journal* **26,** 1913–1923 (2007).

161. Lee, S., Kim, S., Sun, X., Lee, J. H. & Cho, H. Cell cycle-dependent mitochondrial biogenesis and dynamics in mammalian cells. *Biochemical and Biophysical Research Communications* **357,** 111–117 (2007).

162. Rasbach, K. A. & Schnellmann, R. G. Signaling of mitochondrial biogenesis following oxidant injury. *Journal of Biological Chemistry* **282,** 2355–2362 (2007).

163. Nisoli, E. *et al.* Mitochondrial biogenesis in mammals: the role of endogenous nitric oxide. *Science (New York, N.Y.)* **299,** 896–899 (2003).

164. McLeod, C. J., Pagel, I. & Sack, M. N. The mitochondrial biogenesis regulatory program in cardiac adaptation to ischemia--a putative target for therapeutic intervention. *Trends in cardiovascular medicine* **15,** 118–23 (2005).

165. DiMauro, S. & Schon, E. A. Mitochondrial respiratory-chain diseases. *The New England journal of medicine* **348,** 2656–2668 (2003).

166. Wallace, D. C. Mitochondrial defects in neurodegenerative disease. *Mental retardation and developmental disabilities research reviews* **7,** 158–66 (2001).

167. Klaus, S., Casteilla, L., Bouillaud, F. & Ricquier, D. The uncoupling protein UCP: a membraneous mitochondrial ion carrier exclusively expressed in brown adipose tissue. *The International journal of biochemistry* **23,** 791–801 (1991).

168. Wu, H. *et al.* Regulation of mitochondrial biogenesis in skeletal muscle by CaMK. *Science (New York, N.Y.)* **296,** 349–352 (2002).

169. Handschin, C., Rhee, J., Lin, J., Tarr, P. T. & Spiegelman, B. M. An autoregulatory loop controls peroxisome proliferator-activated receptor gamma coactivator 1alpha expression in muscle. *Proceedings of the National Academy of Sciences of the United States of America* **100,** 7111–7116 (2003).

170. Treuter, E., Albrektsen, T., Johansson, L., Leers, J. & Gustafsson, J. A. A regulatory role for RIP140 in nuclear receptor activation. *Molecular endocrinology (Baltimore, Md.)* **12,** 864–881 (1998).

171. Powelka, A. M. *et al.* Suppression of oxidative metabolism and mitochondrial biogenesis by the transcriptional corepressor RIP140 in mouse adipocytes. *Journal of Clinical Investigation* **116,** 125–136 (2006).

172. White, R. *et al.* Role of RIP140 in metabolic tissues: Connections to disease. *FEBS Letters* **582,** 39–45 (2008).

173. Fan, M. *et al.* Suppression of mitochondrial respiration through recruitment of p160 myb binding protein to PGC-1α: Modulation by p38 MAPK. *Genes and Development* **18,** 278–289 (2004).

174. Chang, J. S. *et al.* Regulation of NT-PGC-1alpha subcellular localization and function by protein kinase A-dependent modulation of nuclear export by CRM1. *The Journal of biological chemistry* **285,** 18039–18050 (2010).

175. Witczak, C. A., Sharoff, C. G. & Goodyear, L. J. AMP-activated protein kinase in skeletal muscle: from structure and localization to its role as a master regulator of cellular metabolism. *Cellular and molecular life sciences : CMLS* **65,** 3737–3755 (2008).

176. Ignoul, S. & Eggermont, J. CBS domains: structure, function, and pathology in human proteins. *American journal of physiology. Cell physiology* **289,** C1369–78 (2005).

177. Woods, A. *et al.* LKB1 Is the Upstream Kinase in the AMP-Activated Protein Kinase Cascade. *Current Biology* **13,** 2004–2008 (2003).

178. Woods, A. *et al.* Ca2+/calmodulin-dependent protein kinase kinase-beta acts upstream of AMP-activated protein kinase in mammalian cells. *Cell metabolism* **2,** 21–33 (2005).

179. Reznick, R. M. *et al.* Aging-Associated Reductions in AMP-Activated Protein Kinase Activity and Mitochondrial Biogenesis. *Cell Metabolism* **5,** 151–156 (2007).

180. Xiao, B. *et al.* Structure of mammalian AMPK and its regulation by ADP. *Nature* **472,** 230–233 (2011).

181. Mihaylova, M. M. & Shaw, R. J. The AMPK signalling pathway coordinates cell growth, autophagy and metabolism. *Nature cell biology* **13,** 1016–1023 (2011).

182. Gwinn, D. M. *et al.* AMPK Phosphorylation of Raptor Mediates a Metabolic Checkpoint. *Molecular Cell* **30,** 214–226 (2008).

183. Kalender, A. *et al.* Metformin, independent of AMPK, inhibits mTORC1 in a rag GTPase-dependent manner. *Cell Metabolism* **11,** 390–401 (2010).

184. Jung, C. H., Ro, S.-H., Cao, J., Otto, N. M. & Kim, D.-H. mTOR regulation of autophagy. *FEBS letters* **584,** 1287–95 (2010).

185. Meley, D. *et al.* AMP-activated protein kinase and the regulation of autophagic proteolysis. *The Journal of biological chemistry* **281,** 34870–34879 (2006).

186. McGee, S. L. *et al.* AMP-activated protein kinase regulates GLUT4 transcription by phosphorylating histone deacetylase 5. *Diabetes* **57,** 860–867 (2008).

187. Chang, S., Bezprozvannaya, S., Li, S. & Olson, E. N. An expression screen reveals modulators of class II histone deacetylase phosphorylation. *Proceedings of the National Academy of Sciences of the United States of America* **102,** 8120–8125 (2005).

188. Mihaylova, M. M. *et al.* Class IIa histone deacetylases are hormone-activated regulators of FOXO and mammalian glucose homeostasis. *Cell* **145,** 607–621 (2011).

189. Cantó, C. *et al.* AMPK regulates energy expenditure by modulating NAD+ metabolism and SIRT1 activity. *Nature* **458,** 1056–1060 (2009).

190. Cantó, C. *et al.* Interdependence of AMPK and SIRT1 for Metabolic Adaptation to Fasting and Exercise in Skeletal Muscle. *Cell Metabolism* **11,** 213–219 (2010).

191. Narkar, V. A. *et al.* AMPK and PPAR?? Agonists Are Exercise Mimetics. *Cell* **134,** 405–415 (2008).

192. Han, D., Williams, E. & Cadenas, E. Mitochondrial respiratory chain-dependent generation of superoxide anion and its release into the intermembrane space. *The Biochemical journal* **353,** 411–416 (2001).

193. Wu, S.-B., Ma, Y.-S., Wu, Y.-T., Chen, Y.-C. & Wei, Y.-H. Mitochondrial DNA mutation-elicited oxidative stress, oxidative damage, and altered gene expression in cultured cells of patients with MERRF syndrome. *Molecular neurobiology* **41,** 256–266 (2010).

194. Ma, Y. S., Wu, S. B., Lee, W. Y., Cheng, J. S. & Wei, Y. H. Response to the increase of oxidative stress and mutation of mitochondrial DNA in aging. *Biochimica et Biophysica Acta - General Subjects* **1790,** 1021–1029 (2009).

195. Menzies, K. J., Robinson, B. H. & Hood, D. A. Effect of thyroid hormone on mitochondrial properties and oxidative stress in cells from patients with mtDNA defects. *American journal of physiology. Cell physiology* **296,** C355–C362 (2009).

196. Lu, C. Y., Wang, E. K., Lee, H. C., Tsay, H. J. & Wei, Y. H. Increased expression of manganese-superoxide dismutase in fibroblasts of patients with CPEO syndrome. *Molecular Genetics and Metabolism* **80,** 321–329 (2003).

197. Majora, M. *et al.* Functional consequences of mitochondrial DNA deletions in human skin fibroblasts: increased contractile strength in collagen lattices is due to oxidative stress-induced lysyl oxidase activity. *The American journal of pathology* **175,** 1019–1029 (2009).

198. Van Eijsden, R. G. E. *et al.* Termination of damaged protein repair defines the occurrence of symptoms in carriers of the m.3243A > G tRNA(Leu) mutation. *Journal of medical genetics* **45,** 525–534 (2008).

199. Scarpulla, R. C. Transcriptional paradigms in mammalian mitochondrial biogenesis and function. *Physiological reviews* **88,** 611–638 (2008).

200. Choi, H. C. *et al.* Reactive nitrogen species is required for the activation of the AMP-activated protein kinase by statin in vivo. *The Journal of biological chemistry* **283,** 20186–20197 (2008).

201. Cao, C. *et al.* EGFR activation confers protections against UV-induced apoptosis in cultured mouse skin dendritic cells. *Cellular Signalling* **20,** 1830–1838 (2008).

202. Cidad, P., Almeida, A. & Bolaños, J. P. Inhibition of mitochondrial respiration by nitric oxide rapidly stimulates cytoprotective GLUT3-mediated glucose uptake through 5'-AMP-activated protein kinase. *The Biochemical journal* **384,** 629–636 (2004).

203. Wang, S., Song, P. & Zou, M.-H. AMP-activated protein kinase, stress responses and cardiovascular diseases. *Clinical science (London, England : 1979)* **122,** 555–73 (2012).

204. Egan, D. F. *et al.* Phosphorylation of ULK1 (hATG1) by AMP-activated protein kinase connects energy sensing to mitophagy. *Science (New York, N.Y.)* **331,** 456–461 (2011).

205. Kim, J., Kundu, M., Viollet, B. & Guan, K.-L. AMPK and mTOR regulate autophagy through direct phosphorylation of Ulk1. *Nature cell biology* **13,** 132–141 (2011).

206. Hardie, D. G. AMPK and autophagy get connected. *The EMBO journal* **30,** 634–5 (2011).

207. Shang, L. *et al.* Nutrient starvation elicits an acute autophagic response mediated by Ulk1 dephosphorylation and its subsequent dissociation from AMPK. *Proceedings of the National Academy of Sciences of the United States of America* **108,** 4788–4793 (2011).

208. Tian, W. *et al.* Phosphorylation of ULK1 by AMPK regulates translocation of ULK1 to mitochondria and mitophagy. *FEBS letters* **589,** 1847–54 (2015).

209. Corton, J. M., Gillespie, J. G., Hawley, S. A. & Hardie, D. G. 5-aminoimidazole-4-carboxamide ribonucleoside. A specific method for activating AMP-activated protein kinase in intact cells? *European journal of biochemistry / FEBS* **229,** 558–65 (1995).

210. Sanz, P. AMP-activated protein kinase: structure and regulation. *Current protein & peptide science* **9,** 478–492 (2008).

211. Cool, B. *et al.* Identification and characterization of a small molecule AMPK activator that treats key components of type 2 diabetes and the metabolic syndrome. *Cell Metabolism* **3,** 403–416 (2006).

212. Sanders, M. J. *et al.* Defining the mechanism of activation of AMP-activated protein kinase by the small molecule A-769662, a member of the thienopyridone family. *The Journal of biological chemistry* **282,** 32539–48 (2007).

213. Zhou, G. *et al.* Role of AMP-activated protein kinase in mechanism of metformin action. *Journal of Clinical Investigation* **108,** 1167–74 (2001).

214. Li, H.-B., Ge, Y., Zheng, X.-X. & Zhang, L. Salidroside stimulated glucose uptake in skeletal muscle cells by activating AMP-activated protein kinase. *European journal of pharmacology* **588,** 165–169 (2008).

215. Gruzman, A. *et al.* Novel D-xylose derivatives stimulate muscle glucose uptake by activating AMP-activated protein kinase α. *Journal of Medicinal Chemistry* **51,** 8096–8108 (2008).

216. Ahn, J., Lee, H., Kim, S., Park, J. & Ha, T. The anti-obesity effect of quercetin is mediated by the AMPK and MAPK signaling pathways. *Biochemical and Biophysical Research Communications* **373,** 545–549 (2008).

217. Hwang, J. T. *et al.* Genistein, EGCG, and capsaicin inhibit adipocyte differentiation process via activating AMP-activated protein kinase. *Biochemical and Biophysical Research Communications* **338,** 694–699 (2005).

218. Kim, T., Davis, J., Zhang, A. J., He, X. & Mathews, S. T. Curcumin activates AMPK and suppresses gluconeogenic gene expression in hepatoma cells. *Biochemical and Biophysical Research Communications* **388,** 377–382 (2009).

219. Cheng, Z. *et al.* Berberine-stimulated glucose uptake in L6 myotubes involves both AMPK and p38 MAPK. *Biochimica et Biophysica Acta - General Subjects* **1760,** 1682–1689 (2006).

220. Lin, C. L. & Lin, J. K. Epigallocatechin gallate (EGCG) attenuates high glucose-induced insulin signaling blockade in human hepG2 hepatoma cells. *Molecular Nutrition and Food Research* **52,** 930–939 (2008).

221. Park, C. E. *et al.* Resveratrol stimulates glucose transport in C2C12 myotubes by activating AMP-activated protein kinase. *Experimental & molecular medicine* **39,** 222–229 (2007).

222. Kola, B., Boscaro, M., Rutter, G. A., Grossman, A. B. & Korbonits, M. Expanding role of AMPK in endocrinology. *Trends in Endocrinology and Metabolism* **17,** 205–215 (2006).

223. Fryer, L. G. D., Parbu-Patel, A. & Carling, D. Protein kinase inhibitors block the stimulation of the AMP-activated protein kinase by 5-amino-4-imidazolecarboxamide riboside. *FEBS letters* **531,** 189–192 (2002).

224. Landree, L. E. *et al.* C75, a fatty acid synthase inhibitor, modulates AMP-activated protein kinase to alter neuronal energy metabolism. *The Journal of biological chemistry* **279,** 3817–27 (2004).

225. LUFT, R., IKKOS, D., PALMIERI, G., ERNSTER, L. & AFZELIUS, B. A case of severe hypermetabolism of nonthyroid origin with a defect in the maintenance of mitochondrial respiratory control: a correlated clinical, biochemical, and morphological study. *The Journal of clinical investigation* **41,** 1776–804 (1962).

226. ENGEL, W. K. & CUNNINGHAM, G. G. RAPID EXAMINATION OF MUSCLE TISSUE. AN IMPROVED TRICHROME METHOD FOR FRESH-FROZEN BIOPSY SECTIONS. *Neurology* **13,** 919–23 (1963).

227. Liang, C., Ahmad, K. & Sue, C. M. The broadening spectrum of mitochondrial disease: Shifts in the diagnostic paradigm. *Biochimica et Biophysica Acta - General Subjects* **1840,** 1360–1367 (2014).

228. Walker, U. A., Collins, S. & Byrne, E. Respiratory chain encephalomyopathies: a diagnostic classification. *European neurology* **36,** 260–267 (1996).

229. Bernier, F. P. *et al.* Diagnostic criteria for respiratory chain disorders in adults and children. *Neurology* **59,** 1406–1411 (2002).

230. Thorburn, D. R. & Smeitink, J. Diagnosis of mitochondrial disorders: clinical and biochemical approach. *Journal of inherited metabolic disease* **24,** 312–6 (2001).

231. Wolf, N. I. & Smeitink, J. A. M. Mitochondrial disorders: a proposal for consensus diagnostic criteria in infants and children. *Neurology* **59,** 1402–1405 (2002).

232. Blass, J. P., Avigan, J. & Uhlendorf, B. W. A defect in pyruvate decarboxylase in a child with an intermittent movement disorder. *Journal of Clinical Investigation* **49,** 423–432 (1970).

233. Engel, A. G. & Angelini, C. Carnitine deficiency of human skeletal muscle with associated lipid storage myopathy: a new syndrome. *Science (New York, N.Y.)* **179,** 899–902 (1973).

234. DiMauro, S. & DiMauro, P. M. Muscle carnitine palmityltransferase deficiency and myoglobinuria. *Science (New York, N.Y.)* **182,** 929–31 (1973).

235. Willems, J. L. *et al.* Leigh's encephalomyelopathy in a patient with cytochrome c oxidase deficiency in muscle tissue. *Pediatrics* **60,** 850–7 (1977).

236. DiMauro, S., Bonilla, E., Zeviani, M., Nakagawa, M. & DeVivo, D. C. Mitochondrial myopathies. *Annals of neurology* **17,** 521–38 (1985).

237. DiMauro, S. Mitochondrial diseases. *Biochimica et biophysica acta* **1658,** 80–8 (2004).

238. DiMauro, S. & Hirano, M. Mitochondrial DNA Deletion Syndromes. (2011).

239. DiMauro, S. & Hirano, M. MELAS. (2013).

240. Sproule, D. M. & Kaufmann, P. Mitochondrial encephalopathy, lactic acidosis, and strokelike episodes: Basic concepts, clinical phenotype, and therapeutic management of MELAS syndrome. *Annals of the New York Academy of Sciences* **1142,** 133–158 (2008).

241. DiMauro, S. & Hirano, M. MERRF. (2015).

242. Mancuso, M. *et al. A novel mitochondrial tRNAPhe mutation causes MERRF syndrome. Neurology* **62,** 2119–2121 (2004).

243. Thorburn, D. R. & Rahman, S. Mitochondrial DNA-Associated Leigh Syndrome and NARP. (2014).

244. Holt, I. J., Harding, A. E., Petty, R. K. & Morgan-Hughes, J. A. *A new mitochondrial disease associated with mitochondrial DNA heteroplasmy. American journal of human genetics* **46,** 428–433 (1990).

245. Vázquez-Memije, M. E. *et al.* Comparative biochemical studies of ATPases in cells from patients with the T8993G or T8993C mitochondrial DNA mutations. *Journal of Inherited Metabolic Disease* **21,** 829–836 (1998).

246. Sadun, A. A., La Morgia, C. & Carelli, V. Leber's Hereditary Optic Neuropathy. *Current treatment options in neurology* **13,** 109–17 (2011).

247. Triepels, R. H., Van Den Heuvel, L. P., Trijbels, J. M. & Smeitink, J. A. Respiratory chain complex I deficiency. *American journal of medical genetics* **106,** 37–45 (2001).

248. Bourgeron, T. *et al. Mutation of a nuclear succinate dehydrogenase gene results in mitochondrial respiratory chain deficiency. Nature genetics* **11,** 144–149 (1995).

249. Lagier-Tourenne, C. *et al.* ADCK3, an Ancestral Kinase, Is Mutated in a Form of Recessive Ataxia Associated with Coenzyme Q10 Deficiency. *American Journal of Human Genetics* **82,** 661–672 (2008).

250. Zhu, Z. *et al.* SURF1, encoding a factor involved in the biogenesis of cytochrome c oxidase, is mutated in Leigh syndrome. *Nature genetics* **20,** 337–43 (1998).

251. Sacconi, S. *et al.* Mutation screening in patients with isolated cytochrome c oxidase deficiency. *Pediatric Research* **53,** 224–230 (2003).

252. Visapää, I. *et al.* GRACILE syndrome, a lethal metabolic disorder with iron overload, is caused by a point mutation in BCS1L. *American journal of human genetics* **71,** 863–876 (2002).

253. De Meirleir, L. *et al. Respiratory chain complex V deficiency due to a mutation in the assembly gene ATP12. Journal of medical genetics* **41,** 120–124 (2004).

254. Hirano, M. *et al.* Defects of intergenomic communication: autosomal disorders that cause multiple deletions and depletion of mitochondrial DNA. *Seminars in cell & developmental biology* **12,** 417–427 (2001).

255. Spinazzola, A. & Zeviani, M. Disorders of nuclear-mitochondrial intergenomic communication. in *Bioscience Reports* **27,** 39–51 (2007).

256. Shoubridge, E. A. Diseases caused by nuclear genes affecting mtDNA stability. *American Journal of Medical Genetics - Seminars in Medical Genetics* **106,** 53–61 (2001).

257. Hirano, M. & DiMauro, S. ANT1, Twinkle, POLG, and TP: new genes open our eyes to ophthalmoplegia. *Neurology* **57,** 2163–5 (2001).

258. Nishino, I., Spinazzola, A. & Hirano, M. Thymidine phosphorylase gene mutations in MNGIE, a human mitochondrial disorder. *Science (New York, N.Y.)* **283,** 689–692 (1999).

259. Kaukonen, J. *et al.* Role of adenine nucleotide translocator 1 in mtDNA maintenance. *Science (New York, N.Y.)* **289,** 782–785 (2000).

260. Van Goethem, G., Dermaut, B., Löfgren, A., Martin, J. J. & Van Broeckhoven, C. Mutation of POLG is associated with progressive external ophthalmoplegia characterized by mtDNA deletions. *Nature genetics* **28,** 211–212 (2001).

261. Spelbrink, J. N. *et al.* Human mitochondrial DNA deletions associated with mutations in the gene encoding Twinkle, a phage T7 gene 4-like protein localized in mitochondria. *Nature genetics* **28,** 223–231 (2001).

262. Saada, A. *et al.* Mutant mitochondrial thymidine kinase in mitochondrial DNA depletion myopathy. *Nature genetics* **29,** 342–344 (2001).

263. Salviati, L. *et al.* Mitochondrial DNA depletion and dGK gene mutations. *Annals of Neurology* **52,** 311–317 (2002).

264. Okamoto, K. *et al.* The protein import motor of mitochondria: A targeted molecular ratchet driving unfolding and translocation. *EMBO Journal* **21,** 3659–3671 (2002).

265. Fenton, W. A. Mitochondrial protein transport--a system in search of mutations. *American journal of human genetics* **57,** 235–8 (1995).

266. Roesch, K., Curran, S. P., Tranebjaerg, L. & Koehler, C. M. Human deafness dystonia syndrome is caused by a defect in assembly of the DDP1/TIMM8a-TIMM13 complex. *Human molecular genetics* **11,** 477–86 (2002).

267. Hansen, J. J. *et al.* Hereditary spastic paraplegia SPG13 is associated with a mutation in the gene encoding the mitochondrial chaperonin Hsp60. *American journal of human genetics* **70,** 1328–1332 (2002).

268. Barth, P. G. *et al.* X-linked cardioskeletal myopathy and neutropenia (Barth syndrome) (MIM 302060). in *Journal of Inherited Metabolic Disease* **22,** 555–567 (1999).

269. Schlame, M. *et al.* Deficiency of tetralinoleoyl-cardiolipin in Barth syndrome. *Annals of Neurology* **51,** 634–637 (2002).

270. Delettre, C. *et al.* Nuclear gene OPA1, encoding a mitochondrial dynamin-related protein, is mutated in dominant optic atrophy. *Nature genetics* **26,** 207–210 (2000).

271. Schon, E. A. & Manfredi, G. Neuronal degeneration and mitochondrial dysfunction. *The Journal of clinical investigation* **111,** 303–12 (2003).

272. Tabrizi, S. J. *Mitochondrial Disorders in Neurology 2*. *Blue Books of Practical Neurology* **26,** (Elsevier, 2002).

273. Beal, M. F. Aging, energy, and oxidative stress in neurodegenerative diseases. *Annals of Neurology* **38,** 357–366 (1995).

274. Chomyn, a *et al.* MELAS mutation in mtDNA binding site for transcription termination factor causes defects in protein synthesis and in respiration but no change in levels of upstream and downstream mature transcripts. *Proceedings of the National Academy of Sciences of the United States of America* **89,** 4221–4225 (1992).

275. Schwartz, M. & Vissing, J. Paternal inheritance of mitochondrial DNA. *The New England journal of medicine* **347,** 576–80 (2002).

276. Viscomi, C., Bottani, E. & Zeviani, M. Emerging concepts in the therapy of mitochondrial disease. *Biochimica et biophysica acta* **1847,** 544–557

277. Giordano, C. *et al.* Efficient mitochondrial biogenesis drives incomplete penetrance in Leber's hereditary optic neuropathy. *Brain* **137,** 335–353 (2014).

278. Bastin, J., Aubey, F., Rötig, A., Munnich, A. & Djouadi, F. Activation of peroxisome proliferator-activated receptor pathway stimulates the mitochondrial respiratory chain and can correct deficiencies in patients' cells lacking its components. *Journal of Clinical Endocrinology and Metabolism* **93,** 1433–1441 (2008).

279. Wenz, T., Diaz, F., Spiegelman, B. M. & Moraes, C. T. Activation of the PPAR/PGC-1alpha pathway prevents a bioenergetic deficit and effectively improves a mitochondrial myopathy phenotype. *Cell metabolism* **8,** 249–56 (2008).

280. Wenz, T., Wang, X., Marini, M. & Moraes, C. T. A metabolic shift induced by a PPAR panagonist markedly reduces the effects of pathogenic mitochondrial tRNA mutations. *Journal of cellular and molecular medicine* **15,** 2317–25 (2011).

281. Noe, N. *et al.* Bezafibrate improves mitochondrial function in the CNS of a mouse model of mitochondrial encephalopathy. *Mitochondrion* **13,** 417–26 (2013).

282. Viscomi, C. *et al.* In vivo correction of COX deficiency by activation of the AMPK/PGC-1α axis. *Cell metabolism* **14,** 80–90 (2011).

283. Golubitzky, A. *et al.* Screening for active small molecules in mitochondrial complex I deficient patient's fibroblasts, reveals AICAR as the most beneficial compound. *PLoS ONE* **6,** (2011).

284. Cerutti, R. *et al.* NAD(+)-dependent activation of Sirt1 corrects the phenotype in a mouse model of mitochondrial disease. *Cell metabolism* **19,** 1042–9 (2014).

285. Khan, N. A. *et al.* Effective treatment of mitochondrial myopathy by nicotinamide riboside, a vitamin B3. *EMBO Molecular Medicine* **6,** 721–731 (2014).

286. Lopes Costa, A. *et al.* Beneficial effects of resveratrol on respiratory chain defects in patients' fibroblasts involve estrogen receptor and estrogen-related receptor alpha signaling. *Human molecular genetics* **23,** 2106–19 (2014).

287. Hofer, A. *et al.* Defining the action spectrum of potential PGC-1α activators on a mitochondrial and cellular level in vivo. *Human molecular genetics* **23,** 2400–15 (2014).

288. Chae, S. *et al.* A systems approach for decoding mitochondrial retrograde signaling pathways. *Science signaling* **6,** rs4 (2013).

289. Jeppesen, T. D. *et al.* Aerobic training is safe and improves exercise capacity in patients with mitochondrial myopathy. *Brain* **129,** 3402–3412 (2006).

290. Wenz, T., Diaz, F., Hernandez, D. & Moraes, C. T. Endurance exercise is protective for mice with mitochondrial myopathy. *Journal of applied physiology (Bethesda, Md. : 1985)* **106,** 1712–1719 (2009).

291. Safdar, A. *et al.* Endurance exercise rescues progeroid aging and induces systemic mitochondrial rejuvenation in mtDNA mutator mice. *Proceedings of the National Academy of Sciences of the United States of America* **108,** 4135–4140 (2011).

292. Viscomi, C. *et al. Combined treatment with oral metronidazole and N-acetylcysteine is effective in ethylmalonic encephalopathy. Nature medicine* **16,** 869–871 (2010).

293. Bratic, A. & Larsson, N. G. The role of mitochondria in aging. *Journal of Clinical Investigation* **123,** 951–957 (2013).

294. Raimundo, N. *et al.* Mitochondrial stress engages E2F1 apoptotic signaling to cause deafness. *Cell* **148,** 716–726 (2012).

295. Chinnery, P., Majamaa, K., Turnbull, D. & Thorburn, D. Treatment for mitochondrial disorders. *Cochrane database of systematic reviews (Online)* CD004426 (2006). doi:10.1007/s11825-012-0347-7

296. Garrido-Maraver, J. *et al.* Coenzyme q10 therapy. *Molecular syndromology* **5,** 187–97 (2014).

297. Nishino, I., Spinazzola, A. & Hirano, M. MNGIE: from nuclear DNA to mitochondrial DNA. *Neuromuscular disorders : NMD* **11,** 7–10 (2001).

298. Taanman, J. W., Muddle, J. R. & Muntau, A. C. Mitochondrial DNA depletion can be prevented by dGMP and dAMP supplementation in a resting culture of deoxyguanosine kinase-deficient fibroblasts. *Human Molecular Genetics* **12,** 1839–1845 (2003).

299. Cámara, Y. *et al.* Administration of deoxyribonucleosides or inhibition of their catabolism as a pharmacological approach for mitochondrial DNA depletion syndrome. *Human Molecular Genetics* **23,** 2459–2467 (2014).

300. Johnson, S. C. *et al.* mTOR inhibition alleviates mitochondrial disease in a mouse model of Leigh syndrome. *Science (New York, N.Y.)* **342,** 1524–8 (2013).

301. Nunnari, J. & Suomalainen, A. Mitochondria: In sickness and in health. *Cell* **148,** 1145–1159 (2012).

302. Santra, S., Gilkerson, R. W., Davidson, M. & Schon, E. A. Ketogenic treatment reduces deleted mitochondrial DNAs in cultured human cells. *Annals of Neurology* **56,** 662–669 (2004).

303. Ahola-Erkkilä, S. *et al.* Ketogenic diet slows down mitochondrial myopathy progression in mice. *Human Molecular Genetics* **19,** 1974–1984 (2010).

304. Schiff, M. *et al.* Mouse studies to shape clinical trials for mitochondrial diseases: High fat diet in Harlequin mice. *PLoS ONE* **6,** (2011).

305. Roe, C. R., Sweetman, L., Roe, D. S., David, F. & Brunengraber, H. Treatment of cardiomyopathy and rhabdomyolysis in long-chain fat oxidation disorders using an anaplerotic odd-chain triglyceride. *Journal of Clinical Investigation* **110,** 259–269 (2002).

306. Watmough, N. J. *et al.* Impaired mitochondrial β-oxidation in a patient with an abnormality of the respiratory chain studies in skeletal muscle mitochondria. *Journal of Clinical Investigation* **85,** 177–184 (1990).

307. Rasola, A. & Bernardi, P. The mitochondrial permeability transition pore and its involvement in cell death and in disease pathogenesis. *Apoptosis* **12,** 815–833 (2007).

308. Merlini, L. *et al.* Cyclosporin A corrects mitochondrial dysfunction and muscle apoptosis in patients with collagen VI myopathies. *Proceedings of the National Academy of Sciences of the United States of America* **105,** 5225–5229 (2008).

309. Mingozzi, F. & High, K. A. Therapeutic in vivo gene transfer for genetic disease using AAV: progress and challenges. *Nature reviews. Genetics* **12,** 341–355 (2011).

310. Gao, G.-P. *et al.* Novel adeno-associated viruses from rhesus monkeys as vectors for human gene therapy. *Proceedings of the National Academy of Sciences of the United States of America* **99,** 11854–11859 (2002).

311. Flierl, A., Chen, Y., Coskun, P. E., Samulski, R. J. & Wallace, D. C. Adeno-associated virus-mediated gene transfer of the heart/muscle adenine nucleotide translocator (ANT) in mouse. *Gene therapy* **12,** 570–8 (2005).

312. Di Meo, I. *et al.* Effective AAV-mediated gene therapy in a mouse model of ethylmalonic encephalopathy. *EMBO Molecular Medicine* **4,** 1008–1014 (2012).

313. Torres-Torronteras, J. *et al.* Gene Therapy Using a Liver-targeted AAV Vector Restores Nucleoside and Nucleotide Homeostasis in a Murine Model of MNGIE. *Molecular therapy : the journal of the American Society of Gene Therapy* 1–7 (2014). doi:10.1038/mt.2014.6

314. Hirano, M. *et al.* Allogeneic stem cell transplantation corrects biochemical derangements in MNGIE. *Neurology* **67,** 1458–1460 (2006).

315. Pañeda, A. *et al.* Effect of adeno-associated virus serotype and genomic structure on liver transduction and biodistribution in mice of both genders. *Human gene therapy* **20,** 908–17 (2009).

316. Bouaita, A. *et al.* Downregulation of apoptosis-inducing factor in Harlequin mice induces progressive and severe optic atrophy which is durably prevented by AAV2-AIF1 gene therapy. *Brain* **135,** 35–52 (2012).

317. Bonnet, C. *et al.* Allotopic mRNA localization to the mitochondrial surface rescues respiratory chain defects in fibroblasts harboring mitochondrial DNA mutations affecting complex I or v subunits. *Rejuvenation research* **10,** 127–144 (2007).

318. Kaltimbacher, V. *et al.* mRNA localization to the mitochondrial surface allows the efficient translocation inside the organelle of a nuclear recoded ATP6 protein. *RNA (New York, N.Y.)* **12,** 1408–1417 (2006).

319. Bonnet, C. *et al.* The optimized allotopic expression of ND1 or ND4 genes restores respiratory chain complex I activity in fibroblasts harboring mutations in these genes. *Biochimica et biophysica acta* **1783,** 1707–17 (2008).

320. Ellouze, S. *et al.* Optimized Allotopic Expression of the Human Mitochondrial ND4 Prevents Blindness in a Rat Model of Mitochondrial Dysfunction. *American Journal of Human Genetics* **83,** 373–387 (2008).

321. Muratovska, A. *et al.* Targeting peptide nucleic acid (PNA) oligomers to mitochondria within cells by conjugation to lipophilic cations: implications for mitochondrial DNA replication, expression and disease. *Nucleic acids research* **29,** 1852–63 (2001).

322. Wang, G. *et al.* PNPASE regulates RNA import into mitochondria. *Cell* **142,** 456–467 (2010).

323. Wang, G. *et al.* Correcting human mitochondrial mutations with targeted RNA import. *Proceedings of the National Academy of Sciences* **109,** 4840–4845 (2012).

324. Bacman, S. R., Williams, S. L., Hernandez, D. & Moraes, C. T. Modulating mtDNA heteroplasmy by mitochondria-targeted restriction endonucleases in a 'differential multiple cleavage-site' model. *Gene therapy* **14,** 1309–1318 (2007).

325. Bacman, S. R., Williams, S. L., Duan, D. & Moraes, C. T. Manipulation of mtDNA heteroplasmy in all striated muscles of newborn mice by AAV9-mediated delivery of a mitochondria-targeted restriction endonuclease. *Gene Therapy* (2011). doi:10.1038/gt.2011.196

326. Srivastava, S. & Moraes, C. T. Manipulating mitochondrial DNA heteroplasmy by a mitochondrially targeted restriction endonuclease. *Human molecular genetics* **10,** 3093–3099 (2001).

327. Gammage, P. A., Rorbach, J., Vincent, A. I., Rebar, E. J. & Minczuk, M. Mitochondrially targeted ZFNs for selective degradation of pathogenic mitochondrial genomes bearing large-scale deletions or point mutations. *EMBO Molecular Medicine* **6,** 458–466 (2014).

328. Bacman, S. R., Williams, S. L., Pinto, M., Peralta, S. & Moraes, C. T. Specific elimination of mutant mitochondrial genomes in patient-derived cells by mitoTALENs. *Nature medicine* **19,** 1111–3 (2013).

329. Tanaka, M. *et al.* Gene therapy for mitochondrial disease by delivering restriction endonuclease SmaI into mitochondria. *Journal of biomedical science* **9,** 534–541 (2002).

330. Bayona-Bafaluy, M. P., Blits, B., Battersby, B. J., Shoubridge, E. A. & Moraes, C. T. Rapid directional shift of mitochondrial DNA heteroplasmy in animal tissues by a mitochondrially targeted restriction endonuclease. *Proceedings of the National Academy of Sciences of the United States of America* **102,** 14392–14397 (2005).

331. Bacman, S. R., Williams, S. L., Garcia, S. & Moraes, C. T. Organ-specific shifts in mtDNA heteroplasmy following systemic delivery of a mitochondria-targeted restriction endonuclease. *Gene therapy* **17,** 713–720 (2010).

332. Kim, Y. G., Cha, J. & Chandrasegaran, S. Hybrid restriction enzymes: zinc finger fusions to Fok I cleavage domain. *Proceedings of the National Academy of Sciences of the United States of America* **93,** 1156–1160 (1996).

333. Smith, J. *et al.* Requirements for double-strand cleavage by chimeric restriction enzymes with zinc finger DNA-recognition domains. *Nucleic acids research* **28,** 3361–3369 (2000).

334. Park, S. G., Schimmel, P. & Kim, S. Aminoacyl tRNA synthetases and their connections to disease. *Proceedings of the National Academy of Sciences of the United States of America* **105,** 11043–11049 (2008).

335. Li, R. & Guan, M.-X. Human mitochondrial leucyl-tRNA synthetase corrects mitochondrial dysfunctions due to the tRNALeu(UUR) A3243G mutation, associated with mitochondrial encephalomyopathy, lactic acidosis, and stroke-like symptoms and diabetes. *Molecular and cellular biology* **30,** 2147–2154 (2010).

336. Rorbach, J. *et al.* Overexpression of human mitochondrial valyl tRNA synthetase can partially restore levels of cognate mt-tRNAVal carrying the pathogenic C25U mutation. *Nucleic Acids Research* **36,** 3065–3074 (2008).

337. Kolesnikova, O. A. *et al.* Nuclear DNA-encoded tRNAs targeted into mitochondria can rescue a mitochondrial DNA mutation associated with the MERRF syndrome in cultured human cells. *Human Molecular Genetics* **13,** 2519–2534 (2004).

338. Comte, C. *et al.* Mitochondrial targeting of recombinant RNAs modulates the level of a heteroplasmic mutation in human mitochondrial DNA associated with Kearns Sayre Syndrome. *Nucleic Acids Research* **41,** 418–433 (2013).

339. Alexander, C. *et al.* OPA1, encoding a dynamin-related GTPase, is mutated in autosomal dominant optic atrophy linked to chromosome 3q28. *Nature genetics* **26,** 211–215 (2000).

340. Züchner, S. *et al.* Mutations in the mitochondrial GTPase mitofusin 2 cause Charcot-Marie-Tooth neuropathy type 2A. *Nature genetics* **36,** 449–451 (2004).

341. Cogliati, S. *et al.* Mitochondrial cristae shape determines respiratory chain supercomplexes assembly and respiratory efficiency. *Cell* **155,** 160–171 (2013).

342. Cassidy-Stone, A. *et al.* Chemical inhibition of the mitochondrial division dynamin reveals its role in Bax/Bak-dependent mitochondrial outer membrane permeabilization. *Developmental cell* **14,** 193–204 (2008).

343. Wang, D. *et al.* A small molecule promotes mitochondrial fusion in mammalian cells. *Angewandte Chemie - International Edition* **51,** 9302–9305 (2012).

344. Perales-Clemente, E. *et al.* Restoration of electron transport without proton pumping in mammalian mitochondria. *Proceedings of the National Academy of Sciences of the United States of America* **105,** 18735–18739 (2008).

345. Dassa, E. P. *et al.* Expression of the alternative oxidase complements cytochrome c oxidase deficiency in human cells. *EMBO molecular medicine* **1,** 30–36 (2009).

346. Hakkaart, G. A. J., Dassa, E. P., Jacobs, H. T. & Rustin, P. Allotopic expression of a mitochondrial alternative oxidase confers cyanide resistance to human cell respiration. *EMBO reports* **7,** 341–345 (2006).

347. Tachibana, M. *et al.* Mitochondrial gene replacement in primate offspring and embryonic stem cells. *Nature* **461,** 367–372 (2009).

348. Israeli, E. Towards germline gene therapy of inherited mitochondrial diseases. *Israel Medical Association Journal* **15,** 255 (2013).

349. Craven, L. *et al.* Pronuclear transfer in human embryos to prevent transmission of mitochondrial DNA disease. *Nature* **465,** 82–85 (2010).

350. Pavlakis, S. G., Phillips, P. C., DiMauro, S., De Vivo, D. C. & Rowland, L. P. *Mitochondrial myopathy, encephalopathy, lactic acidosis, and strokelike episodes: a distinctive clinical syndrome. Annals of neurology* **16,** 481–488 (1984).

351. Holt, I. J., Harding, A. E. & Morgan-Hughes, J. A. Deletions of muscle mitochondrial DNA in patients with mitochondrial myopathies. *Nature* **331,** 717–719 (1988).

352. Wong, L.-J. C. Pathogenic mitochondrial DNA mutations in protein-coding genes. *Muscle & nerve* **36,** 279–293 (2007).

353. Ruiz-Pesini, E. *et al.* An enhanced MITOMAP with a global mtDNA mutational phylogeny. *Nucleic Acids Research* **35,** (2007).

354. Hilton, G. MELAS: a mitochondrial encephalomyopathy syndrome. *The Journal of neuroscience nursing : journal of the American Association of Neuroscience Nurses* **27,** 278–282 (1995).

355. Scaglia, F. & Northrop, J. L. The mitochondrial myopathy encephalopathy, lactic acidosis with stroke-like episodes (MELAS) syndrome: A review of treatment options. *CNS Drugs* **20,** 443–464 (2006).

356. Iizuka, T. *et al.* Regional cerebral blood flow and cerebrovascular reactivity during chronic stage of stroke-like episodes in MELAS - Implication of neurovascular cellular mechanism. *Journal of the Neurological Sciences* **257,** 126–138 (2007).

357. Naini, A. *et al.* Hypocitrullinemia in patients with MELAS: An insight into the 'MELAS paradox'. in *Journal of the Neurological Sciences* **229-230,** 187–193 (2005).

358. El-Hattab, A. W., Emrick, L. T., Chanprasert, S., Craigen, W. J. & Scaglia, F. Mitochondria: Role of citrulline and arginine supplementation in MELAS syndrome. *International Journal of Biochemistry and Cell Biology* **48,** 85–91 (2014).

359. Wu, G. & Morris, S. M. Arginine metabolism: nitric oxide and beyond. *The Biochemical journal* **336 (Pt 1,** 1–17 (1998).

360. El-Hattab, A. W. *et al.* Glucose metabolism derangements in adults with the MELAS m.3243A>G mutation. *Mitochondrion* **18,** 63–9 (2014).

361. Jeppesen, T. D. *et al.* Muscle phenotype and mutation load in 51 persons with the 3243A>G mitochondrial DNA mutation. *Archives of neurology* **63,** 1701–6 (2006).

362. Goto, Y., Nonaka, I. & Horai, S. A mutation in the tRNA(Leu)(UUR) gene associated with the MELAS subgroup of mitochondrial encephalomyopathies. *Nature* **348,** 651–3 (1990).

363. Kobayashi, Y. *et al.* A point mutation in the mitochondrial tRNA(Leu)(UUR) gene in MELAS (mitochondrial myopathy, encephalopathy, lactic acidosis and stroke-like episodes). *Biochemical and biophysical research communications* **173,** 816–22 (1990).

364. Hess, J. F., Parisi, M. A., Bennett, J. L. & Clayton, D. A. Impairment of mitochondrial transcription termination by a point mutation associated with the MELAS subgroup of mitochondrial encephalomyopathies. *Nature* **351,** 236–9 (1991).

365. Flierl, A., Reichmann, H. & Seibel, P. Pathophysiology of the MELAS 3243 transition mutation. *The Journal of biological chemistry* **272,** 27189–96 (1997).

366. Chomyn, A., Enriquez, J. A., Micol, V., Fernandez-Silva, P. & Attardi, G. The mitochondrial myopathy, encephalopathy, lactic acidosis, and stroke-like episode syndrome-associated human mitochondrial tRNALeu(UUR) mutation causes aminoacylation deficiency and concomitant reduced association of mRNA with ribosomes. *Journal of Biological Chemistry* **275,** 19198–209 (2000).

367. Wittenhagen, L. M. & Kelley, S. O. Dimerization of a pathogenic human mitochondrial tRNA. *Nature structural biology* **9,** 586–90 (2002).

368. Kirino, Y. *et al.* Codon-specific translational defect caused by a wobble modification deficiency in mutant tRNA from a human mitochondrial disease. *Proceedings of the National Academy of Sciences of the United States of America* **101,** 15070–5 (2004).

369. Kirino, Y. & Suzuki, T. Human mitochondrial diseases associated with tRNA wobble modification deficiency. *RNA biology* **2,** 41–4 (2005).

370. Kirby, D. M. *et al.* Mutations of the mitochondrial ND1 gene as a cause of MELAS. *Journal of medical genetics* **41,** 784–789 (2004).

371. James, A. M., Wei, Y. H., Pang, C. Y. & Murphy, M. P. Altered mitochondrial function in fibroblasts containing MELAS or MERRF mitochondrial DNA mutations. *The Biochemical journal* **318 (Pt 2,** 401–407 (1996).

372. Wong, E. & Cuervo, A. M. Autophagy gone awry in neurodegenerative diseases. *Nature neuroscience* **13,** 805–811 (2010).

373. Cheldi, A. *et al.* POLG1 mutations and stroke like episodes: a distinct clinical entity rather than an atypical MELAS syndrome. *BMC neurology* **13,** 8 (2013).

374. Yatsuga, S. *et al.* MELAS: A nationwide prospective cohort study of 96 patients in Japan. *Biochimica et Biophysica Acta - General Subjects* **1820,** 619–624 (2012).

375. Uusimaa, J. *et al.* Prevalence, segregation, and phenotype of the mitochondrial DNA 3243A>G mutation in children. *Annals of neurology* **62,** 278–87 (2007).

376. Chinnery, P. F. & Turnbull, D. M. Epidemiology and treatment of mitochondrial disorders. *American journal of medical genetics* **106,** 94–101 (2001).

377. Neargarder, S. A., Murtagh, M. P., Wong, B. & Hill, E. K. *The neuropsychologic deficits of MELAS: evidence of global impairment. Cognitive and behavioral neurology : official journal of the Society for Behavioral and Cognitive Neurology* **20,** 83–92 (2007).

378. Hirano, M. & Pavlakis, S. G. Mitochondrial myopathy, encephalopathy, lactic acidosis, and strokelike episodes (MELAS): current concepts. *Journal of child neurology* **9,** 4–13 (1994).

379. Hirano, M. *et al. Melas: an original case and clinical criteria for diagnosis. Neuromuscular disorders : NMD* **2,** 125–135 (1992).

380. Thambisetty, M., Newman, N. J., Glass, J. D. & Frankel, M. R. A practical approach to the diagnosis and management of MELAS: case report and review. *The neurologist* **8,** 302–12 (2002).

381. Kuwabara, T. *et al.* Mitochondrial encephalomyopathy: elevated visual cortex lactate unresponsive to photic stimulation--a localized 1H-MRS study. *Neurology* **44,** 557–559 (1994).

382. Kaufmann, P. *et al.* Cerebral lactic acidosis correlates with neurological impairment in MELAS. *Neurology* **62,** 1297–302 (2004).

383. Lin, D. D. M., Crawford, T. O. & Barker, P. B. Proton MR spectroscopy in the diagnostic evaluation of suspected mitochondrial disease. *AJNR. American journal of neuroradiology* **24,** 33–41 (2003).

384. El-Hattab, A. W., Adesina, A. M., Jones, J. & Scaglia, F. MELAS syndrome: Clinical manifestations, pathogenesis, and treatment options. *Molecular genetics and metabolism* (2015). doi:10.1016/j.ymgme.2015.06.004

385. Santa, K. M. Treatment options for mitochondrial myopathy, encephalopathy, lactic acidosis, and stroke-like episodes (MELAS) syndrome. *Pharmacotherapy* **30,** 1179–1196 (2010).

386. Shanske, S. *et al.* Varying loads of the mitochondrial DNA A3243G mutation in different tissues: implications for diagnosis. *American journal of medical genetics. Part A* **130A,** 134–7 (2004).

387. Mancuso, M. *et al.* A non-syndromic hearing loss caused by very low levels of the mtDNA A3243G mutation. *Acta Neurologica Scandinavica* **110,** 72–74 (2004).

388. Tatuch, Y. *et al. Heteroplasmic mtDNA mutation (T----G) at 8993 can cause Leigh disease when the percentage of abnormal mtDNA is high. American journal of human genetics* **50,** 852–858 (1992).

389. Hancock, D. K., Schwarz, F. P., Song, F., Wong, L. J. C. & Levin, B. C. Design and use of a peptide nucleic acid for detection of the heteroplasmic low-frequency mitochondrial encephalomyopathy, lactic acidosis, and stroke-like episodes (MELAS) mutation in human mitochondrial DNA. *Clinical Chemistry* **48,** 2155–2163 (2002).

390. Wong, L. J. & Senadheera, D. Direct detection of multiple point mutations in mitochondrial DNA. *Clinical chemistry* **43,** 1857–61 (1997).

391. Bai, R. K. & Wong, L. J. C. Detection and quantification of heteroplasmic mutant mitochondrial DNA by real-time amplification refractory mutation system quantitative PCR analysis: A single-step approach. *Clinical Chemistry* **50,** 996–1001 (2004).

392. Gigarel, N. *et al.* Single cell quantification of the 8993T>G NARP mitochondrial DNA mutation by fluorescent PCR. *Molecular genetics and metabolism* **84,** 289–92 (2005).

393. White, H. E. *et al.* Accurate detection and quantitation of heteroplasmic mitochondrial point mutations by pyrosequencing. *Genetic testing* **9,** 190–199 (2005).

394. Reiner, J. E. *et al.* Detection of heteroplasmic mitochondrial DNA in single mitochondria. *PloS one* **5,** e14359 (2010).

395. Strand, H., Ingebretsen, O. C. & Nilssen, Ø. Real-time detection and quantification of mitochondrial mutations with oligonucleotide primers containing locked nucleic acid. *Clinica Chimica Acta* **390,** 126–133 (2008).

396. Fan, H. *et al.* Detection of common disease-causing mutations in mitochondrial DNA (mitochondrial encephalomyopathy, lactic acidosis with stroke-like episodes MTTL1 3243 A>G and myoclonic epilepsy associated with ragged-red fibers MTTK 8344A>G) by real-time polymerase ch. *The Journal of molecular diagnostics : JMD* **8,** 277–81 (2006).

397. Montagna, P. *et al. MELAS syndrome: characteristic migrainous and epileptic features and maternal transmission. Neurology* **38,** 751–754 (1988).

398. Ohno, K., Isotani, E. & Hirakawa, K. MELAS presenting as migraine complicated by stroke: case report. *Neuroradiology* **39,** 781–4 (1997).

399. Kärppä, M., Syrjälä, P., Tolonen, U. & Majamaa, K. Peripheral neuropathy in patients with the 3243A>G mutation in mitochondrial DNA. *Journal of neurology* **250,** 216–21 (2003).

400. Anglin, R. E., Garside, S. L., Tarnopolsky, M. A., Mazurek, M. F. & Rosebush, P. I. The psychiatric manifestations of mitochondrial disorders: a case and review of the literature. *The Journal of clinical psychiatry* **73,** 506–12 (2012).

401. Sproule, D. M. *et al.* Wolff-Parkinson-White syndrome in Patients With MELAS. *Archives of neurology* **64,** 1625–1627 (2007).

402. Fujii, A. *et al.* Gastric dysmotility associated with accumulation of mitochondrial A3243G mutation in the stomach. *Internal medicine (Tokyo, Japan)* **43,** 1126–1130 (2004).

403. Maassen, J. A. *et al.* Mitochondrial Diabetes: Molecular Mechanisms and Clinical Presentation. *Diabetes* **53,** 103S–109 (2004).

404. Yorifuji, T. *et al.* Nephropathy and growth hormone deficiency in a patient with mitochondrial tRNA(Leu(UUR)) mutation. *Journal of medical genetics* **33,** 621–2 (1996).

405. Balestri, P. & Grosso, S. *Endocrine disorders in two sisters affected by MELAS syndrome. Journal of child neurology* **15,** 755–758 (2000).

406. Hotta, O. *et al.* Clinical and pathologic features of focal segmental glomerulosclerosis with mitochondrial tRNALeu(UUR) gene mutation. *Kidney International* **59,** 1236–1243 (2001).

407. Barclay, A. R. *et al. Pulmonary hypertension--a new manifestation of mitochondrial disease. Journal of inherited metabolic disease* **28,** 1081–1089 (2005).

408. Sproule, D. M. *et al.* Pulmonary artery hypertension in a child with MELAS due to a point mutation of the mitochondrial tRNA((Leu)) gene (m.3243A>G). *Journal of inherited metabolic disease* **31 Suppl 3,** 497–503 (2008).

409. Karvonen, S. L. *et al.* Increased prevalence of vitiligo, but no evidence of premature ageing, in the skin of patients with bp 3243 mutation in mitochondrial DNA in the mitochondrial encephalomyopathy, lactic acidosis and stroke-like episodes syndrome (MELAS). *The British journal of dermatology* **140,** 634–9 (1999).

410. Kubota, Y., Ishii, T., Sugihara, H., Goto, Y. & Mizoguchi, M. Skin manifestations of a patient with mitochondrial encephalomyopathy with lactic acidosis and strokelike episodes (MELAS syndrome). *Journal of the American Academy of Dermatology* **41,** 469–73 (1999).

411. Finsterer, J. Chronic anemia as a manifestation of MELAS syndrome. *Revista de investigación clínica; organo del Hospital de Enfermedades de la Nutrición* **63,** 100–3

412. FESTENSTEIN, G. N., HEATON, F. W., LOWE, J. S. & MORTON, R. A. A constituent of the unsaponifiable portion of animal tissue lipids (lambda max. 272 m mu). *The Biochemical journal* **59,** 558–66 (1955).

413. CRANE, F. L., HATEFI, Y., LESTER, R. L. & WIDMER, C. Isolation of a quinone from beef heart mitochondria. *Biochimica et biophysica acta* **25,** 220–1 (1957).

414. Quinzii, C. M. & Hirano, M. Coenzyme Q and mitochondrial disease. *Dev Disabil Res Rev* **16,** 183–188 (2010).

415. Turunen, M., Olsson, J. & Dallner, G. Metabolism and function of coenzyme Q. *Biochimica et Biophysica Acta (BBA) - Biomembranes* **1660,** 171–199 (2004).

416. Sena, C. M. *et al.* Supplementation of coenzyme Q10 and alpha-tocopherol lowers glycated hemoglobin level and lipid peroxidation in pancreas of diabetic rats. *Nutrition research (New York, N.Y.)* **28,** 113–21 (2008).

417. Crane, F. L. Biochemical functions of coenzyme Q10. *Journal of the American College of Nutrition* **20,** 591–8 (2001).

418. Armstrong, J. S., Whiteman, M., Rose, P. & Jones, D. P. The Coenzyme Q10 analog decylubiquinone inhibits the redox-activated mitochondrial permeability transition: role of mitcohondrial [correction mitochondrial] complex III. *The Journal of biological chemistry* **278,** 49079–49084 (2003).

419. Groneberg, D. A. *et al.* Coenzyme Q10 affects expression of genes involved in cell signalling, metabolism and transport in human CaCo-2 cells. *The international journal of biochemistry & cell biology* **37,** 1208–1218 (2005).

420. Santos-González, M., Gómez Díaz, C., Navas, P. & Villalba, J. M. Modifications of plasma proteome in long-lived rats fed on a coenzyme Q10-supplemented diet. *Experimental Gerontology* **42,** 798–806 (2007).

421. Tran, U. C. & Clarke, C. F. Endogenous synthesis of coenzyme Q in eukaryotes. *Mitochondrion* **7,** (2007).

422. Bentinger, M., Tekle, M. & Dallner, G. Coenzyme Q--biosynthesis and functions. *Biochemical and biophysical research communications* **396,** 74–9 (2010).

423. Papucci, L. *et al.* Coenzyme q10 prevents apoptosis by inhibiting mitochondrial depolarization independently of its free radical scavenging property. *The Journal of biological chemistry* **278,** 28220–8 (2003).

424. Quinzii, C. *et al.* A mutation in para-hydroxybenzoate-polyprenyl transferase (COQ2) causes primary coenzyme Q10 deficiency. *American journal of human genetics* **78,** 345–349 (2006).

425. López-Martín, J. M. *et al.* Missense mutation of the COQ2 gene causes defects of bioenergetics and de novo pyrimidine synthesis. *Human Molecular Genetics* **16,** 1091–1097 (2007).

426. Quinzii, C. M., Hirano, M. & DiMauro, S. CoQ10 deficiency diseases in adults. *Mitochondrion* **7,** (2007).

427. Mollet, J. *et al.* Prenyldiphosphate synthase, subunit 1 (PDSS1) and OH-benzoate polyprenyltransferase (COQ2) mutations in ubiquinone deficiency and oxidative phosphorylation disorders. *Journal of Clinical Investigation* **117,** 765–772 (2007).

428. Balreira, A. *et al.* ANO10 mutations cause ataxia and coenzyme Q_{10} deficiency. *Journal of neurology* **261,** 2192–8 (2014).

429. Miyamae, T. *et al.* Increased oxidative stress and coenzyme Q10 deficiency in juvenile fibromyalgia: amelioration of hypercholesterolemia and fatigue by ubiquinol-10 supplementation. *Redox report : communications in free radical research* **18,** 12–9 (2013).

430. Chen, R. S., Huang, C. C. & Chu, N. S. *Coenzyme Q10 treatment in mitochondrial encephalomyopathies. Short-term double-blind, crossover study. European neurology* **37,** (1997).

431. E.I., G. *et al.* A randomized trial of coenzyme Q10 in mitochondrial disorders. *Muscle and Nerve* **42,** 739–748 (2010).

432. Marriage, B., Clandinin, M. T. & Glerum, D. M. Nutritional cofactor treatment in mitochondrial disorders. *Journal of the American Dietetic Association* **103,** 1029–1038 (2003).

433. Schmelzer, C. *et al.* Functions of coenzyme Q10 in inflammation and gene expression. *BioFactors (Oxford, England)* **32,** 179–183 (2008).

434. Cordero, M. D. *et al.* Can coenzyme q10 improve clinical and molecular parameters in fibromyalgia? *Antioxidants & redox signaling* **19,** 1356–61 (2013).

435. Wu, Y.-T., Wu, S.-B. & Wei, Y.-H. Metabolic reprogramming of human cells in response to oxidative stress: implications in the pathophysiology and therapy of mitochondrial diseases. *Current pharmaceutical design* **20,** 5510–26 (2014).

436. Abadi, A. *et al.* Supplementation with α-Lipoic Acid, CoQ10, and Vitamin E Augments Running Performance and Mitochondrial Function in Female Mice. *PLoS ONE* **8,** (2013).

437. Lee, S. K. *et al.* Coenzyme Q10 increases the fatty acid oxidation through AMPK-mediated PPARα induction in 3T3-L1 preadipocytes. *Cellular Signalling* **24,** 2329–2336 (2012).

438. Tsai, K. L. *et al.* Coenzyme Q10 suppresses oxLDL-induced endothelial oxidative injuries by the modulation of LOX-1-mediated ROS generation via the AMPK/PKC/NADPH oxidase signaling pathway. *Molecular Nutrition and Food Research* **55,** (2011).

439. Matthews, P. M. *et al.* Coenzyme Q10 with multiple vitamins is generally ineffective in treatment of mitochondrial disease. *Neurology* **43,** 884–890 (1993).

440. Hargreaves, I. P., Duncan, A. J., Heales, S. J. R. & Land, J. M. The effect of HMG-CoA reductase inhibitors on coenzyme Q10: possible biochemical/clinical implications. *Drug safety* **28,** 659–76 (2005).

441. Matthews, R. T., Yang, L., Browne, S., Baik, M. & Beal, M. F. Coenzyme Q10 administration increases brain mitochondrial concentrations and exerts neuroprotective effects. *Proceedings of the National Academy of Sciences of the United States of America* **95,** 8892–7 (1998).

442. Napolitano, A. *et al. Long-term treatment with idebenone and riboflavin in a patient with MELAS. Neurological sciences : official journal of the Italian Neurological Society and of the Italian Society of Clinical Neurophysiology* **21,** S981–S982 (2000).

443. Lekoubou, A. *et al.* Effect of long-term oral treatment with L-arginine and idebenone on the prevention of stroke-like episodes in an adult MELAS patient. *Revue Neurologique* **167,** 852–855 (2011).

444. Depeint, F., Bruce, W. R., Shangari, N., Mehta, R. & O'Brien, P. J. Mitochondrial function and toxicity: Role of the B vitamin family on mitochondrial energy metabolism. *Chemico-Biological Interactions* **163,** 94–112 (2006).

445. Halliwell, B. Antioxidants in human health and disease. *Annual review of nutrition* **16,** 33–50 (1996).

446. Longnus, S. L., Wambolt, R. B., Parsons, H. L., Brownsey, R. W. & Allard, M. F. 5-Aminoimidazole-4-carboxamide 1-beta -D-ribofuranoside (AICAR) stimulates myocardial glycogenolysis by allosteric mechanisms. *American journal of physiology. Regulatory, integrative and comparative physiology* **284,** R936–44 (2003).

447. Drake, J. C., Alway, S. E., Hollander, J. M. & Williamson, D. L. AICAR treatment for 14 days normalizes obesity-induced dysregulation of TORC1 signaling and translational capacity in fasted skeletal muscle. *American journal of physiology. Regulatory, integrative and comparative physiology* **299,** R1546–R1554 (2010).

448. Towler, M. C. & Hardie, D. G. AMP-activated protein kinase in metabolic control and insulin signaling. *Circulation Research* **100,** 328–341 (2007).

449. Sabina, R. L., Patterson, D. & Holmes, E. W. 5-Amino-4-imidazolecarboxamide riboside (Z-riboside) metabolism in eukaryotic cells. *Journal of Biological Chemistry* **260,** 6107–6114 (1985).

450. Jin, X., Townley, R. & Shapiro, L. Structural Insight into AMPK Regulation: ADP Comes into Play. *Structure* **15,** 1285–1295 (2007).

451. Hayashi, T. *et al.* Metabolic stress and altered glucose transport: activation of AMP-activated protein kinase as a unifying coupling mechanism. *Diabetes* **49,** 527–531 (2000).

452. Vincent, M. F., Erion, M. D., Gruber, H. E. & Van den Berghe, G. Hypoglycaemic effect of AICAriboside in mice. *Diabetologia* **39,** 1148–1155 (1996).

453. Pokrywka, A. *et al.* Metabolic modulators of the exercise response: doping control analysis of an agonist of the peroxisome proliferator-activated receptor δ (GW501516) and 5-aminoimidazole-4-carboxamide ribonucleotide (AICAR). *Journal of physiology and pharmacology : an official journal of the Polish Physiological Society* **65,** 469–76 (2014).

454. Koga, Y. *et al. L-arginine improves the symptoms of strokelike episodes in MELAS. Neurology* **64,** (2005).

455. Koga, Y. *et al.* MELAS and l-arginine therapy. *Mitochondrion* **7,** 133–139 (2007).

456. El-Hattab, A. W. *et al.* Restoration of impaired nitric oxide production in MELAS syndrome with citrulline and arginine supplementation. *Molecular Genetics and Metabolism* **105,** 607–614 (2012).

457. Tarnopolsky, M. A., Roy, B. D. & MacDonald, U. R. A randomized, controlled trial of creatine monohydrate in patients with mitochondrial cytopathies. *Muscle and Nerve* **20,** 1502–1509 (1997).

458. Rodriguez, M. C. *et al.* Beneficial effects of creatine, CoQ10, and lipoic acid in mitochondrial disorders. *Muscle and Nerve* **35,** 235–242 (2007).

459. Scarpelli, M. *et al.* Mitochondrial Sensorineural Hearing Loss: A Retrospective Study and a Description of Cochlear Implantation in a MELAS Patient. *Genetics research international* **2012,** 287432 (2012).

460. Taivassalo, T. & Haller, R. G. Implications of exercise training in mtDNA defects--use it or lose it? *Biochimica et biophysica acta* **1659,** 221–231 (2004).

461. King, M. P. & Attardi, G. Human cells lacking mtDNA: repopulation with exogenous mitochondria by complementation. *Science (New York, N.Y.)* **246,** 500–503 (1989).

462. Rustin, P. *et al.* Biochemical and molecular investigations in respiratory chain deficiencies. in *Clinica Chimica Acta* **228,** 35–51 (1994).

463. Spinazzi, M., Casarin, A., Pertegato, V., Salviati, L. & Angelini, C. Assessment of mitochondrial respiratory chain enzymatic activities on tissues and cultured cells. *Nature Protocols* **7,** 1235–1246 (2012).

464. Bradford, M. M. A rapid and sensitive method for the quantitation of microgram quantities of protein utilizing the principle of protein-dye binding. *Analytical biochemistry* **72,** 248–254 (1976).

465. Erbrich, U., Naujok, A., Petschel, K. & Zimmermann, H. W. The fluorescent staining of mitochondria in living HeLa- and LM-cells with new acridine dyes (author's transl). *Histochemistry* **74,** 1–7 (1982).

466. Jacobson, J., Duchen, M. R. & Heales, S. J. R. Intracellular distribution of the fluorescent dye nonyl acridine orange responds to the mitochondrial membrane potential: Implications for assays of cardiolipin and mitochondrial mass. *Journal of Neurochemistry* **82,** 224–233 (2002).

467. Trounce, I. A., Kim, Y. L., Jun, A. S. & Wallace, D. C. Assessment of mitochondrial oxidative phosphorylation in patient muscle biopsies, lymphoblasts, and transmitochondrial cell lines. *Methods in enzymology* **264,** 484–509 (1996).

468. James, A. M., Sheard, P. W., Wei, Y. H. & Murphy, M. P. Decreased ATP synthesis is phenotypically expressed during increased energy demand in fibroblasts containing mitochondrial tRNA mutations. *European journal of biochemistry / FEBS* **259,** 462–9 (1999).

469. Gajewski, C. D., Yang, L., Schon, E. A. & Manfredi, G. New insights into the bioenergetics of mitochondrial disorders using intracellular ATP reporters. *Molecular biology of the cell* **14,** 3628–35 (2003).

470. Byrne, E. Biochemical defects in mitochondrial cytopathies: a new classification. *Australian paediatric journal* **24 Suppl 1,** 58–61 (1988).

471. Yoneda, M. *et al. Pleiotropic molecular defects in energy-transducing complexes in mitochondrial encephalomyopathy (MELAS). Journal of the neurological sciences* **92,** 143–158 (1989).

472. Muller-Hocker, J. *et al.* Generalized mitochondrial microangiopathy and vascular cytochrome c oxidase deficiency: Occurrence in a case of MELAS syndrome with mitochondrial cardiomyopathy-myopathy and combined complex I/IV deficiency. *Archives of Pathology and Laboratory Medicine* **117,** 202–210 (1993).

473. Davidson, M. M., Walker, W. F., Hernandez-Rosa, E. & Nesti, C. Evidence for nuclear modifier gene in mitochondrial cardiomyopathy. *Journal of Molecular and Cellular Cardiology* **46,** 936–942 (2009).

474. Janssen, A. J. M. *et al.* Muscle 3243A???G mutation load and capacity of the mitochondrial energy-generating system. *Annals of Neurology* **63,** 473–481 (2008).

475. Zhang, J. & Ney, P. A. Reticulocyte mitophagy: Monitoring mitochondrial clearance in a mammalian model. *Autophagy* **6,** 405–408 (2010).

476. Kim, I. & Lemasters, J. J. Mitophagy selectively degrades individual damaged mitochondria after photoirradiation. *Antioxidants & redox signaling* **14,** 1919–1928 (2011).

477. Youle, R. J. & Narendra, D. P. Mechanisms of mitophagy. *Nature reviews. Molecular cell biology* **12,** 9–14 (2011).

478. Asencio, C. *et al.* Severe encephalopathy associated to pyruvate dehydrogenase mutations and unbalanced coenzyme Q10 content. *European journal of human genetics : EJHG* (2015). doi:10.1038/ejhg.2015.112

479. Nisoli, E., Clementi, E., Moncada, S. & Carruba, M. O. Mitochondrial biogenesis as a cellular signaling framework. *Biochemical Pharmacology* **67,** 1–15 (2004).

480. Garrabou, G. *et al.* Reversible inhibition of mitochondrial protein synthesis during linezolid-related hyperlactatemia. *Antimicrobial Agents and Chemotherapy* **51,** 962–967 (2007).

481. Wu, Z., Puigserver, P. & Spiegelman, B. M. Transcriptional activation of adipogenesis. *Current Opinion in Cell Biology* **11,** 689–694 (1999).

482. Zong, H. *et al.* AMP kinase is required for mitochondrial biogenesis in skeletal muscle in response to chronic energy deprivation. *Proceedings of the National Academy of Sciences of the United States of America* **99,** 15983–15987 (2002).

483. Sano, M. *et al.* Intramolecular control of protein stability, subnuclear compartmentalization, and coactivator function of peroxisome proliferator-activated receptor γ coactivator 1α. *Journal of Biological Chemistry* **282,** 25970–25980 (2007).

484. Li, X., Monks, B., Ge, Q. & Birnbaum, M. J. Akt/PKB regulates hepatic metabolism by directly inhibiting PGC-1alpha transcription coactivator. *Nature* **447,** 1012–1016 (2007).

485. Rodgers, J. T., Haas, W., Gygi, S. P. & Puigserver, P. Cdc2-like Kinase 2 Is an Insulin-Regulated Suppressor of Hepatic Gluconeogenesis. *Cell Metabolism* **11,** 23–34 (2010).

486. Anderson, R. M. *et al.* Dynamic regulation of PGC-1α localization and turnover implicates mitochondrial adaptation in calorie restriction and the stress response. *Aging Cell* **7,** 101–111 (2008).

487. Lerin, C. *et al.* GCN5 acetyltransferase complex controls glucose metabolism through transcriptional repression of PGC-1alpha. *Cell metabolism* **3,** 429–38 (2006).

488. Houtkooper, R. H., Cantó, C., Wanders, R. J. & Auwerx, J. The secret life of NAD+: An old metabolite controlling new metabolic signaling pathways. *Endocrine Reviews* **31,** 194–223 (2010).

489. Fernandez-Marcos, P. & Auwerx, J. Regulation of PGC-1a , a nodal regulator of mitochondrial biogenesis. *The American journal of clinical ...* **93,** 884–890 (2011).

490. Morita, M. *et al.* MTORC1 controls mitochondrial activity and biogenesis through 4E-BP-dependent translational regulation. *Cell Metabolism* **18,** 698–711 (2013).

491. Cunningham, J. T. *et al.* mTOR controls mitochondrial oxidative function through a YY1-PGC-1alpha transcriptional complex. *Nature* **450,** 736–740 (2007).

492. Shin, J. H. *et al.* PARIS (ZNF746) repression of PGC-1α contributes to neurodegeneration in parkinson's disease. *Cell* **144,** 689–702 (2011).

493. Yamamoto, H. *et al.* NCoR1 is a conserved physiological modulator of muscle mass and oxidative function. *Cell* **147,** 827–839 (2011).

494. Tangeman, L., Wyatt, C. N. & Brown, T. L. Knockdown of AMP-activated protein kinase alpha 1 and alpha 2 catalytic subunits. *Journal of RNAi and gene silencing : an international journal of RNA and gene targeting research* **8,** 470–8 (2012).

495. Hawley, S. A. *et al.* Characterization of the AMP-activated protein kinase kinase from rat liver and identification of threonine 172 as the major site at which it phosphorylates AMP-activated protein kinase. *Journal of Biological Chemistry* **271,** 27879–27887 (1996).

496. Bakala, H., Hamelin, M., Mary, J., Borot-Laloi, C. & Friguet, B. Catalase, a target of glycation damage in rat liver mitochondria with aging. *Biochimica et Biophysica Acta - Molecular Basis of Disease* **1822,** 1527–1534 (2012).

497. Zelko, I. N., Mariani, T. J. & Folz, R. J. Superoxide dismutase multigene family: A comparison of the CuZn-SOD (SOD1), Mn-SOD (SOD2), and EC-SOD (SOD3) gene structures, evolution, and expression. *Free Radical Biology and Medicine* **33,** 337–349 (2002).

498. Yun, H. *et al.* AMP-activated protein kinase mediates the antioxidant effects of resveratrol through regulation of the transcription factor FoxO1. *The FEBS journal* **281,** 4421–38 (2014).

499. Sanchez, A. M. J. *et al.* AMPK promotes skeletal muscle autophagy through activation of forkhead FoxO3a and interaction with Ulk1. *Journal of Cellular Biochemistry* **113,** 695–710 (2012).

500. Levine, B. & Kroemer, G. Autophagy in the Pathogenesis of Disease. *Cell* **132,** 27–42 (2008).

501. Egan, D., Kim, J., Shaw, R. J. & Guan, K. L. The autophagy initiating kinase ULK1 is regulated via opposing phosphorylation by AMPK and mTOR. *Autophagy* **7,** 643–644 (2011).

502. Tadaishi, M. *et al.* Effect of exercise intensity and AICAR on isoform-specific expressions of murine skeletal muscle PGC-1{alpha} mRNA: a role of {beta}2-adrenergic receptor activation. *American journal of physiology. Endocrinology and metabolism* **300,** E341–9 (2011).

503. Lamperti, C. *et al.* MELAS-like encephalomyopathy caused by a new pathogenic mutation in the mitochondrial DNA encoded cytochrome c oxidase subunit I. *Neuromuscular Disorders* **22,** 990–994 (2012).

504. McKenzie, M. *et al.* Mitochondrial ND5 gene variation associated with encephalomyopathy and mitochondrial ATP consumption. *Journal of Biological Chemistry* **282,** 36845–36852 (2007).

505. Koga, Y., Davidson, M., Schon, E. A. & King, M. P. Analysis of cybrids harboring MELAS mutations in the mitochondrial tRNA(Leu(UUR)) gene. in *Muscle and Nerve* **18,** (1995).

506. Picard, M. *et al.* Progressive increase in mtDNA 3243A>G heteroplasmy causes abrupt transcriptional reprogramming. *Proceedings of the National Academy of Sciences of the United States of America* **111,** E4033–42 (2014).

507. Feuermann, M. *et al.* The yeast counterparts of human 'MELAS' mutations cause mitochondrial dysfunction that can be rescued by overexpression of the mitochondrial translation factor EF-Tu. *EMBO reports* **4,** 53–58 (2003).

508. Montanari, A. *et al.* Yeast as a model of human mitochondrial tRNA base substitutions: investigation of the molecular basis of respiratory defects. *Rna* **14,** 275–283 (2008).

509. Ernster, L. & Dallner, G. Biochemical, physiological and medical aspects of ubiquinone function. in *Biochimica et Biophysica Acta - Molecular Basis of Disease* **1271,** 195–204 (1995).

510. Mileykovskaya, E. & Dowhan, W. Cardiolipin-dependent formation of mitochondrial respiratory supercomplexes. *Chemistry and Physics of Lipids* **179,** 42–48 (2014).

511. Pfeiffer, K. *et al.* Cardiolipin Stabilizes Respiratory Chain Supercomplexes. *Journal of Biological Chemistry* **278,** 52873–52880 (2003).

512. Chen, Y. C. *et al.* Identification of a protein mediating respiratory supercomplex stability. *Cell Metabolism* **15,** 348–360 (2012).

513. Brandner, K. *et al.* Taz1, an outer mitochondrial membrane protein, affects stability and assembly of inner membrane protein complexes: implications for Barth Syndrome. *Molecular biology of the cell* **16,** 5202–5214 (2005).

514. Palikaras, K. & Tavernarakis, N. Mitochondrial homeostasis: The interplay between mitophagy and mitochondrial biogenesis. *Experimental Gerontology* **56,** 182–188 (2014).

515. Rossmanith, W. *et al. Isolated cytochrome c oxidase deficiency as a cause of MELAS. Journal of medical genetics* **45,** 117–121 (2008).

516. Pessina, S. *et al.* Snf1/AMPK promotes S-phase entrance by controlling CLB5 transcription in budding yeast. *Cell Cycle* **9,** 2189–2200 (2010).

517. Hardie, D. G. The AMP-activated protein kinase pathway--new players upstream and downstream. *Journal of cell science* **117,** 5479–5487 (2004).

518. Mackenzie, R. M. *et al.* Mitochondrial reactive oxygen species enhance AMP-activated protein kinase activation in the endothelium of patients with coronary artery disease and diabetes. *Clinical science (London, England : 1979)* **124,** 403–11 (2013).

519. Wu, S.-B. & Wei, Y.-H. AMPK-mediated increase of glycolysis as an adaptive response to oxidative stress in human cells: implication of the cell survival in mitochondrial diseases. *Biochimica et biophysica acta* **1822,** 233–47 (2012).

520. Salminen, A. & Kaarniranta, K. AMP-activated protein kinase (AMPK) controls the aging process via an integrated signaling network. *Ageing Research Reviews* **11,** 230–241 (2012).

521. Alcocer-Gómez, E. *et al.* Metformin and caloric restriction induce an AMPK-dependent restoration of mitochondrial dysfunction in fibroblasts from Fibromyalgia patients. *Biochimica et biophysica acta* **1852,** 1257–67 (2015).

522. Wu, S.-B., Wu, Y.-T., Wu, T.-P. & Wei, Y.-H. Role of AMPK-mediated adaptive responses in human cells with mitochondrial dysfunction to oxidative stress. *Biochimica et biophysica acta* **1840,** 1331–44 (2014).

523. Chen, H. & Chan, D. C. Emerging functions of mammalian mitochondrial fusion and fission. *Human Molecular Genetics* **14,** (2005).

524. Detmer, S. A. & Chan, D. C. Functions and dysfunctions of mitochondrial dynamics. *Nature reviews. Molecular cell biology* **8,** 870–879 (2007).

525. Hoppins, S., Lackner, L. & Nunnari, J. The machines that divide and fuse mitochondria. *Annual review of biochemistry* **76,** 751–780 (2007).

526. Garcia-Roves, P. M., Osler, M. E., Holmström, M. H. & Zierath, J. R. Gain-of-function R225Q mutation in AMP-activated protein kinase γ3 subunit increases mitochondrial biogenesis in glycolytic skeletal muscle. *Journal of Biological Chemistry* **283,** 35724–35734 (2008).

527. Meijer, A. J. & Codogno, P. Autophagy: Regulation by energy sensing. *Current Biology* **21,** (2011).

528. Wolf, D. E. *et al.* Coenzyme Q. I. Structure Studies on the Coenzyme Q Group. *Journal of the American Chemical Society* **80,** 4752–4752 (1958).

529. Dröge, W. Free radicals in the physiological control of cell function. *Physiological reviews* **82,** 47–95 (2002).

530. Valko, M. *et al.* Free radicals and antioxidants in normal physiological functions and human disease. *The international journal of biochemistry & cell biology* **39,** 44–84 (2007).

531. Cardaci, S., Filomeni, G. & Ciriolo, M. R. Redox implications of AMPK-mediated signal transduction beyond energetic clues. *Journal of Cell Science* **125,** 2115–2125 (2012).

532. Zmijewski, J. W. *et al.* Exposure to hydrogen peroxide induces oxidation and activation of AMP-activated protein kinase. *Journal of Biological Chemistry* **285,** 33154–33164 (2010).

533. Sarkar, S. *et al.* Complex Inhibitory Effects of Nitric Oxide on Autophagy. *Molecular Cell* **43,** 19–32 (2011).

534. Dalle-Donne, I., Rossi, R., Colombo, R., Giustarini, D. & Milzani, A. Biomarkers of oxidative damage in human disease. *Clinical Chemistry* **52,** 601–623 (2006).

535. Ott, M., Gogvadze, V., Orrenius, S. & Zhivotovsky, B. Mitochondria, oxidative stress and cell death. *Apoptosis : an international journal on programmed cell death* **12,** 913–922 (2007).

536. Tian, G. *et al.* Ubiquinol-10 Supplementation Activates Mitochondria Functions to Decelerate Senescence in Senescence-Accelerated Mice. *Antioxidants & redox signaling* 1–51 (2013). doi:10.1089/ars.2013.5406

537. Armstrong, J. S. The Coenzyme Q10 Analog Decylubiquinone Inhibits the Redox-activated Mitochondrial Permeability Transition: ROLE OF MITOCHONDRIAL RESPIRATORY COMPLEX III. *Journal of Biological Chemistry* **278,** 49079–49084 (2003).

538. Sliwoski, G., Kothiwale, S., Meiler, J. & Lowe, E. W. Computational methods in drug discovery. *Pharmacological reviews* **66,** 334–95 (2014).

539. García-Alcover, I. *et al.* Development of a Drosophila melanogaster spliceosensor system for in vivo high-throughput screening in myotonic dystrophy type 1. *Disease models & mechanisms* **7,** 1297–306 (2014).

540. Ma, D. Applications of yeast in drug discovery. *Progress in drug research. Fortschritte der Arzneimittelforschung. Progres des recherches pharmaceutiques* **57,** 117–162 (2001).

541. Saada, A. The use of individual patient's fibroblasts in the search for personalized treatment of nuclear encoded OXPHOS diseases. *Molecular Genetics and Metabolism* **104,** 39–47 (2011).

542. Montini, G., Malaventura, C. & Salviati, L. Early Coenzyme Q10 Supplementation in Primary Coenzyme Q10 Deficiency. *New England Journal of Medicine* **358,** 2849–2850 (2008).

543. Sacconi, S. *et al.* Coenzyme Q10 is frequently reduced in muscle of patients with mitochondrial myopathy. *Neuromuscular Disorders* **20,** 44–48 (2010).

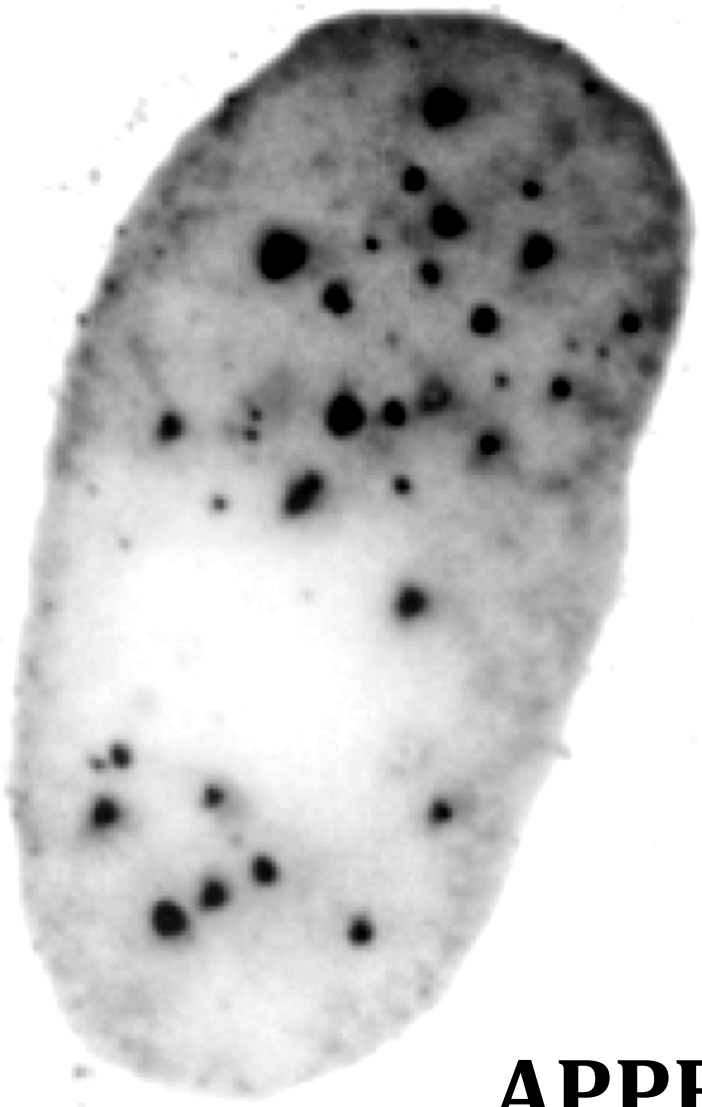

APPENDIX

APPENDIX

A-I. List of figures and tables

Figures

Tables

A-II. Publications

- ♦ **Garrido-Maraver J**, Villanueva Paz M, Cordero MD, Bautista-Lorite J, Oropesa-Ávila M, de la Mata M, Delgado Pavón A, de Lavera I, Alcocer-Gómez E, Galán F, Ybot González P, Cotán D, Jackson S and Sánchez-Alcázar JA. (2015) Critical role of AMP-activated protein kinase in the balance between mitophagy and mitochondrial biogenesis in MELAS disease. *Molecular Basis of Disease*. 1852(11):2535-2553. Article.
- ○ **Garrido-Maraver J**, Cordero MD, Oropesa-Ávila M, Fernandez Vega A, de la Mata M, Delgado Pavón A, de Miguel M, Pérez Calero C, Villanueva Paz M, Cotán D, Sánchez-Alcázar JA. (2014) Coenzyme Q10 therapy. *Molecular syndromology* 3-4, 187-197. Review.
- ○ **Garrido-Maraver J**, Cordero MD, Oropesa-Avila M, Vega AF, de la Mata M, Pavón AD, Alcocer-Gómez E, Calero CP, Paz MV, Alanis M, de Lavera I, Cotán D, Sanchez-Alcázar JA. (2014) *Clinical applications of coenzyme Q10*. *Frontiers in Bioscience* 19, 619-633. Review.
- ♦ **Garrido-Maraver J,** Cordero MD, Moñino ID, Pereira-Arenas S, Lechuga-Vieco AV, Cotán D, De la Mata M, Oropesa-Ávila M, De Miguel M, Bautista Lorite J, Rivas Infante E, Alvarez-Dolado M, Navas P, Jackson S, Francisci S, Sánchez-Alcázar JA. (2012) Screening of effective pharmacological treatments for MELAS syndrome using yeasts, fibroblasts and cybrids models of the disease. *British Journal of Pharmacology* 167, 1311-1328. Article.

A-III. Patents

- ○ Method for screening/assessment of the effectiveness of drugs for treatment of MELAS syndrome and mitochondrial diseases. (2012). Reference: P201230936.

Note: This thesis has been mainly based in the highlighted articles (♦).

A-IV. Acknowledgements

I amar prestar aen… Han mathon ne nen… Han mathon ne chae… A han noston ned gwilith[1]…. Llega el final, y toca dedicarles unas palabras a aquellos que creyeron en que este libro podría algún día llegar a ser más que un sueño. Ese día es hoy.

Parece que fue ayer, pero ocho años han pasado ya desde que un estudiante de biotecnología empezaba a deambular como alumno interno por el CABD. Ocho, que se dicen pronto… El principio, fue difícil. Perdido, dubitativo, completamente fuera de lugar, e incluso a veces con la sensación de haber tomado la dirección equivocada. Mucho ha llovido desde entonces, y muchas cosas he visto, oído y aprendido. Muchas personas he conocido desde aquellos primeros días que han dejado huella de una u otra manera en la persona que hoy escribe estas líneas…. Puff… Era cierto. Es duro esto de escribir los agradecimientos de tu propia tesis… Probablemente, me dejaré a muchos por el camino y espero que me perdonen por ello, pero si algo he aprendido durante estos años, es que la primera conclusión de una tesis debería ser siempre que un doctorado pasa factura en tu memoria. Espero que sepan disculparme.

Como no podía ser de otro modo, me gustaría empezar dando las gracias a la persona que me abrió las puertas del mundo de la investigación, a José Antonio Sánchez Alcázar. Fue él, y no otro, quien me ofreció la oportunidad de adentrarme en este laberinto de conocimiento y de incógnitas. Me llevo en el zurrón, tu capacidad de luchar, enfrentarte a las adversidades, preocuparte (y al mismo tiempo reírte) de los problemas, tu sana obsesión investigadora y tu forma de ser tan particular. Hemos trabajado duro desde que nos conocimos y espero que te sientas orgulloso de lo que hemos logrado juntos. Muchas gracias por enseñarme la puerta que tenía que cruzar.

Nada más entrar, fuiste tú... Mario David. Me tocó aprender contigo desde antes que se pusieran las calles... Mucho hemos hablado, trabajado y colaborado juntos. Muchos consejos, confesiones y hasta algún que otro reproche… No me olvido, no. Muchas gracias por coordinar aquellos dos primeros años en los que supiste guiarme de baldosa en baldosa por donde pocos sabían moverse como tú.

Por el laboratorio 210, pasan muchas personas. Algunas ya no están, otras siguen, y otras no han hecho más que llegar… Muchas caras, muchos nombres, muchas formas de pensar y todos ellos diferentes: David, Manuel, Mario, Ana, Isa, Marina, Mónica, Juana, Irene, Ana Victoria, Macarena, Alex y Raquel. A todos ellos, y en diferente medida tengo

[1] "El mundo ha cambiado. Lo siento en el agua. Lo siento en la tierra. Lo huelo en el aire". La canción de Galandriel traducida del sindarin (élfico gris). The Lord of the Rings: The Fellowship of the Ring. Versión filmográfica. 2001.

que agradecerles que me hayan enseñado como la profesionalidad, el compañerismo y la amistad a veces caminan de la mano por una delgada línea fácil de confundir… Pero, ante todo, me quedo con lo inesperado, los momentos fugaces de aquellos que supieron aprehender, aquellos que cuando menos te lo esperas, te sorprenden, te escuchan, te regalan su complicidad y las nubes negras se apartan... A veces, cuando no te lo esperas, la vida va y te sorprende, te regala momentos que sabes que no se repetirán, recuerdos imposibles de borrar... Gracias por cada uno de esos segundos que he vivido y que bien sabes que no voy a olvidar.

Toca cambiar de laboratorio… En primer lugar, me gustaría dar las gracias a Acaimo González Reyes por devolverme al camino, demostrarme que hay un más allá y no permitir que me conforme. Tu exigencia, tu capacidad para ver a través de los problemas, de desenmarañar la maraña con tres pinceladas, tu pasión por la ciencia y tu convicción… todas ellas, te aseguro que han dejado huella. Gracias por mostrarme tu mundo de Drosophila y las bellísimas personas que velan por él.

Primera planta a la izquierda, así empieza la aventura del 111/114. Y lo digo en singular porque uno no se puede concebir sin el otro. Los buenos momentos que me llevo, me obligan a apretarlos en el zurrón para que quepan todos. Son infinitos los detalles conmigo, las buenas intenciones, las sonrisas, la alegría, las bromas,… en definitiva el conjunto. Las magnificas personas que he conocido en este rincón del CABD ha sido de lo mejor. Los Lola, Bea, Andrea, Ceci, Besaid, Carmina, Inka, Gema, Clara, Juanjo, Bea Estrada, Acaimo, Mari Carmen, Alicia, mi archienemiga María y Alfon, son una combinación perfecta que reúne a gente brutalmente sincera, crítica, humilde y trabajadora, interesante, directa, sana, sin complejos, buena, artista, ilusionada, observadora, políticamente correcta, vividora, empática, amiga, lazarilla, defensora, abogada, sindicada al por qué de las cosas, fieles… Son muchos los sentimientos encontrados frente al aluvión de momentos que me vienen a la retina. Gracias a todos, pero vais a tener que permitirme que me detenga en el 114… Gracias a Alicia por tu capacidad para formar personas correctas, críticas con el sistema, luchadoras e inconformistas. Sin lugar a dudas, he aprendido muchísimo de ti, a veces hasta sin tú saberlo... Gracias a María, por tu capacidad crítica, tu personalidad grabada a fuego, la energía que desbordas, tus ansias de descifrar los misterios (casi 11 eran…), tus ganas de vivir el momento, tu Fe en ti misma. Eres envidiable, María. En especial, me gustaría destacar la labor fundamental que ha realizado Mari Carmen, tanto en el laboratorio como conmigo. Esta chica es para mí un ejemplo de tenacidad, ilusión e imaginación elevadas a su máximo exponente, una visionaria de este tiempo (no exagero), fuerte y luchadora, preparada y lista como el hambre, con una capacidad para unir a quien le rodea digna de admirar… Tu forma de ser no pasa desapercibida y créeme cuando te digo, que ojalá hubiese más personas cómo tú en este mundo. Por favor, no dejes de buscar las bolas mágicas…

Y a mi Alfon, Gracias, gracias, gracias. Bien sabes que hemos pasado grandes momentos juntos frente a nuestra chimenea: riéndonos, siguiéndonos el uno al otro cual pollitos en una granja, poniéndonos motes, discutiendo, tirándonos cosas, pegándonos,… En definitiva, aprendiendo el uno del otro. Muchas gracias por llevarme de la mano a la

realidad, por enseñarme a enfrentarme al mundo con más convicción, creyendo en lo que pienso y defendiendo contra viento y marea lo que creo. Gracias por enseñarme a montar y ser mi agenda, por tener paciencia conmigo, por esforzarte en comprenderme, por darme la oportunidad de conocer a esa Alfon detrás de la otra Alfon, gracias por ofrecerme tu siempre correcta sinceridad, por mostrarme que lo que uno considera un problema en realidad no significa tanto, por tu apoyo incondicional, por tu capacidad para alentarme a continuar, por defender férreamente tu forma tan particular de ver la política, la religión y la familia (hasta de eso he aprendido de ti)… Pero sobretodo, me quedo con tu capacidad para superar los obstáculos. Me has dejado boquiabierto… Verdaderamente, desprendes luz, Alfon. Espero que la vida sople a tu favor como te mereces y empieces a recoger los frutos que has ido sembrando.

No me voy a olvidar del "Coffee-time group". Gracias a Elena, Mario, Calero, Sofía, Miriam, Esmeralda, Helena, Mariam, David, Kathy, Marta y Ana, por alegrarme la sobremesa cada día, por enseñarme el valor del buen ambiente que debe imperar en un centro de investigación, por crear un grupo tan diverso como las áreas que tiene el centro. Vuestra capacidad para absorber la amistad, las risas y chistes, los secretos, diluir los problemas, de unirse cuando es necesario (tanto como para organizar un flash mob un domingo en el CABD)… En definitiva, increíbles momentos que no puedo dejar de recordar y agradecer. Sois el ejemplo a seguir de todo estudiante de doctorado.

Me gustaría destacar el papel que han jugado los compañeros del área de Biología Celular durante mis primeros años: Sara, Mariví, Gloria, Guille, Carlos, Luis, Isa, Mª Ángeles, Emilio, Eli, Ángela y Elena. De todos ellos, sin tutorizarme oficialmente, he aprendido muchísimo y han sido el centro de mi atención cada vez que compartían su saber. Grandes profesionales todos ellos. Asimismo, de todos ellos me gustaría agradecer especialmente a Elena por enseñarme la punta del iceberg de la gran persona que hay detrás de esa sonrisa, por su sinceridad, su saber escuchar y darme su confianza. Con tu alegría y desparpajo, ibas sembrando fresas allá por donde fueras. Gracias, Elena.

Me voy dejando a muchas personas por el camino, soy consciente de ello… Mi memoria ya no es la que era. Quiero agradecer también a las compañeras del grupo del área de microscopía Kathy, Corín y Lesly por su inestimable ayuda durante estos años, su confianza y sus palabras de apoyo. Un fuerte abrazo a las tres. También al servicio técnico de Cocina y Limpieza del que destaco a Natalia, Tamara y Mª Ángeles, ya que solo ellas saben cómo de temprano he entrado a trabajar durante todos estos años y conocen al dedillo los entresijos de las tierras de Mordor. A mis compañeros de estancia en Nueva York Ainhoa, Dolors, Xiaoling y al resto. Por hacerme sentir como en casa. También, a mi Tyrion, que desde mi regazo me ha ayudado a escribir gran parte de esta tesis.

A mis inquebrantables amigos Irene, Julián y Carmen, que han sabido estar ahí siempre para darme el aliento que a veces perdía, por ser mis eternos confesores y compartir mi carga… En definitiva, Gracias por llegar a descifrarme y, aun así, seguir ahí… GRACIAS. A mis cucharillas (Isa y Celia), a Kike, a Carmencita… En definitiva, a mis amigos, que desde la distancia se acuerdan de mí y no olvidan el cariño que desde aquí se les profesa.

Juntos hemos compartido muchas cosas, vivido momentos difíciles y también inolvidables. Vosotros sois los pilares sobre los que me sostengo. Sin vosotros al frente, no sería nada.

Finalmente, y no por ello menos importante, no puedo dejar de acordarme de las personas a las que más les debo, a mi familia. En especial a mis padres que desde su humildad y esfuerzo, pusieron toda la carne en el asador por que pudiese llegar donde hoy me encuentro. Gente sencilla, que me ha guiado por la senda del trabajo duro, el tesón, la constancia y el continuo "más-difícil-todavía". Gente trabajadora que ve desde la barrera como su hijo sigue adelante, superando esas barreras para seguir luchando más allá… cual martilleo incesante sobre el yunque. Mi triunfo o fracaso, es también el vuestro. Espero no defraudaros nunca. En este momento, no puedo evitar acordarme de mis abuelos sin emocionarme. Seguramente hoy estarían orgullosos de su nieto. En especial mi abuela, que ya en su día se saltó todos los protocolos de mi graduación para señalarle a la Dra. Margarita Salas desde el atril quién era su nieto y lo orgullosa que se sentía de él. En fin, así era ella…

Por último, quiero agradecer a la Luna de mi vida, Loly Mary, por saber acompañarme hasta el final por este sendero de trabajo infinito, exigencia y cosas inentendibles salvo en la cabeza de uno mismo. Ha sido muy duro. Mucho. Hemos atravesado juntos lo que para mí ha sido probablemente el camino más difícil tomado hasta ahora. Vendrán más…, pero después de esto, estoy completamente seguro que juntos podremos salir adelante.

Finalmente, no me gustaría acabar sin esperar que el presente documento haya hecho reflexionar y comprometerse al lector con la problemática existente en torno a las enfermedades raras y la necesidad de su estudio, para que paso a paso, sigamos contribuyendo a dar esperanza a un colectivo desatendido y ansioso de resultados. Seguiremos luchando.

Gracias a todo el que creyó en mí.

"La ciencia siempre vale la pena porque
sus descubrimientos, tarde o temprano,
siempre se aplican".

Severo Ochoa


UNIVERSIDAD
SEVILLA
AÑO 1997
PABLO DE OLAVIDE

MELAS (mitochondrial encephalomyopathy, lactic acidosis and stroke-like episodes) is a mitochondrial disorder caused mainly by the m.3243A>G mutation in mitochondrial DNA. In this thesis, we report on how the severity of pathophysiological alterations is differently expressed in fibroblasts derived from patients with MELAS disease. We evaluated mitophagy activation and mitochondrial biogenesis which are the main mechanisms regulating the degradation and genesis of mitochondrial mass in transmitochondrial cybrids and fibroblasts derived form MELAS patients. Our results suggest a critical balance between mitophagy and mitochondrial biogenesis which leads to the expression of different degrees of pathological severity among MELAS fibroblast cell lines according to their heteroplasmy load and the activation of AMP-activated protein kinase (AMPK). AMPK-activators such as 5-aminoimidazole-4-carboxamide 1-β-D-ribofuranoside (AICAR) or coenzyme Q_{10} (CoQ) increased peroxisome proliferator-activated receptor alpha (PGC-1α) nuclear translocation, mitochondrial biogenesis, antioxidant enzyme system response, autophagic flux and ultimately improved pathophysiological alterations in MELAS fibroblasts with the most severe phenotype. Our findings support the hypothesis that mitochondrial biogenesis, increased antioxidant response and autophagy clearance serve as compensatory mechanisms in response to mitophagic degradation of dysfunctional mitochondria and point out that AMPK is an important player in this balance.

These results are particularly important since currently no efficient treatments are available for this chronic progressive disorder. Furthermore, in this thesis we propose the evaluation of the effectiveness of putative beneficial pharmacological agents in the treatment of MELAS by using cellular models such as transmitochondrial cybrids and fibroblasts with high mutational load. According to our results, supplementation with riboflavin or coenzyme Q_{10} effectively reversed the pathologic alterations in MELAS cybrid and fibroblast cell models. Our results indicate that cell models manifesting severe pathophysiological alterations and high heteroplasmy load have great potential as a screening and validation assays of novel drug candidates for MELAS treatment and presumably also for other diseases with mitochondrial impairment.